Université de Sherbrooke

Homéostasie des ions cuivre et fer au cours de la germination fongique.

par
Samuel Plante
Département de biochimie

Thèse présentée à la Faculté de médecine et des sciences de la santé
en vue de l'obtention du grade de *Philosophiæ doctor* (*Ph.D.*) en biochimie

Jury d'évaluation :

Pre Amélie Fradet-Turcotte, département de biologie moléculaire, biochimie médicale et pathologie Université Laval
Pr Alexandre Maréchal, département de biologie
Pr François Bachand, département de biochimie
Pr Simon Labbé, département de biochimie

Sherbrooke, Québec
Avril 2019

The true delight is in the finding out
rather than the knowing

Isaac Asimov

RÉSUMÉ DE LA THÈSE

Homéostasie des ions cuivre et fer au cours de la germination fongique

Rédigée par Samuel Plante
Programme de biochimie

Présentée à la Faculté de médecine et des sciences de la santé en vue de l'obtention du diplôme de *Philosophiae doctor* (Ph.D.) en biochimie

La germination fongique est un processus cellulaire qui coordonne les changements métaboliques et morphologiques permettant à une spore en dormance de retrouver une forme végétative et une croissance mitotique. Les spores doivent jauger adéquatement leur environnement afin d'identifier les conditions propices à leur germination. La régulation fine de la germination est essentielle puisque l'activation des spores implique la renonciation à leurs caractéristiques protectrices.

L'objectif de mon projet est de comprendre les besoins des spores en micronutriments comme le Cu et le Fe au moment où ils doivent produire l'énergie, les macromolécules et les organelles afin de supporter la reprise du cycle cellulaire et les changements morphologiques associés. La levure fissipare (*S. pombe*) est le modèle que j'ai choisi pour l'étude de la germination. J'ai utilisé une souche hétérothallique que j'ai faite sporuler dans un milieu carencé en azote. Après l'isolement des spores, j'ai pu induire leur germination de manière synchrone.

Mes travaux ont révélé que les ions Cu et Fe sont requis pour la germination. Une carence en Cu induite par l'ajout du chélateur TTM, ou une carence de Fe induite par l'ajout du chélateur Dip lors de la germination inhibe pareillement l'éclosion des spores et l'apparition des projections. J'ai démontré que les transporteurs de Cu Ctr4, Ctr5 et Ctr6 sont requis pour la complétion de la germination. Ctr4 et Ctr5 co-localisent à la membrane plasmique de la projection en émergence. Dans le cas de Ctr6, il se localise à la membrane des vacuoles. Quant aux vacuoles, elles s'accumulent préférentiellement dans la vieille portion des spores en éclosion. Ces trois transporteurs sont requis pour la pleine activation da la superoxyde dismutase Cu/Zn SOD1. L'activité antioxydante de SOD1 est nécessaire pour l'éclosion des spores.

De plus, mes résultats révèlent le rôle crucial du sidérophore ferrichrome (FC) pour la germination. Le FC est synthétisé chez *S. pombe* par une voie impliquant les enzymes Sib1 et Sib2. La délétion de *sib1*+ et *sib2*+ inhibe complétement la synthèse de FC, entraînant un arrêt de la germination avant l'éclosion des spores. Les spores peuvent acquérir du FC exogène via le transporteur Str1 pour assurer la complétion de la germination. Str1 se localise à la membrane plasmique des spores en croissance isotrope. Sa fonction de transport du FC est dépendante de deux résidus tyrosine conservés (Tyr^{553} et Tyr^{567}) dans ce qui est prédit pour être la dernière boucle extracellulaire de Str1.

Dans l'ensemble, j'ai mis en évidence que l'assimilation adéquate de Cu et de Fe est nécessaire pour satisfaire le métabolisme des spores en germination. L'activation de la SOD1 et l'accumulation de FC sont des pré-requis cruciaux qui permettent l'adaptation de la spore à la transition vers une forme végétative.

Mots clés : Levure, Germination, Cuivre, Fer, superoxyde dismutase, Sidérophores

TABLE DES MATIÈRES

LISTE DES FIGURES

INTRODUCTION

RÉSULTATS

Chapitre premier

Chapitre deuxième

DISCUSSION

LISTE DES TABLEAUX

RÉSULTATS

LISTE DES ABRÉVIATIONS

AMP ..... Adénosine monophosphate
ATP ..... Adénosine triphosphate
ATPase ..... Adénosine triphosphatase
Cao ..... Amine oxydase cuivre-dépendante
CCM ..... Chromatographie sur couche mince
CcO ..... Cytochrome *c* oxydase
CRIB ..... *Cdc41/Ras – interactive binding*
CuSEs ..... *Copper sensing elements*
Ctrs ..... *Copper Transporters*, transporteurs de cuivre
Dip ..... 2,2' Dipyridyl
FC ..... Ferrichrome
GFP ..... *Green Fluorescent Protein*, protéine fluorescente verte
GTP ..... Guanosine triphosphate
GTPase ..... Guanosine triphosphatase
IMS ..... Espace intermembranaire de la mitochondrie
MT ..... Métallothionéines
NADPH ..... Nicotinamide adenine dinucleotide phosphate
NBT ..... Nitro bleu de tétrazolium
NES ..... *Nuclear Export Signal*, signal d'export nucléaire
NLS ..... *Nuclear Localisation Signal*, signal de localisation nucléaire
NOX ..... NADPH oxydase
NRPS ..... *Non Ribosomal Peptide Synthase*
PKA ..... Protéine Kinase A
ROS ..... *Reactive oxygen species*, espèces réactives de l'oxygène
SOD ..... Superoxyde dismutase
TPQ ..... 2,4,5-trihydroxyphénylalanine quinone
TTM ..... Tétrathiomolybdate
YES ..... *Yeast Extract plus supplement*

INTRODUCTION

1. Organismes fongiques

Les organismes fongiques, nommés aussi mycètes, sont des eucaryotes distincts des plantes ou des animaux, qui ont été regroupés dans le règne des *Fungi*. Ils sont de formes très variées, allant d'organismes unicellulaires simples nommés levures, à de complexes réseaux d'hyphes ou des champignons macroscopiques. Ils ont des rôles essentiels dans les écosystèmes terrestres ainsi qu'une grande importance économique et médicale (Kendrick, 2011).

Jusqu'à 92 % des plantes vasculaires bénéficient d'une association symbiotique, nommée mycorhize, entre leurs racines et un mycète (Bonfante, 2018). Ses hyphes sont généralement très étendus au-delà des racines et fournissent à la plante hôte une source d'eau et de minéraux, alors que le mycète se nourrit des exsudats des racines, riches en sucres et en acides aminés (Botha, 2011).

Les mycètes sont d'importants décomposeurs de matière organique, principalement les résidus végétaux (Boer et al., 2005). La cellulose représente la source de carbone majoritaire dans ces résidus, mais elle est isolée dans une matrice récalcitrante de lignine, de cutine ou chitine. Une propriété unique des mycètes consiste au fait qu'ils peuvent infiltrer ces matrices via leurs hyphes ou encore, les diriger en sécrétant des enzymes extracellulaires (Boer et al., 2005).

Les mycètes peuvent aussi contaminer les fruits, plantes et animaux, incluant l'homme. *Fusarium oxysporum*, *Magnaporthe oryzae*, *Fusarium graminearum*, et *Ustilago maydis,* entre autres, ont de grandes répercussions économiques en raison des ravages qu'ils peuvent causer aux récoltes et aux champs (Callan and

Carris, 2004). Les autorités de santé publique sont concernées par certains mycètes tels *Aspergillus fumigatus*, *Candida albicans* et *Cryptococcus neoformans* qui peuvent causer des infections pulmonaires, septicémies ou des méningites (Nosanchuk, 2015).

Dans presque tous les cas, les mycètes colonisent un nouvel environnement sous la forme de spores (Calhim et al., 2018). Les spores fongiques sont de petites cellules spécialisées au rôle central dans la survie, la reproduction et la dispersion des mycètes. Le règne des *fungi* a été initialement divisé en considération de la formation des spores (Lee et al., 2010). Les ascomycètes (*ascomycota*) sont une des plus importantes classes de mycètes. Les spores sexuelles de cette classe, nommées ascospores, sont maturées au sein d'un asque (voir *figure 1* pour un exemple d'asque), alors que les spores de basidiomycètes, nommées basidiospores, se forme par bourgeonnement sur la face apical d'un basidium. Les basidia sont très souvent regroupés dans des *fruiting bodies* qui sont des structures multicellulaires spécialisées dans la formation et la dispersion des spores (Silar, 2014). Le sujet principal de cette thèse étant un ascomycète, je n'élaborerai pas d'avantage concernant la famille des basiodiomycètes.

1.1. Organismes modèles

La levure à bourgeon *Saccharomyces cerevisiae* est connue pour sa contribution à l'industrie alimentaire. Elle est utilisée dans la fabrication du pain, le brassage de la bière et la fermentation du vin. Elle fait depuis longtemps l'objet de recherches visant à mieux comprendre son métabolisme afin d'augmenter ses rendements industriels (Liti, 2015). *S. cerevisiae* sert également de modèle pour l'étude de plusieurs processus biologiques fondamentaux. De fait, ses conditions

de culture simples et relativement peu couteuses sont modifiables selon les génotypes des souches utilisées. Puis, des outils très efficaces de génétiques ont été développés, permettant la délétion spécifique de gènes et l'étude de leur fonction (Botstein et al., 1997). Le séquençage de son génome en 1996, le premier génome eucaryote séquencé, a mis en lumière que ~31 % des séquences codantes de *S. cerevisiae* avait une homologie significative avec des cadres de lecture codant pour des protéines de mammifères (Goffeau et al., 1996). Malgré tous ces avantages, des divergences importantes, notamment son mode de division asymétrique par bourgeonnement et l'absence de système d'interférence à l'ARN, la distinguent de beaucoup d'autres mycètes et des métazoaires (Drinnenberg et al., 2009).

D'autres espèces prouvent toujours leur utilité comme modèles en laboratoire. Notamment, l'ascomycète filamenteux *N. crassa*, qui a pavé la voie aux études génétiques, contribue par exemple à l'étude du développement des hyphes et du cycle circadien (Mehra et al., 2009; Riquelme et al., 2011). Les espèces pathogènes *A. fumigatus*, *C. neoformans*, et *U. maydis* servent comme modèle pour l'étude des déterminants de la pathogénèse, et ce, autant chez l'humain que chez les plantes (Perez-Nadales et al., 2014).

1.1.1. Schizosaccharomyces pombe

La levure à fission *Schizosaccharomyces pombe* occupe divers habitats dans lesquels des composés riches en sucres s'y retrouvent tels des fruits, le miel; et la sève de canne et de palme (Florenzano et al., 1977; Jeffares, 2018; Jeffares et al., 2015). *S. pombe* participe à la fermentation des sucres botaniques que l'on retrouve sur les fruits de *Coffea arabica* et *Theobroma cacao* ou certains breuvages comme le *kombucha* ou le vin de palme (Gomes et al., 2002; Hoffman et al., 2015).

S. pombe a fait son entrée dans les laboratoires de recherche au début des années 1950. Sa manipulation relativement facile et sa culture rapide dans des conditions diverses et flexibles rendent cette levure attrayante comme organisme modèle. Comme chez *S. cerevisiae*, des techniques efficaces de génétique moléculaire ont été développées pour *S. pombe* (Forsburg, 2001). Le séquençage de son génome en 2002 a révélé que *S. pombe* n'aurait que peu évolué depuis la divergence des différentes levures (Hedges, 2002; Wood et al., 2002). Sa proximité phylogénique avec l'ancêtre commun des ascomycètes explique la conservation de caractéristiques biologiques partagées avec les métazoaires telles que le système d'interférence à l'ARN, le système d'épissage des ARNs, la structure des chromosomes et la division cellulaire par fission. *S. pombe* a aussi été utilisée pour l'étude de son cycle de vie sexuelle et la formation des spores (Hoffman et al., 2015; Kuramae et al., 2006; Yanagida, 2002).

2. Sporulation

La sporulation est le processus de différenciation cellulaire qui mène à la formation de spores qui sont de petites cellules en latence ayant développé une résistance à une multitude de facteurs environnementaux compromettant l'intégrité de cellules végétatives. Il se forme aussi, chez certaines espèces, des structures qui facilitent la dispersion des spores.

La sporulation fongique peut suivre une division mitotique. Dans un tel cas, une division asymétrique produit une cellule qui conservera son caractère végétatif et une autre qui se différenciera en spore. De telles spores, dites asexuelles, se nomment conidies. Elles sont produites en chaîne. Plusieurs ascomycètes sont bien

connus pour en produire, comme *N. crassa*, et plusieurs levures du genre *Aspergillus* (Adams et al., 1998; Park and Yu, 2012).

Pour le besoin de cette thèse, je vais m'attarder à la sporulation, dite sexuelle, de *S. pombe* (figure 1). Cette dernière se produit via une division méiotique. La progression de la méiose et de la différenciation des spores est conduite par quatre grandes vagues d'expression génique régulées par des facteurs de transcription (Yamamoto, 1996), ce qui contribue à synchroniser finement les événements afin d'assurer la division fidèle du matériel génétique et les chances de survie de la progéniture.

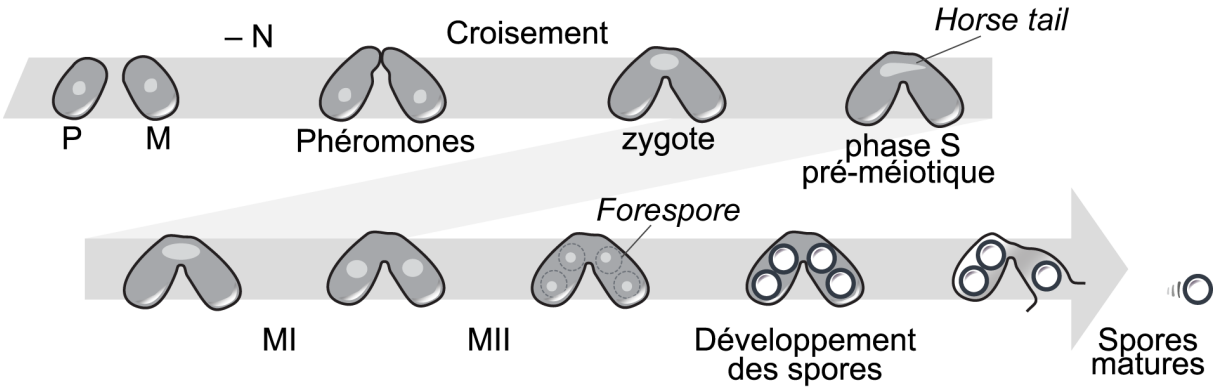

Figure 1- Illustration des principales étapes de la méiose chez *S. pombe*.
La carence en azote (-N) induit la communication par phéromones entre les cellules de type P et type M. Le croisement entre cellules de types complémentaires crée un zygote diploïde. La phase pré-méiotique S se caractérise par une déformation du noyau qui est appelée « horse tail ». Deux rondes successives de division du matériel génétique (MI et MII) se concluent par la formation de quatre jeux haploïdes de chromosomes. Chaque noyau haploïde est alors inclus dans un organite nommé "forespore" qui se développera en spore. À la fin de la maturation des spores, l'asque se lyse, permettant ainsi la libération des spores matures.

2.1. Méiose

La méiose est une division cellulaire essentielle pour la reproduction et la survie des organismes sexués. Elle mène à la formation des gamètes haploïdes (spermatozoïdes chez les mâles, ovules chez les femelles et spores chez les mycètes) à partir d'une cellule germinale diploïde nommée zygote.

Chez *S. pombe*, la sporulation est initiée par une carence nutritionnelle, plus particulièrement une carence en azote, qui mène à l'induction de Ste11. Ce facteur entraîne d'abord l'arrêt du cycle cellulaire en phase G1 et la différenciation sexuelle (Mata et al., 2007; Otsubo and Yamamoto, 2012). Il active la transcription des gènes de différenciation au locus *mat1*$^{+}$, qui peuvent être de deux types : *M* ou *P*.

La différenciation sexuelle comprend la sécrétion d'une phéromone; une cellule M sécrète la phéromone M qui est dérivée des protéines Mfm1-3; alors qu'une cellule de type P sécrète la phéromone P dérivée de la protéine Map2. Chacun des types présente à sa surface le récepteur à la phéromone du type opposé (Nielsen and Davey, 1995).

La communication par les phéromones amplifie la différenciation sexuelle et induit la croissance des cellules en direction de la source de la phéromone détectée, ce qui mène à la fusion entre deux cellules de types opposés pour former un zygote (Merlini et al., 2013). Si la carence nutritionnelle persiste, une cascade moléculaire impliquant notamment l'inactivation de la kinase Pat1 engage définitivement le zygote en méiose (Harigaya and Yamamoto, 2007).

Le génome diploïde du zygote est d'abord dupliqué durant la phase S pré-méiotique. Cette étape est suivie d'une prophase qui est caractérisée par des mouvements du noyau de la cellule précurseur diploïde qui lui donne une forme allongée nommée *horse tail*. Sous cette forme, il se produit des événements de recombinaison entre chromosomes homologues (Davis and Smith, 2001). Ces échanges de matériel chromosomique confèrent de nouvelles propriétés aux cellules descendantes. Deux rondes de division du matériel génétique se succèdent. D'abord, la séparation des chromosomes homologues, dénommée *méiose I*, puis la séparation des chromatides sœurs, dénommée *méiose II*. Quatre jeux haploïdes de chromosomes en résultent, chacun enfermé dans une membrane nucléaire. Chez les ascomycètes, dont *S. pombe*, les divisions méiotiques se font au sein du zygote et les spores y sont conservées jusqu'à la fin de leur maturation (Tanaka and Hirata, 1982).

2.2. Morphogénèse des spores

La formation des spores chez *S. pombe* commence par l'inclusion de chacun des quatre noyaux haploïdes dans une double membrane lipidique, nommée *forespore membrane*. Une paroi aux couches extérieures uniques aux spores y est ensuite déposée. Elle est composée de chitosane et un dépôt de la protéine Isp3 (Fukunishi et al., 2014). La paroi des spores est plus épaisse que celle qui recouvre les cellules végétatives. Elle contribue à la résistance des spores face à une multitude de stresses et conditions adverses comme la dessiccation, les variations de température extrêmes, les enzymes digestives et les solvants organiques (Fukunishi et al., 2014).

Les spores entrent dans un état de dormance qui est caractérisé par une faible activité métabolique. Les spores accumulent aussi des molécules protectrices comme le disaccharide tréhalose. Le tréhalose protège les macromolécules (ADN, protéines, lipides) des chocs thermiques et de la dessiccation en minimisant le besoin en eau dans leur environnement (Doxastakis et al., 2005; Magazù et al., 1999; Thevelein, 1984). Il contribue certainement au maintien de la dormance.
Le zygote initial est remodelé pour résulter en la formation d'un asque qui contient les quatre spores matures. Puis, l'asque se lyse spontanément, ce qui libère les spores.

3. Germination

Les spores fongiques se maintiennent en dormance sur de longues périodes, et ce, qui peuvent s'étendre sur plusieurs années pour certaines espèces (Bruns et al., 2009). Au retour des conditions adéquates pour la croissance cellulaire, les spores s'engagent alors en germination (figure 2). Ce programme de différenciation coordonne les changements métaboliques et morphologiques nécessaires au retour à une forme végétative et à la croissance cellulaire mitotique. D'abord les spores s'activent et quittent leur état de dormance. Puis, leur volume augmente de manière isotrope. La croissance polarisée est ensuite stabilisée, ce qui mène à l'émergence d'une projection qui est appelée le tube germinal. Finalement, une première division cellulaire sépare la cellule fille végétative de la spores mère.

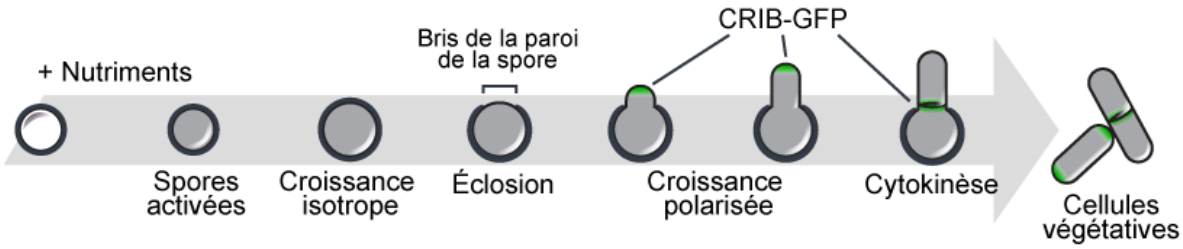

Figure 2 – Schématisation des étapes de la germination chez *S. pombe*.
Les spores en dormance sont activées par la présence de glucose dans leur environnement. Les spores doublent de volume tout en restant sphériques durant la période de croissance dite isotrope. Puis, il se produit un bris de la paroi des spores qui est nommée l'éclosion. Une projection émerge alors de la spore. La croissance polarisée peut être confirmée par la présence du marqueur de croissance CRIB-GFP. La première division cellulaire par fission à la base de la projection forme la première cellule végétative.

3.1. Dispersion des spores

Les spores doivent premièrement se retrouver dans des conditions favorables à leur germination. Bien que les conditions locales autour des spores puissent changer en leur faveur, il est possible que les spores aient été délocalisées par des facteurs externes tels des aérosols et des fluides pour trouver une nouvelle niche (Chitarra et al., 2004). Contrairement aux spores des mycètes filamenteux tels *Aspergillus spp.* et *N. crassa* qui sont produites sur un hyphe aérien qui les portent à l'air pour accélérer leur dispersion, la libération des spores de *S. pombe* n'implique pas de dispersion rapide. D'autres facteurs, tels les insectes, peuvent servir de vecteurs aux spores fongiques (Bunyard, 2007). Les levures sur les fruits mûrs en fermentation servent d'attracteurs et de diète pour la mouche *D. melanogaster* (Becher et al., 2012). Les cellules végétatives des levures *S. cerevisiae* et *S. pombe* sont tuées par leur passage dans le tractus digestif des mouches, alors que leurs ascospores survivent. L'analyse des fèces des mouches qui ont été nourries par des cultures de levures montre la présence de spores intactes

(Coluccio et al., 2008). Il s'agirait d'un vecteur plus efficace que la dispersion passive par l'air ou l'eau puisqu'ils exploitent la locomotion et la chimio-attraction des mouches qui déposeront les spores sur leur prochain lieu d'alimentation, soit un environnement riche en nutriments.

3.2. Activation des spores

La germination des spores débute par leur activation. Cette étape implique la sortie des spores de leur état de dormance qui est induit par des signaux environnementaux. De manière répandue, la présence d'eau et de nutriments comme un sucre est requise pour activer les spores (d'Enfert, 1997). Les spores de certaines espèces ont besoin de signaux spécifiques pour initier leur germination. C'est le cas des spores de *N. crassa* pour lesquelles un choc thermique est nécessaire pour leur activation (Lindegren, 1932). Ces besoins reflètent l'écologie variée des mycètes. *N. crassa* est une des premières levures saprophytes à croître sur les débris végétaux suivant un feu de forêt. Les spores de cette espèce fongique sont amenées sur des substrats qui ont chauffé et dont la chaleur est encore souvent présente.

La présence d'un sucre fermentable, le glucose idéalement, dans l'environnement des spores de *S. pombe* est suffisante pour initier leur germination (Shimoda, 1980) (figure 3). Le signal de la présence du glucose est d'abord reconnu par la sous-unité α de la protéine G nommée Gpa2. Cette protéine est associée au récepteur de glucose Git3 à la membrane plasmique (Welton and Hoffman, 2000). Le signal entraîne ensuite l'augmentation de la synthèse d'AMP cyclique, ce qui active la sous-unité catalytique de la protéine kinase AMP-cyclique-dépendante Pka1. L'activation de Pka1 est critique pour la germination des spores autant

chez *S. pombe* que pour plusieurs mycètes comme *S. cerevisiae*, *C. gloeosporioides*, *A. nidulans* et *M. grisea* (Barhoom and Sharon, 2004; Hatanaka and Shimoda, 2001; Kang et al., 1999). L'activation de la Pka1 entraîne l'utilisation rapide des réserves de tréhalose des spores. La tréhalase Ntp1 et une seconde tréhalase prédite comme spore-spécifique sont responsables de l'hydrolyse du tréhalose (Beltran et al., 2000; Inoue and Shimoda, 1981). Ce processus causerait un appel osmotique d'eau et une reprise du métabolisme. Chez *S. pombe*, cette étape n'implique pas de changement majeur de morphologie, sauf pour ce qui est d'une diminution de la réfractilité qui est détectable par microscopie à contraste de phase (Hatanaka and Shimoda, 2001). De plus, l'activation synchronisée d'une population se détecte par une diminution d'environ 20 % de la densité optique de la culture.

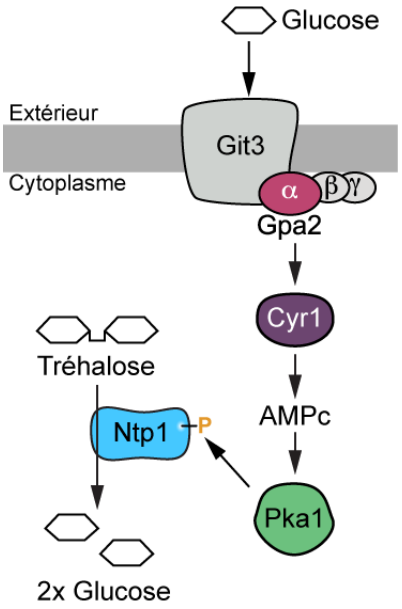

Figure 3 – Activation des spores
La présence de glucose dans l'environnement des spores est détectée par le récepteur Git3 à la membrane plasmique. La protéine G α Gpa2 couplée au récepteur active l'adénylate cyclase Cyr1. L'accumulation d'AMPc active la protéine kinase Pka1. Cette dernière phosphoryle entre autres la tréhalase Ntp1. La phosphorylation de Ntp1 active sa fonction d'hydrolyse du tréhalose dans les spores en activation.

3.3. Croissance isotrope

Le premier changement morphologique à survenir durant la germination est une croissance isotrope, durant laquelle les spores doublent leur volume tout en restant sphériques. Après l'initiation de la germination, le processus s'accompagne de la reprise de plusieurs activités métaboliques comme l'entrée d'eau et de nutriments, la respiration cellulaire ainsi que la synthèse d'ARN et de protéines (Allen, 1965). Les cellules initient d'ailleurs le cycle cellulaire en phase G1. Au cours de cette étape, les spores ne possèdent qu'une copie de génome (Hatanaka and Shimoda, 2001). La croissance à cette étape n'est pas parfaitement isotrope. En fait, une polarisation transitoire de la croissance a été détectée à cette étape. Un pôle de croissance est visible au pourtour des spores, mais son emplacement n'est pas constant (Bonazzi et al., 2014). La croissance polarisée serait inhibée par la tension dans la paroi de la spore. Ce processus qui déstabilise le pôle le force à se déplacer constamment. En somme, la croissance presqu'isotrope serait la somme de toutes ces tentatives de croissance polarisée autour de la spore.

L'augmentation du volume des spores est visible au microscope. De plus, cette croissance cause une augmentation de la densité optique de la culture de spores en germination à partir de la deuxième heure après le début de la germination.

3.4. Éclosion et croissance polarisée

La croissance perdure de manière isotrope jusqu'à ce que la spore ait doublé son volume. À ce point, la tension physique dans sa paroi est prédite pour être très élevée, ce qui causerait une rupture de la paroi (Bonazzi et al., 2014). L'éclosion de la spore est l'élément déterminant dans la poursuite de la germination. Le pôle de croissance est stabilisé au site de la rupture.

Le pôle de croissance a pu être détecté, notamment par la présence du régulateur clé de la polarisation, la guanosine triphosphatase (GTPase) de la famille *rho* Cdc42 sous sa forme active liée au guanosine triphosphate (GTP). Cette protéine peut être localisée grâce à l'utilisation d'un domaine rapporteur nommé CRIB (*Cdc42/Rac Interactive Binding*) qui est fusionné à la GFP (Das et al., 2012). Ce domaine est retrouvé dans les protéines effectrices interagissant directement avec Cdc42-GTP. Chez *S. pombe*, Cdc42-GTP active notamment la kinase Shk1 qui régule l'organisation du cytosquelette d'actine (Marcus et al., 1995; Ottilie et al., 1995).

La croissance polarisée au point de rupture de la paroi de la spore entraîne la croissance d'une projection germinative. Parce que le reste de la spore conserve sa forme sphérique, cela donne à la cellule une forme de poire caractéristique de cette étape de la germination. L'émergence de la projection crée une césure dans la paroi de la spore. La projection croît alors avec sa propre paroi nouvellement synthétisée qui est typique d'une cellule végétative (Bonazzi et al., 2014).

L'éclosion des spores est concomitante avec le début de la phase S du cycle cellulaire. En effet, les spores avec une projection en croissance contiennent deux copies de génome (Hatanaka and Shimoda, 2001). Ces deux copies sont ensuite divisées par mitose qui est suivie d'une cytokinèse par fission à la base de la projection pour produire une première cellule végétative fille à partir de la spore mère.

4. Ions cuivre et fer en biologie

Les ions Cu et Fe sont essentiels pour la vie aérobique. Une variété de protéines exploitent le potentiel redox des couples Cu(I)/Cu(II) ou Fe(II)/Fe(III), en tant que

cofacteurs catalytiques essentiels. Les enzymes Cu et Fe-dépendantes catalysent des réactions d'oxydo-réduction souvent cruciales pour les organismes (Kaplan and Ward, 2013; Nevitt et al., 2012).

Entre autres, les ions Cu sont essentiels à la détoxification des anions superoxyde (superoxyde dismutase), le transport du Fe (ceruloplasmine), la respiration cellulaire (cytochrome c oxydase), la synthèse de pigments (tyrosinase) et la coagulation sanguine (Facteurs V et VIII).

Les ions Fe sont des cofacteurs cruciaux pour le transport de l'oxygène (hémoglobine), la détoxyfication du peroxyde d'hydrogène (catalase), la respiration cellulaire (cytochromes), la biosynthèse d'acides aminés (acides aminés oxydase), le métabolisme des lipides (acides gras désaturase) et la biosynthèse d'ADN (ribonucléotides réductase). L'incorporation du fer aux sites catalytiques des enzymes se fait généralement sous la forme d'un centre fer-soufre (Fe-S), d'un groupement hème ou d'un complexe binucléaire de fer.

Cependant, la capacité des ions Cu et Fe à changer d'état d'oxydation leur donne un potentiel cytotoxique. Ils peuvent produire des dérivés oxygénés tel qu'illustré par la réaction de Fenton :

$$Cu(I) + H_2O_2 \longrightarrow Cu(II) + HO^- + \bullet OH$$

$$Fe(II) + H_2O_2 \longrightarrow Fe(III) + HO^- + \bullet OH$$

Au cours de cette réaction, le radical hydroxyl est produit. Ce radical cause des dommages délétères aux protéines, lipides et acides nucléiques (Halliwell and Gutteridge, 1992; Valko et al., 2005)

D’une part, les organismes ont développé des stratégies afin d’acquérir les ions Cu et Fe et les distribuer en quantité suffisante et sécuritaire aux métalloprotéines. De plus, des systèmes de stockage et de détoxification sont présents afin de prévenir les effets nocifs de ions Cu et Fe libres dans les cellules (Howard, 1999; Kim et al., 2008).

Chez l’humain, de sérieuses tares génétiques sont associées à des défauts de l’assimilation ou la régulation des ions Cu ou du Fe, telles que la maladie de Wilson, la maladie de Menkes, l’anémie microcytique hypochromique, l'hémochromatose ou l'ataxie de Friedreich (Kodama et al., 2012; Silva and Faustino, 2015). Les symptômes qui y sont reliés sont dus à la perte de fonction des métalloprotéines ou la toxicité des ions qui s’accumulent. De plus, l’accessibilité aux ions Cu et Fe est déterminante pour l’invasion par des microorganismes pathogènes. Des défauts dans l’acquisition ou la régulation des ions Cu ou Fe chez *C. neoformans*, *A. nidulans*, *A. fumigatus*, ou *C. albicans* atténuent grandement la virulence de ces pathogènes fongiques (Gerwien et al., 2018). L'étude des mécanismes qui régissent l'acquisition, l'entreposage et l'utilisation du Cu et Fe revêt donc une importance capitale.

Les prochaines sections de cette thèse seront consacrées à la description des composantes pertinentes participant à l’homéostasie des ions Cu et Fe chez *S. pombe*.

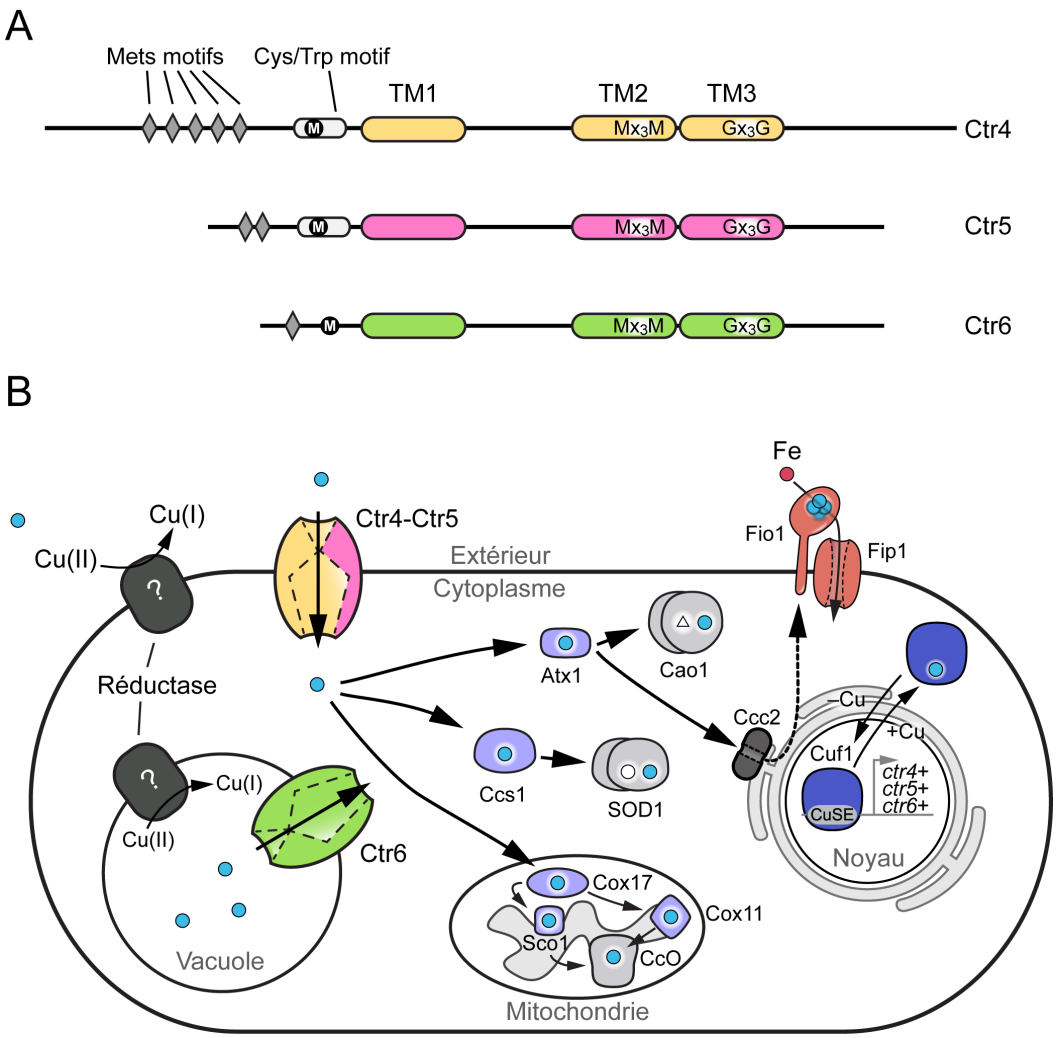

Figure 4 – Homéostasie des ions Cu chez *S. pombe*.
A) Schématisation des transporteurs de Cu Ctr4, Ctr5 et Ctr6 de *S. pombe*. Ils possèdent 3 domaines transmembranaires (TM1-3). Les motifs Mx_3M et Gx_3G sont conservés dans les TM2 et TM3, respectivement. Des motifs riches en résidus méthionines (Mets motifs, losanges gris) sont présents en nombre variables dans la portion N-terminale des transporteurs. Une méthionine (M) à environ 20 résidus en amont du premier TM est aussi conservée. Ctr4 et Ctr5 possèdent de plus un motif de cystéine et tryptophane (cys/trp motif) qui a une fonction *in vitro* dans la liaison du Cu(I). B) Le facteur de transcription Cuf1 active la transcription des gènes *ctr*4+ *ctr*5+ et *ctr*6+ en carence de Cu (-Cu) alors qu'en abondance (+Cu), Cuf1 lie le Cu et est exporté hors du noyau. Ctr4 et Ctr5 forment un hétérocomplexe à la membrane plasmique, alors que Ctr6 homotrimérise à la membrane vacuolaire. Les ions Cu sont réduits potentiellement par la réductase Frp1. La chaperonne Atx1 distribue le Cu à la protéine Ccc2 dans le sentier de sécrétion et également à l'amine oxydase Cao1. La chaperonne Ccs1 distribue spécifiquement le Cu à la superoxyde dismutase SOD1. Cox17 est la chaperonne du Cu spécifique à la mitochondrie. Les protéines Sco1 et Cox11 sont aussi impliquées dans l'activation de la cytochrome c oxydase (CcO). Rond bleu, ions Cu; rond blanc, Zinc; triangle blanc, TPQ.

5. Homéostasie des ions Cu

5.1. Transporteurs de la famille *Ctr*

L'environnement oxydant sur la terre favorise la forme oxydée Cu(II). Pourtant, ce sont les ions Cu(I) qui sont assimilés par les levures (Hassett and Kosman, 1995). Ainsi, préalablement à leur acquisition, les ions Cu doivent être réduits à la forme Cu(I). Chez *S. cerevisiae*, les métalloréductases Fre1 et Fre2 catalysent près de la totalité de l'activité ferriréductase à la membrane plasmique. Elles participent aussi à l'acquisition des ions Cu en réduisant les ions Cu(II). Chez *S. pombe*, l'activité ferriréductase à la surface des cellules est effectuée par Frp1, un homologue de Fre1 et Fre2 de *S. cerevisiae* (Roman et al., 1993).

L'acquisition des ions Cu chez les eucaryotes est assurée par une famille de transporteurs à haute affinité, nommée *Ctr* (*i.e. Copper Transporter*). Ctr1, Ctr2 et Ctr3 de *S. cerevisiae* ont été les premiers transporteurs de cette famille à avoir été identifiés, ce qui fait de cette levure un modèle important dans l'étude de l'homéostasie du Cu (Dancis et al., 1994; Kampfenkel et al., 1995; Peña et al., 2000). Elle a permis la découverte des *Ctrs* chez un grand nombre d'eucaryotes à cause du haut degré d'homologie de cette famille de transporteurs, notamment chez l'humain (Zhou and Gitschier, 1997), la souris (Lee et al., 2000), le ver *Caenorhabditis elegans* (Yuan et al., 2018), la mouche *Drosophila melanogaster* (Zhou et al., 2003) et la plante *Arabidopsis thaliana* (Kampfenkel et al., 1995).

Les *Ctrs* sont intégrés aux membranes par trois domaines transmembranaires (TM) (figure 4a). Leur extrémité N-terminale étant orientée vers le milieu extracel-

lulaire et l'extrémité C-terminal dans le cytoplasme. Les *Ctrs* s'assemblent en trimère, créant un canal (Feo et al., 2009). Un motif GxxxG dans le 3e TM est essentiel pour cet assemblage.

Leur portion N-terminale extracellulaire est riche en résidus méthionine (M) organisés en motifs MxM ou MxxM, nommés les mets motifs qui sont importants pour la captation des ions Cu et pour l'efficacité de transport par les *Ctrs* (Puig et al., 2002) (figure 4a). Une méthionine hautement conservée à environ 20 résidus en amont du premier TM est cruciale pour la coordination du Cu avant sa translocation vers le cytoplasme. Le motif MxxxM dans le 2e TM est impliqué dans le passage des ions Cu à travers la membrane (Puig et al., 2002).

Un motif cystéine/tryptophane a aussi été identifié dans la portion N-terminale de certains *Ctrs* fongiques (*e.g. S. pombe*, *S. cerevisiae*, *Colletotrichum gloeosporioides*). Des essais *in vitro* ont confirmé la capacité de ce domaine à lier et à stabiliser les ions Cu(I) (Okada and Miura, 2016; Okada et al., 2017).

Le mécanisme de transport du Cu par les *Ctrs* n'est pas dépendant de l'ATP. Sans être parfaitement décrit, le flux d'ions Cu de l'environnement extracellulaire vers le cytoplasme serait soutenu par un gradient d'affinité (Pope et al., 2012). Les ions seraient ainsi échangés d'un site de liaison à un autre de plus forte affinité jusqu'au cytoplasme. Chez Ctr1 humain, il est proposé qu'un motif HCH dans le domaine C-terminal sert de site énergétiquement favorable pour la liaison d'un ion Cu à la sortie du canal (Feo et al., 2009).

La levure à fission *S. pombe* présente deux transporteurs de Cu de haute affinité à sa surface, dénommés Ctr4 et Ctr5 (figure 4). Ils sont interdépendants du fait que l'expression de l'un ou de l'autre seul n'est pas suffisant pour permettre l'acquisition des ions Cu (Zhou and Thiele, 2001). Ctr4 ou Ctr5 exprimé seul n'est

pas correctement maturé et acheminé jusqu'à la membrane plasmique. Il est plutôt retenu au réticulum endoplasmique. Il a été déterminé qu'une molécule Ctr5 et deux molécules Ctr4 s'assemblent en un hétérocomplexe fonctionnel à la membrane plasmique (Ioannoni et al., 2010).

Une souche qui ne possède plus ces transporteurs (*ctr4*Δ *ctr5*Δ) présente plusieurs signes de déficience en Cu. Une conséquence directe est la perte d'activité des plusieurs enzymes Cu-dépendantes, comme la superoxyde dismutase SOD1, la cytochrome c oxydase, la multi-Cu oxydase Fio1 et l'amine oxydase Cu-dépendante Cao1 (Beaudoin et al., 2011a; Laliberté et al., 2004; Peter et al., 2008).

Ctr6 est un transporteur localisé à la membrane des vacuoles chez *S. pombe*. Il y fonctionne en homotrimère dans le but de mobiliser les réserves de Cu vacuolaires (Bellemare et al., 2002). En effet, les vacuoles fongiques servent notamment de réserve à plusieurs oligoéléments dont le Cu (Blaby-Haas and Merchant, 2014). La délétion *ctr6*Δ cause une diminution de l'activité de la SOD1, alors que sa surexpression augmente la sensibilité des cellules au Cu. Ces données suggèrent que Ctr6 participe à augmenter le bassin d'ions Cu cytoplasmiques disponibles pour les cuproenzymes.

L'ajout de Cu exogène (≥25 μM) au milieu de culture permet de rétablir l'activité des cuproenzymes, malgré les délétions *ctr4*Δ *ctr5*Δ. Cette observation suggère la présence d'au moins une voie d'assimilation à plus faible affinité. Le transporteur à faible affinité d'ions métalliques (dont le Cu et le Fe) Fet4 chez *S. cereviae* a un homologue du même nom chez *S. pombe* (Dainty et al., 2008). Cependant, la fonction de Fet4, ni d'aucune autre protéine, dans l'assimilation à faible affinité de Cu chez *S. pombe* n'a été déterminée.

5.2. Distribution aux cuproenzymes.

Une fois assimilés, les ions Cu sont pris en charge par des chaperonnes, ne laissant virtuellement aucun ion Cu libre dans le cytoplasme des cellules (Field et al., 2002). Alors que la concentration de Cu dans le cytoplasme est bien en dessous des limites d'affinité des cuproenzymes, ces dernières nécessitent les chaperonnes pour obtenir leur cofacteur métallique. D'une part, cela permet de limiter la toxicité des ions Cu et, d'autre part, augmente la spécificité ainsi que le contrôle de leur incorporation dans les protéines. Dans les prochaines lignes, je décrirai brièvement quatre sentiers de distribution.

5.2.1. Chaperonne Ccs1 et enzyme SOD1

La Cu/Zn superoxyde dismutase (SOD1) est un enzyme principalement cytosolique, qui catalyse la disproportion des anions superoxyde (O_2^-) en peroxyde d'hydrogène et en oxygène moléculaire (figure 5) (McCord and Fridovich, 1969).

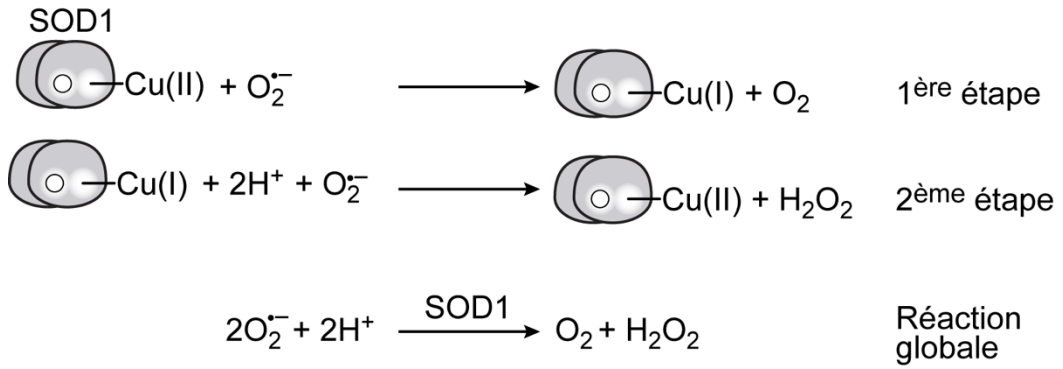

Figure 5 – Réaction catalysée par la SOD1.
La réaction globale de disproportion des anions superoxydes (tout en bas) peut être divisée en deux étapes. Une première étape durant laquelle il y a réduction du Cu catalytique et une seconde durant laquelle il y a oxydation du Cu.

Cette réaction enzymatique vaut à SOD1 un rôle central dans la protection contre des dérivés oxygénés toxiques. Elle est remarquablement hautement conservée chez les organismes aérobiques. La déficience en activité SOD1 augmente la sensibilité des cellules au stress oxydatif et provoque d'importants défauts métaboliques en condition aérobique (Reddi and Culotta, 2013; Wallace et al., 2004). La SOD1 est retrouvée sous forme dimérique. Son activité est dépendante d'un ion zinc (Zn) et Cu. Le zinc a une fonction structurale, alors que l'ion Cu participe directement à la réaction de disproportion de l'anion superoxyde. Le site catalytique de SOD1 contient quatre résidus histidine (*e.g.* H47, H49, H64 et H121, chez *S. pombe*) qui ont pour rôle de coordonner la liaison de l'atome de Cu au site catalytique.

La *Copper Chaperone for SOD1* (Ccs1) est responsable d'activer la SOD1 en l'approvisionnant spécifiquement en ion Cu et en facilitant sa maturation (Boyd et al., 2019; Culotta et al., 1997). Le mécanisme par lequel l'ion Zn est incorporé n'est pas connu à ce jour, mais il est indépendant de Ccs1.

Trois domaines (domaine I, II et III) ont été identifiés chez Ccs1 de *S. cerevisiae* (Schmidt et al., 1999). Le domaine I en N-terminal possède une pochette de liaison au Cu formé du motif MxCxxC, qui est conservée chez la chaperonne de Cu Atx1 et le transporteur de Cu Ccc2 (Pufahl et al., 1997). Le domaine I a une fonction de liaison du Cu qui favorise son transfert à SOD1 *in vivo* en condition de carence en Cu (Lamb et al., 2001).

Le domaine II de Ccs1 possède une similarité de séquence et de structure avec SOD1. Cependant, ce domaine ne peut pas lier d'ion Cu ni d'ion Zn, ce qui le rend catalytiquement inactif. Le domaine II sert à l'accostement ("docking") entre

les 2 protéines (Ccs1 et SOD1), ainsi qu'à stabiliser leur interaction lors du transfert du Cu d'une protéine à l'autre, ce qui est crucial à l'activation de SOD1 (Lamb et al., 2001; Schmidt et al., 2000).

Le domaine III en C-terminal est celui qui est le plus conservé à travers les espèces. Il compte un motif CxC qui se lie à l'ion de Cu *in vitro*. Ce domaine est indispensable pour le transfert de l'ion Cu à SOD1 (Lamb et al., 1999).

La chaperonne Ccs1 de *S. pombe* possède un quatrième domaine qui n'est pas présent chez Ccs1 de *S. cerevisiae*. Le domaine IV chez *S. pombe* est dispensable pour la fonction d'activation de la SOD1 (Laliberté et al., 2004). Le domaine IV est très similaire aux métallothionéines. En effet, il est riche en cystéines qui sont retrouvées majoritairement en paire selon l'arrangement CC. Ces résidus Cys sont connus pour jouer un rôle essentiel sur le plan de la coordination des ions Cu chez les métallothionéines. Des résultats suggèrent que le domaine IV de Ccs1 chez *S. pombe* contribue à la résistance au Cu en séquestrant ce dernier (Laliberté et al., 2004). Ccs1 joue donc au moins 2 fonctions : celle de chaperonne et de séquestreur d'ions Cu afin d'éviter que ces derniers deviennent libres dans la cellule.

5.2.2. Chaperonne Atx1, l'enzyme Cao1 et le sentier de sécrétion

Chez *S. cerevisiae* et *S. pombe*, une délétion du gène *ATX1* cause un défaut d'assimilation de Fe (Lin et al., 1997). C'est qu'*ATX1* code pour une protéine, Atx1, qui distribue spécifiquement les ions Cu au sentier de sécrétion. La principale cuproenzyme qui requiert des ions Cu pour sa maturation en vue d'être dirigée à la membrane plasmique est la multi-Cu oxydase Fet3, qui est essentielle pour l'assimilation de Fe (voir section 6.1). Fet3 obtient le cofacteur métallique alors

qu'elle transite du réticulum endoplasmique vers l'appareil de golgi. L'incorporation du Cu à la multi-Cu oxydase est dépendant de l'ATPase Ccc2, qui transporte activement les ions Cu vers la lumière du golgi (Yuan et al., 1995). Une interaction directe entre Atx1 et Ccc2 rend possible le transfert d'un ion Cu à Ccc2. Plus précisément, Atx1 interagit avec la portion N-terminale de Ccc2 (Banci et al., 2006). Cette dernière comporte deux domaines similaires à ceux retrouvés chez Atx1 et qui sont constitués des acides aminés Met et Cys selon l'arrangement suivant : MxCxxC.

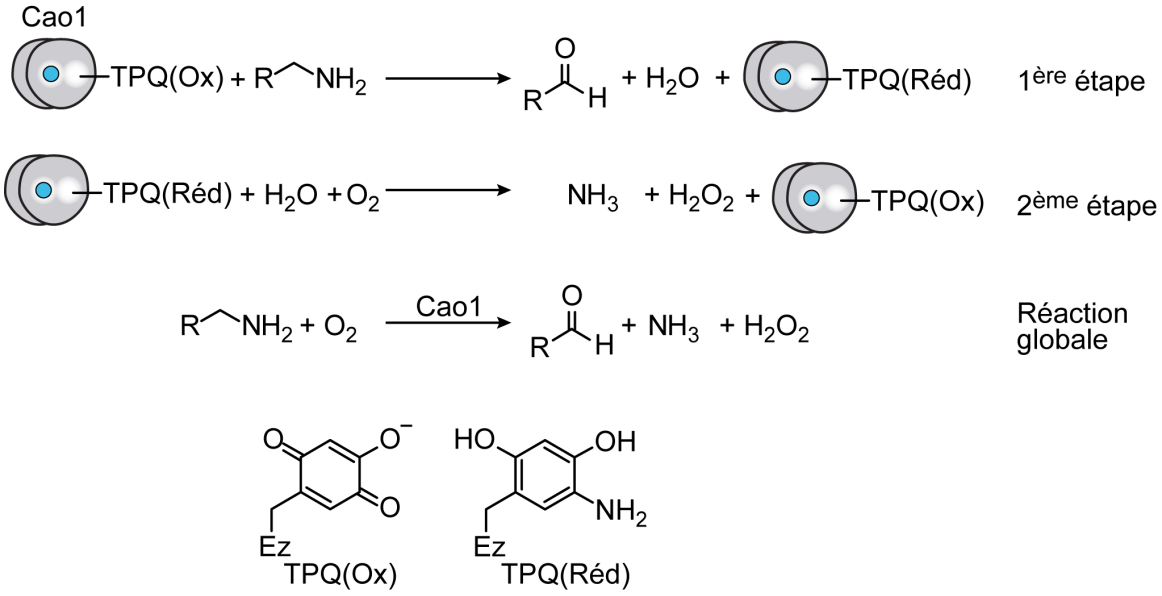

Figure 6 – Réaction catalysée par les CAO.
De haut en bas : la première et la deuxième étape de la réaction dans lesquelles il y a réduction et oxydation du cofacteur TPQ, respectivement; la réaction globale d'oxydation d'un amine primaire en aldéhyde, formant de l'ammonium et du peroxyde d'hydrogène; les structures du TPQ sous forme oxydée (Ox) et réduite (Réd).

Atx1 de *S. pombe* partage 57 % de similarité avec la chaperonne de *S. cerevisiae*. Elle possède un rôle identique à la protéine Atx1 de *S. cerevisiae*, soit celui de distribuer le Cu au transporteur Ccc2. Toutefois, une seconde fonction a été iden-

tifiée pour cette protéine. En effet, Atx1 possède également la capacité d'acheminer les ions Cu à la protéine amine oxydase Cao1 (Peter et al., 2008). Cao1 appartient à une classe d'enzymes qui catalysent l'élimination d'une amine primaire pour former de l'ammoniac ainsi qu'un aldéhyde et, du même fait, produisant du peroxyde d'hydrogène. Un ion Cu(II) est nécessaire à la formation du cofacteur organique TPQ (2,4,5-trihydroxyphénylalanine) qui est dérivé d'une tyrosine conservée du site actif (Janes et al., 1992; Rinaldi et al., 1998). Le TPQ participe à la réaction d'oxydation de l'amine primaire (figure 6). Seuls quelques organismes sont connus pour ne pas posséder d'amine oxydase Cu-dépendante. Ces organismes incluent *S. cerevisiae*, *C. elegans* et *D. melanogaster*. Atx1 peut interagir physiquement avec Cao1. Cette interaction entre Atx1 et Ccc2 requiert la portion N-terminale de cette dernière protéine (Peter et al., 2008).

5.2.3. Chaperonne Cox17 et la mitochondrie

La cytochrome *c* oxydase (CcO, ou complexe IV) est un complexe protéique intégré à la membrane interne de la mitochondrie. Ce complexe est la dernière étape de la chaîne de transport des électrons à la mitochondrie qui est impliquée dans la génération d'énergie par la phosphorylation oxydative. La CcO catalyse l'oxydation du cytochrome *c*, en la couplant à la réduction de l'oxygène moléculaire et la translocation de quatre protons dans l'espace intermembranaire (IMS). Les sous-unités catalytiques Cox1 et Cox2 sont Cu-dépendantes. D'ailleurs, l'ion Cu de Cox1 participe directement à la réduction de l'oxygène en eau. L'hème, le magnésium et le sodium sont aussi essentiels pour l'activité du complexe. La chaperonne Cox17 est importante pour fournir les ions Cu aux sous-unités Cox1 et Cox2 qui sont codées par l'ADN mitochondrial et produites dans la mitochondrie

(Glerum et al., 1996). La Cox17 de *S. pombe* partage 47 % de similarité avec son homologue chez *S. cerevisiae*. La délétion de *cox17*$^{+}$ et *COX17* chez *S. pombe* et *S. cerevisiae*, respectivement, entraîne une perte de fonction de la CcO qui se traduit par une incapacité de cette souche à croire sur un milieu non-fermentable. Cox17 de *S. cerevisiae* acquiert le Cu à partir d'une molécule dont la nature moléculaire n'a pas été encore définie (Cobine et al., 2004). Cette molécule apporterait le Cu dans l'IMS et permettrait le transfert du cofacteur à Cox17, qui elle, à son tour transfère le Cu à deux protéines intégrées à la membrane interne, Sco1 et Cox11 (Horng et al., 2004). Sco1 lie un ion Cu via un motif CxxxC, il le transfère spécifiquement à Cox2, qui est l'une des composantes du cœur catalytique de CcO (Cobine et al., 2006). Cox11 forme un dimère et chacun des monomères peut lier un ion Cu. Après son chargement en Cu via Cox17, Cox11 interagit spécifiquement avec Cox1 et permet le transfert du Cu entre les deux protéines, procurant ainsi le Cu à Cox1 (Cobine et al., 2006). Sco1 et Cox11 chez *S. pombe* sont des homologues des 2 protéines qui viennent d'être décrites de *S. cerevisiae*. Malgré le fait qu'elles n'aient pas été encore caractérisées chez la levure à fission, Sco1 et Cox11 de *S. pombe* ont une forte homologie de séquence avec les 2 protéines de *S. cerevisiae*, ce qui suggère qu'elles ont les mêmes fonctions respectives.

5.3. Régulation des transporteurs de Cu

La régulation transcriptionnelle des transporteurs de Cu est un aspect central dans le contrôle de l'homéostasie du Cu. La transcription des gènes *ctr4*$^{+}$, *ctr5*+ et *ctr6*+ est induite en carence de Cu, alors qu'elle est réprimée lorsqu'il y a abondance de Cu (Zhou and Thiele, 2001). Cela permet d'une part d'acquérir par haute

affinité les ions Cu lorsqu'ils se font rares, puis d'autre part de restreindre leur entrée lorsqu'ils sont abondants afin de limiter leur toxicité. Le facteur Cuf1 est responsable de cette régulation transcriptionnelle. La délétion *cuf1*Δ entraîne des phénotypes reliés à une déficience en Cu. En l'absence de Cuf1, les gènes qui codent pour les transporteurs de Cu ne sont plus induits, ce qui mène à la perte de fonction des cuproenzymes en carence de Cu (Beaudoin et al., 2003).

L'activation de la transcription par Cuf1 dépend des éléments de régulation en *cis* nommés CuSE (*Cu Signaling Elements*). Les CuSEs sont constitués des paires de bases formant la séquence consensus *5*'- D(A/T)DDHGCTGD -*3*' (où D = A, G ou T; H= A, C ou T) et qui sont retrouvés dans les promoteurs des gènes cibles. Cuf1 lie directement les CuSEs, ce qui permet sa fonction d'activation de la transcription. Les 174 premiers résidus de Cuf1 sont suffisants pour lier les éléments CuSEs *in vitro* (Beaudoin et al., 2003). En carence de Cu, le signal de localisation nucléaire (NLS) de Cuf1 (résidus 11 à 53) lui permet de se localiser au noyau où il peut activer la transcription des gènes *ctr4*+, *ctr5*+ et *ctr6*+. À l'opposé, en abondance de Cu, une séquence riche en cystéines (résidus 328 à 342) dans Cuf1 lierait alors du Cu. Des changements structuraux seraient alors induits. La protéine adopterait alors une conformation qui masquerait le NLS, inhibant son transport au noyau et sa capacité à se lier à l'ADN (Beaudoin and Labbé, 2006). Ce changement conformationnel exposerait le signal d'export nucléaire (NES) de Cuf1. Une accumulation de Cuf1 au cytoplasme, dépendante de l'exportine Crm1, est alors observée, empêchant de ce fait l'activation transcriptionnelle des gènes cibles (Beaudoin and Labbé, 2007).

Après une transition à un environnement abondant en Cu, l'hétérocomplexe Ctr4 – Ctr5 à la membrane plasmique est internalisé (Ioannoni et al., 2010). Cette

forme de régulation n'est toutefois pas aussi sensible que la régulation transcriptionnelle. Alors que des concentrations de l'ordre du nanomolaire en Cu sont suffisantes à la répression des transporteurs, il faut ≥25 μM de Cu pour observer l'endocytose des transporteurs. L'hétérocomplexe Ctr4 – Ctr5 internalisé peut être recyclé à la membrane plasmique lorsque les ions Cu se font à nouveau rares (Ioannoni et al., 2010). Les composantes et les mécanismes moléculaires responsables de l'endocytose et du recyclage des transporteurs sont toujours inconnus.

6. Homéostasie des ions Fe

Bien que le Fe soit un des éléments les plus abondants sur Terre, il n'est que très peu biodisponible. Cela s'explique par le fait qu'il est majoritairement retrouvé à l'état oxydé (Fe(III)) dans les conditions aérobiques. Il adopte alors différentes formes insolubles, incluant des précipités d'hydroxydes insolubles (Spiro et al., 1966). Les organismes ont dû développer des stratégies pour solubiliser et acquérir le Fe de leur environnement.

Je présente ici trois systèmes de haute affinité utilisés par *S. pombe* afin d'assimiler des ions Fe : i) l'acquisition du Fe inorganique qui requiert sa réduction ; ii) l'acquisition d'hème et iii) l'acquisition de Fe par des sidérophores. Les systèmes de transport d'ions Fe chez *S. pombe* et leurs composantes moléculaires sont illustrés à la figure 7

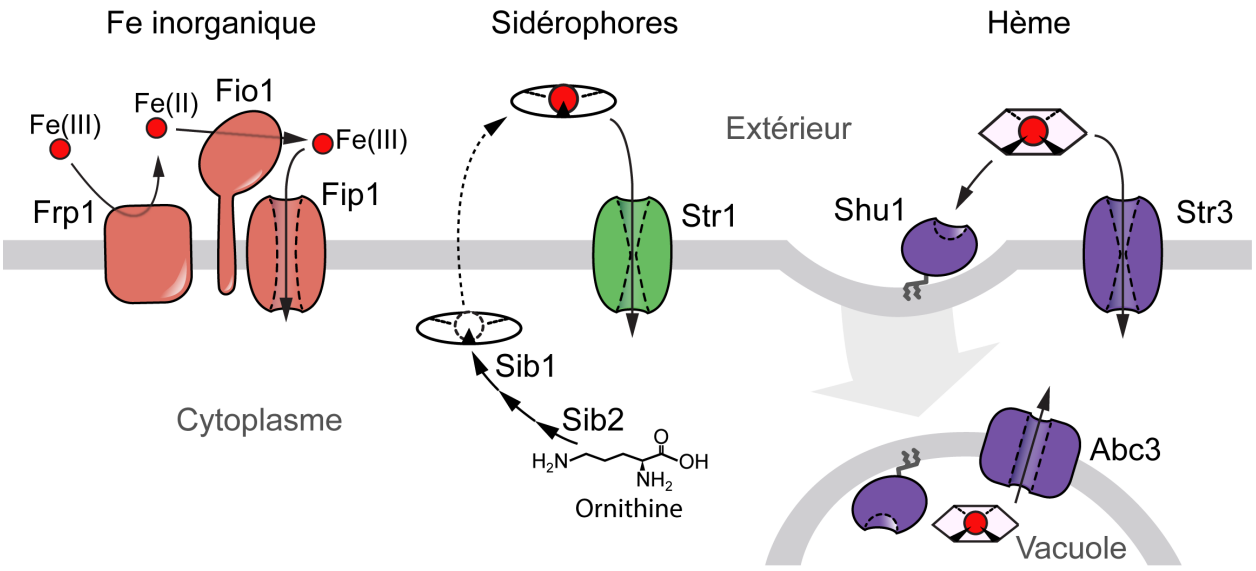

Figure 7 – Schématisation des systèmes d'acquisition du Fe chez *S. pombe*.
L'acquisition des ions Fe inorganiques dépend de la réductase de surface Frp1 et du complexe composé de l'oxydase Fio1 et de la perméase Fip1. Le sidérophore ferrichrome est synthétisé à partir de l'ornithine par un sentier impliquant les protéines Sib1 et Sib2. Le ferrichrome est ensuite sécrété dans l'environnement. Les sidérophores liés au Fe sont ensuite assimilés via le transporteur Str1 à la membrane plasmique. L'hème peut être capté par le récepteur Shu1 ou assimilé via le transporteur Str3. L'acquisition d'hème par Shu1 dépend de l'internalisation de l'hème et du récepteur jusqu'à la vacuole. L'utilisation de l'hème par cette voie implique le transporteur vacuolaire Abc3.

6.1. Acquisition du Fe inorganique qui requiert sa réduction

Le Fe(III) dans l'environnement immédiat des levures peut être solubilisé par sa réduction en Fe(II). La levure *S. pombe* exprime à sa surface la ferriréductase Frp1, qui, comme Fre1 et Fre2 de *S. cerevisiae*, catalyse la réduction des ions Fe(III) en Fe(II) (Roman et al., 1993). Fre1 possède des sites de liaison au NADP et au FAD qui servent de donneurs d'électron pour la réaction de réduction. Fre1

lie également deux molécules d'hème qui sont cruciales pour son activité (Shatwell et al., 1996). À cause de leur homologie de séquence, Frp1 est prédite pour utiliser un mécanisme d'action enzymatique semblable à Fre1.

Les ions Fe(II) sont ensuite pris en charge par le complexe de haute affinité composé de la multicuivre oxydase Fio1 et la perméase Fip1. Ces protéines partagent une grande homologie de séquence avec un complexe protéique équivalent chez *S. cerevisiae* qui est composé de la multicuivre oxydase Fet3 et la perméase Ftr1. D'abord, les ions Fe(II) sont oxydés par la multicuivre oxydase Fio1. Cette réaction est dépendante de la présence d'oxygène et d'ions Cu qui sont utilisés comme cofacteurs par Fio1 (Komori and Higuchi, 2015). L'oxydation des ions Fe est nécessaire pour leur transport à travers la membrane plasmique grâce à l'activité de la perméase Fip1. Les perméases Ftr1 et Fip1 arborent deux motifs REXLE. Ces motifs sont essentiels pour le transit des ions Fe(III) à travers la membrane plasmique via l'action de Fip1 (*S. pombe*) et Ftr1 (*S. cerevisiae*) (Severance et al., 2004).

6.2. Acquisition d'hème

L'hème est une molécule vitale composée de l'anneau protoporphyrine IX qui coordonne en son centre un ion Fe. Les cellules possèdent une voie de biosynthèse de l'hème qui est hautement conservée à travers les différentes espèces d'organismes. Cette voie est composée de 8 protéines, dont 4 qui sont mitochondriales, alors que 4 sont cytosoliques. Chacune de ces protéines a été très bien caractérisée chez plusieurs organismes prototrophiques pour l'hème (Heinemann et al., 2008). Un autre moyen pour les cellules d'acquérir l'hème est de médier son transport à l'intérieur des cellules lorsqu'il est présent dans l'environnement.

Chez *S. pombe*, la protéine Shu1 a été caractérisée comme un récepteur d'hème (Mourer et al., 2015). La majorité de la protéine est exposée au milieu extracellulaire. Elle est retenue à la surface des cellules par une ancre glycosylphosphatidylinositol (GPI) qui est attachée à la membrane plasmique. Seuls quelques exemples de tels récepteurs ont été étudiés, incluant les protéines Pga7 et Rbt5 de *C. albicans*, qui sont impliquées dans l'acquisition d'hème chez cette levure pathogène (Kuznets et al., 2014). Un domaine CFEM conservé se retrouve dans les protéines Pga7 et Rbt5. Ce domaine permet aux protéines d'adopter une configuration en type de panier de basketball qui est requis pour la captation de l'hème (Kulkarni et al., 2003). Des huit cystéines composant le domaine CFEM, seulement quatre sont conservées chez Shu1 de *S. pombe*. Elles sont d'ailleurs requises pour le bon fonctionnement de Shu1(Mourer et al., 2015). Une fois associé à Shu1, l'hème est ensuite internalisé jusqu'à la vacuole. Une fois à l'intérieur de la vacuole, un mécanisme permet à l'hème d'être libéré et d'être transporté à l'extérieur de la vacuole vers le cytoplasme. Ce dernier processus requiert le transporteur Abc3 (Mourer et al., 2017).

Une seconde voie d'assimilation de l'hème chez *S. pombe* implique le transporteur Str3. Il se localise à la membrane plasmique où il permet l'entrée d'hème vers le cytoplasme. Str3 possède une boucle extracellulaire dans laquelle un motif de liaison à l'hème s'y retrouve. Il a été démontré que la région peptidique correspondant à cette boucle se lie à l'hème *in vitro* et qu'elle est requise pour l'activité de transport de l'hème par Str3 (Normant et al., 2018). La voie d'assimilation de l'hème sous le contrôle de Str3 est indépendante de la présence de Shu1.

6.3. Acquisition de Fe par des sidérophores

Les sidérophores sont des molécules de petite taille ayant une affinité très élevée pour les ions Fe(III). La constante de formation du complexe Fe-sidérophore peut atteindre 10^{-30} M (Renshaw et al., 2002). Les sidérophores contournent le problème de faible biodisponibilité du Fe en le séquestrant à partir de sources dans lesquelles le Fe est en faibles concentrations; par exemple, les hydroxydes de Fe dans le sol qui ont une solubilité aussi faible que 10^{-9} M, ou à partir de la matière organique dans laquelle le Fe est principalement lié à des protéines. Des sidérophores sont produits par de nombreuses espèces de bactéries, mycètes et plantes. Les sidérophores sont classifiés selon le groupement chimique qui coordonne l'ion Fe(III) tel que le groupement aryl (catéchol ou phénolate), hydroxamate ou carboxylate. Presque tous les sidérophores fongiques sont de type hydroxamate et sont synthétisés à partir de la molécule d'ornithine. Ils peuvent être regroupés en quatre familles définies par leur arrangement structural : acides rhodotoruliques, fusarinines, coprogènes et ferrichromes (voir figure 8) (Haas et al., 2008).

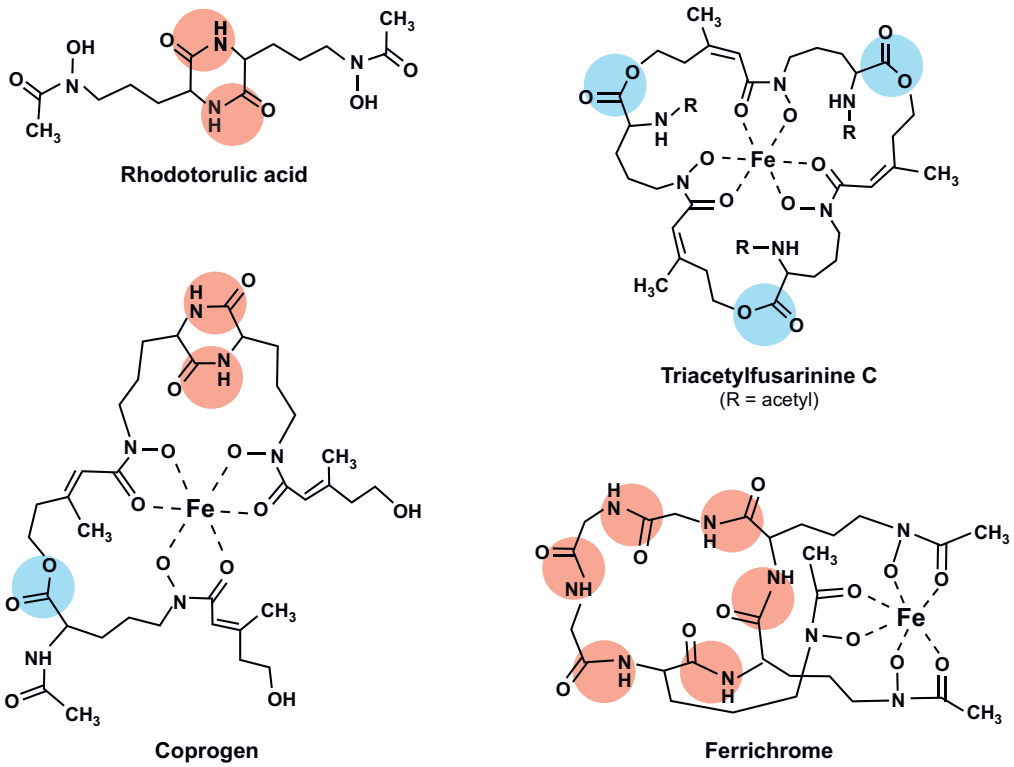

Figure 8 – Sidérophores fongiques.
Exemples de différentes familles de sidérophores fongiques. Les liens peptidiques et ester qui lient les groupements hydroxamates sont encerclés en rouge et en bleu, respectivement.
(tiré de Hass H, et al 2008)

La levure à fission *S. pombe* synthétise, accumule et sécrète le sidérophore ferrichrome (Mercier and Labbé, 2010; Schrettl et al., 2004). Ce sidérophore est un hexapeptide cyclique composé de trois résidus N^5-acétyl-N^5-hydroxyornithine et trois résidus glycine. Chez *S. pombe*, la synthèse du ferrichrome inclut l'hydroxylation de l'ornithine par la *L*-ornithine-N^5-monooxygénase Sib2 et son acétylation par une N^5-transacétylase. Le cadre de lecture *SPBC17G9.06c* est prédit pour coder une protéine ayant cette activité. Puis, l'hexapeptide est assemblé grâce à l'activité de la *non ribosomal peptide synthase* (NRPS) Sib1 qui catalyse la formation des liens peptidiques (Schwecke et al., 2006). Les enzymes Sib1 et Sib2 chez

S. pombe partagent une forte homologie avec l'ornithine-monooxygènase et les NRPS des mycètes producteurs de sidérophores dont *U. maydis*, *A. nidulans* et *A. fumigatu*s (Bushley et al., 2008; Haas et al., 2008). Quelques levures, dont *S. cerevisiae*, *C albicans* et *C. neoformans*, ne produisent pas de sidérophore.

6.3.1. Transporteurs de sidérophores.

Chez les mycètes, l'assimilation des complexes Fe-sidérophores est facilitée par les transporteurs de sidérophores (SITs, *Siderophore-Iron Transporter*s) appartenant à la superfamille *Major Facilitator* (MFS). Les MFS partagent une structure et un mécanisme d'action commun. Ils sont ancrés à la membrane via 12 ou 14 hélices transmembranaires qui sont organisées symétriquement de la façon suivante. Un premier groupe de 6 hélices transmembranaires est relié par de petites boucles. Une longue boucle intracellulaire sépare ces 6 hélices d'un regroupement de 6 autres hélices qui sont disposées de façon identique au premier regroupement d'hélices, de sorte que le transporteur s'organise en deux domaines de 6 hélices qui sont séparés par la longue boucle centrale (Quistgaard et al., 2016). Ces transporteurs peuvent adopter une conformation qui expose le site de liaison du ligand, soit vers le cytoplasme (captation) ou vers l'extérieur (relarguage). Le modèle *rocker-switch* propose qu'après la liaison du ligand, le transporteur change de conformation par une bascule des domaines, ce qui permet au ligand de traverser la membrane (Quistgaard et al., 2016; Yan, 2015). L'acquisition de sidérophores par les SITs est couplée à l'entrée de protons qui est soutenue par le potentiel de membrane (Winkelmann and Huschka, 1984). L'acquisition de Fe par les SITs est une stratégie universelle chez les mycètes, et ce, même pour les levures non productrices de sidérophores. L'utilisation de xenosidérophores reflète la compétition des microorganismes pour le Fe dans des niches qui

peuvent être souvent riches en sidérophores, en particulier les ferrichromes et les ferrioxamines (Winkelmann, 2007). Des travaux sur les SITs, en particulier chez *S. cerevisiae*, *A. fumigatus*, *A. nidulans* et *F. graminearum*, ont révélé qu'ils transportent des substrats spécifiques différents d'un transporteur à l'autre (Haas, 2014; Park et al., 2006; Renshaw et al., 2002; Yun et al., 2000).

Chez *S. pombe*, l'assimilation du ferrichrome depuis le milieu extracellulaire est médiée par Str1, qui a été identifié par homologie de séquence avec les transporteurs Arn1 à 4 de *S. cerevisiae*. D'ailleurs, l'expression hétérologue de Str1 dans une souche de *S. cerevisiae* déficiente en acquisition de Fe, supporte l'utilisation du ferrichrome comme source de Fe (Pelletier et al., 2003). Le rôle physiologique d'un deuxième SIT putatif nommé Str2 reste encore inconnu chez *S. pombe*. Les protéines Arn1 et Arn3 de *S. cerevisiae*, Sit1 de *C. albicans*, MirB de *A. fumigatus*, Sit1 de *C. glabrata* et Sit1 de *F. graminearum* sont connues pour transporter les ferrichromes (Heymann et al., 2002; Nevitt and Thiele, 2011; Park et al., 2016; Yun et al., 2000).

La dernière boucle extracellulaire de Sit1 de *C. glabrata* (longue de 51 résidus) contient un domaine SITD qui est conservé chez plusieurs transporteurs fongiques de sidérophores. Un résidu tyrosine (Y^{575}) localisé dans le domaine SITD de Sit1 est critique pour sa fonction d'assimilation du ferrichrome couplé au Fe (Nevitt and Thiele, 2011). Ce résidu tyrosine est hautement conservé dans les SITs d'un grand nombre de mycètes.

La présence ou non de sidérophores peut affecter la localisation des transporteurs. Sans aucun sidérophore dans l'environnement, les transporteurs Arn1 et Arn3 de *S. cerevisiae* sont dirigés aux endosomes. La présence de leurs ligands (FC pour Arn1 et FC ou ferrioaxamine B pour Arn3) à faible concentration permet

le mouvement des transporteurs jusqu'à la membrane plasmique (Kim et al., 2002). À des plus fortes concentrations de sidérophores, les transporteurs vont à la membrane plasmique et sont ensuite rapidement endocytosés avec leurs cargos. Cette continuelle relocalisation est essentielle pour leur activité.

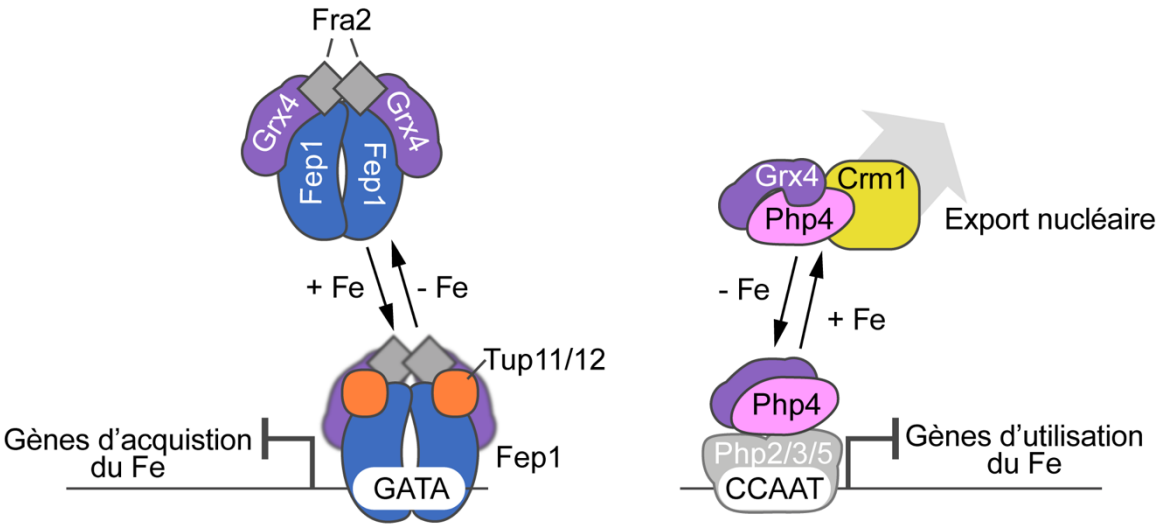

Figure 9 – Régulateurs de l'homéostasie du Fe chez *S. pombe*.
En abondance de Fe, Fep1 lie les éléments GATA dans les promoteurs de ses gènes cibles. Fep1 réprime la transcription des gènes codant pour les gènes d'acquisition du Fe grâce au recrutement des co-répresseurs Tup11 et Tup12. En carence de Fe, Fep1 décroche de la chromatine, permettant la transcription des gènes de transport du Fe. L'inactivation de Fep1 requiert les partenaires Grx4 et Fra2. Toujours en carence de Fe, Php4 forme un complexe avec Php2, 3 et 5 sur les éléments CCAAT dans les promoteurs de ses gènes cibles. Php4 réprime la transcription de plusieurs gènes, dont *fep1*+ et des gènes codant pour des protéines utilisant le Fe. Lorsque le Fe est abondant, Grx4 est primordial pour l'inactivation de Php4, qui permet la levée de la répression de ses gènes cibles. La liaison de Php4 avec le complexe Php2, 3 et 5 est rompue. Grx4 promeut l'export de Php4 hors du noyau via l'exportine Crm1.

6.4. Régulateurs de l'homéostasie du Fe.

Les gènes qui codent pour les composantes des systèmes d'assimilation de Fe sont régulés selon la disponibilité en Fe. En carence de Fe, la transcription de ces gènes est augmentée afin de maximiser l'acquisition de Fe et la mobilisation des réserves, alors que, lorsque le Fe est abondant, la cellule réprime les sentiers d'acquisition et accumule du Fe en réserve (Brault et al., 2015, voir figure 9 pour un résumé chez *S. pombe*). Chez la majorité des mycètes, la répression Fe-dépendante est médiée par un facteur de transcription répondant au Fe de type GATA. Des membres de cette famille ont été identifiés chez *U. maydis* (Urbs1), *Aspergillus spp.* (SREA), *C. albicans* (Sfu1), *C. neoformans* (Cir1) et *S. pombe* (Fep1) (Rutherford and Bird, 2004). La liaison Fe-dépendante à la chromatine de ces facteurs de transcription dépend de la présence d'éléments *cis* GATA (figure 9). Leur séquence consensus est définie par les bases 5'-ATG(A/T)GATA(A/T)-3'. L'élément GATA est reconnu par deux motifs en doigt de zinc conservés qui sont nommés respectivement ZF1 et ZF2. Dans le cas du facteur Fep1 de *S. pombe*, sa portion N-terminale comprend les 2 doigts de zinc et elle est requise pour l'attachement au promoteur des gènes cibles (Pelletier et al., 2005). ZF2 a une fonction prédominante quant à la capacité du facteur à se lier à l'ADN, alors que ZF1 augmente l'affinité du facteur pour sa liaison à l'ADN et du même coup renforce son action de répression transcriptionnelle sur les gènes cibles. Une séquence conservée de 27 résidus contenant quatre cystéines invariantes se trouve entre les motifs ZF1 et ZF2. Ces résidus cystéines servent à la liaison de Fe ainsi que promeuvent la liaison à l'ADN et la répression Fe-dépendante des gènes cibles (Jbel et al., 2009; Pelletier et al., 2005). La fonction de Fep1 est dépendante de sa dimérisation et de son interaction (via son extrémité C-terminale) avec les co-

répresseurs Tup11 et Tup12 (Znaidi et al., 2004). Les protéines de la famille Tup participent aussi à la répression des gènes impliqués dans l'acquisition Fe chez *C. albicans* et *C. neoformans* (Brault et al., 2015).

En contraste, lorsque les ions Fe se font rares, Fep1 se décroche de la chromatine, permettant ainsi l'expression des gènes responsables de l'acquisition du Fe, incluant *frp1*+, *fip1*+, *fio1*+, *sib1*+, *sib2*+, *str1*+, *shu1*+, *str3*+ et *abc3*+ (Pelletier et al., 2002, 2003). Chez *S. pombe*, la glutarédoxine monothiol Grx4 et la protéine Fra2 servent de co-inactivateurs de Fep1. Sans une ou l'autre de ces composantes, Fep1 reste lié au promoteur de ses gènes cibles et les réprime constitutivement, sans égard au statut en Fe (Jbel et al., 2011).

La cellule répond aussi à la carence en Fe par un processus d'économie du Fe qui assure une utilisation adéquate des faibles quantités de Fe. Le facteur de transcription Php4 est le principal régulateur de l'économie du Fe chez *S. pombe* (Mercier et al., 2008). Lors d'une carence, Php4 s'associe au complexe composé de Php2, 3 et 5. Ces 3 dernières protéines déjà présentes sur les éléments régulateurs CCAAT sur l'ADN reçoivent Php4, qui lui, de par sa propriété à pouvoir réprimer permet la régulation négative de plusieurs gènes codant pour des protéines Fe-dépendantes ou impliquées dans des voies métaboliques Fe-dépendantes (Mercier et al., 2006, 2008). La régulation Php4-dépendante permet une diminution de la consommation de Fe par les cellules.

Fep1 et Php4 se régulent mutuellement l'un et l'autre sur le plan transcriptionnel. En carence de Fe, Php4 inhibe la transcription de *fep1*+. Au contraire, lorsque le Fe est abondant, Fep1 inhibe la transcription de ses gènes cibles, dont *php4*+ fait partie. Il est à noter que la protéine Php4 est également inactivée par Grx4. Ce

processus est alors suivi de l'export de Php4 hors du noyau par l'exportine Crm1 (Mercier and Labbé, 2009).

7. Objectifs de recherche

Des travaux antérieurs chez la levure à fission *S. pombe* ont mis en lumière l'importance des ions Cu et Fe pour le développement sexuel de cette levure. La déficience pour l'un ou l'autre de ces ions métalliques provoque un arrêt prématuré de la méiose juste avant la première division méiotique des chromosomes homologues. Ces travaux ont permis d'identifier Mfc1 comme un transporteur de Cu méiose spécifique qui assure, en plus de Ctr6, la distribution des ions Cu aux cuproenzymes comme Cao1 dans les spores en maturation (Beaudoin et al., 2011b; Plante et al., 2014). De plus, l'économie du Fe régulée par Php4 est un élément essentiel à la complétion de la sporulation en carence en Fe (Brault et al., 2016). Les spores formées après la méiose ont le potentiel de germer afin de développer de nouvelles cellules en prolifération mitotique. L'initiation de la germination requiert du glucose, qui, à lui seul, est suffisant pour enclencher la première étape de la germination. Cependant, les exigences nutritionnelles pour la complétion de la germination sont inconnues. Il paraît vraisemblable que les ions Cu et Fe, de par leur nature essentielle, soient requis par les spores en germination afin de compléter les changements métaboliques nécessaires au retour à une forme végétative. Dans cette optique, mon projet de recherche visait à élucider le rôle des ions Cu et Fe, ainsi que des principales composantes moléculaires permettant leur assimilation au cours de la germination chez *S. pombe*.

RÉSULTATS

CHAPITRE PREMIER

Cell-surface copper transporters and superoxide dismutase 1 are essential for outgrowth during fungal spore germination

Par
Samuel Plante, Vincent Normant, Karla M. Ramos-Torres, et Simon Labbé.

Article publié dans *The Journal of Biological Chemistry*, vol. 292, pages 11896 – 11914 (2017)

Contribution

J'ai réalisé la grande majorité des expériences rapportées dans cet article. J'ai monté les figures, à l'exception des images contrôles du traceur de cuivre CNIR4, et participé à la rédaction du manuscrit sous la supervision de Simon Labbé.

Résumé de l'article

La germination fongique est la transition d'une spore en dormance à un état cellulaire végétatif et le retour à une croissance mitotique, mais les déterminants nutritionnels et moléculaires qui sont requis au déroulement de ce processus sont peu connus. Nous rapportons ici que le cuivre est essentiel pour la germination des spores chez *Schizosaccharomyces pombe*. Une projection germinative émerge des spores au cours de leur germination. En carence de cuivre, l'expression des transporteurs de cuivre Ctr4 et Ctr5 est maximale à l'étape d'émergence de la projection. Dans le cas de Ctr6, son expression est plus étendue dans le temps, débutant au tout début du programme et ce, jusqu'à l'émergence de la projection. La germination des spores déficients pour les transporteurs Ctr4, Ctr5

ou encore, du senseur de cuivre Cuf1 est arrêtée prématurément avant l'émergence d'une projection. La délétion de *ctr6* interfère seulement partiellement avec le déroulement de la germination. À l'émergence d'une projection, Ctr4-GFP et Ctr5-Cherry co-localisent au pourtour de la spore, suivi de leur relocalisation autour de la projection à mesure qu'elle croît. Subséquemment, les transporteurs quittent la spore pour se retrouver à la membrane de la cellule fille. Après l'activation des spores, Ctr6 se localise à la membrane des vacuoles, qui elles, sont enrichies dans la spore mère comparativement à la projection. Les résultats utilisant un senseur fluorescent de cuivre indiquent que le cuivre labile s'accumule préférentiellement dans la spore mère. Des analyses génétiques et biochimiques révèlent que Ctr4 et Ctr6 sont nécessaires à l'activation de la superoxyde dismutase 1 (SOD1) durant la germination. Cette activation est cruciale puisque la déficience en activité SOD1 inhibe l'émergence d'une projection en germination. Ensemble, ces résultats indiquent que les transporteurs de cuivre et la SOD1 sont requis pour la complétion du programme de germination.

Cell-surface copper transporters and superoxide dismutase 1 are essential for outgrowth during fungal spore germination

Samuel Plante[1], Vincent Normant[1], Karla M. Ramos-Torres[2], and Simon Labbé[1]*

[1]Département de Biochimie, Faculté de médecine et des sciences de la santé, Université de Sherbrooke, Sherbrooke, QC, J1E 4K8, Canada. [2]Department of Chemistry, University of California, Berkeley, CA, 94720, USA

Running title: Fungal spore outgrowth is a copper-dependent process.

*Address correspondence to: Simon Labbé, Département de Biochimie, Faculté de médecine et des sciences de la santé, Pavillon Z-8, Université de Sherbrooke, 3201, Jean Mignault Street, Sherbrooke (QC) J1E 4K8 Canada. Tel: (819) 821-8000 ext.: 75460; Fax: (819) 820-6831
E-mail: Simon.Labbe@USherbrooke.ca

Keywords: Copper, copper transporters, fission yeast, spore germination, superoxide dismutase 1, yeast physiology.

ABSTRACT

During fungal spore germination, a resting spore returns to a conventional mode of cell division and resumes vegetative growth, but the requirements for spore germination are incompletely understood. Here, we show that copper is essential for spore germination in *Schizosaccharomyces pombe*. Germinating spores develop a single germ tube that emerges from the outer spore wall in a process called outgrowth. Under low copper conditions, the copper transporters Ctr4 and Ctr5 are maximally expressed at the onset of outgrowth. In the case of Ctr6, its expression is broader, taking place before and during outgrowth. Spores lacking Ctr4, Ctr5 and the copper sensor Cuf1 exhibit complete germination arrest at outgrowth. In contrast, *ctr6* deletion only partially interferes with formation of outgrowing spores. At outgrowth, Ctr4-GFP and Ctr5-Cherry first co-localize at the spore contour, followed by relocation to a middle peripheral spore region. Subsequently, they move away from the spore body to occupy the periphery of the nascent cell. After breaking of spore dormancy, Ctr6 localizes to the vacuole membranes that are enriched in the spore body relative to the germ tube. Using a copper-binding tracker, results showed that labile copper is preferentially localized to the spore body. Further analysis showed that Ctr4 and Ctr6 are required for copper-dependent activation of the superoxide dismutase 1 (SOD1) during spore germination. This activation is critical since loss of SOD1 activity blocks spore germination at outgrowth. Taken together, these results indicate that, cell-surface copper transporters and SOD1 are required for completion of the spore germination program.

INTRODUCTION

Schizosaccharomyces pombe cell proliferation generally occurs in a haploid state through rounds of mitotic cell divisions under nutrient-rich conditions. In contrast, under nutrient-starved conditions such as nitrogen deficiency, haploid cells of the opposite mating types conjugate and form precursor diploid cells that can switch from mitosis to meiosis (1). Once in meiosis, diploid cells undergo one round of DNA replication, followed by two successive rounds of chromosome segregation without an intervening S-phase that generate four haploid sets of chromosomes, termed chromatids. Each set of chromatids is then enclosed in a forespore which through a developmental process, results in four mature haploid spores that are enclosed into an ascus (2). After an extended period of time, *S. pombe* asci are autonomously lysed, releasing spores into the environment. However, under unfavorable conditions, spores remain highly resistant to a variety of environmental stresses due to the presence of a spore-specific structure called outer spore wall (OSW) or spore coat. The OSW provides a sealed physical barrier between the outside environment and the fungal spore content (3,4).

Under favorable nutrient and environmental conditions, dormant spores undergo a developmental process called germination in which case each quiescent spore converts itself into a vegetative cell that re-enters the mitotic cell cycle to resume growth and division (5,6). Spore germination in *S. pombe* is divided into distinct stages. First, dormancy of spores is stopped and their activation is accompanied by loss of spore refractility that can be observed by light microscopy and a decrease in optical absorbance of the spore suspension. Second, spores undergo an isotropic swelling process that results in doubling of their volume. Third, swollen spores enter outgrowth. This stage is characterized by a singular rupture in the OSW that is accompanied by an initial emergence of the germ-tube, resulting in the formation of pear-shaped spores. Fourth, the germ tube emerges at one side and grows away from the spore body in an unidirectional manner. Fifth, the duplicated chromosomal material migrates into the cylindrical part and then the new daughter cell is divided by septation from the mother spore body (5). Previous studies have shown that fungal spore germination is a multi-step process whose nutritional requirements differed at the early stage of germination in comparison to subsequent stages such as outgrowth (6-8). In *S. pombe*, the presence of glucose without any additional nutrients is sufficient for spores to exit dormancy as measured by the loss of spore refractility (9). However, subsequent morphogenesis development fails to occur in glucose-grown spores for which swelling and germ-tube formation are defective and absent, respectively (6). Based on the fact that spore germination implies a profound change in the resting state

of the spore, which involves major morphological and metabolic modifications towards its activation, it is expected that essential nutrients are required to satisfy the physiological demand of this multi-step developmental process.

Copper is an obligatory micronutrient for aerobic organisms (10). It serves as a catalytic or structural cofactor in a variety of enzymes, including cytochrome *c* oxidase, copper-zinc superoxide dismutase (SOD1), multicopper ferroxidase, and copper amine oxidase (CAO). These enzymes are respectively essential to fundamental cellular processes such as respiration, superoxide anion detoxification, iron transport, and xenobiotic amine metabolism (11). In the model organism *S. pombe*, the copper transport machinery has mostly been studied in dividing cells that grow mitotically. In these cells, copper is taken up by a two-component transporting complex that is composed of the Ctr4 and Ctr5 proteins located at the cell surface (12-16). Studies have shown that Ctr4 and Ctr5 are unable to function independently in copper acquisition. A clear interdependence between Ctr4 and Ctr5 has been established since the secretion of either protein to the plasma membrane requires the concomitant secretion of the partner protein (12,16). Bimolecular fluorescence complementation experiments have shown that the assembly of a functional heteromeric Ctr4-Ctr5 complex at the cell surface requires the combination of two Ctr4 molecules and one Ctr5 molecule (14). *ctr4Δ*, *ctr5Δ* or *ctr4Δ ctr5Δ* mutants exhibit phenotypes associated with copper deficiency. These mutants are characterized by their inability to take up radioactive ^{64}Cu and their inability to grow in low copper medium. In addition, the mutant cells display alterations in copper-dependent enzyme activities, including SOD1, copper amine oxidase 1 (Cao1), and cytochrome *c* oxidase (15,17). As is the case for most members of the Ctr family in fungal species, *ctr4*$^+$ and *ctr5*$^+$ genes are regulated at the level of transcription as a function of copper availability. They are induced under conditions of copper starvation and repressed in response to high copper concentrations. The transcription factor Cuf1 is required to activate *ctr4*$^+$ and *ctr5*$^+$ gene expression (18-20). Cuf1 associates with *ctr4*$^+$ and *ctr5*$^+$ promoters in copper-starved cells *in vivo*. In contrast, high concentrations of copper inhibit the binding of Cuf1 to chromatin (15).

Based on the fact that meiosis requires copper to successfully undertake and complete its differentiation program, expression and localization of the Ctr4 and Ctr5 proteins have been investigated in meiotic and sporulating cells (21,22). When the cells switch from mitosis to meiosis, expression and localization profiles of Ctr4 and Ctr5 show that the two proteins are still synchronously co-expressed, and co-localized at the cell surface of zygotes but only during the early steps of the meiotic program (22). After meiotic divisions, transcript levels of *ctr4*$^+$ and *ctr5*$^+$ are extinguished with concomitant disappearance of their encoded proteins. At this stage, the meiosis-specific cop-

per transporter Mfc1 is expressed and subsequently appears at the forespore membrane of ascospores where it serves to transport copper for accurate and timely meiotic differentiation under low copper conditions (21).

In *S. pombe*, Ctr6 is a third member of the Ctr family that localizes at the membrane of vacuoles in cells proliferating in mitosis under copper-limiting conditions (23). Ctr6 is an integral membrane protein that assembles as a homotrimer (23). A deletion of the *ctr6*$^{+}$ gene (*ctr6Δ*) results in a reduction of SOD1 activity (22,23). Similarly, inactivation of *ctr4*$^{+}$ (*ctr4Δ*) also causes a decrease of SOD1 activity but to a greater extent. When both *ctr6*$^{+}$ and *ctr4*$^{+}$ genes are inactivated, the double mutant (*ctr6Δ ctr4Δ*) fails to display measurable SOD1 activity, revealing a functional contribution of Ctr6 and Ctr4 in providing copper to at least one cytosolic copper-dependent enzyme under low copper conditions (22,23). On the basis of studies on Ctr6 and its ortholog Ctr2 in *Saccharomyces cerevisiae* (24,25), Ctr6 has been predicted to function as a vacuolar membrane copper transporter that mobilizes stored copper from the vacuole to the cytosol, thereby participating to a pathway by which copper could be distributed within cells from the organelle according to copper needs. In the case of cells that undergo meiotic differentiation, Ctr6 localizes at the membrane of vacuoles during the first stages of meiosis (22). After meiotic divisions, Ctr6 undergoes an intracellular relocation to co-localize with the forespore membrane at late anaphase II (22). Although the relocation of Ctr6 to the nascent forespore membrane is still unclear, one possibility may be a potential role in transporting stored copper from the prespore to the cytosol where meiotic copper-dependent enzymes are present such as SOD1. As opposed to the expression of *ctr4*$^{+}$ and *ctr5*$^{+}$ that is exclusively dependent on the presence of Cuf1, *ctr6*$^{+}$ expression is broader throughout the entire meiotic process and relies on two distinct regulators, Cuf1 and Mei4 (22).

In the present study, we have determined that *S. pombe* spore outgrowth is a copper-dependent developmental process. During spore germination, *ctr4*$^{+}$ and *ctr5*$^{+}$ genes are primarily co-expressed in response to low concentrations of copper through Cuf1, with peaks of expression at the end of isotropic swelling and at the onset of outgrowth. In the case of *ctr6*$^{+}$, its expression slightly increases in a time-dependent manner from the exit dormancy to outgrowth. Although *ctr6*$^{+}$ expression is more robust under low copper conditions in the presence of Cuf1, a low and constitutive level of expression is observed under basal and copper-replete conditions that is Cuf1-independent. Spores lacking Ctr4, Ctr5 or Cuf1 exhibit a germination arrest at the onset of outgrowth. In the case of *ctr6Δ* mutant spores, production of developing spores and newborn vegetative cells is reduced in comparison to wild-type spores. During the formation of the polar cap, Ctr4 and Ctr5 co-localize at the periphery of the spore and, subsequently at the plasma membrane of the new daughter cell. In the case of Ctr6, it localizes on the membrane of vacuoles. Using the fluorescent copper-

binding tracker CNIR4, labile copper is preferentially detected in the spore body, whereas the germ tube exhibits less CNIR4-copper complexes-associated fluorescence. Furthermore, results showed the critical importance of copper transport to a specific copper-dependent target since removal of SOD1 leads to a spore developmental arrest at the onset of outgrowth. Taken together, our findings highlight the essential requirement of copper and copper transport proteins for the developmental process of spore germination and outgrowth under low copper conditions.

RESULTS

Spore germination and outgrowth in S. pombe. A non-dividing haploid spore represents a resting state in fission yeast. Haploid spores are more resistant to different environmental stresses than vegetative cells that proliferate in mitosis (3,4). Purified spores are highly refractile when they are observed by phase-contrast microscopy (5,6). Herein, we used differential interference contrast (DIC or Nomarski) microscopy as a complementary approach (Fig 1A). Although DIC microscopy gives lower image brightness than standard brightfield microscopy, it provides far more highly defined images of the spore morphology. To monitor morphological changes, we therefore used DIC microscopy and spores harboring a *CRIB-GFP* allele (26,27). In *S. pombe*, the GTP-bound form of Cdc42 binds and activates a group of proteins that possess the CRIB (Cdc42/Rac-interactive binding) domain (27). By itself the CRIB domain fused to GFP associates with the GTP-bound form of Cdc42 that localizes at new growing cell end(s). CRIB-GFP is therefore used as a marker for spore outgrowth dynamics. Dormant purified spores were first incubated in the presence of calcofluor (10 μg/ml) in glucose-free media. After a 30-min incubation period, dormant spores were washed and synchronously induced to enter germination in glucose-containing and calcofluor-free media in the presence of $CuSO_4$ (50 μM). After initiation of spore germination, we observed that the optical density (OD_{600}) of the spore suspension decreased (Fig. 1B). This observation was consistent with previous reports in which results have shown that light-refractile spores became dark after 2 to 3 h of induction of germination (5,6). During the bright- to dark-phase transition, the optical density (OD_{600}) of the spore suspension decreased in parallel with darkening (6). Spores then increased their size for approximately 4 to 6 h (Fig. 1A). After 7 – 8 h of spore germination, a protrusion (also called germ tube) began to emerge at one side of each enlarged spore (Fig. 1A). At this stage and thereafter, an outgrowing spore adopted a bottle-like shape and the germ tube grew away from the spore body to eventually produce a calcofluor-free daughter cell (Fig. 1, A and

B). DNA content was determined by flow cytometry (FACS) analysis to assess whether ungerminated spores were restricted to single genome content (1C DNA). At the 0-time point and over a time period of 6 h after induction of germination, spores primarily exhibited 1C DNA content (Fig. 1C). Results showed that spores duplicated their genome (2C DNA) when they entered outgrowth (8-h time point, Fig. 1). At the end of outgrowth, developing spores solely exhibited 2C DNA content (10- and 12-h time points). In addition, forward light scatter (FSC) and side-scatter (SSC) analysis were performed after spores had been synchronously induced into germination. Results showed that at the 0-time point, the FSC/SSC cytogram exhibited the lowest values, which was consistent with a population of single spores that possessed small sizes (FSC) and very low internal granularity (SSC) (Fig. 1D). After 6 h of induction of germination, swollen spores increased their dimensions, which resulted in slightly higher FSC values with a global distribution of points moving towards the right (Fig. 1D). At the 12-h time point, the germ-tube has emerged and expended, causing an increase in size of individual cell. This increase in size correlated well with the highest FSC values, whereas further differentiation of cells growing away from the spore body produced higher SSC values, presumably due to formation of organelles that were detected as granularity signals (Fig. 1D).

Copper deficiency blocks the outgrowth of developing spores. Although yeast cells require copper as redox cofactor when they are committed to the aerobic mitotic cell cycle or to the meiotic program, little is known about the role of copper in spore germination. To investigate whether insufficient concentrations of copper would perturb spore germination, purified dormant spores harboring a *CRIB-GFP* allele were incubated in the presence of calcofluor to stain spore walls. Spores were then washed and synchronously induced to enter in germination in the presence of the copper chelator TTM (200 μM) or copper (50 μM). Spores that had been treated with TTM proceeded through the initial phases of germination, including breaking of spore dormancy until they reached isotropic swelling. At this stage, they stopped their differentiation and exhibited a germination arrest (Fig. 2A). A clear phenotype of the TTM-mediated block was the lack of germ-tube formation and, therefore, absence of outgrowth.

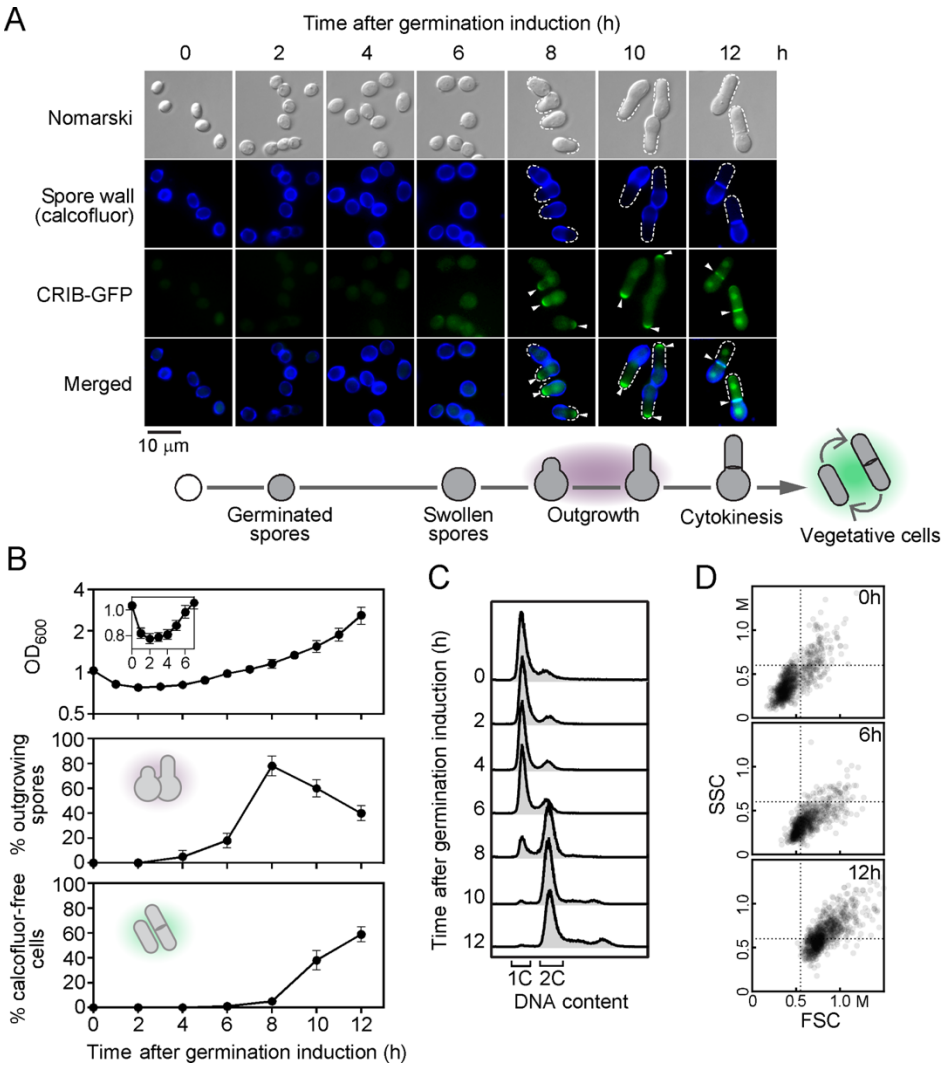

Figure 1. *Changes in morphology during spore germination and outgrowth*. *A,* Purified spores containing a *CRIB-GFP* allele were synchronously induced to initiate and proceed through germination in the presence of copper (50 μM). When expressed in germinating spores, CRIB-GFP was used as a marker to highlight the new cell tip during outgrowth and the site of cell division (septum) during cytokinesis (*center bottom*). Calcofluor (*blue*) was used as a marker to indicate the spore wall and the mother spore side, especially during outgrowth (*center top*). New cell side of outgrowing cells is indicated with *white dashed lines*, whereas white arrowheads show examples of CRIB-GFP cellular locations. The merged images are shown in the *far bottom* panels. Nomarski optics (*far top*) was used to examine spore and cell morphologies. Schematic representations of morphological changes of spores during germination and outgrowth are shown below microscopy panels. Results of microscopy are representative of five independent experiments. *B,* Total growth was measured at OD_{600} as a function of time after induction of germination. Inset indicates measurements at OD_{600} for the first 7 h of spore germination (*top*). The percentage of spores undergoing outgrowth (*middle*) and the percentage of calcofluor-free vegetative cells (*bottom*) were determined as a function of time after induction of germination. Values represent the average +/- S.D. of three independent experiments. *C,* FACS analysis of purified spores that contained one nucleus with a single complete genome (1C DNA). Following induction of germination, outgrowing spores duplicated their genome (2C DNA) as shown by FACS analysis. *D,* Dot plot of FSC versus SSC in which each dot represents a single spore or a calcofluor-free cell during early (0 h), middle (6 h),

and late (12 h) phases, respectively, of the germination program. FSC is proportional to spore size, whereas SSC is proportional to spore granularity.

Copper insufficient spores failed to reach the development stage where CRIB-GFP could be localized at one side of an enlarged spore, which represents the site of cell tip emergence. In contrast, spores that had been treated with copper proceeded through the entire germination program and formed bottle-like shaped spores with an outgrowing tip where CRIB-GFP was observed (Fig. 2B). After their entry in germination, optical density (OD_{600}) of spores was assessed under copper-replete conditions (50 μM) or in the presence of increasing concentrations of TTM (50, 100, and 200 μM). After initiation of spore germination, light-refractile spores became dark within 2 – 3 h. During the bright- to dark-phase transition, the optical density (OD_{600}) of the spore suspension decreased in parallel with darkening (Fig. 2C). After 3 h of germination, spores then increased their size through a process called isotropic swelling. At this stage (3-h time point) and until the 6-h time point, the optical density (OD_{600}) of the spore suspension progressively increased (Fig. 2C). During the first 6 h of observations, spectrophotometric absorbance values (OD_{600}) were similar, irrespective of the presence of TTM or copper (Fig. 2C). After 8 h of germination, at which point there was formation and emergence of a germ tube in copper-replete spores, the presence of TTM inhibited outgrowth of spores as a function of the increase in TTM concentration (Fig. 2C). In the presence of 200 μM TTM, outgrowing spores were absent, whereas 22.3% and 76.5% less outgrowing spores were detected in medium containing 50 and 100 μM TTM, respectively, as compared to that of copper-replete spores (Fig. 2C, bottom left panel). After 12 h of germination, outgrowing spores led to production of vegetative cells that were calcofluor-free, which represent 62% of the total population (outgrowing spores plus new vegetative daughter cells) in the presence of copper (Fig. 2C). Under conditions of copper starvation, production of calcofluor-free cells decreased by 21%, 42%, and 92% in medium containing 50, 100, and 200 μM TTM, respectively, as compared to that of calcofluor-free cells in medium containing copper (Fig. 2C, bottom right panel). Spores that underwent germination in the presence of 50 μM copper and 200 μM TTM were analyzed by FACS. At the time of outgrowth (8-h time point), the majority of copper-treated spores exhibited a 2C DNA content, whereas most of TTM-treated spores had a 1C DNA content and were blocked at the stage of isotropic swelling (Fig. 2D). Consistently, the FSC/SSC values for these TTM-treated spores were much lower than those of copper-treated spores after 12 h of germination (Fig. 2D), especially with respect to spore/cell internal granularity (SSC). We investigated whether copper-insufficient spores could be relieved of isotropic swelling-like arrest by

transferring the spores to a copper-replete medium. Spores that displayed a germination block were washed and resuspended in a medium containing copper (50 μM), iron (100 μM), zinc (100 μM), nickel (100 μM), manganese (100 μM), or cobalt (100 μM). Results showed that removal of the copper chelator TTM, followed by the addition of exogenous copper, triggered a rescue of spore germination. We noticed that a delay of ~6 h occurred when copper-insufficient spores were rescued by exogenous copper as compared to control spores for which copper was available during the germination program (Fig. 2E). Although a delayed rescue was observed, supplementation with copper restored spore germination including outgrowth and generation of novel calcofluor-free cells. Under copper supplement conditions, pre-treated TTM spores that had been rescued produced calcofluor-free cells with a percentage of 50% with respect to the total population (calcofluor-positive and calcofluor-free cells) as compared to control spores in which case copper was available (78% among total population: calcofluor-positive and calcofluor-free cells) (Fig. 2E, right panel, 16-h time point). Among the metal ions tested (copper, iron, zinc, nickel, manganese, and cobalt), only copper was able to rescue spore germination caused by copper deficiency (Fig. 2E). Taken together, the results showed that copper is required for spore germination. The evidence is based on the observation that copper deficiency leads to germination arrest at the onset of outgrowth and that arrest of spore germination could be rescue by the addition of copper.

Temporal expression profiles of ctr4$^+$, ctr5$^+$, ctr6$^+$, and cuf1$^+$ transcripts during spore germination and outgrowth. In response to copper starvation conditions, proliferating cells that grow mitotically exhibit transcriptional induction of the copper transport genes and their activation requires the copper-dependent transcription factor Cuf1 (20). In contrast, *ctr4*$^+$, *ctr5*$^+$, and *ctr6*$^+$ transcripts are repressed in *cuf1*$^+$ cells in response to copper. Taking into account the fact that copper was required for morphological changes of spores during outgrowth, we examined *ctr4*$^+$, *ctr5*$^+$, and *ctr6*$^+$ transcription profiles during spore germination as a function of time and copper availability. Purified *cuf1*$^+$ and *cuf1Δ* spores were synchronously induced into germination and treated with TTM (50 μM) or $CuSO_4$ (50 μM). Aliquots of cultures were taken after induction of germination and steady-state levels of *ctr4*$^+$, *ctr5*$^+$, *ctr6*$^+$, and *cuf1*$^+$ mRNA were analyzed by RNase protection assays. Results showed that *ctr4*$^+$ and *ctr5*$^+$ mRNA levels were primarily detected in *cuf1*$^+$ spores treated with TTM (Fig. 3).

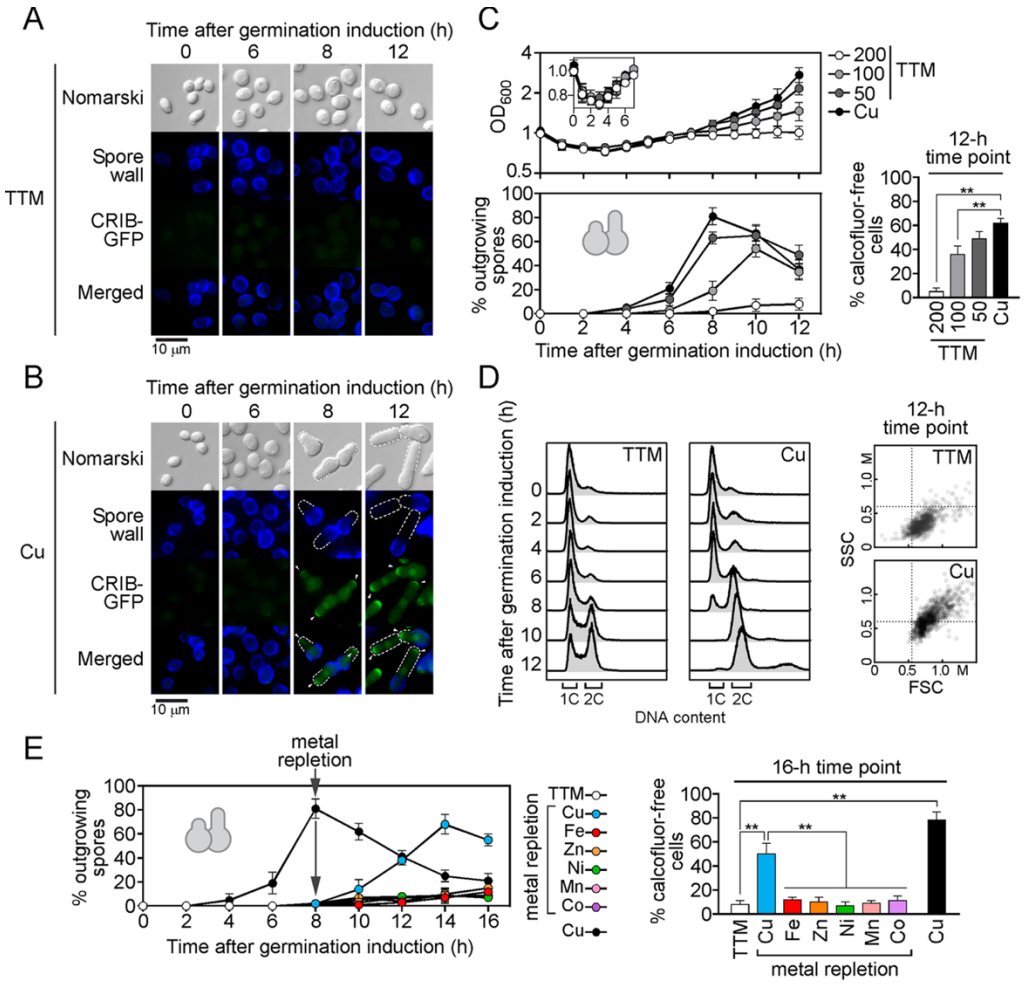

Figure 2. *Copper insufficient germinating spores undergo arrest at outgrowth*. Wild-type spores harboring a *CRIB-GFP* allele were synchronously induced into germination in the presence of TTM (200 μM) (*panel A*) or copper (50 μM) (*panel B*). Shown are three representative stages of spore germination and outgrowth that occurred after 6, 8, and 12 h of induction. The spore wall was stained with calcofluor (*center top*). The daughter cell tip marker CRIB-GFP is shown in green (also indicated with white arrowheads) (*center bottom*). Spore morphology was examined by Nomarski optics (*top*). Merged images of calcofluor and CRIB-GFP are shown at the bottom of each panel. Examples of new daughter cell ends are indicated with white dashed lines. *C*, Total growth was measured at OD_{600} in the presence of copper (50 μM) or three different concentrations of TTM (50, 100, and 200 μM). Inset indicates OD_{600} values up to 7 h post induction of germination (*top*). The percentage of spores undergoing outgrowth (*bottom*) and the percentage of calcofluor-free cells after 12 h of induction of germination were determined under the indicated conditions of incubation (*far right*). *D*, Shown is FACS analysis of spores that underwent synchronous germination in the presence of TTM (200 μM) (*left*) or copper (50 μM) (*right*). Fluorescence intensities corresponding to 1C and 2C DNA content are indicated. At the 12-h time point, dot plots of FSC versus SSC that correspond to spore size (FSC) and spore granularity (SSC) under low (TTM) and copper (50 μM) conditions. *E*, Aliquots of spores used in *panel C* (blocked at outgrowth) were incubated in the presence of exogenous $CuSO_4$ (Cu, 50μM) (*blue*), $FeSO_4$ (Fe, 100μM) (*red*), $ZnSO_4$ (Zn, 100 μM) (*orange*), $NiCl_2$ (Ni, 100 μM) (*green*), $MnCl_2$ (Mn, 100 μM) (*pink*), or $CoCl_2$ (Co, 100 μM) (*violet*). The graph (*left*) depicts the germination profiles of spores. A minimum of 200 spores or calcofluor-free cells were examined every 2 h and under each one of the conditions.

The graph on the *far right* represents the percentage of calcofluor-free cells after 16 h of incubation that included copper supplementation (at the 8-h time point) following a TTM block. Results are shown as the averages +/- S.D. of a minimum of three independent experiments. The asterisks (**) correspond to $p < 0.001$ (paired Student's *t*-test).

Under this low copper condition, *ctr4*$^+$ and *ctr5*$^+$ transcript levels were relatively low within the first 4 h compared to their transcript levels detected 6 and 8 h after induction of germination (3 to 33-fold lower for *ctr4*$^+$ and, 7- to 8-fold lower for *ctr5*$^+$). Maximal levels of *ctr4*$^+$ and *ctr5*$^+$ transcription were observed 6 and 8 h after induction of germination. This was followed by a reduction of *ctr4*$^+$ (6- to 13-fold) and *ctr5*$^+$ (4- to 5-fold) mRNA levels within 10 – 12 h (compared with levels observed after 6 and 8 h of induction of germination). As controls, *ctr4*$^+$ and *ctr5*$^+$ mRNAs were virtually absent in wild-type spores treated with copper (Fig. 3). Similarly, RNA samples prepared from *cuf1Δ* mutant spores showed loss of copper starvation-dependent induction of *ctr4*$^+$ and *ctr5*$^+$ gene expression, indicating that the copper-dependent regulation of *ctr4*$^+$ and *ctr5*$^+$ mRNAs required Cuf1 during germination and outgrowth.

Although transcript levels of *ctr6*$^+$ were detected under all conditions tested, the presence of copper or disruption of Cuf1 (*cuf1Δ*) resulted in reduced *ctr6*$^+$ mRNA levels in comparison with those recorded in the case of wild-type (*cuf1*$^+$) spores incubated under low copper conditions (Fig. 3). Under this latter condition, *ctr6*$^+$ mRNA levels progressively increased between 2 and 10 h after induction of germination. This was followed by a slight reduction of *ctr6*$^+$ mRNA levels within 12 h. Under copper-replete conditions, results showed that steady-state levels of *ctr6*$^+$ transcripts remained low compared with levels observed in the case of spores that had been exposed to TTM (Fig. 3). Under both conditions (TTM and $CuSO_4$), disruption of Cuf1 (*cuf1Δ*) resulted in decreased *ctr6*$^+$ transcript levels in comparison to those observed in copper-starved *cuf1*$^+$ control spores (Fig. 3). In the absence of Cuf1 (*cuf1Δ*), although a low level of *ctr6*$^+$ mRNA was still observed, its expression was not altered by the presence of TTM or copper (Fig. 3).

Steady-state levels of *cuf1*$^+$ transcripts were constitutively present within the first 12 h of induction of germination. Furthermore, *cuf1*$^+$ mRNA levels were expressed to a similar extent under copper-starved and copper-replete conditions (Fig. 3). As a control, the *cuf1*$^+$ mRNA was absent in *cuf1Δ* spores as determined by RNase protection assays (Fig. 3). Taken together, results showed that *ctr4*$^+$ and *ctr5*$^+$ mRNA levels are induced in response to copper starvation in a Cuf1-dependent manner, exhibiting maximal expression during isotropic swelling and outgrowing stages of germination. Furthermore, results indicated that expression of *ctr6*$^+$ transcript requires Cuf1 for its maximal induction under copper-limiting conditions during spore germination.

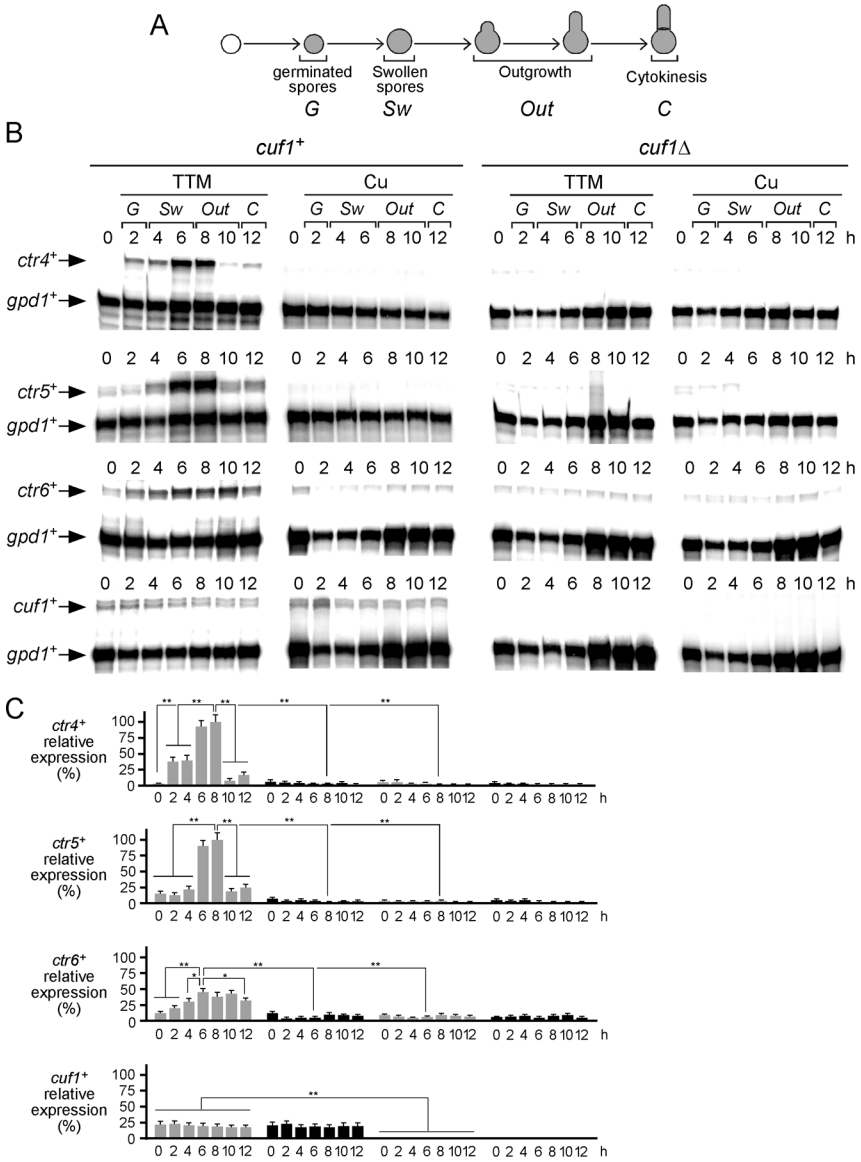

Figure 3. *Expression profiles of ctr4$^+$, ctr5$^+$, ctr6$^+$, and cuf1$^+$ mRNAs during germination and outgrowth*. *A,* Shown is a schematic representation of different steps during germination and outgrowth. *B,* Wild-type (*cuf1$^+$*) and *cuf1Δ* mutant spores were synchronously induced to undergo germination in the presence of TTM (50 μM) or copper (Cu, 50 μM). Total RNA was isolated from culture aliquots taken at the indicated time points. Following RNA isolation, *ctr4$^+$, ctr5$^+$, ctr6$^+$,* and *cuf1$^+$* steady-state mRNA levels were analyzed by RNase protection assays. The zero time point (0 h) refers to the onset of germination induction. *C,* Graphs represent quantification of the results of three independent RNase protection assays, including experiments shown in *panel B*. Values are represented as the averages +/- S.D. The asterisks correspond to $p < 0.001$ (**) and $p < 0.05$ (*) (paired Student's *t*-test).

Copper transport proteins Ctr4, Ctr5 and, to a lesser extent Ctr6, are required for spore outgrowth under conditions of copper starvation. Taking into account the fact that copper ions were required during the spore germination program (Fig. 2), we hypothesized that Ctr4, Ctr5, and Ctr6 could also play important roles in spore germination under low copper conditions. To test this hypothesis, *ctr4Δ*, *ctr5Δ*, *ctr6Δ*, *ctr4Δ ctr6Δ*, and *cuf1Δ* spores were used and results compared to wild-type control spores (Fig. 4, A – F). Purified spores were treated with TTM (50 μM) or $CuSO_4$ (50 μM) immediately after induction of germination. In the case of wild-type spores, loss of spore refractility occurred within 2 h, isotropic swelling between 4 and 6 h, and formation of an outgrowing tip between 8 and 10 h following induction of germination, irrespective of the copper status (Figs 1 and 4, G and H). In the case of *ctr4Δ*, *ctr5Δ*, *ctr4Δ ctr6Δ*, and *cuf1Δ* mutant spores, the progression of germination primarily stopped at the onset of outgrowth, although loss of spore refractility and isotropic swelling steps were still observed under low copper conditions (Fig. 4, B, C, E, F, and G). Expression of the CRIB-GFP reporter produced a fluorescence signal that was visible at the tips of outgrowing wild-type spores after 8 h of induction of germination (Fig. 4A, wild-type). In contrast, there was an absence of CRIB-GFP signal in *ctr4Δ*, *ctr5Δ*, *ctr4Δ ctr6Δ*, and *cuf1Δ* mutant spores after 8 and 12 h of induction of germination in the presence of TTM (Fig. 4, B, C, E, and F). Furthermore, observations of *ctr4Δ*, *ctr5Δ*, *ctr4Δ ctr6Δ*, and *cuf1Δ* mutant spores using Nomarski optics showed that these spores stopped their morphogenesis progression and exhibited an arrest at the isotropic swelling stage (as compared to wild-type spores) (Fig. 4, B, C, E, F, and G). After 12 h of induction of germination, DNA content of *ctr4Δ*, *ctr5Δ*, *ctr4Δ ctr6Δ*, and *cuf1Δ* mutant spores was determined by FACS analysis (Fig. 4, B, C, E, and F). Results showed that 40 to 55% of mutant spores had 1C DNA content, whereas another 45 to 60% had a 2C DNA content. As a control at the 12-h time point, wild-type spores had 2C DNA content (Fig. 4A). Under copper-limiting conditions, these mutant spores failed to enter outgrowth (>98%) (Fig. 4G) and did not produce newborn calcofluor-free cells (Fig. 4I). Germ tube formation defect of these mutants could be corrected by addition of $CuSO_4$ (50 μM) to the growth medium (Fig. 4H). Indeed, under copper-replete conditions, *ctr4Δ*, *ctr5Δ*, *ctr4Δ ctr6Δ*, and *cuf1Δ* mutant spores entered outgrowth with formation of bottle-like shape outgrowing spores in a manner comparable to that found in wild-type spores (Fig. 4H). In the case of *ctr6Δ* mutant spores, the outgrowth defect was present but to a lesser extent than *ctr4/5Δ* and *cuf1Δ* mutants (Fig. 4, D and G). Deletion of *ctr6* lowered the number of outgrowing spores by 17% (8-h time point), 19% (10-h time point), and 4% (12-h time point) as compared to wild-type spores (Fig. 4, D and G). Inactivation of *ctr6* also reduced by 14% the proportion of resulting calcofluor-free cells that were generated and growing away from

spore bodies after 12 h of induction of germination (Fig. 4I). As opposed to *ctr4/5Δ* and *cuf1Δ* mutants, a large proportion of *ctr6Δ* mutant spores had 2C DNA content after 12 h of induction of germination (Fig. 4D). Similarly to *ctr4/5Δ* and *cuf1Δ* mutants, the addition of exogenous copper to the growth medium rescued the outgrowth defect phenotype of *ctr6Δ* mutant spores (Fig. 4H). In summary, deletion of *ctr4Δ*, *ctr5Δ*, and *cuf1Δ* stopped progression of spore germination at out-growth, whereas deletion of *ctr6Δ* only partially interfered with the formation of outgrowing spores.

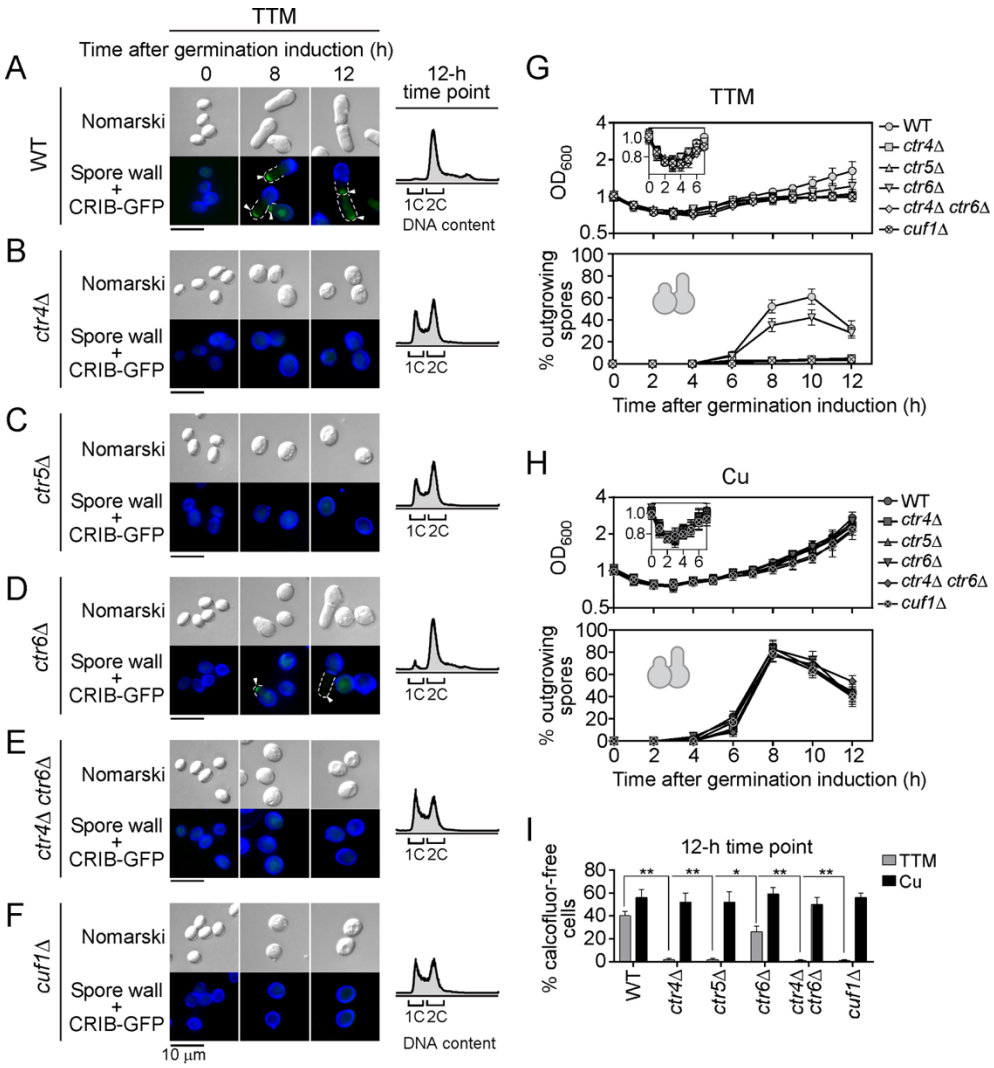

Figure 4. *Effect of the absence of Ctr4, Ctr5, Ctr6 or Cuf1 on the emergence of the germ tube at one side of spores under low copper conditions.* Wild-type (*WT*) spores and spores harboring deletions of the *ctr4*$^+$ (*ctr4Δ*), *ctr5*$^+$ (*ctr5Δ*), *ctr6*$^+$ (*ctr6Δ*), *ctr4*$^+$ *ctr6*$^+$ (*ctr4Δ ctr6Δ*), and *cuf1*$^+$ (*cuf1Δ*) genes were synchronously induced to undergo germination under copper-depleted (50 µM TTM)

and copper-replete (50 μM $CuSO_4$) conditions. *A – F*, Representative microscopic images revealed defective outgrowth of *ctr4Δ*, *ctr5Δ*, *ctr4Δ ctr6Δ*, and *cuf1Δ* spores compared to wild-type (*WT*) spores under copper starvation conditions (TTM). In the case of *ctr6Δ* spores, two populations were observed: spores with and without an outgrowing tip. Although wild-type and all mutant spores possess an integrated *CRIB-GFP* allele, its green fluorescent product was only detected in wild-type and some *ctr6Δ* germinated spores (*panels A and D*). CRIB-GFP (*white arrowheads*) was used as a marker of the new cell side tip of an outgrowing spore. Calcofluor (*blue*) was used to stain the wall of the spore body. Morphology of spores was examined by Nomarski optics. At the 12-h time point, FACS analysis of wild-type and mutant spores is shown next to microscopic images (*far right*). *G – H*, In the case of each indicated strain, graphs depict growth profiles of spores after induction of germination under copper-starved (*panel G*) and copper-replete (*panel H*) conditions. *I*, Shown is the percentage of calcofluor-free cells that were produced after 12 h of induction of germination under conditions of low and high levels of copper. A minimum of 200 spores and germinated cells were examined under each condition. Data are represented as the averages +/- S.D. of three independent experiments. The asterisks correspond to $p < 0.001$ (**) and $p < 0.05$ (*) (paired Student's *t*-test).

Ctr4-GFP and Ctr5-Cherry first co-localize at the spore contour at the onset of outgrowth and then move away from the spore body to occupy the periphery of the nascent cell. Exogenous copper is transported across the plasma membrane by the Ctr4-Ctr5 heteromeric complex in dividing cells that grow mitotically (12,16,21,28). We next sought to determine the location of Ctr4 and Ctr5 during spore germination since steady-state levels of *ctr4*$^{+}$ and *ctr5*$^{+}$ transcripts were poorly expressed in early stages of spore germination. However, Ctr4 and Ctr5 were expressed at higher levels at the end of isotropic swelling and at the onset of outgrowth. The experiments were set by integrating functional *ctr4*$^{+}$*-GFP* and *ctr5*$^{+}$*-Cherry* alleles into *ctr4Δ ctr5Δ* cells. After production and purification of spores, they were synchronously induced to undergo germination in the presence of TTM (50 μM) or $CuSO_4$ (50 μM). Under low Cu conditions, Ctr4-GFP and Ctr5-Cherry fluorescent proteins were first co-detected after 4 to 6 h of induction of germination (Fig. 5A). Their initial intracellular detection revealed the appearance of cytoplasmic vesicular structures within the spore (Fig. 5A). At the onset of outgrowth (8-h time point), Ctr4-GFP and Ctr5-Cherry fluorescent proteins co-localized at the spore contour, except for a short peripheral region that may correspond to the polar cap where there is a local rupture of the OSW (Fig. 5A). After 9 h of induction of germination, green and red fluorescence signals associated with Ctr4-GFP and Ctr5-Cherry, respectively, were primarily seen in a middle peripheral region of the outgrowing elongated spore (Fig. 5A). Ctr4-GFP and Ctr5-Cherry fluorescent signals progressively displayed local shifting toward the germ projection that emerged at one side of the enlarged spore (10-h time point). At 12 h, Ctr4-GFP and Ctr5-Cherry fluorescent signals were mainly restricted to the periphery of the new

daughter cells (Fig. 5A). Consistent with the clear interdependence between Ctr4 and Ctr5, Ctr4-GFP- and Ctr5-Cherry-associated fluorescent signals co-localized during spore germination.

To further detect the presence of Ctr4-GFP and Ctr5-Cherry proteins, aliquots of TTM-treated spore cultures were taken at various time points after induction of germination and steady-state levels of Ctr4-GFP and Ctr5-Cherry were analyzed by Western blots. Results showed that steady-state protein levels of Ctr4-GFP followed those of Ctr5-Cherry as they were present during the same stages of spore germination (Fig. 5B). The two approaches (fluorescence microscopy and immunoblotting) indicated the absence of both proteins during the first 2 h of spore germination, whereas their presence was detected between 4 and 12 h (Fig. 5, A and B). Because transcription of the *ctr4*$^{+}$ and *ctr5*$^{+}$ genes were repressed under copper-replete conditions (Fig. 3), results showed that Ctr4-GFP and Ctr5-Cherry steady-state levels (expressed under their native promoters) were undetectable by immunoblot assays in copper-treated spores, irrespective of the indicated time point after induction of germination (Fig. 5C). Taken together, the results revealed that at the end of spore germination, the plasma membrane of a new daughter cell is the preferred location of Ctr4 and Ctr5 where their presence is highly enriched as observed by fluorescence microscopy.

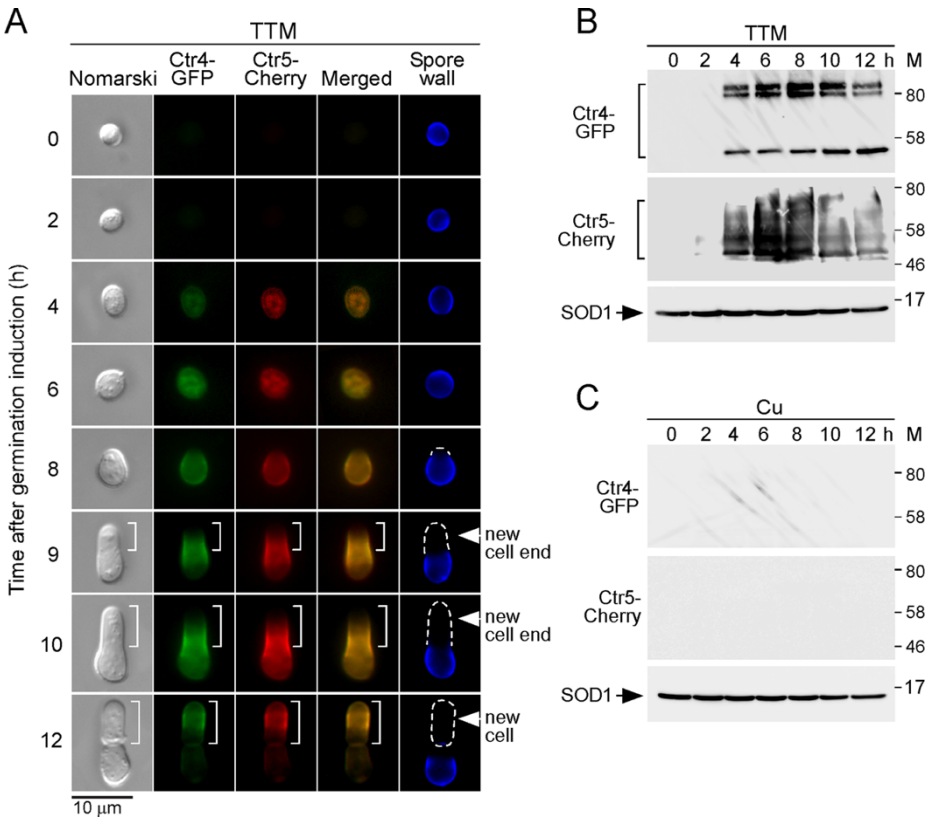

Figure 5. *Colocalization of Ctr4-GFP and Ctr5-Cherry during spore germination and outgrowth. A*, *ctr4Δ ctr5Δ* spores harboring functional *ctr4*$^{+}$*-GFP* and *ctr5*$^{+}$*-Cherry* alleles were synchronously induced to undergo germination. Once induced, spores were allowed to germinate in the presence of TTM (50 μM). Fluorescence signals of Ctr4-GFP and Ctr5-Cherry were observed at different stages of germination (center left). Merged images of Ctr4-GFP and Ctr5-Cherry are shown in the center right panels. Nomarski optics (far left) were used to examine spore or cell morphology. Calcofluor staining was performed to visualize the spore wall (far right). White brackets, dashed lines and arrowheads indicate the formation of a new cell tip that subsequently produced a new cell. *B – C*, At the indicated time points, lysates from aliquots of copper-starved or copper-replete spores were analyzed by immunoblotting using anti-GFP, anti-Cherry, and anti-SOD1 antibodies. Positions of the molecular weight standards (*M*) are indicated to the right in panels *B* and *C*.

Ctr6 localizes in the vacuole membranes of swollen spores and spores that undergo outgrowth. In the case of Ctr6, it is known that it localizes to the membrane of vacuoles in cells proliferating in mitosis under copper-limiting conditions (22,23). A similar localization was observed when a functional Ctr6-HA$_4$ fusion protein was expressed in *ctr6Δ* cells grown in malt medium after 1 day of incubation in the presence of TTM (50 μM) (Fig. 6A). As previously reported (22), Ctr6-HA$_4$ underwent an intracellular re-location and co-localized with the forespore membrane after 2 and 3 days (malt medium) that corresponded to late meiosis (Fig. 6A). Once spores were formed and released from the ascus, Ctr6-HA$_4$-associated fluorescence progressively disappeared after 4 days in malt medium (Fig. 6A). Spores were then purified and cultured under conditions to induce synchronous germination. Under low copper conditions, the Ctr6-HA$_4$ fluorescent signal was barely detectable during the first 2 h of germination which corresponded to breaking of spore dormancy. In contrast, during isotropic swelling, Ctr6-HA$_4$-associated fluorescence progressively appeared in the vacuolar membranes of spores, especially after 6 h of induction of germination (Fig. 6B). Swollen spores were also incubated in the presence of the vacuole-staining dye FM4-64 (Fig. 6C). Results showed that Ctr6-HA$_4$ and FM4-64 exhibited similar subcellular location patterns within the spores, especially after 6 h of induction of germination (Fig. 6, B and C). In the case of outgrowing spores, results showed that vacuoles were enriched in the spore body, which was the portion stained with calcofluor (Fig. 6C). Consistently, results showed that Ctr6-HA$_4$-associated fluorescence was also enriched in the spore body of outgrowing spores after 10 – 12 h of induction of germination (Fig. 6B). Aliquots of single-spore cultures were analyzed at various time points after induction of germination in the presence of TTM (50 μM) or $CuSO_4$ (50 μM). Immunoblotting analysis showed that Ctr6-HA$_4$ was detected at each time point under copper-starved conditions (Fig. 6D). Steady-state levels of Ctr6-HA$_4$ increased after 6, 8, and 10 h of induction of germination and were ex-

pressed to a lesser degree after 12 h (Fig. 6D). Immunoblotting analysis showed that protein extracts from copper-treated swelling and outgrowing spores were negative for the presence of Ctr6-HA_4 (Fig. 6E). Taken together, the results revealed that Ctr6-HA_4 localizes in the vacuole membranes of spores that had undergone germination and that it is enriched in the spore body following production of a newborn daughter cell.

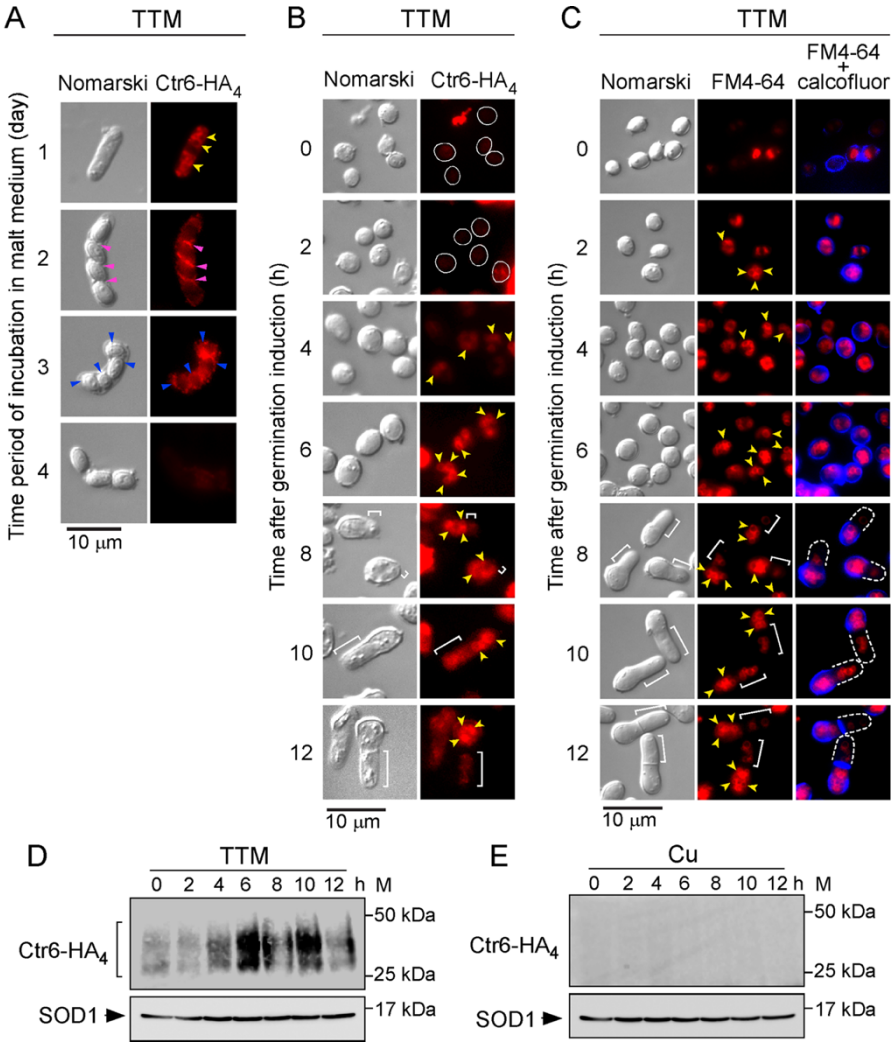

Figure 6. *Subcellular localization of Ctr6-HA_4 during spore germination and outgrowth. A*, a h^{90} *ctr6Δ* strain expressing a *ctr6*$^{+}$*-HA_4* allele was incubated on ME media under low copper conditions (50 μM TTM). Four representative stages of the sporulation program that occurred within 4 days are shown. Cells, asci, and spores were analyzed by indirect immunofluorescence microscopy to assess subcellular localization of Ctr6-HA_4. Yellow arrowheads indicate examples of vacuole membranes in which Ctr6-HA_4 was found (day 1). During the forespore membrane formation (violet arrowheads) (day 2), Ctr6-HA_4 is known to become resident of the spore membrane (blue arrowheads) (day 3). Ctr6-HA_4-associated fluorescence disappeared from the surface of spores that had been released from asci after 4 days of meiotic induction. *B*, Purified *ctr6Δ* mutant spores

expressing Ctr6-HA_4 were induced into germination in the presence of TTM (50 μM) or copper (50 μM) for the indicated time points. Fixed cells were observed by indirect immunofluorescence (Ctr6-HA_4; *right*) and Normarski optics (*left*). White circles indicate cells observed within 2 h after induction of germination. After the 4-h time point, Ctr6-HA_4-associated fluorescent signal was more prominent and was detected in the vacuole membranes (yellow arrowheads). White brackets indicate examples of new cell tips of outgrowing spores. *C*, FM4-64 (middle) staining was visualized by fluorescence microscopy as a marker of vacuolar membranes (yellow arrowheads). Double staining (FM4-64 plus calcofluor) was performed to identify spore walls (blue). After the 8-h time point, calcofluor-associated fluorescent signal (blue) was found at the bottom part of the bottle-like shape of spores that had undergone outgrowth. *D – E*, At the indicated time points, total-extracts from aliquots of spores used in *panel B* under low and high (not shown by fluorescence microscopy due to the absence of fluorescent signal) copper conditions were analyzed by immunoblotting using anti-HA and anti-SOD1 antibodies. Positions of the molecular weight standards (*M*) are indicated to the right in panels *D* and *E*.

Ctr4 and Ctr6 are required for the production of a fully active SOD1 during spore germination and outgrowth. Previous studies have shown that Ctr4 and Ctr6 transporters are required to produce a fully active copper-dependent SOD1 enzyme in cells undergoing vegetative growth or meiosis for production of spores (22,23). To determine whether Ctr4 or Ctr6 was needed to provide copper to SOD1 during spore germination, purified h^{90} wild-type (*ctr4*$^+$ *ctr6*$^+$), *ctr4Δ*, *ctr6Δ*, and *ctr4Δ ctr6Δ* spores were synchronously induced to undergo germination in the presence of TTM (50 μM) or $CuSO_4$ (50 μM). SOD activity was assayed from spore lysates using a standard in-gel assay with nitro blue tetrazolium staining (22). In the case of wild-type spores, results showed that levels of SOD1 activity increased as a function of germination time to reach maximal activity within 12 h under both copper-depleted and copper-replete conditions (Fig. 7). During the first 6 h of induction of germination (isotropic swelling), copper-starved *ctr4Δ* mutant spores exhibited a weak SOD1 activity comparable to that of wild-type spores (Fig. 7). At 8 h and later time points, results showed that SOD1 activity of *ctr4Δ* spores was 5.3- (8 h), 3.3- (10 h), and 4.3-fold (12 h) lower than that of wild-type spores (Fig. 7). In the case of copper-starved *ctr6Δ* spores, SOD1 activity was 3.5-, 5.3-, 6.7-, and 2.7-fold lower than that of wild-type spores after 2, 4, 6, and 8 h of induction of germination, respectively (Fig. 7). At 10- and 12-h time points, *ctr6Δ* spores exhibited SOD1 activity levels comparable to those of wild-type spores. In the case of *ctr4Δ ctr6Δ* double mutant spores, results showed an absence of measurable SOD1 activity under low copper conditions, highlighting the fact that both Ctr4 and Ctr6 were required to provide copper to SOD1 during spore germination and outgrowth (Fig. 7). To assess expression of SOD1 in wild-type and mutant spores, whole spore extracts were analyzed by Western blots at the indicated time points during germination and outgrowth (Fig. 7). Results showed that SOD1 was present in wild-type and mutant spores,

revealing that the decrease or lack of activity was not due to the absence of SOD1 expression. As shown in previous studies and reported here, SOD1 activity could be rescued by addition of exogenous $CuSO_4$ concentrations (50 μM) to the spores (Fig. 7). This copper-remedial phenotype was likely due to the fact that copper ions were assimilated by way of a putative low-affinity copper transport system, therefore circumventing requirements for high-affinity Ctr copper transporters. Taken together, the results revealed a distinct requirement of Ctr4 and Ctr6 for activation of SOD1 under copper starvation during spore germination. Although Ctr6 plays an important role during early stages of germination such as isotropic swelling, Ctr4 is needed to ensure maximal SOD1 activity during outgrowth and cytokinesis.

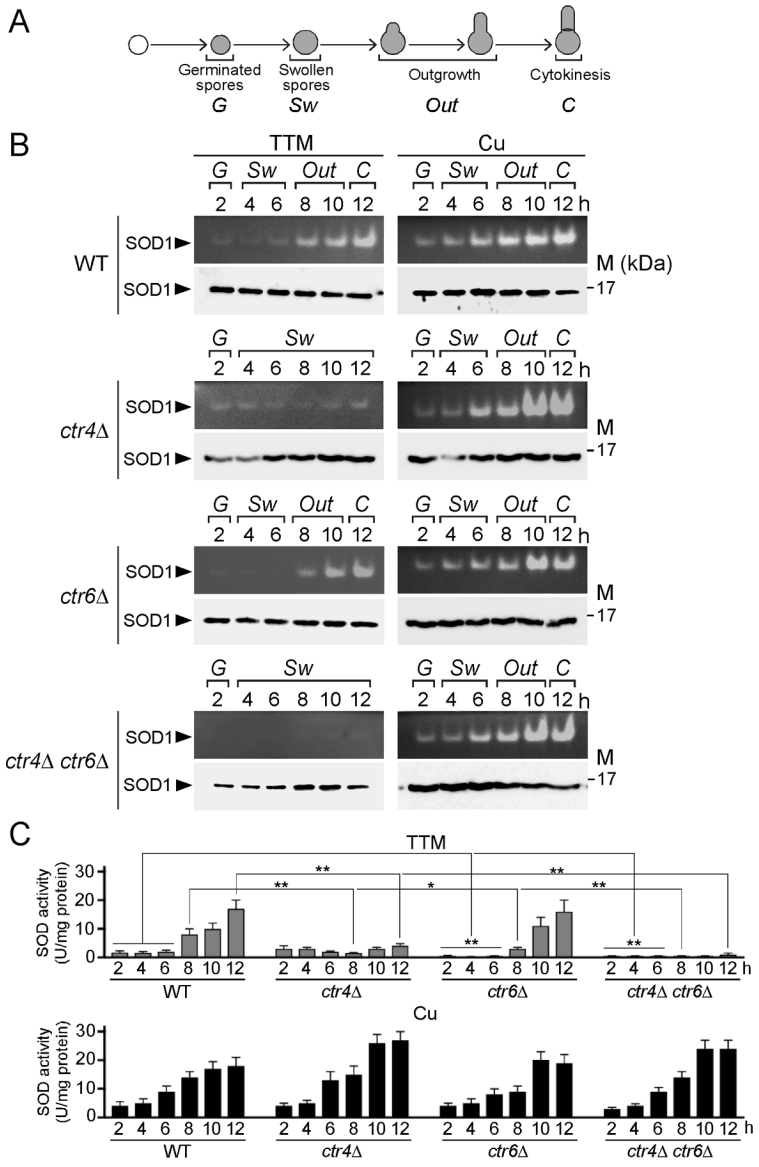

Figure 7. *Effect of ctr4Δ, ctr6Δ, and ctr4Δ ctr6Δ deletions on SOD1 activity during germination and outgrowth. A*, Shown is a schematic representation of different steps during germination and outgrowth. *B,* Wild-type (*WT*), *ctr4Δ*, *ctr6Δ*, and *ctr4Δ ctr6Δ* spores were synchronously induced to undergo germination under copper-starved (50 μM TTM) and copper-replete (50 μM $CuSO_4$) conditions. At the indicated time points, total extracts from aliquots of cultures were analyzed for SOD1 activity using an in-gel assay (*upper panels*). Protein extracts were analyzed for steady-state protein levels of SOD1 by immunoblotting using an anti-SOD1 antibody (*lower panels*). *M*, position of the molecular weight reference band (17 kDa) is indicated to the right in panel *B*. *C*, Spectrophotometric determination of SOD activity was also performed from these wild-type and mutant spores using a cytochrome c/xanthine oxidase method. Values are represented as the averages +/- S.D. of three independent experiments. The asterisks correspond to $p < 0.001$ (**) and $p < 0.05$ (*) (paired Student's *t*-test).

Labile copper pools primarily remain in the spore body during outgrowth. The physiological contribution of copper and cuproproteins to spore germination led us to investigate the status of labile copper pools at different stages of the germination process. Wild-type *ctr4*$^{+}$ *ctr6*$^{+}$ and *ctr4Δ*, *ctr6Δ*, and *ctr4Δ ctr6Δ* mutant spores were used in these experiments. We utilized the fluorescent copper-binding probe CNIR4 to track exchangeable copper pools in living cells or spores. CNIR4 is a second-generation silicon rhodamine analog of the silicon rhodol CSR1 (29). As chemical control analogs, Ctrl-CNIR4 and Ctrl-CNIR4-S2 were used under the same conditions as CNIR4. These control probes, in which metal-interacting sulfur atoms have been partially or completely replaced by isosteric carbon atoms, do not bind copper but have the same dye scaffold as CNIR4 and thus can be used to help disentangle metal- and dye-dependent signals (29,30). We first tested CNIR4 and its control analogs using *ctr4*$^{+}$ *ctr6*$^{+}$ cells that were proliferating in mitosis. Cells were cultured to mid-logarithmic phase and then grown in the presence of $CuSO_4$ (5 μM) for 1 h. The treatment ensured intracellular copper sequestration by the cells. After washings, cells were incubated in low copper (~0.16 nM $CuSO_4$; a concentration which is 100 times lower than standard culture conditions)-containing EMM medium in the presence of 5 μM CNIR4, Ctrl-CNIR4, Ctrl-CNIR4-S2 or were left untreated (no probe) for 30 min. Results showed that the cells displayed fluorescent CNIR4-copper complexes that were distributed throughout the cells with a preferred location to the yeast secretory pathway, including the endoplasmic reticulum (Fig. 8A). As expected, there was an absence of fluorescence in the case of Ctrl-CNIR4 and Ctrl-CNIR4-S2 analogs (Fig. 8A). *ctr4*$^{+}$ *ctr6*$^{+}$ *ish1Δ* + *ish1*$^{+}$*-Cherry* cells were grown under similar conditions in the absence of CNIR4, Ctrl-CNIR4, or Ctrl-CNIR4-S2 (Fig. 8B, *top center*). Cellular location of the Ish1-GFP fluorescent signal was detected as a nuclear envelope/endoplasmic reticulum resident

marker (31). In the presence of CNIR4, results showed that a fraction of CNIR4-copper-associated fluorescence appeared in a common perinuclear region where Ish1-GFP was detected (Fig. 8B).

To assess copper distribution during spore germination, wild-type *ctr4*$^{+}$ *ctr6*$^{+}$ and *ctr4Δ*, *ctr6Δ*, and *ctr4Δ ctr6Δ* mutant strains were plated on ME media that contained $CuSO_4$ (5 μM). After sporulation and purification, spores from each strain were synchronized to initiate and proceed through the germination program. At the indicated time points, spores were harvested and resuspended in the presence of CNIR4 (5 μM) for 30 min and then analyzed by direct fluorescence microscopy. After 6 h of germination, CNIR4-copper complexes generated a fluorescent signal that was dispersed within the spores, irrespective of the presence or absence of Ctr4, Ctr6 or both. In the case of *ctr4*$^{+}$ *ctr6*$^{+}$ and *ctr6Δ* spores undergoing outgrowth, CNIR4-copper-associated fluorescence was primarily observed within the old spore body after 8, 10, and 12 h of germination induction (Fig 8C). In contrast, the CNIR4-copper fluorescent signal was weak at the new germ projection end in comparison with that of the spore body. In the case of *ctr4Δ* and *ctr4Δ ctr6Δ* spores, there were no changes in the pattern of fluorescence signal of CNIR4-copper complexes after 8, 10 and 12 h of induction of germination in comparison to that observed after 6 h, since spore outgrowth was blocked in these mutants (Fig. 8C). Taken together, these results suggested the existence of a mechanism whereby labile copper pools are preferentially retained in the spore body during outgrowth.

Cuproprotein SOD1 is required for spore outgrowth. Based on the fact that copper and copper transporters were required for spore outgrowth, we hypothesized that a copper-dependent enzyme may be necessary to ensure spore outgrowth during germination. Given that previous studies had suggested that the loss of copper-dependent SOD1 activity negatively affected fungal spore germination (32-34), we tested the outcome of the absence of SOD1 on the germination and outgrowth of spores. We used *sod1Δ* cells carrying an integrated empty vector or expressing either a re-integrated wild-type *sod1*$^{+}$ or *sod1H64A* mutant allele and compared the behavior to *sod1*$^{+}$ control cells. When these strains were proliferating in mitosis, wild-type (*sod1*$^{+}$) cells exhibited high levels of SOD1 activity (Fig. 9A). In contrast, there was no detectable SOD1 activity in *sod1Δ* null cells harboring an empty plasmid or expressing the *sod1H64A* mutant allele which was expected to alter both structural and catalytic properties of the enzyme (35,36) (Fig. 9A).

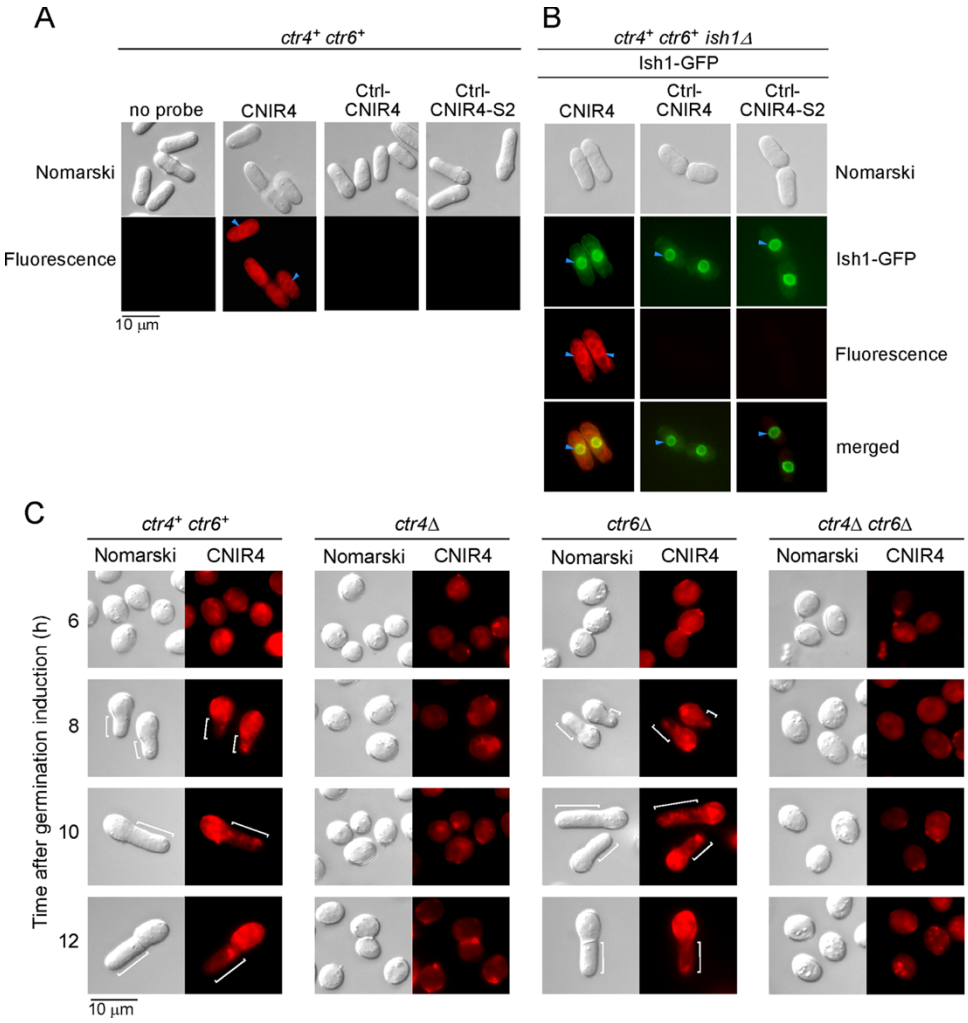

Figure 8. *Intracellular copper distribution during spore germination and outgrowth*. *A – B*, Live cell copper imaging with the fluorescent copper-binding probe CNIR4 (5 μM) in *ctr4*$^{+}$ *ctr6*$^{+}$ cells (*panel A*) or *ctr4*$^{+}$ *ctr6*$^{+}$ *ish1Δ* cells expressing Ish1-GFP (*panel B*) as a marker of the nuclear envelope/endoplasmic reticulum secretory network. Cells proliferating in mitosis were first incubated in the presence of copper (5 μM) and then transferred and analyzed in a low copper-containing media. Ctrl-CNIR4 and Ctrl-CNIR4-S2 are control analogs that cannot bind to copper due to the fact that metal-interacting sulfur atoms had been replaced by isosteric carbon atoms. Nomarski microscopy was used to examine cell morphology (*upper panels*). Fluorescent CNIR4-Cu complexes were detected with a transmission window at 640 nm (*red*) (*fluorescence*). The merged images are shown in the bottom right (*panel B*). *C*, Live cell copper imaging with CNIR4 (5 μM) after 6, 8, 10, and 12 h of induction of germination in *ctr4*$^{+}$ *ctr6*$^{+}$, *ctr4Δ*, *ctr6Δ*, and *ctr4Δ ctr6Δ* cells. White brackets indicate the new cell tips during outgrowth.

In *sod1Δ* mutant strain, the loss of SOD1 activity was rescued to ~50% of the activity of control parental strain by returning a wild-type copy of the *sod1*$^{+}$ gene expressed from an integrated plasmid (Fig. 9A). To ascertain that SOD1 and its H64A mutant version were expressed in *sod1Δ* cells,

total protein extracts from transformed cells were analyzed by Western blots. Results showed that SOD1 and the H64A mutant were produced in *sod1Δ* cells, indicating that the absence of SOD1 activity in *H64A* mutant cells was not due to the lack of SOD1-H64A expression (Fig. 9A).

Each strain was cultured on ME medium for 4 days and spore production was monitored. We observed that during the procedure of spore isolation and purification, *sod1Δ* mutant cells that harbored an empty vector or that expressed the *sod1H64A* allele exhibited dramatic decreased levels of spore production in comparison to wild-type control cells or *sod1Δ* cells expressing an integrated *sod1*$^{+}$ gene (Fig. 9B). Results showed that the two strains that lacked a functional SOD1 produced almost two orders of magnitude less spores, which corresponded to 99.7% (empty vector) and 99.6% (SOD1H64A) less spores than those of cells expressing SOD1. However, there was a sufficient number of spores to allow their isolation and purification from each strain. Purified spores containing the *CRIB-GFP* allele were induced to synchronous germination and were examined at the indicated time points (Fig. 9C). Results showed that after 8 h of induction of germination, a germ tube emerged in spores expressing active SOD1. In contrast, there was no emergence and elongation of a germ tube in spores that were defective in SOD1 activity. The CRIB-GFP reporter was observed at the outgrowing tips of wild-type *sod1*$^{+}$ spores, whereas CRIB-GFP did not show formation of outgrowing polar caps in *sod1Δ* or *sod1H64A* mutants (Fig. 9C). Results further showed that the breaking of dormancy occurred in both wild-type (*sod1*$^{+}$) and mutant (*sod1Δ* or *sod1H64A*) spores since we detected the loss of refractility (phase-contrast microscope) and a decrease in optical absorbance of spore suspensions after 2 h of induction of germination (Fig. 9D, inset). In contrast, spore outgrowth and production of new calcofluor-free cells were exclusively seen in spores that were competent for SOD1 activity (Fig. 9, D and E). Taken together, these results indicated that deletion or inactivation of SOD1 leads to a defect in spore outgrowth, blocking the production of new daughter cells from the mother spore.

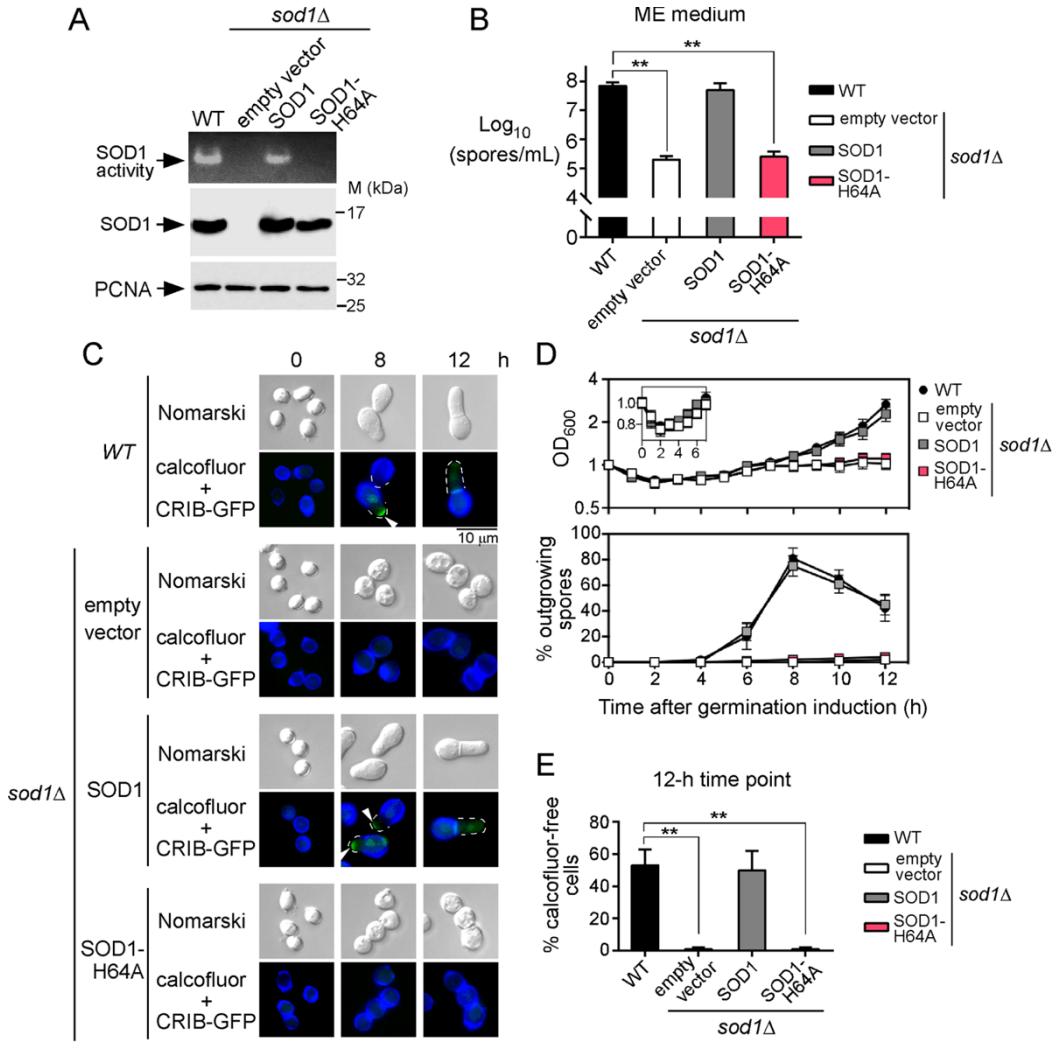

Figure 9. *An active SOD1 is required to undergo spore outgrowth*. *A*, Cell extracts were prepared from mitotically proliferating strains and analyzed for SOD1 activity using an in-gel assay. A *sod1Δ* mutant strain was transformed with an empty vector or a plasmid encoding the *sod1*$^{+}$ or *sod1*$^{+}$*H64A* mutant allele. The wild-type (WT) strain was used as a control. Protein extracts prepared from these strains were analyzed for steady-state levels of SOD1 by immunoblotting using anti-SOD1 and anti-PCNA antibodies. *B*, Production of spores was determined from the same strains of *panel A* after incubation on ME medium for four days. *C*, *h*^{90} *sod1Δ* mutant cells containing a *CRIB-GFP* allele were transformed with an empty vector and plasmid pJK*sod1*$^{+}$ or plasmid pJK*sod1H64A*. After sporulation, dormant spores were purified and synchronously induced to germinate. Wild-type (WT) spores were used as a germination control. Three representative stages of the germination and outgrowth that occurred at the 0-time point and after 8 and 12 h of induction are shown. Calcofluor (blue) was used as a marker to visualize the spore wall. Nomarski optics (*top*) was used to monitor spore morphology. *D*, Total growth was measured at OD_{600} as a function of time after induction of germination. Inset indicates measurements at OD_{600} for the first 7 h of spore germination. The percentage of spores undergoing outgrowth were determined as a function of time after induction of germination. *E*, In the case of each indicated strain, the graph represents the percentage of calcofluor-free cells (new vegetative cells) that were produced after 12 h of induction of germination. A minimum of 200 spores and germinated cells were examined in

the case of each condition. Data are represented as the averages +/- S.D. of three independent experiments. The asterisks correspond to $p < 0.001$ (**) (paired Student's *t*-test).

DISCUSSION

Spores are thought to be infectious particles for many pathogenic organisms, including bacteria, fungi, and protozoa (37,38). Spores are highly resistant to harsh conditions under which vegetative cells lose their viability. Spores are adapted to resist environmental stress and for efficient dispersal through airflow or fluids (39). When conditions are favorable, spores undergo a specialized program called germination. This process requires copper since copper-insufficient spores proceeded through the initial phases of germination until they reached outgrowth and then they stopped their differentiation (Fig. 2). The observation that copper can be a limiting factor for complete and normal progression of fungal spore germination suggests that copper acquisition may depend of specialized transport proteins to deliver copper to critical copper-dependent enzymes essential to germination.

This situation is reminiscent of that found in the fungal plant pathogen *Colletotrichum gloeosporioides* in which case copper is necessary for pathogenic spore germination (32). In *C. gloeosporioides*, CgCtr2 is a protein of the Ctr family that localizes to the membrane of vacuoles. CgCtr2 is involved in intracellular delivery of copper to copper-requiring cytosolic enzymes, including SOD1 (32). *Cgctr2* mutant cells consistently display reduced SOD1 activity and reduced spore germination rates (32). In the present study, results showed that under low copper conditions, spores lacking the vacuolar membrane copper transporter Ctr6 (*ctr6Δ*) displayed less SOD1 activity compared to that of wild-type spores, especially during the first 8 h after induction of germination. Furthermore, the percentage of calcofluor-free cells that were produced by *ctr6Δ* mother spores were 35% lower than that of wild-type spores. This analogy between the two yeast models reinforces the notion that spore germination is a developmental process that requires mobilization of intravacuolar stores of copper.

An additional intriguing observation is the fact that results showed a preferential retention of vacuoles and Ctr6 in the spore body during emergence and elongation of the germ tube. The fact that vacuoles are known to play a role as copper storage compartment (24,25,40-42), this may favor a reserve of copper within the mother spore. Consistent with this possibility, experiments using the fluorescent CNIR4 copper probe revealed a preferential accumulation of labile copper pools in the spore body as compared to the germ tube. Before losing its OSW, a mother spore could produce three consecutive and distinct germ tubes that subsequently results in three novel daughter cells (5).

Because of these three rounds of outgrowth, it is presumed that the mother spore contains high levels of micronutrients such as copper to fulfill the demand of three consecutive formations of germ tubes. Concerning the preferential retention of vacuoles in the spore body, one possible explanation is that autophagy would be more active in this area where spore wall un-coating occurs to resume mitotic cell growth. The process of spore development may implicate delivery of cellular materials to the vacuole for degradation. In contrast, a weak autophagic activity is predicted during the formation of a germ tube in which *de novo* protein and organelle biogenesis occurs to produce a novel daughter cell.

Consistent with an asymmetric copper distribution between mother spore and germ tube, results showed that Ctr4 and Ctr5 were preferentially expressed at the germ tube periphery in comparison to that of the spore body after 12 h of induction of germination. Given the fact that labile copper pools are lower in the germ projection, the asymmetric enrichment of Ctr4 and Ctr5 at the cell-surface of the germ tube could compensate and contribute to mediate copper uptake in this new cellular portion. Furthermore, the preferential germ tube localization of Ctr4 and Ctr5 may contribute to save labile copper ions that are present in the spore body. Elucidating the molecular nature of this asymmetric Ctr4 and Ctr5 distribution between the spore body and a germ tube is an interesting challenge for future studies.

Analyses of expression profiles of *ctr4*$^+$ and *ctr5*$^+$ have shown that these two genes are co-expressed in response to low-copper conditions during the mitotic cell cycle and during the early stages of meiosis (16,22). In both cell-cycle programs, expression of *ctr4*$^+$ and *ctr5*$^+$ requires the copper-responsive transcription factor Cuf1 (16,20,22). In the case of spores undergoing a transition from cellular dormancy to proliferation, expression profiles of *ctr4*$^+$ and *ctr5*$^+$ showed that the two genes were still co-expressed, reaching a maximum 6 – 8 h after induction of germination. At this middle germination phase, spores entered outgrowth that was followed by an extension process of a single germ tube that hatches out the OSW. As observed in the case of mitotic and meiotic cells, expression of *ctr4*$^+$ and *ctr5*$^+$ during spore germination was copper starvation- and Cuf1-dependent. Although copper-regulated gene expression profiling during spore germination has not been characterized in other fungal species, global gene expression patterns in *S. cerevisiae* has revealed that a response to nutrients other than glucose occurs during the second phase of germination (8). This second phase is known to occur after breaking of spore dormancy and is accompanied by loss of spore refractility. Therefore, based on the general transcription program of spore germination in *S. cerevisiae* (8,43), the highest expression levels of *ctr4*$^+$ and *ctr5*$^+$ appear to be consistent with a timely response that occurs after the first phase of germination, especially in the context of the onset and promotion of spore outgrowth.

In the case of *cuf1*$^+$, its expression pattern differed from that of *ctr4*$^+$ and *ctr5*$^+$. The *cuf1*$^+$ gene exhibited a constitutive transcription that was independent of developmental stage or copper availability during spore germination. The transcription of *ctr6*$^+$ was detected in all stages of spore germination and was slightly increased after 6, 8 and 10 h of induction of germination, which corresponds to the period where *ctr4*$^+$ and *ctr5*$^+$ mRNA levels were highly expressed (except for the 10-h time point). Deletion of *cuf1*$^+$ (*cuf1Δ*) resulted to a significant decrease of *ctr6*$^+$ mRNA levels under low copper conditions. However, its expression was not completely abolished and remained detectable throughout the spore germination process under both low and high copper conditions. On the basis of these observations, *ctr6*$^+$ expression is predicted to require at least an additional transcriptional regulator to ensure the continuous presence of Ctr6 during the developmental program. This observation was reminiscent of cells undergoing meiosis in which case *ctr6*$^+$ expression relies on Cuf1 and the meiosis-specific transcription factor Mei4. Under conditions whereby Cuf1 is inactive, Mei4 ensures the expression of Ctr6 during the meiotic divisions and the process of spore formation, especially under basal and copper-replete conditions (22). Due to the fact that Mei4 is a meiosis-specific regulator that is required for expression of several middle-phase genes (44), it is unlikely that Mei4 co-regulates the timely expression of *ctr6*$^+$ during spore germination. In *S. cerevisiae*, spore germination is driven by a gene expression program during which several genes are induced or repressed as a function of the developmental path (8,43). Although such transcriptional regulatory network is still awaiting characterization in fission yeast, it is possible that one (or more) transcriptional regulator involved in the control of germination is also required for the expression of *ctr6*$^+$ gene.

Previous studies have shown that *S. pombe* cells lacking Ctr4 and Ctr6 (*ctr4Δ ctr6Δ*) are devoid of measurable SOD1 activity under copper-limiting conditions. This phenotype has been observed in cells proliferating in mitosis as well as in meiotic and sporulating cells (22,23). When *ctr4Δ ctr6Δ* double mutant spores were induced to undergo germination under low copper conditions, SOD1 activity was undetectable. Furthermore, *ctr4Δ ctr6Δ* spores exhibited a developmental block at the onset of outgrowth. Based on these phenotypic observations, we sought to further examine whether *sod1Δ* mutant spores or spores expressing a catalytically inactive mutant form of SOD1 (SOD1H64A) underwent a block of spore germination. Results showed an arrest of spore germination at the onset of outgrowth, suggesting a role for SOD1 in the formation or maintenance of the germ tube. In fungal species, spore outgrowth involves the establishment of a polarized growth axis that is visualized by a tip extension. After hatching out the OSW, a polar cap serves as a platform to foster local membrane addition and cell-wall remodeling that are needed for polar growth. In filamentous fungi, it is generally accepted that polarized growth by tip extension must

exhibit apical dominance whereby the growing tip is dominant, suppressing the formation of other tips in its vicinity. One contributing factor of the enforcement of apical dominance is the localized accumulation of reactive oxygen species (ROS) in the apical region of polarized cells. According to previous studies, ROS are produced by NADPH oxidase-like proteins or related flavoproteins (45,46). In *A. nidulans*, ROS accumulation is detected using nitro blue tetrazolium (NBT). When NBT is reduced by superoxide ions, it forms a readily detectable blue-purple formazan precipitate. In the case of *A. nidulans* spores that undergo germination and formation of a germ tube, NBT stains primarily the tip of the germ tube 12 h after germination induction (45). Discrete superoxide ions accumulation at the tip of the germ tube suggests the presence of active SOD1 to protect the sequential development of the germ tube against oxidative insults, including membrane damage due to lipid peroxidation. Assuming that an analogous situation occurs to establish a polarized growth axis for formation of germ tubes in *S. pombe*, this possibility could largely explain the reason why SOD1 activity is required to ensure protection against ROS accumulation at the growing tips of germ tubes during apical dominance.

EXPERIMENTAL PROCEDURES

Strains, media, sporulation and spore purification. Genotypes of *S. pombe* strains used in this study are described in Table 1. Standard yeast genetic methods were used for growth, mating, and sporulation of cells (1). Untransformed strains were cultured on yeast extract medium (YES) that was supplemented with 225 mg/l of adenine, histidine, leucine, uracil and lysine. Cells transformed with gene-swap knock-out or knock-in cassettes were selected on YES medium supplemented with the geneticin antibiotic (G418, 200 μg/ml) (Sigma-Aldrich). When plasmid integration was required, *S. pombe* h^{90} cells were cultured in synthetic dextrose minimal (SD) medium containing bacto-yeast nitrogen base (0.67%), dextrose (2%), and 225 mg/l of adenine, uracil and lysine. Leucine was omitted in SD medium to allow selection and maintenance of the integrated DNA fragment into the yeast genome (47).

Table 1. *S. pombe* strains used in this study.

Strain	Genotype	source or refererence
FY12806	*h^{90} ura4-Δ18 ade6-M210 leu1-32*	(57)
SPY09	*h^{90} ura4-Δ18 ade6-M210 leu1-32 ctr4Δ::KAN^r*	This study
SPY10	*h^{90} ura4-Δ18 ade6-M210 leu1-32 ctr5Δ::KAN^r*	This study
SPY11	*h^{90} ura4-Δ18 ade6-M210 leu1-32 ctr6Δ::KAN^r*	This study

SPY12	*h^{90} ura4-Δ18 ade6-M210 leu1-32 ctr6Δ::loxP ctr4Δ::KAN^{r}*	This study
SPY13	*h^{90} ura4-Δ18 ade6-M210 leu1-32 cuf1Δ::KAN^{r}*	This study
SPY14	*h^{90} ura4-Δ18 ade6-M210 leu1-32 ctr4-GFP:loxP ctr5-mCherry:KAN^{r}*	This study
SPY15	*h^{90} ura4-Δ18 ade6-M210 leu1-32 ctr6-HA$_4$:KAN^{r}*	This study
SPY17	*h^{90} ura4-Δ18 ade6-M210 leu1-32 sod1Δ::KAN^{r}*	This study
SPY18	*h^{90} ura4-Δ18 ade6-M210 leu1-32 ish1Δ::KAN^{r}*	This study
SPY19	*h^{90} ura4-Δ18 ade6-M210 leu1-32 ish1Δ::KAN^{r} ish1^{+}-GFP:leu1^{+}*	This study
FY435	*h^{+} his7-366 leu1-32 ura4-Δ18 ade6-M210*	(53)
VNY10	*h^{+} his7-366 leu1-32 ura4-Δ18 ade6-M210 ish1Δ::KAN^{r}*	This study
VNY11	*h^{+} his7-366 leu1-32 ura4-Δ18 ade6-M210 ish1Δ::KAN^{r} ish1^{+}-GFP:leu1^{+}*	This study

To obtain spores, homothallic *h^{90}* cells were freshly pre-cultured in YES until the mid-logarithmic phase. Cells were then washed and plated on malt extract (ME) medium for four days. Sporulation efficiency was assessed by light microscopy examination. Although *S. pombe* asci break down by themselves, preparations containing ascospores, spores, vegetative cells and cellular debris were digested by glusulase (5%) for 1 h. The glusulase-dependent step ensured killing of the remaining vegetative cells. The digested mixture was washed and spores were purified by Percoll gradient centrifugation as described (48,49). After centrifugation at 15,000 x g at 4^{o}C for 1 h, the top three layers (50, 60, and 70% Percoll in 2.5 M sucrose and 0.5% Triton X-100) consisting of vegetative cells and debris were removed and discarded. The remaining layer (80% Percoll) containing spores was washed three times with 0.5% Triton X-100. Spores were then suspended in water and stored at 4^{o}C. To synchronize spores for their entry into germination, they were adjusted to a titer of 1 x 10^{7} spores/ml in glucose-free YE medium. At this point, glucose was added to induce germination and spore differentiation was monitored by optical density measurements at 600 nm and microscopic examination of changes in spore morphology.

Plasmids. *Saccharomyces cerevisiae GIC2* coding region corresponding to amino acid residues 1 – 208, denoted the CRIB domain (27), was isolated by PCR and then cloned into the EcoRI and SalI sites of pJK148 plasmid (50). The resulting construct was named pJKCRIB. The *GFP* coding sequence was isolated by PCR using primers designed to generate SalI and ApaI sites at the 5' and 3' termini, respectively, of the *GFP* gene. The resulting DNA fragment was digested with SalI and ApaI, and then fused in-frame with CRIB into the corresponding sites of pJKCRIB, generating pJKCRIB-GFP. The *S. pombe shk1^{+}* promoter up to -636 from the start codon of the *shk1^{+}* gene was isolated by PCR and then inserted into pJKCRIB-GFP at the SacI and EcoRI sites. We therefore ensured that the expression of the CRIB-GFP reporter, which localizes to the cell tips and to

the site of cell division, was under the control of the *shk1*$^{+}$ promoter and was used as described previously (27).

To create *h*^{90} strains in which GFP, Cherry, and HA_4 coding sequences were integrated at the chromosomal locus of *ctr4*$^{+}$, *ctr5*$^{+}$, and *ctr6*$^{+}$, respectively, a cassette-based gene replacement approach was used. In the case of Ctr4, a *ctr4*$^{+}$-*GFP* DNA fragment containing a sub-region of the *ctr4*$^{+}$ locus (starting at +514 downstream of the first base of the translational initiator codon) up to the stop codon of GFP was amplified by PCR from pJK*ctr4*$^{+}$-*GFP* plasmid (22). The resulting DNA fragment was inserted into the BamHI and EcoRI sites of pKSloxP-kanMX6-loxP. Similarly, a 320-bp SalI-Asp718 PCR-amplified DNA segment containing a 3'-UTR region of the *ctr4*$^{+}$ locus was inserted downstream of the second loxP sequence using the SalI and Asp718 sites of pKSloxP-kanMX6-loxP. Once generated, the *ctr4*$^{+}$-*GFP*-loxP-kanMX6-loxP-*ctr4-3'UTR* cassette was isolated using NheI and Asp718 digestion and then integrated at the chromosomal locus of *ctr4*$^{+}$. In the case of Ctr5, a *ctr5*$^{+}$-*Cherry* DNA fragment containing a sub-region of the *ctr5*$^{+}$ locus (starting at +314 downstream of the first base of the translational initiator codon) up to the stop codon of Cherry was amplified by PCR of the pJK*ctr5*$^{+}$-*Cherry* plasmid (22). The resulting DNA fragment was inserted into the SpeI and EcoRI sites of pKSloxP-kanMX6-loxP. Likewise, a 336-bp SalI-Asp718 PCR-amplified DNA segment containing a 3'-UTR region of the *ctr5*$^{+}$ locus was inserted downstream of the second loxP sequence using the SalI and Asp718 sites of pKSloxP-kanMX6-loxP. Once generated, the *ctr5*$^{+}$-*Cherry*-loxP-kanMX6-loxP-*ctr5-3'UTR* cassette was isolated using SpeI and Asp718 digestion and then integrated at the chromosomal locus of *ctr5*$^{+}$. In the case of Ctr6, a *ctr6*$^{+}$-HA_4 DNA fragment containing the *ctr6*$^{+}$ locus starting at -350 from the translational initiator codon up to the stop codon was amplified by PCR of the pJK*ctr6*$^{+}$-HA_4 plasmid (22). The resulting DNA fragment was inserted into the NotI and EcoRI sites of pKSloxP-kanMX6-loxP. Similarly, a 452-bp SalI-Asp718 PCR-amplified DNA segment containing a 3'-UTR region of the *ctr6*$^{+}$ locus was inserted downstream of the second loxP sequence using the SalI and Asp718 sites of pKSloxP-kanMX6-loxP. Once generated, the *ctr6*$^{+}$-HA_4-loxP-kanMX6-loxP-*ctr6-3'UTR* cassette was isolated using NotI and Asp718 digestion and then integrated at the chromosomal locus of *ctr6*$^{+}$.

To generate the integrative pJK*sod1*$^{+}$ plasmid, a 1115-bp EcoRI-XhoI PCR-amplified DNA segment containing the *S. pombe sod1*$^{+}$ locus starting at position -650 from the translational start codon up to the stop codon was inserted into the EcoRI and XhoI sites of pJK148. Nucleotide substitutions that gave rise to *sod1H64A* mutant allele were performed by an overlap extension method as described previously (51).

RNA isolation and analysis. Total RNA was isolated using a standard hot phenol method as described previously (52). Analysis of gene transcript levels was performed using RNase protection assays as described previously (53). To detect *gpd1*$^+$ mRNA levels, a plasmid pSK*gpd1*$^+$ was created by inserting a 154-bp BamHI-EcoRI fragment from the *gpd1*$^+$ gene into the same restriction sites of pBluescript SK (Stratagene, La Jolla, CA). The antisense RNA hybridizes to the region between positions +51 and +205 downstream of the first base of the translational start codon of *gpd1*$^+$. Plasmids pSK*ctr4*$^+$ (18), pSK*ctr5*$^+$-v1, pSK*ctr6*$^+$-v2 (22), pSK*cuf1*$^+$-v7 (21), and pSK*gpd1*$^+$ were used to produce antisense RNA probes, allowing the detection of steady-state levels of *ctr4*$^+$, *ctr5*$^+$, *ctr6*$^+$, *cuf1*$^+$, and *gpd1*$^+$ mRNAs, respectively. ^{32}P-labeled antisense RNA probes were produced using the above-mentioned BamHI-linearized plasmids, [α-^{32}P]UTP, and the T7 RNA polymerase, as described previously (53). The *gpd1*$^+$ riboprobe was used to detect *gpd1*$^+$ transcript as an internal control for normalization during quantification of the RNase protection products.

Calcofluor, FM4-64, and CNIR4 labeling of spores and outgrowing cells. To stain the OSW, dormant spores that were found to be refractile under phase-contrast microscopy, were incubated in the presence of calcofluor (10 μg/ml) in glucose-free media. After a 30-min incubation, dormant spores were washed and synchronously induced to enter in germination in glucose-containing and calcofluor-free media. At zero time point, when spores had just entered germination and for the subsequent time points, aliquots were retrieved every hour. At each time point, spores were subjected to microscopic analysis using a 1000X magnification and the following filters: 340 – 380 nm (calcofluor), 465 – 495 nm (GFP) (when spores contained an integrated *CRIB-GFP* or *ctr4*$^+$-*GFP* allele), and 510 – 560 nm (Cherry) (when spores harbored an integrated *ctr5*$^+$-*Cherry* allele). This microscopic procedure allowed monitoring of the progression of germination of individual spores and, simultaneously visualization of fluorescent markers. Calcofluor was used to stain the outer spore wall since it binds to constituents in the spore wall of *S. pombe*. CRIB-GFP was used as a marker of the new cell end during outgrowth.

Vacuole membrane staining using FM4-64 (Sigma-Aldrich) was performed as described previously (54), except that germinating spores were not resuspended in distilled water prior to microscope analysis. At the indicated germination phase, aliquots were harvested, washed, and resuspended in germination YES media containing FM4-64 (16 μM) for 30 min at 30^{o}C. After this step, spores and outgrowing spores were pelleted, washed and resuspended in fresh germination YES media and then incubated at 30^{o}C for an additional 30 min before performing fluorescence microscopy.

Wild-type h^{90} cells were grown mitotically in the presence of $CuSO_4$ (5 μM) to an A_{600} (optical density) of 1.0 at 30ºC. This step allowed accumulation of copper within cells. Subsequently, cells were harvested, washed and resuspended in low copper-containing media (0.16 nM $CuSO_4$, which corresponds 100 times less copper than basal conditions). Cells were divided into four treatment groups as follows: no addition of copper sensor (control) but addition of the same concentration of DMSO when a chemical probe was added; addition of CNIR4 (5 μM in 1% DMSO); addition of Ctrl-CNIR4 (5 μM in 1% DMSO); addition of Ctrl-CNIR4-S2 (5 μM in 1% DMSO). After 30 min following each treatment, aliquots were examined by direct fluorescence microscopy. Ctrl-CNIR4 and Ctrl-CNIR4-S2 are control analogs where the metal-interacting sulfur atoms are replaced by isosteric carbons. Ctrl-CNIR4 has no sulfur atoms and Ctrl-CNIR4-S2 contains two sulfur atoms. These control probes do not respond to copper but have the same dye scaffold as CNIR4 and thus can be used to help disentangle metal- and dye-dependent signals (29,30). To study intracellular copper distribution during spore germination and outgrowth, wild-type h^{90} and h^{90} *ctr4Δ*, h^{90} *ctr6Δ*, and h^{90} *ctr4Δ ctr6Δ* mutant strains were plated on ME media that contained $CuSO_4$ (5 μM). After sporulation and purification of spores from each strain, spores were induced to undergo germination in low copper-containing media. At the indicated step of germination, spores or outgrown spores were harvested, washed, and resuspended in the presence of CNIR4 (5 μM in 1% DMSO) for 30 min and then analyzed by direct fluorescence microscopy using 1,000X magnification at 633 nm excitation to match the absorption maximum of the Cu^{+}-bound CNIR4 probe.

Indirect immunofluorescence microscopy. Localization of Ctr6-HA_4 in meiotic and sporulating cells was performed as described previously (22). In the case of Ctr6-HA_4 localization during germination and outgrowth, purified h^{90} *ctr6Δ* mutant spores harboring a *ctr6*$^{+}$*-HA*$_4$ allele were induced to germinate in the presence of TTM (50 μM) for the indicated time points. Germinating spores were fixed and adsorbed on poly-*L*-lysine-coated (0.1%) multiwall slides as described previously (23). After a 30-min block with TNB (10 mM Tris/HCl, pH 7.5, 150 mM NaCl, 1% BSA, 0.02% sodium azide), spores were incubated with an anti-HA antibody (F-7) (Santa Cruz Biotechnology) diluted 1:250 in TNB. After an 18 h period of incubation at 4ºC, spores were washed with TNB and incubated for 4 h with a goat anti-mouse Alexa Fluor 546-labelled IgG antibody (Invitrogen) diluted 1:250 in TNB. After spores were washed, mounting media (Invitrogen) was added to each well prior to microscopic examination. Fluorescence and differential interference contrast images of germinating spores and outgrown cells were obtained using a Nikon Eclipse E800 epifluorescent microscope (Nikon, Melville, NY) equipped with a Hamamatsu ORCA-ER digital cooled

charge-coupled device (CCD) camera (Hamamatsu, Bridgewater, NJ). Merged images were obtained using the Simple PCI software version 5.3.0.1102 (Compix, Sewickly, PA). Cell fields shown in this study represent a minimum of five independent experiments.

Flow cytometry analysis. At various time points after spores had entered germination, aliquots of germinating spores were retrieved and fixed with cold ethanol to perform flow cytometry assays as described previously (55). Spores were stained with propidium iodide and analyzed using a CytoFLEX (or FACScan) flow cytometer with an argon laser tuned to 488 nm. The FL3 detector with a 670/690-nm long pass filter was used to collect propidium iodide fluorescence. Results were analyzed using the FlowJo version 10 software (FlowJo LLC).

SOD activity and Western blot assays. At the indicated time points, germinating spores or outgrown cells were harvested and washed with lysis buffer containing 25 mM Tris-HCl, pH 7.5, 150 mM NaCl, 1 mM PMSF, 1 mM DTT, 0.1 mM Na_3VO_4 and a protease inhibitor cocktail (Sigma-Aldrich; P8340). After washings, germinating spores were suspended in lysis buffer, and then disrupted with an equivalent volume of glass beads using a Fastprep instrument (MP Biomedicals). Lysates were centrifuged at 13,000 x *g* and then the supernatants that contained soluble proteins were partially purified using Spin-X centrifuge tube filters (Costar-Corning; 8161). Equal concentrations of lysates were analyzed on 10% native polyacrylamide gels as described previously (56), and SOD activity assays were carried out using in-gel nitro blue tetrazolium staining as described previously (20). Spectrophotometric determination of SOD activity was performed using a cytochrome *c*/xanthine oxidase method (23).

In the case of Ctr4-GFP, Ctr5-Cherry, Ctr6-HA_4 and SOD1 detection, germinating spore lysates were centrifuged at 100,000 x *g* for 30 min at 4^{o}C. The supernatant that contained soluble proteins was set aside for SOD1 detection, whereas the membrane fraction (pellet) was treated with 1% Triton X-100 for 30 min on ice, and then re-fractionated at 100,000 x *g*. The resulting supernatant fraction contained solubilized membrane proteins. The following antibodies were used for immunodetection of Ctr4-GFP, Ctr5-Cherry, Ctr6-HA_4, and SOD1: monoclonal anti-GFP antibody B-2 (Santa Cruz Biotechnology), polyclonal anti-Cherry antibody 16D7 (Thermo Fisher Scientific), monoclonal anti-HA antibody F-7, and polyclonal anti-SOD1 antibody 100 (Stressgen), respectively. Following incubation, Western blot membranes were washed and incubated with the appropriate horseradish peroxidase-conjugated secondary antibodies (Amersham Biosciences), developed with enhanced chemiluminescence (ECL) reagents (Amersham Biosciences), and visualized

by chemiluminescence using an ImageQuant LAS 4000 instrument (GE Healthcare) equipped with a Fujifilm High Sensitivity F0.85 43 mm camera.

ACKNOWLEDGMENTS
We are indebted to Dr. Gilles Dupuis for critical review of the manuscript and for his valuable comments, as well as Dr. Chris Chang for help in providing copper probes. We gratefully acknowledge Dr. Léonid Volkov for excellent assistance in flow cytometry experiments. The *S. pombe* strain FY12806 was provided by the Yeast Genetic Resource Center of Japan (YGRC/NBRP; http://yeast.lab.nig.ac.jp/nig/). S.P. is recipient of an Alexander Graham Bell Canada Graduate Doctoral studentship from the Natural Sciences and Engineering Research Council of Canada (NSERC). K.M.R.T. was partially supported by a Chemical Biology training studentship from the NIH (T32 GM066698) and NIGMS (GM79465). This study was supported by the grant MOP-CP-243929 from the Canadian Institutes of Health Research (CIHR) to S.L.

CONFLICT OF INTEREST
The authors declare that they have no conflict of interest with the content of this article.

AUTHOR CONTRIBUTIONS
S.P. designed and performed most of the experiments. V.N. produced several DNA constructs and performed a number of fluorescence microscopy experiments. K.M.R.T. produced and purified the fluorescent-based copper probe and its chemical control analogs. S.P., V.N., and S.L. analyzed data. S.P. and S.L. conceptualized research and wrote the manuscript. All authors reviewed the results and approved the final version of the manuscript.

REFERENCES
1. Sabatinos, S. A., and Forsburg, S. L. (2010) Molecular genetics of *Schizosaccharomyces pombe*. *Methods Enzymol.* **470**, 759-795
2. Shimoda, C. (2004) Forespore membrane assembly in yeast: coordinating SPBs and membrane trafficking. *J. Cell Sci.* **117**, 389-396
3. Fukunishi, K., Miyakubi, K., Hatanaka, M., Otsuru, N., Hirata, A., Shimoda, C., and Nakamura, T. (2014) The fission yeast spore is coated by a proteinaceous surface layer comprising mainly Isp3. *Mol. Biol. Cell* **25**, 1549-1559
4. Garcia, I., Tajadura, V., Martin, V., Toda, T., and Sanchez, Y. (2006) Synthesis of alpha-glucans in fission yeast spores is carried out by three alpha-glucan synthase paralogues, Mok12p, Mok13p and Mok14p. *Mol. Microbiol.* **59**, 836-853
5. Bonazzi, D., Julien, J. D., Romao, M., Seddiki, R., Piel, M., Boudaoud, A., and Minc, N. (2014) Symmetry breaking in spore germination relies on an interplay between polar cap stability and spore wall mechanics. *Dev. Cell* **28**, 534-546
6. Hatanaka, M., and Shimoda, C. (2001) The cyclic AMP/PKA signal pathway is required for initiation of spore germination in *Schizosaccharomyces pombe*. *Yeast* **18**, 207-217
7. Herman, P. K., and Rine, J. (1997) Yeast spore germination: a requirement for Ras protein activity during re-entry into the cell cycle. *EMBO J.* **16**, 6171-6181
8. Joseph-Strauss, D., Zenvirth, D., Simchen, G., and Barkai, N. (2007) Spore germination in *Saccharomyces cerevisiae*: global gene expression patterns and cell cycle landmarks. *Genome Biol.* **8**, R241
9. Shimoda, C. (1980) Differential effect of glucose and fructose on spore germination in the fission yeast *Schizosaccharomyces pombe*. *Can. J. Microbiol.* **26**, 741-745

10. Kim, B. E., Nevitt, T., and Thiele, D. J. (2008) Mechanisms for copper acquisition, distribution and regulation. *Nat. Chem. Biol.* **4**, 176-185
11. Festa, R. A., and Thiele, D. J. (2011) Copper: an essential metal in biology. *Curr. Biol.* **21**, R877-883
12. Beaudoin, J., Laliberté, J., and Labbé, S. (2006) Functional dissection of Ctr4 and Ctr5 amino-terminal regions reveals motifs with redundant roles in copper transport. *Microbiology* **152**, 209-222
13. Beaudoin, J., Thiele, D. J., Labbé, S., and Puig, S. (2011) Dissection of the relative contribution of the *Schizosaccharomyces pombe* Ctr4 and Ctr5 proteins to the copper transport and cell surface delivery functions. *Microbiology* **157**, 1021-1031
14. Ioannoni, R., Beaudoin, J., Mercier, A., and Labbé, S. (2010) Copper-dependent trafficking of the Ctr4-Ctr5 copper transporting complex. *PloS One* **5**, e11964
15. Labbé, S., Beaudoin, J., and Ioannoni, R. (2013) in *Metals in Cells* (Culotta, V. C., and Scott, R. S., eds) pp. 163-174, John Wiley & Sons, Chichester, UK
16. Zhou, H., and Thiele, D. J. (2001) Identification of a novel high affinity copper transport complex in the fission yeast *Schizosaccharomyces pombe*. *J. Biol. Chem.* **276**, 20529-20535
17. Peter, C., Laliberté, J., Beaudoin, J., and Labbé, S. (2008) Copper distributed by Atx1 is available to copper amine oxidase 1 in *Schizosaccharomyces pombe*. *Eukaryot. Cell* **7**, 1781-1794
18. Beaudoin, J., and Labbé, S. (2001) The fission yeast copper-sensing transcription factor Cuf1 regulates the copper transporter gene expression through an Ace1/Amt1-like recognition sequence. *J. Biol. Chem.* **276**, 15472-15480
19. Beaudoin, J., Mercier, A., Langlois, R., and Labbé, S. (2003) The *Schizosaccharomyces pombe* Cuf1 is composed of functional modules from two distinct classes of copper metalloregulatory transcription factors. *J. Biol. Chem.* **278**, 14565-14577
20. Labbé, S., Peña, M. M. O., Fernandes, A. R., and Thiele, D. J. (1999) A copper-sensing transcription factor regulates iron uptake genes in *Schizosaccharomyces pombe*. *J. Biol. Chem.* **274**, 36252-36260
21. Beaudoin, J., Ioannoni, R., Lopez-Maury, L., Bähler, J., Ait-Mohand, S., Guérin, B., Dodani, S. C., Chang, C. J., and Labbé, S. (2011) Mfc1 is a novel forespore membrane copper transporter in meiotic and sporulating cells. *J. Biol. Chem.* **286**, 34356-34372
22. Plante, S., Ioannoni, R., Beaudoin, J., and Labbé, S. (2014) Characterization of *Schizosaccharomyces pombe* Copper Transporter Proteins in Meiotic and Sporulating Cells. *J. Biol. Chem.* **289**, 10168-10181
23. Bellemare, D. R., Shaner, L., Morano, K. A., Beaudoin, J., Langlois, R., and Labbé, S. (2002) Ctr6, a vacuolar membrane copper transporter in *Schizosaccharomyces pombe*. *J. Biol. Chem.* **277**, 46676-46686
24. Rees, E. M., Lee, J., and Thiele, D. J. (2004) Mobilization of intracellular copper stores by the ctr2 vacuolar copper transporter. *J. Biol. Chem.* **279**, 54221-54229
25. Rees, E. M., and Thiele, D. J. (2007) Identification of a vacuole-associated metalloreductase and its role in Ctr2-mediated intracellular copper mobilization. *J. Biol. Chem.* **282**, 21629-21638
26. Das, M., Wiley, D. J., Chen, X., Shah, K., and Verde, F. (2009) The conserved NDR kinase Orb6 controls polarized cell growth by spatial regulation of the small GTPase Cdc42. *Curr. Biol.* **19**, 1314-1319
27. Tatebe, H., Nakano, K., Maximo, R., and Shiozaki, K. (2008) Pom1 DYRK regulates localization of the Rga4 GAP to ensure bipolar activation of Cdc42 in fission yeast. *Curr. Biol.* **18**, 322-330

28. Beaudoin, J., Ekici, S., Daldal, F., Ait-Mohand, S., Guérin, B., and Labbé, S. (2013) Copper transport and regulation in *Schizosaccharomyces pombe*. *Biochem. Soc. Trans.* **41**, 1679-1686
29. Ackerman, C. M., Lee, S., and Chang, C. J. (2017) Analytical Methods for Imaging Metals in Biology: From Transition Metal Metabolism to Transition Metal Signaling. *Anal. Chem.* **89**, 22-41
30. Cotruvo, J. A., Jr., Aron, A. T., Ramos-Torres, K. M., and Chang, C. J. (2015) Synthetic fluorescent probes for studying copper in biological systems. *Chem. Soc. Rev.* **44**, 4400-4414
31. Taricani, L., Tejada, M. L., and Young, P. G. (2002) The fission yeast ES2 homologue, Bis1, interacts with the Ish1 stress-responsive nuclear envelope protein. *J. Biol. Chem.* **277**, 10562-10572
32. Barhoom, S., Kupiec, M., Zhao, X., Xu, J. R., and Sharon, A. (2008) Functional characterization of CgCTR2, a putative vacuole copper transporter that is involved in germination and pathogenicity in *Colletotrichum gloeosporioides*. *Eukaryot. Cell* **7**, 1098-1108
33. Lambou, K., Lamarre, C., Beau, R., Dufour, N., and Latge, J. P. (2010) Functional analysis of the superoxide dismutase family in *Aspergillus fumigatus*. *Mol. Microbiol.* **75**, 910-923
34. Yao, S. H., Guo, Y., Wang, Y. Z., Zhang, D., Xu, L., and Tang, W. H. (2016) A cytoplasmic Cu-Zn superoxide dismutase SOD1 contributes to hyphal growth and virulence of *Fusarium graminearum*. *Fungal Genet. Biol.* **91**, 32-42
35. Graden, J. A., Ellerby, L. M., Roe, J. A., Valentine, J. S. (1994) Role of the bridging histidyl imidazolate ligand in yeast copper-zinc superoxide dismutase. Characterization of the His63Ala mutant. *J. Am. Chem. Soc.* **116**, 9743-9744
36. Strange, R. W., Antonyuk, S., Hough, M. A., Doucette, P. A., Rodriguez, J. A., Hart, P. J., Hayward, L. J., Valentine, J. S., and Hasnain, S. S. (2003) The structure of holo and metal-deficient wild-type human Cu, Zn superoxide dismutase and its relevance to familial amyotrophic lateral sclerosis. *J. Mol. Biol.* **328**, 877-891
37. Botts, M. R., and Hull, C. M. (2010) Dueling in the lung: how *Cryptococcus* spores race the host for survival. *Curr. Opin. Microbiol.* **13**, 437-442
38. Oiartzabal-Arano, E., Perez-de-Nanclares-Arregi, E., Espeso, E. A., and Etxebeste, O. (2016) Apical control of conidiation in *Aspergillus nidulans*. *Curr. Genet.* **62**, 371-377
39. Geib, E., Gressler, M., Viediernikova, I., Hillmann, F., Jacobsen, I. D., Nietzsche, S., Hertweck, C., and Brock, M. (2016) A Non-canonical Melanin Biosynthesis Pathway Protects *Aspergillus terreus* Conidia from Environmental Stress. *Cell Chem. Biol.* **23**, 587-597
40. Eide, D. J., Bridgham, J. T., Zhao, Z., and Mattoon, J. R. (1993) The vacuolar H(+)-ATPase of *Saccharomyces cerevisiae* is required for efficient copper detoxification, mitochondrial function, and iron metabolism. *Mol. Gen. Genet.* **241**, 447-456
41. Portnoy, M. E., Schmidt, P. J., Rogers, R. S., and Culotta, V. C. (2001) Metal transporters that contribute copper to metallochaperones in *Saccharomyces cerevisiae*. *Mol. Genet. Genomics* **265**, 873-882
42. Szczypka, M. S., Zhu, Z., Silar, P., and Thiele, D. J. (1997) *Saccharomyces cerevisiae* mutants altered in vacuole function are defective in copper detoxification and iron-responsive gene transcription. *Yeast* **13**, 1423-1435
43. Geijer, C., Pirkov, I., Vongsangnak, W., Ericsson, A., Nielsen, J., Krantz, M., and Hohmann, S. (2012) Time course gene expression profiling of yeast spore germination reveals a network of transcription factors orchestrating the global response. *BMC Genomics* **13**, 554
44. Mata, J., Wilbrey, A., and Bahler, J. (2007) Transcriptional regulatory network for sexual differentiation in fission yeast. *Genome Biol.* **8**, R217

45. Semighini, C. P., and Harris, S. D. (2008) Regulation of apical dominance in *Aspergillus nidulans* hyphae by reactive oxygen species. *Genetics* **179**, 1919-1932
46. Takemoto, D., Tanaka, A., and Scott, B. (2007) NADPH oxidases in fungi: diverse roles of reactive oxygen species in fungal cellular differentiation. *Fungal Genet. Biol.* **44**, 1065-1076
47. Matsuyama, A., Yabana, N., Watanabe, Y., and Yamamoto, M. (2000) *Schizosaccharomyces pombe* Ste7p is required for both promotion and withholding of the entry to meiosis. *Genetics* **155**, 539-549
48. Kloimwieder, A., and Winston, F. (2011) A Screen for Germination Mutants in *Saccharomyces cerevisiae*. *G3* **1**, 143-149
49. Shi, L., Li, Z., Tachikawa, H., Gao, X. D., and Nakanishi, H. (2014) Use of yeast spores for microencapsulation of enzymes. *Appl. Environ. Microbiol.* **80**, 4502-4510
50. Keeney, J. B., and Boeke, J. D. (1994) Efficient targeted integration at leu1-32 and ura4-294 in *Schizosaccharomyces pombe*. *Genetics* **136**, 849-856
51. Ho, S. N., Hunt, H. D., Horton, R. M., Pullen, J. K., and Pease, L. R. (1989) Site-directed mutagenesis by overlap extension using the polymerase chain reaction. *Gene* **77**, 51-59
52. Chen, D., Toone, W. M., Mata, J., Lyne, R., Burns, G., Kivinen, K., Brazma, A., Jones, N., and Bähler, J. (2003) Global transcriptional responses of fission yeast to environmental stress. *Mol. Biol. Cell* **14**, 214-229
53. Mercier, A., Watt, S., Bähler, J., and Labbé, S. (2008) Key function for the CCAAT-binding factor Php4 to regulate gene expression in response to iron deficiency in fission yeast. *Eukaryot. Cell* **7**, 493-508
54. Iwaki, T., Giga-Hama, Y., and Takegawa, K. (2006) A survey of all 11 ABC transporters in fission yeast: two novel ABC transporters are required for red pigment accumulation in a *Schizosaccharomyces pombe* adenine biosynthetic mutant. *Microbiology* **152**, 2309-2321
55. Sabatinos, S. A., and Forsburg, S. L. (2009) Measuring DNA content by flow cytometry in fission yeast. *Methods Mol. Biol.* **521**, 449-461
56. Laliberté, J., Whitson, L. J., Beaudoin, J., Holloway, S. P., Hart, P. J., and Labbé, S. (2004) The *Schizosaccharomyces pombe* Pccs protein functions in both copper trafficking and metal detoxification pathways. *J. Biol. Chem.* **279**, 28744-28755
57. Itadani, A., Nakamura, T., Hirata, A., and Shimoda, C. (2010) *Schizosaccharomyces pombe* calmodulin, Cam1, plays a crucial role in sporulation by recruiting and stabilizing the spindle pole body components responsible for assembly of the forespore membrane. *Eukaryot. Cell* **9**, 1925-1935

FOOTNOTES

The abbreviations used are: Cao1, copper amine oxidase 1; Cherry, red fluorescent protein; CRIB, Cdc42/Rac interactive-binding; Ctr, copper transporter; Cuf1, copper factor 1; DIC, differential interference contrast; EMM, Edinburgh minimal medium; FACS, fluorescence-activated cell sorting; FSC, forward-scattered light; GFP, green fluorescent protein; ME, malt extract; NBT, nitro blue tetrazolium; ORF, open reading frame; OSW, outer spore wall; PCR, polymerase chain reaction; SOD1, copper-zinc superoxide dismutase 1; SSC, side-scattered light; TTM, ammonium tetrathiomolybdate; YE, yeast extract; YES, yeast extract plus supplements; WT, wild-type.

CHAPITRE DEUXIÈME

Spore germination requires ferrichrome biosynthesis and the siderophore transporter Str1 in Schizosaccharomyces pombe.

Par
Samuel Plante et Simon labbé

Article publié dans *Genetics*, vol. 211, pages 893-911 (2019)

Avant propos

Je rapporte dans le *chapitre premier* nos résultats concernant le rôle des ions Cu dans le développement des spores en germination. Nous avons identifié qu'une assimilation adéquate de Cu est nécessaire au bon déroulement de la germination. Nous nous sommes donc intéressés aux enzymes Cu dépendantes et leur contribution au métabolisme des spores. Plusieures cuproenzymes ont été considérées dans nos recherches, notament, la multicuivre oxydase Fio1 qui est impliquée dans l'oxidation des ions Fe à la membrane plasmique. Fio1 et la perméase Fip1 travaillent en complexe à l'assimilation du Fe. Parce que le métabolisme du Fe est étroitement lié à celui du Cu, nous avons entreprit d'explorer l'importance de l'homéotasie du Fe pour le programme de germination. Rapidement, des résultats préliminaires suggèraient que l'assimilation du Fe était importante pour la germination, ce qui nous a poussé à poursuivre nos investigations. Les résultats de nos travaux concernant le rôle des ions Fe en germination sont rapportés dans le présent chapitre.

Contribution

J'ai accompli toutes les expériences rapportées dans cet article. De plus, j'ai monté toutes les figures, et j'ai contribué à l'écriture du manuscrit sous la supervision de Simon Labbé.

Résumé de l'article

La germination est un processus durant lequel les spores sortent de leur état de dormance pour initier la division mitotique. Chez *Schizosaccharomyces pombe*, l'étape critique de la germination est la formation d'une projection germinative, qui émerge de la spore. Nous montrons ici que la déficience en fer cause l'inhibition de l'émergence d'une projection germinative. La synthétase de sidérophore Sib1 et l'ornithine N^5-oxygénase Sib2 participent à la synthèse de ferrichrome, alors que Str1 participe à l'acquisition du ferrichrome. Les profils d'expression de sib1+, sib2+ et str1+ indiquent qu'ils sont induits rapidement après l'induction de la germination et qu'ils demeurent surexprimés au cours de la germination en condition de carence en fer. Les spores mutants sib1Δ sib2Δ sont incapables de former une projection germinative en carence de fer. L'ajout de ferrichrome exogène renverse ce phénotype lorsque str1+ est présent. Str1 se localise au contour des spores dès 4 heures après l'induction de la germination. À l'émergence d'une projection germinative, Str1 se déplace hors de la spore mère pour le localiser principalement autour de la cellule naissante. Deux résidus tyrosine conservés (Tyr553 et Tyr 567) sont prédits pour être dans la dernière boucle extracellulaire de Str1. Ces résidus sont essentiels pour l'émergence d'une projection germinative en réponse au ferrichrome exogène. Ensemble, les résultats révèlent le besoin

en biosynthèse de ferrichrome ou à son acquisition via Str1 pour la complétion de la germination.

Spore germination requires ferrichrome biosynthesis and the siderophore transporter Str1 in *Schizosaccharomyces pombe*.

Samuel Plante and Simon Labbé*.

Département de Biochimie, Faculté de médecine et des sciences de la santé, Université de Sherbrooke, Sherbrooke, QC, J1E 4K8, Canada.

*Address correspondence to: Simon Labbé, Département de Biochimie, Faculté de médecine et des sciences de la santé, Pavillon Z-8, Université de Sherbrooke, 3201, Jean Mignault, Sherbrooke (QC) J1E 4K8 Canada. Tel: (819) 821-8000 ext.: 75460;
E-mail: Simon.Labbe@USherbrooke.ca

Running title: Outgrowing spores require ferrichrome in fission yeast

Keywords: Iron, iron acquisition, fission yeast, spore germination, ferrichrome, yeast physiology.

Abstract

Spore germination is a process whereby spores exit dormancy to become competent for mitotic cell division. In *Schizosaccharomyces pombe*, one critical step of germination consists in the formation of a germ tube that hatches out the spore wall in a stage called outgrowth. Here, we show that iron deficiency blocks the outgrowth of germinating spores. The siderophore synthetase Sib1 and the ornithine N^5-oxygenase Sib2 participate in ferrichrome biosynthesis, whereas Str1 functions as a ferrichrome transporter. Expression profiles of *sib1*$^+$, *sib2*$^+$, and *str1*$^+$ transcripts reveal that they are induced shortly after induction of germination and their expression remain up-regulated throughout the germination program under low-iron conditions. *sib1Δ sib2Δ* mutant spores are unable to form a germ-tube under iron-poor conditions. Supplementation with exogenous ferrichrome suppresses this phenotype when *str1*$^+$ is present. Str1 localizes at the contour of swollen spores after 4 h of induction of germination. At the onset of outgrowth, localization of Str1 changes and it moves away from the mother spore to primarily localize at the periphery of the new daughter cell. Two conserved Tyr residues (Tyr^{553} and Tyr^{567}) are predicted to be located in the last extracellular loop region of Str1. Results show that these amino acid residues are critical to ensure timely completion of the outgrowth phase of spores in response to exogenous ferrichrome. Taken together, the results reveal the essential requirement of ferrichrome biosynthesis to promote outgrowth as well as the necessity to take up ferrichrome from an external source via Str1 when ferrichrome biosynthesis is blocked.

Introduction

Schizosaccharomyces pombe cells of the opposite mating types respond to nitrogen starvation by forming precursor diploid cells through conjugation (SABATINOS AND FORSBURG 2010). These precursor diploid cells undergo a specialized mode of division known as meiosis (MARSTON AND AMON 2004; SHIGEHISA *et al.* 2010; BLYTH *et al.* 2018). During meiosis, homologous chromosomes and then sister chromatids are successively segregated to generate four haploid sets of chromosomes that are embedded into four spores. After a maturation process, the spore tetrad is enclosed in an ascus sack. In *S. pombe*, spore tetrads are spontaneously released from the ascus after a prolonged period of time (HATANAKA AND SHIMODA 2001). At this stage, spores are dispersed into the environment. One hallmark of spore properties is the fact that they exhibit high levels of resistance to harsh treatments and environmental stresses, including dehydration, chemical exposure, and extreme temperature variations. The strong resistance of *S. pombe* spores is primarily due to the presence of a specific protective shell called the outer spore wall (OSW) or spore coat (GARCIA *et al.* 2006; BONAZZI *et al.* 2014; FUKUNISHI *et al.* 2014). The OSW acts as a strong barrier that protects the fungal spore content against detrimental environmental conditions.

When favorable growth conditions return, spores exit from dormancy and undertake a developmental program called germination (HATANAKA AND SHIMODA 2001; DWORKIN AND SHAH 2010; BONAZZI *et al.* 2014). This program allows quiescent spores to go through metabolic and morphological changes that result in re-entry in the mitotic cell cycle to resume vegetative growth. Germination of *S. pombe* spores is a process that includes the following developmental stages. First, the end of the dormancy period is marked by the

loss of spore refractility under light microscopy examination (HATANAKA AND SHIMODA 2001). It is also accompanied by a transient decrease in optical absorbance of the spore suspension (HATANAKA AND SHIMODA 2001). Second, spores approximately double their size in an isotropic manner. Third, there is a local rupture of the OSW to form the polar cap. This hatching step is followed by emergence of a projection (germ tube) at one side of the swollen spore in a process called outgrowth (HATANAKA AND SHIMODA 2001; BONAZZI *et al.* 2014). At this stage, outgrowing spores adopt a pear-shaped form. Fourth, there is a progressive extension of the polarized tube that grows away in the opposite direction of the spore side. Fifth, segregation of the replicated chromosomal material occurs, allowing the new daughter cell to acquire its own DNA content and break up by septation from the mother spore body (BONAZZI *et al.* 2014).

Although the development of germinating spores requires nutrients to drive re-entry in vegetative growth, each developmental stage has a number of specific nutrient requirements. For instance, activation of dormant *S. pombe* spores is induced *in vitro* by simply adding glucose to the culture solution, as observed by the loss of spore refractility by phase-contrast microscopy (SHIMODA 1980). However, the addition of glucose alone is insufficient to drive the subsequent developmental stages such as isotropic swelling, hatching of the OSW, and outgrowth. In this context, a recent study of *S. pombe* spores has revealed that the essential transition metal copper is dispensable for entry into germination and isotropic swelling but it is strictly required for outgrowth and generation of nascent daughter cells (PLANTE *et al.* 2017). On the basis of these observations, it is expected that iron, one of the most utilized transition metal as cofactor for the function of cellular enzymes, may also be required for the developmental process of spore germination.

Acquisition of iron in *S. pombe* has been primarily studied in the case of mitotically growing cells. Three strategies for iron assimilation in *S. pombe* have been discovered so far (LABBE *et al.* 2013; MOURER *et al.* 2015; NORMANT *et al.* 2018). One strategy uses a reductive iron transport system that is constituted of the ferrireductase Frp1, the ferroxidase Fio1 and the permease Fip1 (ROMAN *et al.* 1993; ASKWITH AND KAPLAN 1997). Under aerobic conditions, iron is oxidized (Fe^{3+}) and is poorly bioavailable. Cell-surface Frp1 reduces Fe^{3+} to Fe^{2+} prior its uptake across the plasma membrane through the activity of the heteromeric Fio1-Fip1 complex. A second strategy for iron acquisition makes use of uptake of extracellular heme. Cell surface-anchored protein Shu1 binds heme with high-affinity and fosters its accumulation within the cell (MOURER *et al.* 2015; MOURER *et al.* 2017). The Shu1-dependent pathway involves initially accumulation of heme in vacuoles, followed by distribution within the cytoplasm (MOURER *et al.* 2017). Str3 is an additional heme transporter that mediates low-affinity heme acquisition and functions independently of the Shu1 pathway (NORMANT *et al.* 2018). A third strategy consists to produce, accumulate intracellularly, and excrete extracellularly the hydroxamate-type siderophore ferrichrome (SCHRETTL *et al.* 2004). After its excretion into the extracellular environment, ferrichrome captures iron from different sources and then ferrichrome-bound iron is retrieved by *S. pombe* cells by way of the siderophore transporter Str1. This mechanism has received support by the fact that heterologous expression of *S. pombe* Str1 in a *Saccharomyces cerevisiae* mutant strain unable to take up iron results in high affinity transport of iron from ferrichrome (PELLETIER *et al.* 2003). As in the case of Str1, a protein denoted Str2 has been classified as a member of the major facilitator superfamily (MFS) of transporters. However, the physiological role of Str2 in *S. pombe* remains to be clearly defined.

As opposed to *Candida albicans* and *S. cerevisiae*, *S. pombe* is able to synthesize the hydroxamate-type siderophore ferrichrome (SCHRETTL *et al.* 2004; MERCIER AND LABBE 2010). The first step involves conversion of ornithine into N^5-hydroxy-ornithine by the ornithine-N^5-oxygenase Sib2. This enzyme exhibits a high degree of sequence homology with that of other well characterized ornithine N^5-oxygenases such as Sid1 and SidA from *Ustilago maydis* and *Aspergillus nidulans*, respectively (HAAS 2003). A N^5-transacetylase encoded by the *SPBC17G9.06c* gene is predicted to catalyze the second enzymatic step in ferrichrome biosynthesis by producing N5-acyl-N5-hydroxy-ornithine (MERCIER AND LABBE 2010). This metabolite is used as a substrate by the non-ribosomal peptide synthetase Sib1 to form ferrichrome. *S. pombe* Sib1 shares common functional domains and high sequence homology with catalytically active non-ribosomal peptide synthetases Sid2 (*U. maydis*) and SidC (*A. nidulans*) (YUAN *et al.* 2001; EISENDLE *et al.* 2003; SCHWECKE *et al.* 2006).

S. pombe genes that encode proteins involved in reductive iron transport (e.g. *frp1*$^+$, *fio1*$^+$, *fip1*$^+$), heme acquisition (e.g. *shu1*$^+$, *str3*$^+$), biosynthesis and uptake of ferrichrome (e.g. *sib1*$^+$, *sib2*$^+$, *str1*$^+$) are regulated at the transcriptional level in response to changes in iron concentrations (PELLETIER *et al.* 2002; PELLETIER *et al.* 2003; MERCIER AND LABBE 2010; MOURER *et al.* 2015). They are induced under iron-deficient conditions and repressed when iron concentrations are high. Iron-sufficient conditions are sensed by the iron-dependent GATA-type transcriptional repressor Fep1, which is a key regulator of iron homeostasis in *S. pombe* (PELLETIER *et al.* 2002; PELLETIER *et al.* 2003; BRAULT *et al.* 2015). Once activated, Fep1 associates with chromatin and down-regulates its target genes. In

contrast, *in vivo* promoter occupancy by Fep1 is lost under conditions of iron deficiency (JBEL *et al.* 2009).

Although it is known that iron is required for normal progression of the mitotic cell cycle and the meiotic program (PHILPOTT *et al.* 1998; BOHNSACK AND HIRSCHI 2004; BRAULT *et al.* 2016), the requirement for iron during fungal spore germination has not yet been investigated in depth. Here, we report that iron insufficient spores exhibit a germination arrest at the onset of outgrowth. Expression profiles of mRNAs corresponding to genes encoding proteins involved in iron acquisition revealed that *sib1*$^+$, *sib2*$^+$, and *str1*$^+$ transcripts are rapidly induced after induction of germination and that their expression increases in a time-dependent manner from the onset to the end, under low-iron conditions. A similar iron starvation-dependent temporal expression profile of *frp1*$^+$, *fio1*$^+$, and *fip1*$^+$ mRNAs is observed, except that their levels of gene expression are lower at the beginning of the germination program. Spores defective in ferrichrome production (*sib1Δ sib2Δ*) exhibit a germination arrest after isotropic swelling and are unable to initiate outgrowth. Results showed that addition of exogenous ferrichrome to *sib1Δ sib2Δ* mutant spores foster a rescue of spore germination when these spores express the wild-type *str1*$^+$ allele. In contrast, *sib1Δ sib2Δ str1Δ* triple mutant spores undergo arrest at outgrowth, irrespective of exogenous ferrichrome supplementation under low concentrations of iron. Taken together, these results revealed that ferrichrome synthesis and the ability to take up ferrichrome from the environment are essential for outgrowth during spore germination under conditions of iron deficiency.

Materials and methods

Strains, media, yeast sporulation and germination. The *S. pombe* strains used in this study are listed in Table 1. Growth, manipulation and transformation of *S. pombe* cells were carried out by using standard methods (SABATINOS AND FORSBURG 2010). Under non-selective conditions, strains were grown on yeast extract plus supplements medium (YES) that contained 0.5% yeast extract, 3% glucose, and 225 mg/l of adenine, histidine, leucine, uracil, and lysine. Targeted gene deletion was performed using gene deletion cassettes that were composed of the kanamycin/G418 resistance gene flanked by short DNA segments homologous to the chromosomal sequences lying upstream and downstream of the gene to be deleted. Selection of gene disruption strains was carried out on YES supplemented with G418 (geneticin) antibiotic (200 μg/ml). *S. pombe* h^{90} cells used for DNA plasmid integration were cultured in synthetic dextrose minimal (SD) medium containing bacto-yeast nitrogen base (0.67%), dextrose (2%), and 225 mg/l of adenine, uracil and lysine.

Homothallic h^{90} cells were cultured in minimal sporulation liquid medium (MSL) to isolate spores (EGEL *et al.* 1994). Cells were grown in MSL to mid-logarithmic phase at 30°C. Subsequently, cells were washed and transferred in MSL lacking a source of nitrogen (MSL-N) for 4 days. The efficiency of sporulation was assessed by observing spore formation (light microscopy). Although *S. pombe* asci break down by themselves, preparations containing ascospores, spores, vegetative cells and cellular debris were digested by glusulase (0.5%) for 1 h. The glusulase-dependent step ensured killing of the remaining vegetative cells. The digested mixture was washed and spores purified by Percoll gradient centrifugation as described previously (KLOIMWIEDER AND WINSTON 2011; SHI *et al.*

2014). After centrifugation at 15,000 X g at 4°C for 1 h, the top three layers (50, 60, and 70% Percoll in 2.5 M sucrose and 0.5% Triton X-100) consisting of vegetative cells and debris were removed and discarded. The remaining layer (80% Percoll) containing spores was washed three times with 0.5% Triton X-100. Spores were then suspended in water and stored at 4°C. To synchronize spores for their entry into germination, they were adjusted to a titer of 1 x 10^7 spores/ml in glucose-free YES medium. At this point, glucose was added to induce germination and spore differentiation was monitored by optical density measurements at A_{600} and microscopic examination of changes in spore morphology.

Table 1 – *S. pombe* strain genotypes

Strain	Genotype	Source or ref.
FY12806	*h^{90} ura4-Δ18 ade6-M210 leu1-32*	PLANTE *et al.* 2017
SPY20	*h^{90} ura4-Δ18 ade6-M210 leu1-32 fep1Δ::KAN^r*	This study
SPY21	*h^{90} ura4-Δ18 ade6-M210 leu1-32 fip1Δ::loxP fio1::KAN^r*	This study
SPY22	*h^{90} ura4-Δ18 ade6-M210 leu1-32 sib1Δ::loxP sib2Δ::KAN^r*	This study
SPY23	*h^{90} ura4-Δ18 ade6-M210 leu1-32 fip1Δ::loxP fio1Δ::loxP sib1Δ::loxP sib2Δ::KAN^r*	This study
SPY24	*h^{90} ura4-Δ18 ade6-M210 leu1-32 str1Δ::KANr*	This study
SPY25	*h^{90} ura4-Δ18 ade6-M210 leu1-32 sib1Δ::loxP sib2Δ::loxP str1Δ::KAN^r*	This study
SPY26	*h^{90} ura4-Δ18 ade6-M210 leu1-32 sib1Δ::loxP sib2Δ::loxP str2Δ::KAN^r*	This study
SPY27	*h^{90} ura4-Δ18 ade6-M210 leu1-32 sib1Δ::loxP sib2Δ::loxP str3Δ::KAN^r*	This study

Plasmids. Construction of the integrative pJKCRIB-GFP plasmid has been described previously (PLANTE *et al.* 2017). The CRIB-GFP protein used as a marker for tip and, to a lesser extent, septum of cells was expressed under the control of the *shk1*$^+$ promoter as described previously (TATEBE *et al.* 2008; PLANTE *et al.* 2017). To generate the integrative

pJK*str1*$^{+}$-*GFP* plasmid, a 2802-bp Asp718-BamHI PCR-amplified DNA fragment containing the *str1*$^{+}$ locus starting at position -966 from the translational start codon up to the penultimate codon was inserted into the Asp718 and BamHI sites of pJK148 (KEENEY AND BOEKE 1994). The resulting construct was denoted pJK*str1*$^{+}$nostop. The *GFP* coding sequence was isolated by PCR using primers designed to generate BamHI and NotI sites at the 5' and 3' termini, respectively, of the *GFP* gene. The resulting DNA fragment was digested with BamHI and NotI and then inserted in-frame with *str1*$^{+}$ into the corresponding sites of pJK*str1*$^{+}$nostop, generating pJK*str1*$^{+}$-GFP. Subsequently, this plasmid was used as a template to substitute the codons corresponding to Tyr^{553} and Tyr^{567} with Ala codons. A PCR overlap extension method was used to create the plasmid pJK*str1-Y553A/Y567A-GFP* that encodes the Str1-Y553A/Y567A mutant protein.

RNA isolation and analysis. Total RNA was extracted using a hot phenol method as described previously (CHEN *et al.* 2003). Gene expression profiles were analyzed using RNase protection assays as described previously (MERCIER *et al.* 2008). To detect *frp1*$^{+}$ mRNA levels, plasmid pSK*frp1*$^{+}$ was constructed by inserting a 192-bp BamHI-EcoRI fragment from the *frp1*$^{+}$ gene into the same restriction sites of pBluescript SK (Stratagene, La Jolla, CA). The antisense RNA hybridizes to the region between positions +55 and +246 downstream of the first base of the initiator codon of *frp1*$^{+}$. In the case of plasmid pSK*sib2*$^{+}$*-v2*, a 195-bp BamHI-EcoRI fragment from the *sib2*$^{+}$ gene that corresponds to the coding region between positions +37 and +231 relative to the initiator of *sib2*$^{+}$ was amplified and inserted into the BamHI-EcoRI sites of pBluescript SK. pSK*sib2*$^{+}$*-v2* was used to produce an antisense RNA probe that paired specifically to *sib2*$^{+}$ mRNA. Plasmids

pSK*fip1*$^+$, pSK*fio1*$^+$ (PELLETIER *et al.* 2002), pSK*str1*$^+$ (PELLETIER *et al.* 2003), pSK*fep1*$^+$ (JBEL *et al.* 2009), pSK*sib1*$^+$ (MERCIER AND LABBE 2010), pSK*shu1*$^+$ (MOURER *et al.* 2015), and pSK*gpd1*$^+$ (PLANTE *et al.* 2017) were used to produce antisense RNA probes, allowing the detection of steady-state levels of *fip1*$^+$, *fio1*$^+$, *str1*$^+$, *fep1*$^+$, *sib1*$^+$, *shu1*$^+$, and *gpd1*$^+$ mRNAs, respectively. ^{32}P-labeled antisense RNA probes were produced using the above-mentioned BamHI-linearized plasmids, [α-^{32}P]UTP, and the T7 RNA polymerase, as described previously (MERCIER *et al.* 2008). The *gpd1*$^+$ riboprobe was used to detect *gpd1*$^+$ transcript as an internal control for normalization during quantification of the RNase protection products.

Flow cytometry analysis. At various time points after spores had entered germination, aliquots of germinating spores were retrieved and fixed with cold ethanol to perform flow cytometry assays as described previously (SABATINOS AND FORSBURG 2009). Spores were stained with propidium iodide and analyzed using a CytoFLEX flow cytometer with an argon laser tuned to 488 nm. The FL3 detector with a 670/690-nm long pass filter was used to collect propidium iodide fluorescence. Results were analyzed using the FlowJo version 10 software (FlowJo LLC).

Detection of siderophores. Ferrichrome (FC) was extracted as described previously (MOORE *et al.* 2003; HISSEN *et al.* 2005; MERCIER AND LABBE 2010), with the following modifications. Spores were induced to undergo synchronous germination and whole spore extracts were subsequently prepared by FastPrep disruption (MP-24 instrument, MP Bio-

medicals) from culture aliquots taken at different time points. Spore lysates were quantified using the Bradford assay and equal amounts of spore extracts in term of protein content were mixed with a saturated ammonium sulfate solution (250 µl) containing $FeCl_3$ (500 µM) and phenol-chloroform-isoamyl alcool (25:24:1) (250 µl). After mixing the samples, they were then centrifuged, and the organic layers were collected. The latter fraction was then diluted with 3 volumes of diethyl ether and mixed by vortexing with water (150 µl). The aqueous layer containing FC was collected by centrifugation, washed with 1 volume of diethyl ether, and lyophilized. Dried samples were resuspended in 4 µl of water and spotted on pre-heated TLC silica gel 60 F_{254} thin-layer chromatography plastic sheets (EMD Millipore, Billerica, MA). Thin-layer chromatography was carried out using a solvent containing 80% aqueous methanol, and FC was revealed by its reddish color.

Protein extraction and spectrophotometric assay using bathophenanthroline disulfonic acid (BPS). At the indicated time points, germinating spores or outgrown cells were harvested and washed with lysis buffer containing 25 mM Tris-HCl, pH 7.5, 150 mM NaCl, 1 mM PMSF, 1 mM DTT, 0.1 mM Na_3VO_4 and a protease inhibitor cocktail (Sigma-Aldrich; P8340). After washings, germinating spores were suspended in lysis buffer, and then disrupted with an equivalent volume of glass beads using a MP-24 Fastprep instrument. Lysates were centrifuged at 100,000 x *g* for 30 min at 4ºC. The supernatant that contained soluble proteins (including SOD1) was partially purified using Spin-X centrifuge tube filters (Costar-Corning; 8161). Equal concentrations of this protein preparation were resolved by electrophoresis on 10% sodium dodecyl sulfate (SDS)-polyacrylamide gels, allowing subsequent transfer of proteins to membranes and detection of SOD1 by Western

blotting. In the case of Str1-GFP detection, the membrane fraction (pellet) from germinating spore lysates (after a first centrifugation at 100,000 x *g*) was treated with 1% Triton X-100 for 30 min on ice, and then re-fractionated at 100,000 x *g*. The resulting supernatant fraction contained solubilized membrane proteins, including Str1-GFP. Dissolved membrane proteins were resuspended and mixed with sodium dodecyl sulfate (SDS) loading buffer (100 mM Tris-HCl, pH 8.0, 1.4 mM β-mercaptoethanol, 1% SDS, 5 mM EDTA, 8 M urea) and heated for 30 min at 37°C. Samples were resolved by electrophoresis on 9% SDS-polyacrylamide gels and analyzed by immunoblot assays. The following antibodies were used for immunodetection of Str1-GFP and SOD1: monoclonal anti-GFP antibody B-2 (Santa Cruz Biotechnology) and polyclonal anti-SOD1 antibody 100 (Stressgen), respectively. Following incubation, Western blot membranes were washed and incubated with the appropriate horseradish peroxidase-conjugated secondary antibodies (Amersham Biosciences), developed with enhanced chemiluminescence (ECL) reagents (Amersham Biosciences), and visualized by chemiluminescence using an ImageQuant LAS 4000 instrument (GE Healthcare) equipped with a Fujifilm High Sensitivity F0.85 43 mm camera. In the case of the BPS-based spectrophotometric method, equal concentrations of protein extracts were treated with citric acid (100 mM, pH 2.0) and then incubated at 60°C for 4 h as described previously (RAD *et al.* 2007). After centrifugation, the supernatant was mixed with an equivalent volume of citric acid and then transferred to a fresh microtube prior the addition of BPS (5 mM) and freshly prepared ascorbic acid (100 mM). After 45 min of incubation at 25°C in dark, the absorbance for sample preparation containing iron was measured at an OD_{535}. The resulting absorbance value was converted in total iron content

using a separate calibration curve as described previously (RAD *et al.* 2007; POULIOT *et al.* 2010).

Calcofluor staining of spores and fluorescence microscopy. Dormant purified spores were incubated in the presence of calcofluor (10 μg/ml) in glucose-free media. After a 30 min incubation period, dormant spores were washed and synchronously induced to enter in germination in glucose-containing and calcofluor-free media. At zero time point, when spores had just entered germination and for the subsequent time points, aliquots were retrieved every hour. At each time point, spores were subjected to microscopic analysis using a 1000X magnification and the following filters: 340 – 380 nm (calcofluor) and 465 – 495 nm (GFP) (when spores contained an integrated *CRIB-GFP* or *str1*$^{+}$*-GFP* allele). This microscopic procedure allowed monitoring of the progression of germination of individual spores and, simultaneously visualization of fluorescent markers. Calcofluor was used to stain OSW since it binds to constituents in the spore wall of *S. pombe*. CRIB-GFP was used as a marker of the new cell end during outgrowth. Both fluorescence and differential interference contrast images (Nomarski) of the cells were obtained using a Nikon Eclipse E800 epifluorescent microscope (Nikon, Melville, NY) equipped with a Hamamatsu ORCA-ER digital cooled camera (Hamamatsu, Bridgewater, NJ). The cell fields shown in this study represent a minimum of five independent experiments. The merged images were obtained using the Simple PCI software version 5.3.0.1102 (Compix, Sewickly, PA).

Data availability statement. The authors affirm that all data necessary for confirming the conclusions of this manuscript are represented fully within the manuscript and its tables

and figures. Figure S1 and table S1 contain additional quantification and oligonucleotide sequence information, respectively.

Results

Iron-insufficient germinating spores exhibit an arrest at the onset of outgrowth. Iron is an essential cofactor when yeast cells divide through mitosis and when they undergo the meiotic program (BOHNSACK AND HIRSCHI 2004; BRAULT *et al.* 2016). However, little is known about a potential requirement for iron during spore germination. To investigate whether iron deficiency hampered spore germination, purified resting spores containing a *CRIB* (Cdc42/Rac interactive binding domain)-*GFP* allele (TATEBE *et al.* 2008; DAS *et al.* 2009; PLANTE *et al.* 2017) were first treated in the presence of calcofluor to stain the spore walls. These spores were synchronously induced to undergo germination in the presence of the iron chelator 2,2'-dipyridyl (Dip, 400 μM) or $FeCl_3$ (Fe, 100 μM). Differential interference contrast (DIC or Nomarski) microscopy that allowed high resolution images of spores in comparison to phase-contrast microscopy was used to monitor morphological changes. In addition, CRIB-GFP was used as a marker to point out the emergence of new developing germ tubes from mother spores in a process called outgrowth. It is known that *S. pombe* germinating spores expressing GFP fused to a CRIB domain specifically binds active Cdc42 that is concentrated at the end of newly growing cells during outgrowth and, to a lesser extent at the septum during cytokinesis (TATEBE *et al.* 2008; DAS *et al.* 2009). Spores that had been treated with Dip underwent the first stages of germination, including breaking of spore dormancy until they increased in size (Fig. 1, A – B). At this developmental point (called isotropic swelling), Dip-treated spores stopped their developmental

progression, exhibiting a germination arrest (Fig. 1B). Consequently, there was absence of germ-tube formation and the expected lack of outgrowth. In contrast, spores that had been incubated in the presence of iron, exhibited normal progression of germination that resulted in formation of bottle-like shaped spores with an outgrowing germ tube where CRIB-GFP was localized at the new cell end (Fig. 1C). The germ tube grew away from each spore body to eventually produce a calcofluor-free protrusion, leading to the formation of a daughter cell.

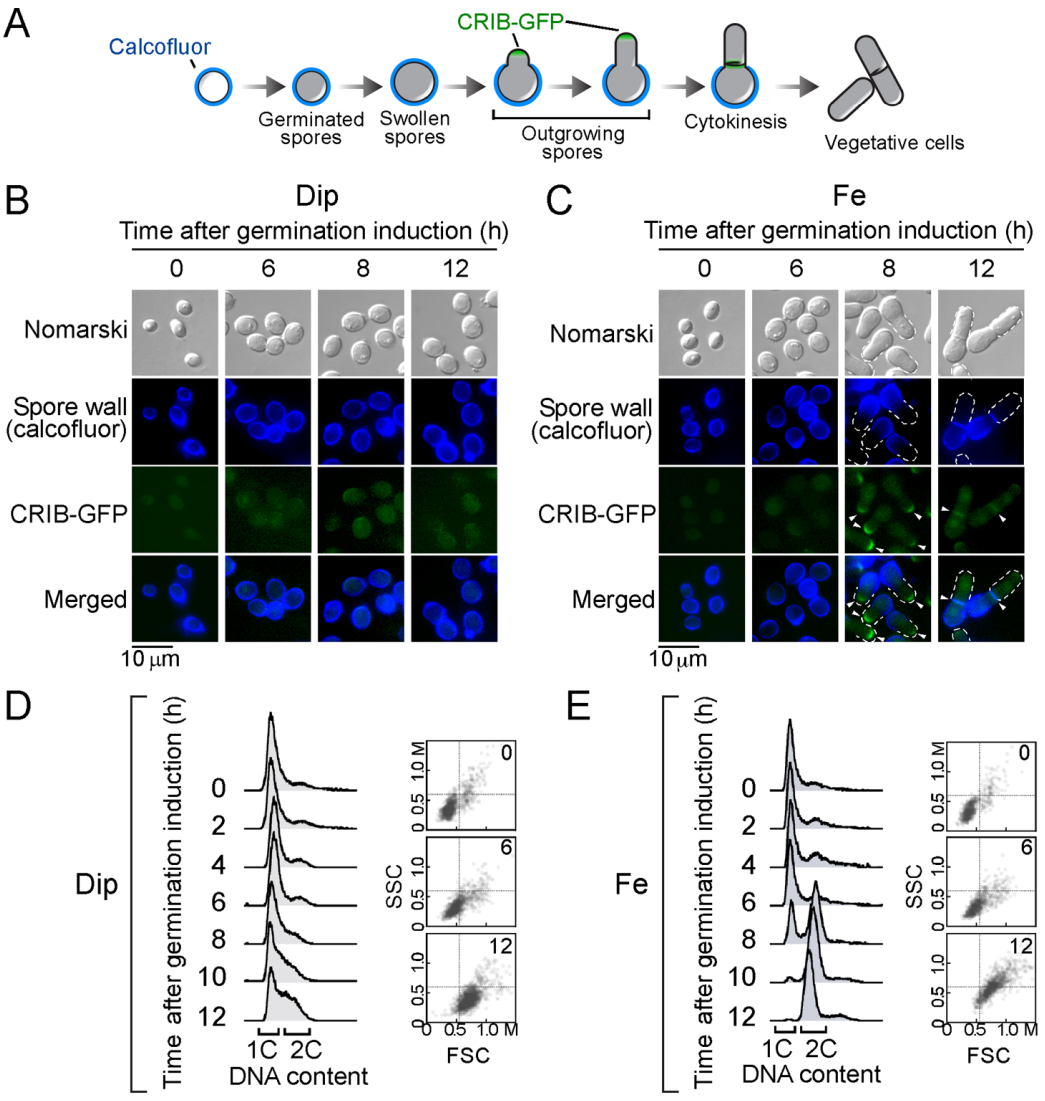

Fig. 1. *Iron deficiency leads to germination arrest at the onset of outgrowth*. *A*, Shown is a schematic representation of distinct developmental stages of spores after induction of germination. Calcofluor (blue) was used as a marker to stain the outer spore wall surrounding the mother spore. CRIB-GFP (green) was expressed as a marker to indicate the new cell tip during outgrowth and the site of cell division (septum) during cytokinesis. *B – C*, Purified spores harboring a *CRIB-GFP* allele were synchronously induced to initiate and proceed through germination in the presence of Dip (400 μM) (*panel B*, *left*) or iron (100 μM) (*panel C*, *right*). Shown are three representative stages of spore germination and outgrowth that occurred after 6, 8, and 12 h of induction. The mother spore wall was stained with calcofluor (*center top*). The daughter cell tip marker CRIB-GFP is shown in green (also indicated with white arrowheads) (*center bottom*). Spore morphology was examined by Nomarski optics (*top*). Merged images of calcofluor and CRIB-GFP are shown at the bottom of each panel. Examples of new daughter cell ends are indicated with white dashed lines. Results of microscopy are representative of five independent experiments. *D – E*, Shown is FACS analysis of spores that underwent synchronous germination in the presence of Dip (400 μM) (*panel D*, *left*) or $FeCl_3$ (100 μM) (*panel E*, *right*). Fluorescence intensities corresponding to purified spores containing one nucleus with a single complete genome (1C DNA) and outgrowing spores that duplicated their genome (2C DNA). Under each condition (Dip or iron), dot plots of FSC versus SSC in which each dot represents a single round spore, a bottle-like shape spore, or a calcofluor-free cell during early (0 h), middle (6 h), and late (12 h) phases, respectively, of the germination program. FSC is proportional to spore size, whereas SSC is proportional to spore granularity.

DNA content status of spores that had undergone germination in the presence of Dip (400 μM) and iron (100 μM) was analyzed by flow cytometry (FACS). In the case of Dip-treated spores, results showed that they exhibited 1C DNA content at the starting point of germination and over a time period of 8 h after induction of germination (Fig. 1D). Although iron-insufficient spores were still blocked at the stage of isotropic swelling after 10 h and 12 h of germination, a small fraction of spores had a 2C DNA content at these two time points (Fig. 1D). The forward light scatter (FSC) and side-scatter (SSC) cytogram of iron-depleted spores exhibited the lowest values as compared with those of iron-replete spores (Fig. 1, D – E). The fact that iron deficiency blocked germ-tube formation contributed to keep spores small in size (low FSC values) with low levels of internal granularity

(low SSC values), presumably due to the absence of developing organelles. In the case of spores that had undergone germination in the presence of iron, more than half of the spores exhibited a 2C DNA content at the time of outgrowth (8-h time point) (Fig. 1E). At the end of outgrowth, most of the germinating spores exhibited a 2C DNA content (10-h and 12-h time points). At this stage, emergence and elongation of the germ tube led to an increase in size of developing spores. This increase in size corresponded well with the highest FSC values (12-h time point) (Fig. 1E). Furthermore, organelle biogenesis that had occurred to produce a novel independent daughter cell from the spore mother correlated well with the highest SSC values, which is associated with an increase in cell internal granularity (12-h time point) (Fig. 1E).

Optical density (OD_{600}) of the spore suspension is known to transiently decrease within 2 to 3 h shortly after initiation of spore germination and then to gradually increase after 4 h when spores increase in size by swelling (HATANAKA AND SHIMODA 2001; PLANTE *et al.* 2017). Immediately after the onset of spore germination, quantification of OD_{600} was monitored under iron-replete conditions ($FeCl_3$, 100 μM) or in the presence of two concentrations of Dip (125 and 400 μM). As expected, OD_{600} values decreased during the first 3 h, irrespective of the presence of Dip or iron (Fig. 2A, inset). However, at the time of outgrowth (8-h time point), the presence of 400 μM Dip resulted in inhibition of formation and emergence of germ tubes, in comparison to iron-replete spores (Fig. 2, A and B).

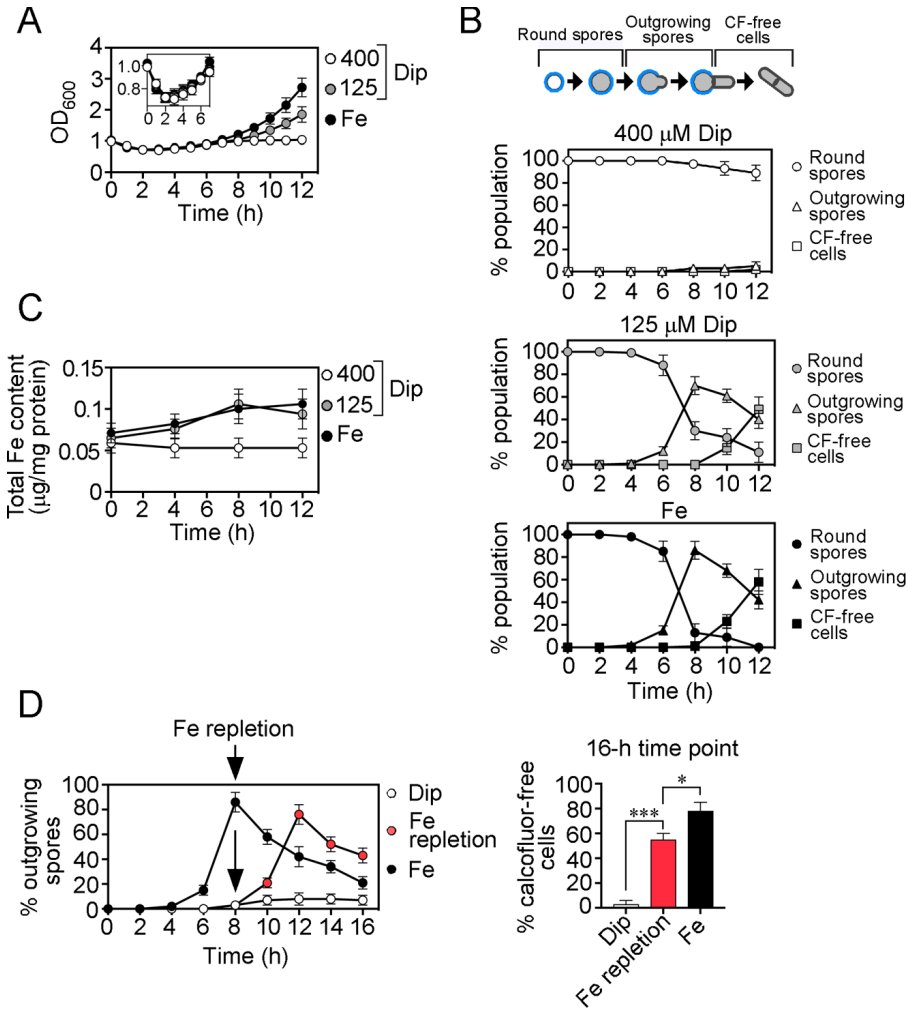

Fig. 2. *Formation of a germ tube in developing spores requires iron. A*, Wild-type spores were synchronously induced to undergo germination. Total growth was measured at OD_{600} as a function of time after induction of spore germination in the presence of iron (100 μM) or two different concentrations of Dip (125 and 400 μM). Inset indicates OD_{600} values up to 7 h post induction of spore germination (*top*). *B*, Shown is a schematic representation of different morphological stages during germination and outgrowth (*top*). The percentage of round and outgrowing spores and the percentage of calcofluor-free (CF) vegetative cells were determined as a function of time after induction of germination under iron-limiting and iron-replete conditions. *C*, At the indicated time points during germination, developing spores were harvested and their total iron content was determined by a BPS-based spectrophotometric method. *D*, Aliquots of DIP-treated (400 μM) spores used in *A* (blocked at the onset of outgrowth) were incubated in the presence of exogenous $FeCl_3$ at the 8-h time point (Fe repletion, 300 μM) (*red*), which led to release from the isotropic swelling stage to undergo outgrowth. An aliquot of spores that entered germination in the presence of iron (*panel A*) was used as a control. The graph (*left*) represents the germination profiles of spores. A minimum of 200 spores or calcofluor-free cells were examined every 2 h and under each one of the conditions. The *graph* on the *far right* represents the percentage of

calcofluor-free cells after 16 h of incubation under each one of the above-mentioned conditions. Results are shown as the averages ± S.D. of a minimum of three independent experiments. The asterisks correspond to $p < 0.01$ (*) and $p < 0.0001$ (***) (paired Student's *t*-test).

In the presence of 125 μM Dip, production of outgrowing spores decreased by 16% compared to that of iron-replete spores (Fig. 2B). At the 12-h time point, when spores had been exposed to 400 μM Dip, less than 3% of spores had differentiated to outgrowing spores (Fig. 2B). In contrast, outgrowing spores that were produced in the presence of 125 μM Dip and iron led to production of cells with elongated germ tubes and new vegetative cells that were free of calcofluor (Fig. 2B). After 12 h of germination, calcofluor-free cells represented 49% and 58% of the total population in the presence of 125 μM Dip and iron, respectively (Fig. 2B). The effect of iron starvation resulted in a 9% and 97% decrease on production of calcofluor-free cells in medium containing 125 μM and 400 μM Dip, respectively, as compared to that of calcofluor-free cells in a medium containing iron (Fig. 2B). Spores that underwent germination in the presence of Dip or iron were analyzed for their iron content by a BPS-based spectrophotometric method (RAD *et al.* 2007; POULIOT *et al.* 2010). After 12 h of induction of germination, iron-replete spores exhibited a total iron concentration of 0.11 μg/mg of protein, whereas the iron-starved spores displayed a total cell iron concentration of 0.09 and 0.05 μg/mg of protein in the presence of 125 μM and 400 μM Dip, respectively. Total cell iron content results revealed that spore iron concentration of 0.05 μg/mg of protein was insufficient to meet the iron requirements at the onset of outgrowth, leading to spore developmental arrest.

We next tested whether iron-insufficient spores could be rescued of isotropic swelling-like arrest by transferring the spores to an iron-replete medium. Spores that exhibited a germination block were washed and resuspended in a medium containing iron ($FeCl_3$, 300 μM). Results showed rescue of spore germination following removal of Dip and addition of exogenous iron. A delay of 4 h occurred when iron-insufficient spores were rescued by exogenous iron (Fig. 2D, left panel) as compared to control spores for which iron was available during the germination program. Despite the fact that a time gap occurred before iron-mediated reactivation of spore differentiation, supplementation with iron rescued spore germination by promoting outgrowth and production of novel vegetative daughter cells (Fig. 2D). At the 16-h time point, when pre-treated Dip spores had been rescued with iron, they produced calcofluor-free cells to a percentage of 55% with respect to the total population of calcofluor-negative and calcofluor-positive cells (Fig. 2D, right panel). In the case of control developing spores in which case iron was available at the beginning of germination, calcofluor-free cells represented 78% of the total population after 16 h of germination (Fig. 2D, right panel). Taken together, the results revealed that iron insufficiency leads to fungal spore germination arrest at the onset of outgrowth and that a block of spore germination could be rescued by iron supplementation.

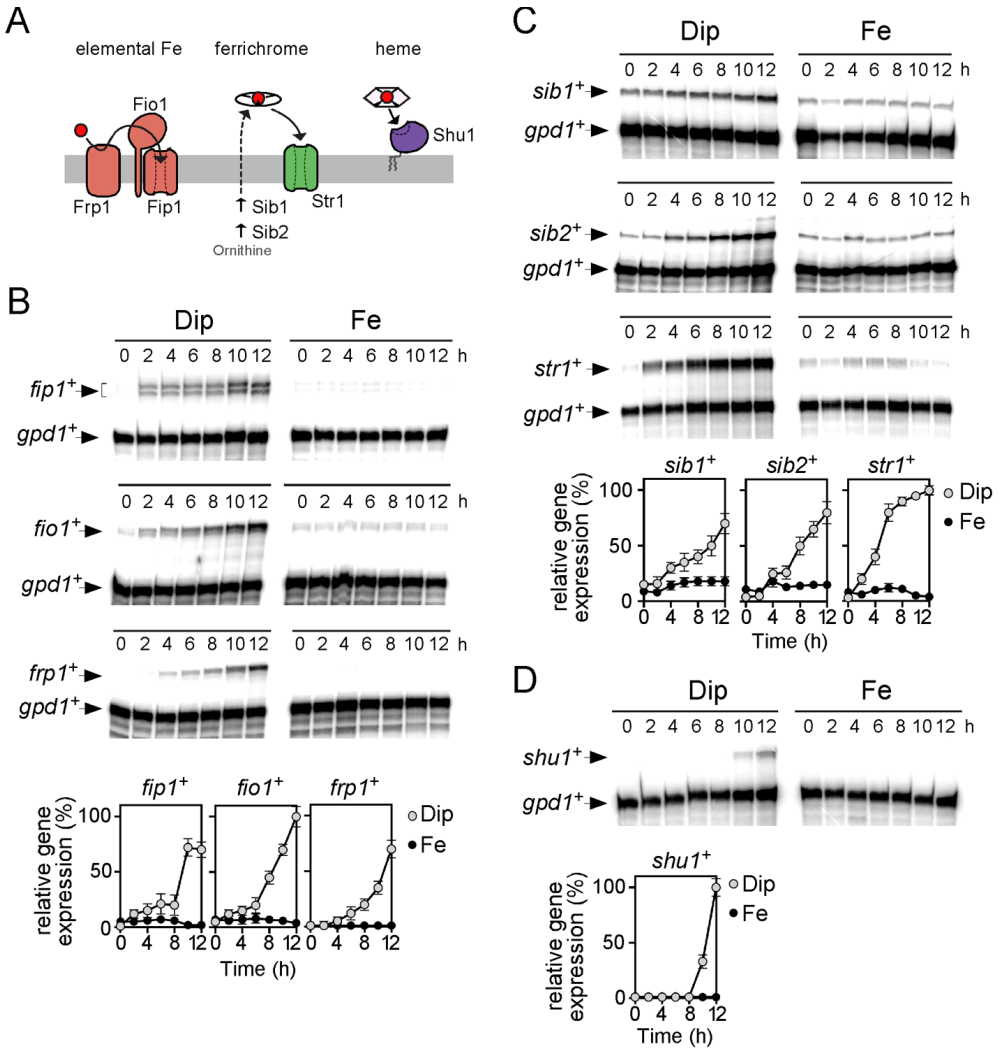

Fig. 3. *Expression profiles of genes that encode proteins related to three iron uptake systems during germination and outgrowth*. *A*, Schematic representation of proteins involved in elemental iron (Frp1, Fio1, and Fip1), ferrichrome-iron (Sib1, Sib1, and Str1), and heme (Shu1) transport systems in *S. pombe*. *B – D*, Wild-type spores were synchronously induced to undergo germination in the presence of Dip (125 μM) or iron (Fe, 100 μM). Total RNA was isolated from culture aliquots harvested at the indicated time points. At zero-time point (0 h), spores had just entered the germination program. Following RNA isolation, *fip1*$^+$, *fio1*$^+$, *frp1*$^+$ (*panel B*), *str1*$^+$, *sib1*$^+$, *sib2*$^+$ (*panel C*), and *shu1*$^+$ (*panel D*) steady-state mRNA levels were analyzed by RNase protection assays (upper part of each panel). Graphs (lower part of each panel) represent quantification of the results of three independent RNase protection assays, including experiments shown in *panels B – D*.

Assessment of the transcript levels of fip1$^+$*, fio1*$^+$*, frp1*$^+$*, str1*$^+$*, sib1*$^+$*, sib2*$^+$*,* and *shu1*$^+$ *during spore germination*. *S. pombe* uses three different transport systems to acquire exogenous iron from external sources (Fig. 3A). Taking into account the fact that iron was essential for formation of outgrowing spores, we investigated expression profiles of representative genes encoding proteins involved in iron acquisition systems in the course of spore germination, and as function of iron availability. Purified spores were induced to undergo synchronous germination and treated with Dip (125 μM) or $FeCl_3$ (100 μM). Aliquots of spore cultures were taken and total RNA isolated at the indicated time points after induction of germination. *fip1*$^+$*, fio1*$^+$*,* and *frp1*$^+$ mRNA levels were analyzed by RNase protection assays. *fip1*$^+$*, fio1*$^+$*,* and *frp1*$^+$ transcripts were primarily detected in germinating spores incubated in the presence of Dip (Fig. 3B). In the case of *fip1*$^+$ and *fio1*$^+$*,* their transcript levels were first detected between 2 h and 8 h, and maximal levels were observed 10 h and 12 h after induction of germination (Fig. 3B). A similar pattern of expression was observed in the case of *frp1*$^+$ mRNA levels, except that *frp1*$^+$ transcripts were first detected after 4 h of induction of germination (Fig. 3B). Results showed that very weak *fip1*$^+$ and *fio1*$^+$ mRNA levels were detected in spores incubated under iron-replete conditions. In the case of *frp1*$^+$, there was a lack of expression in the presence of iron (Fig. 3B).

In the case of genes involved in ferrichrome biosynthesis and transport, steady-state levels of *sib1*$^+$*, sib2*$^+$*,* and *str1*$^+$ transcripts were detected at each time point after induction of germination over a period of 12 h of germination (Fig. 3C). In response to iron starvation, *sib1*$^+$*, sib2*$^+$*,* and *str1*$^+$ mRNA levels were expressed to a higher degree over time compared to spores that had been exposed to $FeCl_3$ (Fig. 3C). After spore entry into germination, expression profiles of *sib1*$^+$*, sib2*$^+$*,* and *str1*$^+$ revealed that they reached a maximum 12 h

after induction of germination under iron-starved conditions (Fig. 3C). Upon addition of Dip, *shu1*$^{+}$ mRNA levels were detected at later times, being detected only 10 h after induction of germination (Fig. 3D). This result was in a marked contrast to expression profiles of *sib1*$^{+}$, *sib2*$^{+}$, and *str1*$^{+}$ for which their transcripts were immediately detected after induction of germination. There was a complete lack of expression of *shu1*$^{+}$ mRNA when germinating spores had been exposed to exogenous iron (Fig. 3D). Taken together, these results revealed that genes encoding proteins involved in elemental iron acquisition and ferrichrome biosynthesis and transport are transcriptionally induced under iron-limiting conditions during early, middle and late germination, with maximum levels of expression at the end of the germination program.

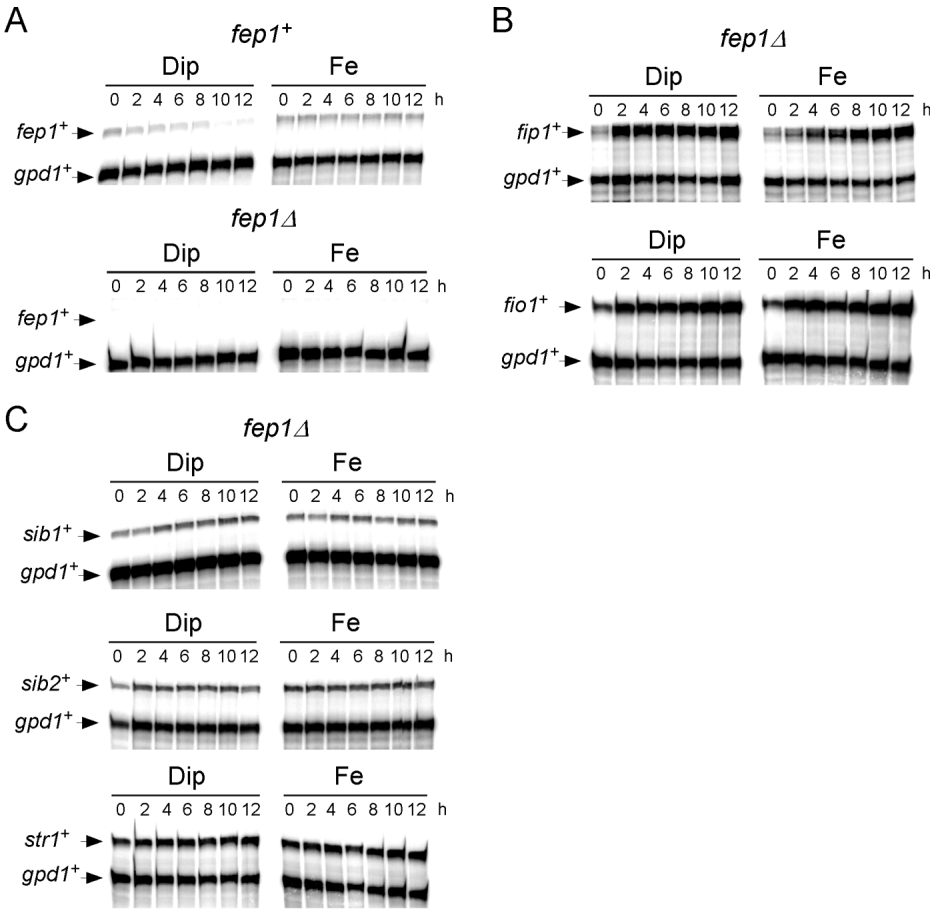

Fig. 4. *Inactivation of Fep1 leads to loss of iron-dependent repression of fip1$^+$, fio1$^+$, str1$^+$, sib1$^+$, and sib2$^+$ transcription during spore germination. A – C*, wild-type (*fep1$^+$*) and *fep1Δ* mutant spores were synchronously induced to germinate in the presence of Dip (125 μM) or $FeCl_3$ (100 μM). At the indicated times, *fep1$^+$, fip1$^+$, fio1$^+$, str1$^+$, sib1$^+$, sib2$^+$*, and *gpd1$^+$* (internal control) steady-state mRNA levels were analyzed by RNase protection assays. For each panel, results are representative of three independent RNase protection assays, including experiments shown in *panels A*, *B* and *C*.

Fep1 is required for iron-mediated repression of fip1$^+$, fio1$^+$, str1$^+$, sib1$^+$, and *sib2$^+$ mRNA levels during spore germination*. When mitotically growing cells undergo a switch from low to high iron concentrations, several gene-encoding proteins involved in iron transport are repressed by the transcription factor Fep1 (PELLETIER *et al.* 2002; PELLETIER *et al.* 2003; LABBE *et al.* 2013). To ascertain whether the *fep1$^+$* gene was expressed during spore germination, purified wild-type and *fep1Δ* mutant spores were synchronously induced to undergo germination in the presence of Dip (125 μM) or iron (100 μM). After spore entry into germination, steady-state levels of *fep1$^+$* mRNA were analyzed by RNase protection assays at various time points. In the case of *fep1$^+$* spores, results showed that *fep1$^+$* transcripts were constitutively present within the first 12 h of induction of germination in the presence of iron (Fig. 4A). When wild-type spores were treated with Dip (125 μM), results showed a decrease of *fep1$^+$* transcript levels within 2 h – 12 h, compared to levels observed in spores treated with iron (Fig. 4A). This iron starvation-dependent downregulation of *fep1$^+$* expression was consistent with the fact that *fep1$^+$* is a known target gene of Php4 under iron starvation conditions (MERCIER *et al.* 2008). As a control, *fep1$^+$* mRNA was absent in *fep1Δ* null spores (Fig. 4A).

We next examined the effect of *fep1Δ* deletion on the expression of *fip1$^+$*, *fio1$^+$*, *sib1$^+$*, *sib2$^+$*, and *str1$^+$* genes during spore germination. In the presence of iron, the loss of Fep1

resulted in increased *fip1*$^+$, *fio1*$^+$, *sib1*$^+$, *sib2*$^+$, and *str1*$^+$ mRNA levels in comparison with those observed in wild-type iron-treated *fep1*$^+$ control spores (Figs 3, 4, and Supplemental Fig. S1). In the absence of Fep1 (*fep1Δ*), *fip1*$^+$, *fio1*$^+$, *sib1*$^+$, *sib2*$^+$ and *str1*$^+$ mRNA levels were elevated and unresponsive to iron for repression (Fig. 4, B and C). As expected, high steady-state levels of *fip1*$^+$, *fio1*$^+$, *sib1*$^+$, *sib2*$^+$, and *str1*$^+$ transcripts were consistently observed in *fep1Δ* spores treated with Dip (Fig. 4, B and C, and Supplemental Fig. S1). Taken together, the results indicated that down regulation of *fip1*$^+$, *fio1*$^+$, *sib1*$^+$, *sib2*$^+$, and *str1*$^+$ genes occurs through the activity of Fep1 that represses to different extents, transcription from these loci in response to iron during spore germination.

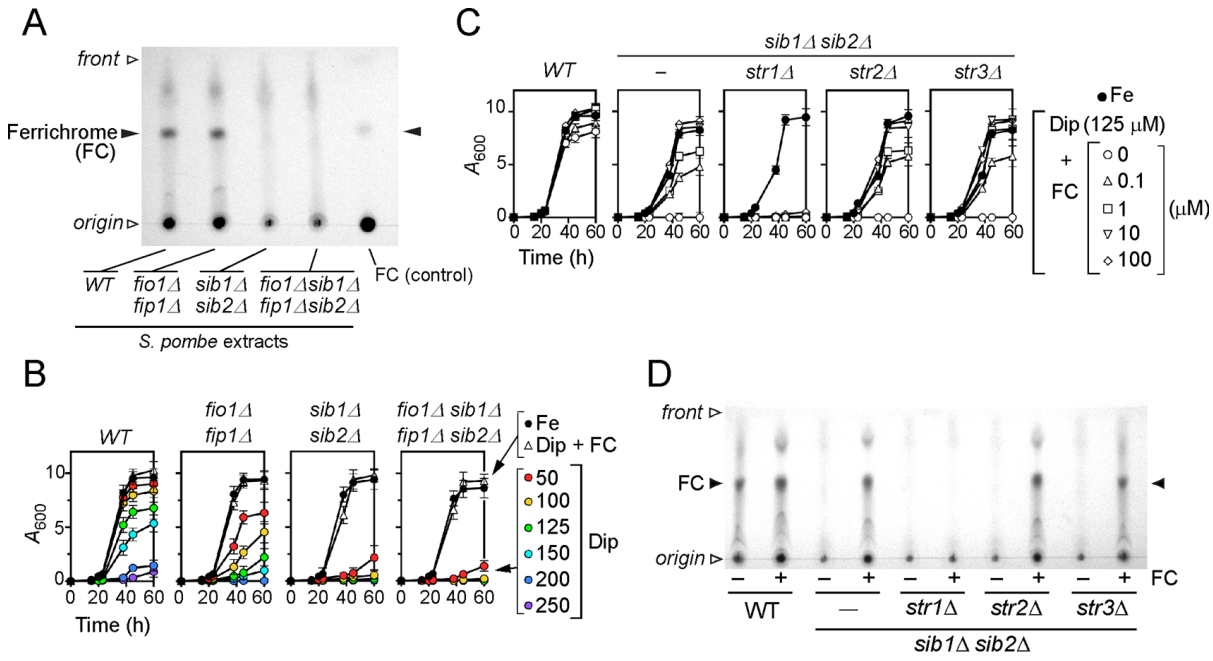

Fig. 5. *Sib1 and Sib2 are required for ferrichrome synthesis, whereas Str1 is required for exogenous ferrichrome acquisition*. *A*, The indicated strains were seeded to an OD_{600} of 0.5 and then mitotically grown in the presence of Dip (125 μM) for 5 h. Total ferrichrome (FC) was extracted and analyzed by thin-layer chromatography on silica gel sheets. Commercially purified FC (15 μg) (*control*) was loaded as a reference. Filled black arrowheads indicate the migrating position of ferrichrome, whereas empty arrowheads show the origin of sample spotting and front of gel migration. Results of thin-layer chromatography anal-

ysis (*panels A and D*) are representative of three independent experiments. *B*, The indicated strains were seeded to an OD_{600} of 0.05 (0-h time point) in the presence of $FeCl_3$ (100 μM, black), Dip (50 μM, red; 100 μM, yellow; 125 μM, green; 150 μM, turquoise; 200 μM, blue; or, 250 μM, purple), or Dip (125 μM) + FC (10 μM) (white) over a period of 20, 40, and 60 h. Graphs represent growth profiles of strains as a function of time. *C*, Growth curves of the indicated strains were measured in the presence of $FeCl_3$ (100 μM) (black) or Dip (125 μM) with increasing concentrations of FC (0, 0.1, 1, 10, and 100 μM) over a period of 0, 20, 40, and 60 h. *D*, Isogenic strains were grown to an OD_{600} of 0.5 and then incubated in the presence of Dip (125 μM) or a combination of Dip and FC (10 μM) for 5 h. Total FC content was analyzed by thin-layer chromatography. In the case of *panels B* and *C*, results are shown as the averages ± S.D. of a minimum of three independent experiments.

Biosynthesis of ferrichrome requires Sib1 and Sib2, whereas exogenous ferrichrome assimilation relies on Str1 in S. pombe. Hydroxamate-type siderophore ferrichrome is produced when *S. pombe* grows under low iron conditions (MERCIER AND LABBE 2010). Although a fraction of ferrichrome is excreted, a significant proportion accumulates intracellularly (SCHRETTL *et al.* 2004). To assess whether the homothallic strains we used accumulated ferrichrome, mitotically growing wild-type, *fio1Δ fip1Δ*, *sib1Δ sib2Δ*, and *fio1Δ fip1Δ sib1Δ sib2Δ* strains were incubated in the presence of Dip (125 μM) for 5 h. Whole cell extracts from all strains were analyzed by thin-layer chromatography (TLC). A ferrichrome signal was detected in wild-type and *fio1Δfip1Δ* strains in which $sib1^+$ $sib2^+$ genes were present encoding proteins that participate in ferrichrome biosynthesis (Fig. 5A). In contrast, mutant strains harboring *sib1Δ* and *sib2Δ* disrupted alleles (*sib1Δ sib2Δ* and *fio1Δ fip1Δ sib1Δ sib2Δ*) were unable to produce ferrichrome (Fig. 5A).

To further investigate whether the ability of cells to produce ferrichrome confered an advantage to grow under iron-limiting conditions, wild-type, *fio1Δ fip1Δ*, *sib1Δ sib2Δ*, and *fio1Δfip1Δ sib1Δ sib2Δ* strains were incubated in the presence of increasing concentrations

of Dip. In the case of the *sib1Δ sib2Δ* double mutant strain, its ability to grow was strongly reduced in the presence of 50, 100, and 125 μM Dip, whereas no growth was observed in the medium containing higher concentrations of Dip (150, 200, and 250 μM). Dip-treated *sib1Δ sib2Δ* cells (50, 100, and 125 μM) exhibited a reduced growth to an A_{600} of 2.17, 0.55, and 0.24, respectively, over a time period of 60 h in comparison with wild-type strain, which exhibited an A_{600} of 9.02, 8.33, and 6.78, respectively, over the same time period (Fig. 5B). These results corresponded to 4.2 ± 0.8-, 15.1 ± 0.7-, and 28.5 ± 0.6-fold less growth for cells lacking *sib1Δ* and *sib2Δ* compared to wild-type strain (Fig. 5B). In the case of the *fio1Δ fip1Δ* mutant strain, its ability to grow was affected in the presence of Dip, but not as severely as that observed in the case of the *sib1Δ sib2Δ* mutant (Fig. 5B). A mutant strain lacking *fio1Δ fip1Δ* exhibited 1.4 ± 0.2-, 1.8 ± 0.4- and 3.1 ± 0.5-fold less growth compared to wild-type strain in the presence of 50, 100, and 125 μM Dip, respectively. Cells with disrupted *fio1*$^+$, *fip1*$^+$, *sib1*$^+$ and *sib2*$^+$ genes (*fio1Δ fip1Δ sib1Δ sib2Δ*) were very sensitive to iron starvation induced by Dip, in which case they exhibited lesser growth than all other strains (Fig. 5B). When growth assays were performed in the presence of iron (100 μM), results showed that wild-type, *fio1Δ fip1Δ*, and *sib1Δ sib2Δ* mutant strains exhibited robust growth, whereas the *fio1Δ fip1Δ sib1Δ sib2Δ* quadruple mutant strain exhibited a slight decrease of growth over a time period of 60 h in comparison to the other three strains. Importantly, the growth inhibitory effect of Dip (125 μM) on wild-type and mutant strains was fully rescued by supplementing the medium with ferrichrome (10 μM), revealing that disruption of *fio1*$^+$, *fip1*$^+$, *sib1*$^+$, and *sib2*$^+$ genes did not interfere with the ability of the cells to take up exogenous ferrichrome-bound iron (Fig. 5B).

We have previously shown that heterologous expression of *S. pombe* Str1 protein complements the ferrichrome assimilation deficiency of *S. cerevisiae* cells defective in the uptake of siderophore iron (PELLETIER *et al.* 2003). To further examine the ability of *S. pombe* to take up ferrichrome, we used a *sib1Δ sib2Δ* double mutant strain in which the ferrichrome biosynthetic pathway was disrupted, thus preventing endogenous biosynthesis of ferrichrome. Based on the knowledge that Str1 triggers ferrichrome assimilation when heterologously expressed in *S. cerevisiae* and that Str2 and Str3 are two potential closely related proteins, we created *sib1Δ sib2Δ str1Δ*, *sib1Δ sib2Δ str2Δ*, and *sib1Δ sib2Δ str3Δ* mutant strains to investigate whether Str1 or Str2 and Str3 may function in ferrichrome acquisition. In the presence of Dip (125 μM) and in the absence of exogenous ferrichrome, *sib1Δ sib2Δ*, *sib1Δ sib2Δ str1Δ*, *sib1Δ sib2Δ str2Δ*, and *sib1Δ sib2Δ str3Δ* cells were unable to grow (Fig. 5C). However, in the case of *sib1Δ sib2Δ*, *sib1Δ sib2Δ str2Δ*, and *sib1Δ sib2Δ str3Δ* cells, their growth defect was rescued when 10 and 100 μM exogenous ferrichrome were added to the medium over a time period of 60 h (Fig. 5C). Although addition of 0.1 and 1 μM ferrichrome resulted in an increase of cell growth, in the case of *sib1Δ sib2Δ*, *sib1Δ sib2Δ str2Δ*, and *sib1Δ sib2Δ str3Δ* cells, their growth levels were only restored to 63 – 70% compared to levels of cells that had been incubated in the presence of 10 or 100 μM ferrichrome (Fig. 5C). In the case of *sib1Δ sib2Δ str1Δ* cells, treatment with different concentrations of ferrichrome (0.1, 1, 10, and 100 μM) failed to restore growth, revealing that Str1 was required for exogenous ferrichrome acquisition in *S. pombe*. Under iron-replete conditions (100 μM $FeCl_3$) in which inorganic iron assimilation in cells is independent of siderophore transporters, all mutant strains exhibited similar growth in comparison to wild-type strain (Fig. 5C).

Extracts from wild-type, *sib1Δ sib2Δ*, *sib1Δ sib2Δ str1Δ*, *sib1Δ sib2Δ str2Δ*, and *sib1Δ sib2Δ str3Δ* mutant strains were analyzed by TLC. In the absence of exogenous ferrichrome, strains lacking *sib1*$^+$ and *sib2*$^+$ (*sib1Δ sib2Δ*) did not show a ferrichrome signal (Fig. 5D). In contrast, a ferrichrome signal was detected in *sib1Δ sib2Δ*, *sib1Δ sib2Δ str2Δ*, and *sib1Δ sib2Δ str3Δ* strains that had been incubated in the presence of exogenous ferrichrome (10 μM) (Fig. 5D). On the other hand, extract preparations from the *sib1Δ sib2Δ str1Δ* mutant strain were devoid of detectable ferrichrome, revealing that Str1 was required for exogenous ferrichrome acquisition. Extracts from wild-type strain, which produces and assimilates exogenous ferrichrome, showed a positive ferrichrome signal in the absence or presence of exogenous ferrichrome in iron-poor media (Fig. 5D). Taken together, these results indicated that ferrichrome synthesis in *S. pombe* requires Sib1 and Sib2, whereas inactivation of Str1 abolishes the capacity of cells to acquire exogenous ferrichrome.

Ferrichrome biosynthesis proteins Sib1 and Sib2 are required for spore outgrowth under low iron conditions. Based on the results that iron deficiency led to a spore germination block (Fig. 1), we examined whether the loss of Fio1, Fip1, Sib1, Sib2 or Str1 could also affect the development of germinating spores. Purified wild-type, *fio1Δ fip1Δ*, *sib1Δ sib2Δ*, *sib1Δ sib2Δ fio1Δ fip1Δ*, *sib1Δ sib2Δ str1Δ*, and *str1Δ* spores were synchronously induced into germination and treated with Dip (125 μM) or iron (100 μM). Wild-type spores that had been incubated in the presence of Dip or iron proceeded through the developmental program by breaking spore dormancy and increasing their size (isotropic swelling).

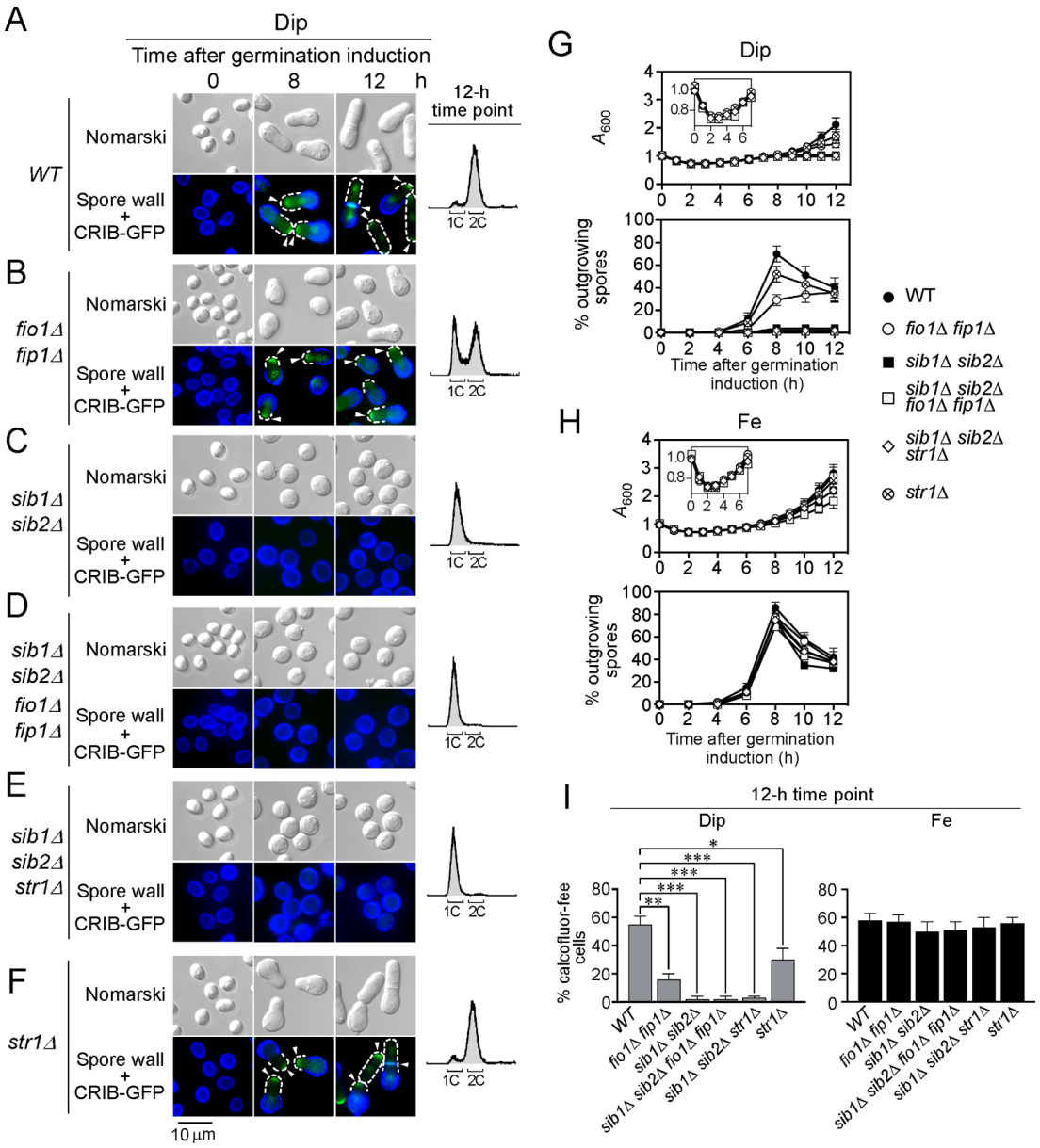

Fig. 6. *Germ-tube formation is defective in the absence of Sib1 and Sib2, whereas germ tube development is delayed in fio1Δ fip1Δ mutant spores.* Wild-type (*WT*) spores and spores harboring deletions of the *fio1*$^+$ *fip1*$^+$ (*fio1Δfip1Δ*), *sib1*$^+$ *sib2*$^+$ (*sib1Δsib2Δ*), *sib1*$^+$ *sib2*$^+$ *fio1*$^+$ *fip1*$^+$ (*sib1Δsib2Δfio1Δfip1Δ*), *sib1*$^+$ *sib2*$^+$ *str1*$^+$ (*sib1Δsib2Δstr1Δ*), and *str1*$^+$ (*str1Δ*) genes were synchronously induced to undergo germination under iron-depleted (Dip, 125 μM) or iron-replete (Fe, 100 μM) conditions. *A – F*, Representative microscopic images showing defective outgrowth of *sib1Δ sib2Δ*, *sib1Δ sib2Δ fio1Δ fip1Δ*, and *sib1Δ sib2Δ str1Δ* spores compared to wild-type (*WT*) spores under iron-limiting conditions (Dip). In the case of *fio1Δ fip1Δ* spores, germ tubes were shorter, exhibiting incomplete outgrowth after 12 h of induction of germination. Although wild-type and all mutant spores contained an integrated *CRIB-GFP* allele, its green fluorescent product was only detected in wild-type spores, *str1Δ* and some *fio1Δ fip1Δ* germinated spores (*panels A*, *B*, and *F*).

CRIB-GFP (*white arrowheads*) was used as a marker to detect new cell tips of nascent daughter cells during outgrowth. Examples of new daughter cell ends are outlined by the white dashed lines. Calcofluor (*blue*) was used as a marker of the spore wall. Morphology of spores at different stages of germination was examined by Nomarski optics. At the 12-h time point, FACS analysis of wild-type and mutant spores is shown next to microscopic images (*far right*). *G – H*, In the case of each indicated strain, graphs represent growth profiles of spores (*top*) and percentages of outgrowing spores (*bottom*) after induction of germination under iron-starved (*panel G*) and iron-replete (*panel H*) conditions. *I*, Shown is the percentage of calcofluor-free cells that were produced after 12 h of induction of germination under the two conditions tested. A minimum of 200 spores and germinated cells was examined under each condition. Results are shown as the averages ± S.D. of three independent experiments. The asterisks correspond to $p < 0.01$ (*), $p < 0.001$ (**), and $p < 0.0001$ (***) (paired Student's *t*-test).

After 8 h of spore germination, wild-type spores adopted a bottle-like shape and a germ tube (calcofluor-free) emerged from the spore body (outgrowth) (Fig. 6A). At the 12-h time point, outgrowing spores produced calcofluor-free vegetative cells and most of them exhibited a 2C DNA content by FACS analysis (Fig. 6, A – I). In the case of Dip-treated *fio1Δ fip1Δ* spores, which exhibited isotropic swelling, the process of formation of outgrowing tip was significantly reduced when compared to wild-type germinating spores (Fig. 6B). At the onset of outgrowth, the polarized germ tube (calcofluor-free) failed to fully expand and exhibited premature arrest during its extension, despite the fact that the hatching step occurred as observed via the detection of the CRIB-GFP marker. As a consequence, there were fewer outgrowing germ tubes and most of them incomplete, therefore preventing production of fully mature daughter cells (Fig. 6, B – I). DNA content of *fio1Δ fip1Δ* spores was determined by FACS after 12 h of germination induction. Results showed that 40% of mutant spores had a 1C DNA content, whereas 60% had a 2C DNA content (Fig. 6B). When spores lacking *sib1* and *sib2* (*sib1Δ sib2Δ*, *sib1Δ sib2Δ fio1Δ fip1Δ*, *sib1Δ sib2Δ str1Δ*) were incubated in the presence of Dip (125 μM), they proceeded through the

initial phases of germination until they reached isotropic swelling. At this stage, *sib1Δ sib2Δ*, *sib1Δ sib2Δ fio1Δ fip1Δ*, and *sib1Δ sib2Δ str1Δ* mutant spores displayed a germination block at the onset of outgrowth and stopped their morphogenesis development when compared to wild-type spores (Fig. 6, A – E). As a consequence of the germination arrest at outgrowth, these mutant spores did not exhibit CRIB-GFP signal and were unable to produce newborn calcofluor-free cells. Furthermore, they had a single genome content (1C DNA) as determined by FACS analysis. However, the absence of germ-tube formation in these mutants could be rescued by supplementation of $FeCl_3$ (100 μM) (Fig. 6H). In fact, *sib1Δ sib2Δ*, *sib1Δ sib2Δ fio1Δ fip1Δ*, and *sib1Δ sib2Δ str1Δ* mutant spores that had been supplemented with high iron concentrations (100 μM) entered and proceeded to outgrowth, leading to formation of germ-tubes and new calcofluor-free vegetative daughter cells in a developmental process comparable to that of wild-type spores (Fig. 6, H – I). In the case of *str1Δ* mutant spores that were induced to undergo germination under conditions of iron starvation, their developmental stages of spore germination were slower than wild-type spores (Fig. 6, A, F – I), but slightly better than *fio1Δ fip1Δ* germinating spores. At the 12-h time point, *str1Δ* spores produced 25% less calcofluor-free cells as compared to control spores (Fig. 6I). Taken together, these results revealed that inactivation of *sib1Δ* and *sib2Δ* leads to a spore developmental arrest at the onset of outgrowth under low iron conditions.

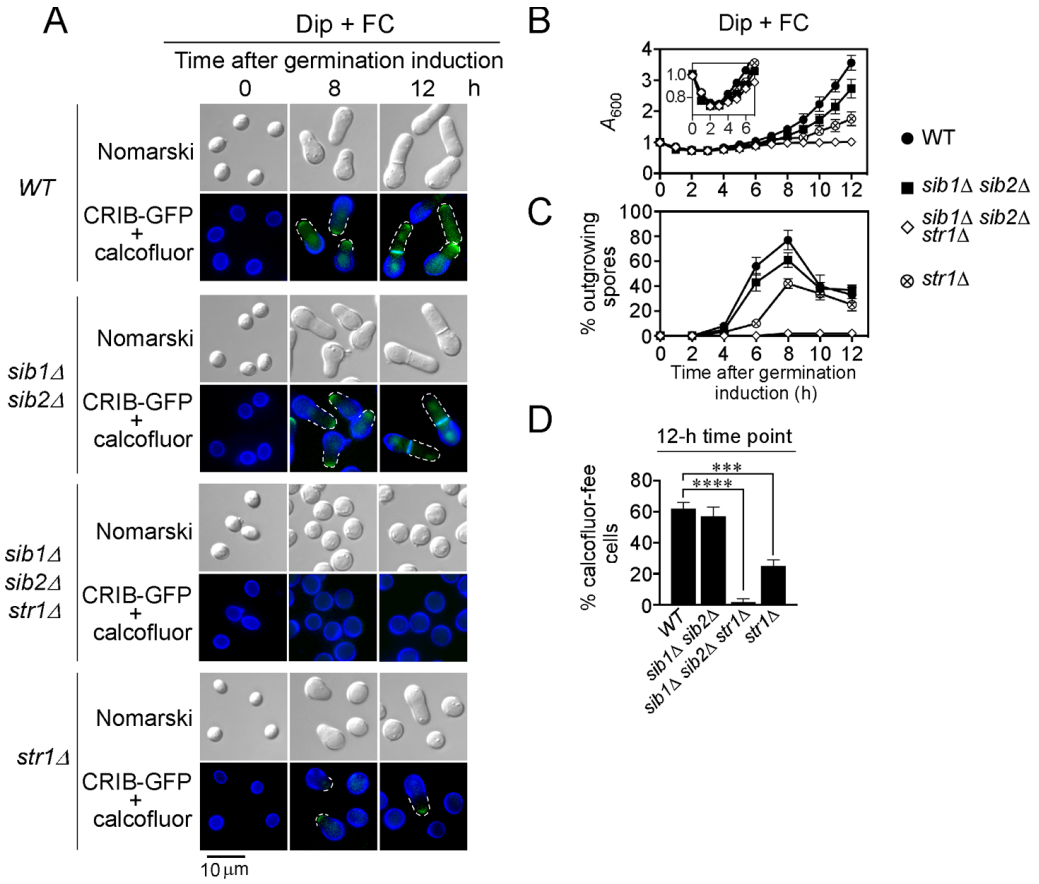

Fig. 7. *Effect of sib1Δ sib2Δ, sib1Δ sib2Δ str1Δ, and str1Δ deletions on the ability of spores to acquire exogenous ferrichrome during germination*. *A*, Synchronous germination of wild-type (*WT*), *sib1Δ sib2Δ*, *sib1Δ sib2Δ str1Δ*, and *str1Δ* spores was carried out in the presence of the iron chelator Dip (125 μM) and FC (10 μM). Three representative stages of the germination and outgrowth are shown, including the zero-time point that corresponds to the onset of induction of germination and the 8-h and 12-h time points. Spores contained the *CRIB-GFP* allele that was used as a marker of new cell tips of outgrowing spores, whereas calcofluor staining was performed to identify the wall of the spores. Examples of new daughter cell ends are indicated with white dashed lines. Spore morphology was monitored by Nomarski optics. *B*, Growth profiles of the indicated spores were analyzed by spectrophotometry at OD_{600} as a function of time after induction of germination. *C*, In the case of each indicated strain, the percentage of germinating spores undergoing outgrowth was determined after induction of germination. *D*, At the 12-h time point, the percentage of calcofluor-free nascent cells was ascertained by examination of a minimum of 200 germinated spores for each strain. Results are shown as the averages ± S.D. of three independent experiments. The asterisks correspond to $p < 0.0001$ (***) and $p < 0.00001$ (****) (paired Student's *t*-test).

Str1 is required to rescue germ-tube formation defect of sib1Δ sib2Δ mutant spores in the presence of exogenous ferrichrome. To further examine whether there was a condition that could rescue spore germination arrest caused by the absence of ferrichrome biosynthesis, purified *sib1Δ sib2Δ* spores were treated with Dip (125 μM) in the presence of exogenous ferrichrome (10 μM). Under this condition, results showed that *sib1Δ sib2Δ* spores underwent the normal germination program, including loss of spore refractility, isotropic swelling, formation of outgrowing tip and production of calcofluor-free vegetative daughter cells in a manner similar to that of wild-type spores (Fig. 7). To test whether Str1 was responsible for the capacity of *sib1Δ sib2Δ* spores to acquire exogenous ferrichrome for their germination, *sib1Δ sib2Δ str1Δ* spores were used to assess the outcome of the absence of Str1 on germination and outgrowth of spores. Results showed that the awakening of dormant *sib1Δ sib2Δ str1Δ* spores occurred because there was a loss of refractility (phase-contrast microscopy) and a slight decrease in optical absorbance in the first 2 h following induction of germination (Fig. 7B, inset). However, the progression of germination stopped at the onset of outgrowth as the mutant spores were unable to hatch (absence of CRIB-GFP signal) and to form a germ tube (Fig. 7). In the case of *str1Δ* mutant spores, the germ-tube formation defect was observed but to a lesser extent than *sib1Δ sib2Δ str1Δ* spores (Fig. 7). When spores normally entered outgrowth (8-h time point), inactivation of *str1Δ* led to a decrease of outgrowing spores by 38% as compared to wild-type spores incubated under low iron in the presence of exogenous ferrichrome (Fig. 7C). Under the same conditions, there was a 6 % and 8% decrease in bottle-like-shaped spores in the case of *str1Δ* spores as compared to control spores at late time-points (10 and 12 h) post-germination (Fig. 7C). Deletion of *str1Δ* resulted also in a decrease of 37% in the proportion of

nascent calcofluor-free cells that were produced 12 h after induction of germination. Collectively, under low concentrations of iron and in the presence of exogenous ferrichrome, results showed that Str1 is required for spore outgrowth in *sib1Δ sib2Δ* mutant spores defective in ferrichrome biosynthesis. In the case of single-*str1Δ* mutants, there is only partial inhibition in their ability to produce pear-shaped spores and new daughter cells compared to control spores.

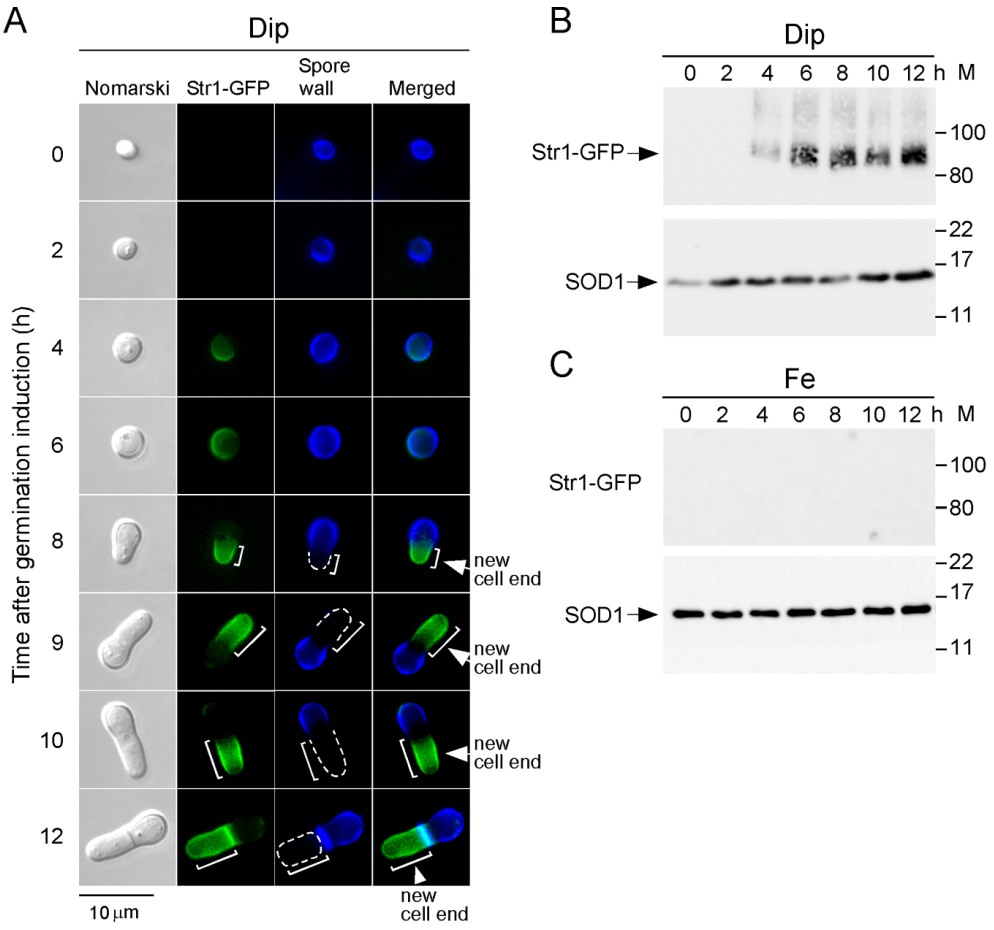

Fig. 8. *Localization of Str1-GFP during spore germination and outgrowth. A*, *str1Δ* spores expressing a functional *str1*$^{+}$*-GFP* allele were synchronously induced to undergo germination under iron-starved (125 μM Dip) or iron-replete (100 μM $FeCl_3$) conditions. The Str1-GFP-associated fluorescence signal was examined by microscopy after induction of germination in the presence of Dip (*center left*). Nomarski optics (*far left*) were used to de-

termine the morphology of germinating spores. Calcofluor staining was performed to detect the spore wall (*center right*). *White brackets*, *dashed lines* and *arrowheads* indicate the formation of germ tube that emerged at one side of the spore body. Merged images of Str1-GFP and calcofluor are shown in the *far right* panels. *B – C*, At the indicated time points after induction of germination, lysates from aliquots of iron-starved (Dip) or iron-replete (Fe) spores were analyzed by immunoblotting using anti-GFP and anti-SOD1 antibodies. Positions of the molecular weight standards (*M*) are indicated to the right in panels *B* and *C*.

Str1-GFP moves away from the spore contour and re-localizes at the periphery of the nascent daughter cell. Based on the fact that Str1 was required to take up exogenous ferrichrome during the formation of outgrowing spores, we next sought to determine its localization during the spore germination program. A fully functional Str1-GFP allele under the control of the *str1*$^{+}$ promoter was integrated in a *h*^{90} *str1Δ* strain. After spores had been produced by mating, they were purified and synchronously induced to undergo germination in the presence of Dip (125 μM) or $FeCl_3$ (100 μM). Str1-GFP was first observed at the spore contour after 4 – 6 h of induction of germination under low iron conditions (Fig. 8A). Only a short peripheral region of the spore did not exhibit a Str1-GFP-associated fluorescence signal, which may correspond to the polar cap where a singular rupture in the OSW takes place. After 8 h of induction of germination, the Str1-GFP fluorescence signal was primarily detected at the periphery of the emerging germ-tube, which was calcofluor-free (Fig. 8A). This new cell end was expending after 9 to 12 h of induction of germination. At the 12-h time point, the green fluorescence signal associated with Str1-GFP was primarily found at the contour of the new daughter cell as well as the site of cell division (septum) between nascent cell and mother spore (Fig. 8A).

To assess the steady-state levels of Str1-GFP during spore germination and outgrowth, immunoblot analyses of proteins were performed at the indicated time points (Fig. 8, B – C). Str1-GFP was first detected 4 h following induction of germination and then Str1 levels were detected throughout the spore germination process under iron-depleted conditions (Fig. 8B). In contrast, there was no signal corresponding to Str1-GFP in spores incubated in the presence of iron. This result was consistent with the fact that *str1*$^{+}$ transcription is known to be strongly repressed in response to iron (PELLETIER *et al.* 2003). Fluorescence microscopy and immunoblotting analysis indicated that there was a delay of 4 h after the start of the germination program before the accumulation of Str1 was observed. Taken together, the results showed that Str1-GFP exhibits a differential localization pattern during spore germination, being first localized at the spore contour and then shifting away from the spore body to accumulate at the cell-surface of the new daughter cell.

Tyr^{553} *and Tyr*^{567} *residues play an important role for maximal exogenous ferrichrome acquisition by Str1 in germinating spores exposed to low iron conditions*. Primary sequence analysis of Str1 predicted that the protein contained amino acid sequences characteristic of members of the MFS-type transporters. Hydrophobicity plot analysis of Str1 predicts the formation of 14 transmembrane spans that are linked by thirteen hydrophilic loops. Among them, the last extracellular loop 13 contained a putative SIderophore Transporter Domain (SITD) (NEVITT AND THIELE 2011).

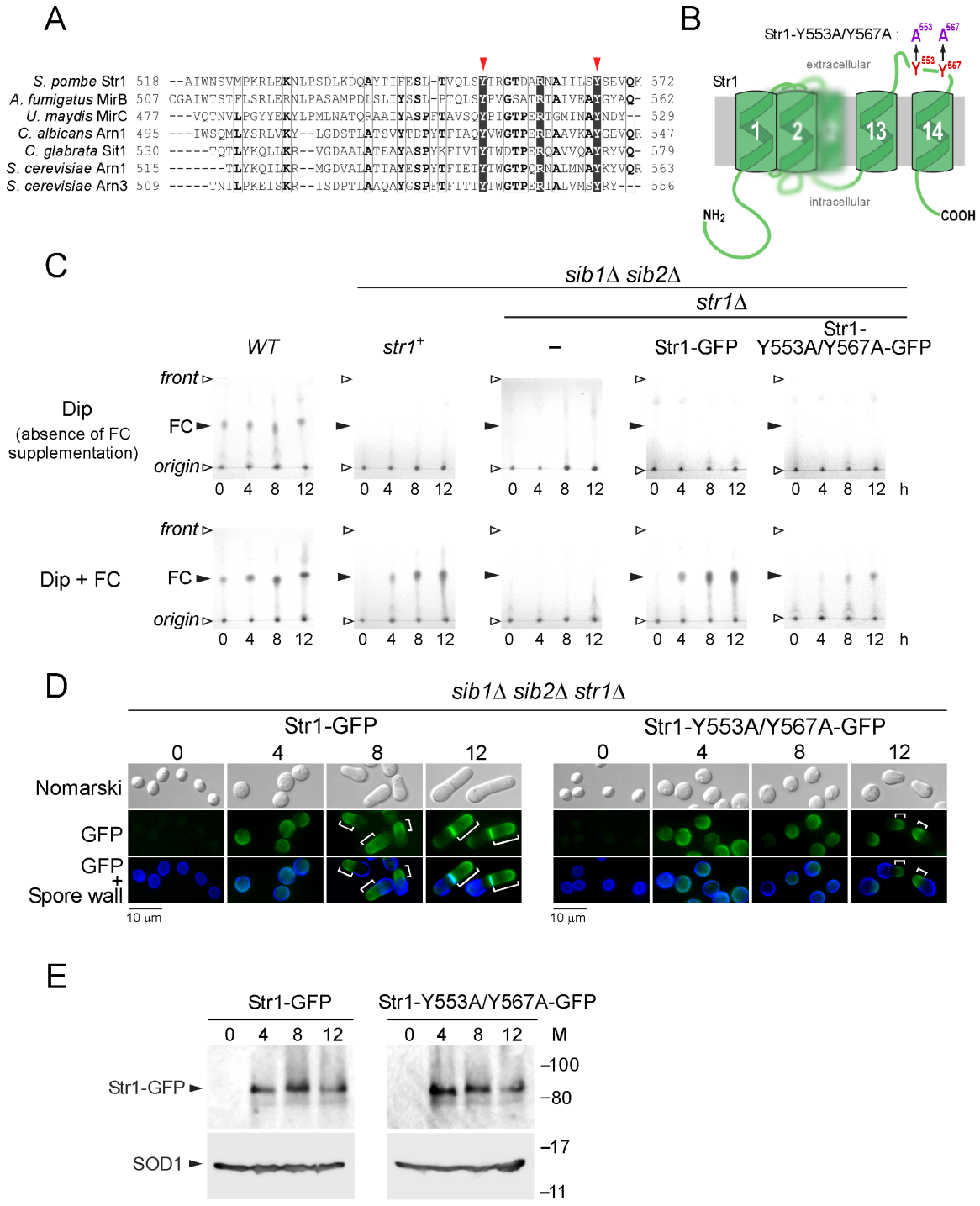

Fig. 9. *Effect of Tyr*^{553}*Ala and Tyr*^{567}*Ala mutations on Str1 function during spore germination*. *A*, Amino acid alignment of *S. pombe* Str1 last predicted external loop (near the carboxyl-terminus) with other carboxyl-terminal loops found in *A. fumigatus* MirB, *U. maydis* MirC, *C. albicans* Arn1, *C. glabrata* Sit1, and *S. cerevisiae* Arn1 and Arn3. *Black arrowheads* indicate two highly conserved Tyr residues. The amino acid sequence numbers refer to the position relative to the first amino acid of each protein. *B,* Schematic

representation of the last extracellular loop found in Str3 in which Tyr^{553} and Tyr^{567} residues are located between transmembrane domains thirteen and fourteen. *C*, Wild-type (*WT*) spores, *sib1Δ sib2Δ* spores expressing *str1*$^+$, and *sib1Δ sib2Δ str1Δ* spores expressing *str1*$^+$*-GFP*, *str1-Y553A/Y567A-GFP*, or an empty vector were synchronously induced to germinate in the presence of Dip (125 μM) supplemented with either 0 or 10 μM ferrichrome (FC). Whole extracts were prepared from spore aliquots taken at the indicated time points. Total FC content was analyzed by thin-layer chromatography on silica gel sheets. *D*, *sib1Δ sib2Δ str1Δ* spores expressing *str1*$^+$*-GFP* or *str1-Y553A/Y567A-GFP* that had been treated with Dip and FC were analyzed by fluorescence microscopy (*green*) after 0, 4, 8, and 12 h of induction of germination. The mother spore wall was stained with calcofluor (*blue*). Morphology of spores and outgrowing spores was examined by Nomarski optics. *E*, Whole extracts from aliquots of spores used in *D* were analyzed by immunoblotting using anti-GFP and anti-SOD1 antibodies. Positions of the molecular weight standards (*M*) are shown to the right.

When the amino acid sequence encompassing the loop 13 of Str1 was aligned with other predicted or known hydroxamate-type siderophore transporters, including MirB (*Aspergillus fumigatus*), MirC (*Ustilago maydis*), Arn1 (*C. albicans*), Sit1 (*C. glabrata*), Arn1, and Arn3 (*S. cerevisiae*), results showed that two Tyr (Tyr^{553} and Tyr^{567} in Str1) residues were highly conserved (Fig. 9A). Furthermore, based on a previous study that had shown the importance of one highly conserved Tyr residue (Tyr^{575}) in the *C. glabrata* Sit1 SITD domain (NEVITT AND THIELE 2011), we constructed a mutant version of Str1, in which case residues Tyr^{553} and Tyr^{567} were replaced by Ala residues (Fig. 9B). To assess Str1-dependent exogenous ferrichrome acquisition during spore germination, a *sib1Δ sib2Δ str1Δ* mutant strain was transformed with an empty plasmid (control), *str1*$^+$*-GFP*, and *str1-Y553A/Y567A-GFP* alleles. *sib1*$^+$ *sib2*$^+$ *str1*$^+$ and *sib1Δ sib2Δ str1*$^+$ strains were also used as additional controls. Purified spores from each strain were synchronously induced to initiate germination under low iron conditions in the absence or presence of exogenous

ferrichrome (10 μM). In the absence of ferrichrome, whole cell extracts from spore preparations failed to display detectable ferrichrome, except in the case of control wild-type spores. In this instance, ferrichrome was endogenously produced through the activity of Sib1 and Sib2 (Fig. 9C). In the presence of exogenous ferrichrome, cell extracts of *sib1Δ sib2Δ str1Δ* spores expressing *str1*$^{+}$*-GFP* displayed a ferrichrome signal 4 and 12 h following induction of germination (Fig. 9C). In these spores, detection of ferrichrome as a function of germination time was similar to *sib1Δ sib2Δ* spores expressing untagged *str1*$^{+}$ wild-type allele, indicating that the Str1-GFP fusion protein retained wild-type function (Fig. 9C). To test whether mutations of Tyr^{553} and Tyr^{567} residues affected the ability of spores to acquire exogenous ferrichrome, whole cell extracts from *sib1Δ sib2Δ str1Δ* spores expressing Str1-Y553A/Y567A-GFP were analyzed by TLC. Results showed that the ferrichrome signal was strongly reduced in spores carrying the *str1-Y553A/Y567A-GFP* allele in comparison with spores harboring the *str1*$^{+}$*-GFP* allele (Fig. 9C). This observation led us to determine the localization of Str1-Y553A/Y567A-GFP during spore germination and the developmental process of spore when Str1-Y553A/Y567A-GFP was expressed under low iron conditions. Synchronized *sib1Δ sib2Δ str1Δ* spores expressing Str1-GFP or Str1-Y553A/Y567A-GFP were observed by fluorescence microscopy at different stages of germination. The Str1-GFP and Str1-Y553A/Y567A-GFP fluorescence signals exhibited the same localization at the spore contour after 4 h of induction of germination (Fig. 9D). In contrast, after 8 h of germination, green fluorescence signals associated with wild-type and Str1-Y553A/Y567A mutant were no longer present at the same location, due to a developmental delay in cellular differentiation in Str1-Y553A/Y567A mutant spores. At the 8-h time point, results showed that the Str1-Y553A/Y567A-GFP fluorescence signal was still

detected at the spore contour, whereas spores expressing Str1-GFP exhibited a fluorescence signal that had moved away from the spore body to occupy the periphery of the emerging germ-tube (Fig. 9D). At the 12-h time point, spores expressing Str1-Y553A/Y567A-GFP had progressed only to the stage corresponding to the onset of outgrowth, which represented a delay of at least 4 h compared to control spores expressing Str1-GFP. At that point in time, the Str1-Y553A/Y567A-GFP fluorescence signal had shifted toward the nascent growing tip that emerged at one side of the spores (Fig. 9D). In the case of spores expressing Str1-GFP, they reached the end of their germination program and displayed a Str1-GFP fluorescence signal that was primarily observed at the periphery of newly formed daughter cells. Results showed that steady-state levels of Str1-GFP and Str1-Y553A/Y567A-GFP proteins were expressed in a manner similar between 4 and 12 h after induction of germination (Fig. 9E). Taken together, although Y553A/Y567A mutations did not lead to a complete loss of Str1 function with respect to ferrichrome acquisition, results showed that the remaining activity was insufficient to sustain normal spore differentiation in the presence of exogenous ferrichrome under iron-starved conditions.

Discussion

Several fungal species produce spores when the amount of bioavailable nutrients is insufficient to ensure their replicative life. Spores possess a number of unique properties that allow them to survive under hostile conditions (COLUCCIO *et al.* 2008; FUKUNISHI *et al.* 2014). When favorable conditions for growth return, spores exit dormancy and undergo

germination. In the case of *S. pombe*, spore dormancy is relieved by the presence of glucose but additional nutrients are required for further development of germinating spores (HATANAKA AND SHIMODA 2001; PLANTE *et al.* 2017). Results have previously shown that copper is required for germinative development of spores as copper-insufficient spores stop their differentiation at the onset of outgrowth (PLANTE *et al.* 2017). Here, we showed that germinating spores that were starved for iron exhibited an arrest immediately following the isotropic swelling phase, which resulted in a phenotype similar to that of copper-insufficient spores.

Based on the fact that iron is required for proper spore germination, we examined the effect of the presence or absence of critical proteins known to be involved in iron acquisition. Results showed that spores lacking *sib1* and *sib2* (*sib1Δ* and *sib2Δ*) were arrested at the onset of outgrowth under low iron conditions in a manner identical to that of iron-insufficient spores which failed to enter outgrowth. As Sib1 and Sib2 are two critical cellular components that participate in ferrichrome biosynthesis, this finding suggested that the ferrichrome product plays an essential role in spore germination, especially at the developmental stage of outgrowth. In *S. pombe*, *de novo* synthesized ferrichrome is found intracellularly and extracellularly (SCHRETTL *et al.* 2004). The hypersensitivity of *sib1Δ sib2Δ* spores to iron starvation may be a consequence of the absence of ferrichrome-bound iron that is normally distributed in an usable form at different intracellular locations where iron-dependent proteins are poised to use the iron cofactor. Alternatively, in the absence of ferrichrome export, its retrieval as source of iron is compromised and may contribute to a spore developmental arrest.

During spore germination, mRNA levels of *fip1*$^+$ and *fio1*$^+$ were primarily co-induced in response to low-iron conditions, reaching a maximum 10 – 12 h after induction of germination. In contrast, their transcript levels were repressed in response to iron in a Fep1-dependent manner. In the case of *sib1*$^+$, *sib2*$^+$, and *str1*$^+$ mRNA levels, although their expression pattern was induced in a comparable manner to that of *fip1*$^+$ and *fio1*$^+$ under low-iron conditions, their mRNA levels remained detectable throughout the spore germination process under high-iron conditions. This observation may suggest the existence of an additional germination-specific transcriptional regulator to ensure a low and constitutive level of expression of *sib1*$^+$, *sib2*$^+$, and *str1*$^+$ even under iron-replete conditions and in the presence of Fep1. This putative mechanism to ensure the continuous expression of siderophore biosynthesis and transport genes is consistent with the fact that previous studies have reported that siderophores are required for spore germination (MATZANKE *et al.* 1987; EISENDLE *et al.* 2006; SCHRETTL *et al.* 2007). In *Neurospora crassa*, the siderophore ferricrocin is thought to serve as iron storage and as a donor of iron during the developmental spore germination process (MATZANKE *et al.* 1987). In *Aspergillus ochraceus* spores, most iron has been found to be in a form bound to a ferrichrome-type siderophore, suggesting that siderophores may serve as an iron reservoir during fungal spore germination (MATZANKE *et al.* 1987). In *Aspergillus nidulans*, *sidA* encodes an ortholog of the *S. pombe* L-ornithine N^5-oxygenase Sib2 (EISENDLE *et al.* 2003). Disruption of *sidAΔ* results in the inability to produce competent spores (EISENDLE *et al.* 2003). Furthermore, the non-ribosomal peptide synthetase SidC and the hydroxamate-type siderophore ferricrocin are required for the emergence of the germ tube in *A. nidulans* germinating spores under iron-depleted conditions (EISENDLE *et al.* 2006). In *Aspergillus fumigatus*, results have shown

that a novel hydroxamate-type siderophore, denoted hydroxyferricrocin, is required for spore outgrowth in the absence of reductive iron uptake activity (SCHRETTL *et al.* 2007). The fact that siderophore biosynthesis is required for spore germination in several fungal species may indicate a strategy that a mother spore uses to recognize an environment favorable for growth. It could be envisioned that swollen spores that are undergoing a transition from a rounded shape to a bottle-like shape may excrete siderophores in the environment to probe whether there is the presence of sufficient bioavailable iron to support the formation of a nascent germ tube. If that were the case, siderophore-bound iron is subsequently recovered and internalized by outgrowing spores, thereby allowing them to acquire sufficient iron that is needed for generation of novel daughter cells. This is an example of autocrine signaling, in which case the same cells generate and respond to a signal for their further differentiation or adaptation. The hypothesis that an excreted siderophore may trigger a developmental switch is reminiscent of that found in *Bacillus subtilis* in which case spores exit dormancy in response to the presence of muropeptide fragments that are released from neighboring growing bacteria (SHAH *et al.* 2008).

At the stage of isotropic swelling, it is plausible that the demand for micronutrients such as iron is high. One reason is that prior to losing its OSW, a mother spore could form three unique and consecutive germ tubes, which in turn, will produce three novel daughter cells (BONAZZI *et al.* 2014). Because of these three repeated phases of outgrowth, it is thought that the mother spore accumulates high concentrations of trace elements such as iron to meet the nutritional requirements of three consecutive formations of germ tubes. In support of this concept, labile pools of copper ions preferentially accumulate in the mother spore in comparison with those of the new germ projection when the fluorescent copper-binding

probe CNIR4 is used to track exchangeable copper pools in germinating spores (PLANTE *et al.* 2017). During the spore germination process, we have shown on our previous work a preferential retention of vacuoles in the spore body during emergence and elongation of the germ tube (PLANTE *et al.* 2017). The fact that vacuoles are known to play an important role as an iron storage compartment may favor a reserve of iron within the mother spore. If labile iron pools are lower in the germ protrusion, this may trigger an asymmetric enrichment of Str1 at the periphery of the germ tube to compensate and contribute to take up ferrichrome-bound iron within the new cellular outgrowing end of the developing daughter cell. For comparative purposes, previous results have shown that in the case of the heteromeric complex formed by the copper transporters Ctr4 and Ctr5, its localization is at the periphery of the newborn daughter cell at the end of the spore germination program (PLANTE *et al.* 2017).

We found that in the absence of *sib1Δ* and *sib2Δ*, production of ferrichrome was absent and spore germination was blocked at the end of the isotropic swelling stage under low iron conditions. A way to circumvent this block and to resume the germination program was to add exogenous ferrichrome, which is the final product of the Sib1-/Sib2-dependent siderophore biosynthesis pathway. Results revealed that exogenous ferrichrome acquisition by *sib1Δ sib2Δ* spores required the cell-surface protein Str1. Indeed, inactivation of *str1Δ* in spores lacking *sib1Δ* and *sib2Δ* resulted in an arrest at the onset of outgrowth, regardless of the presence of exogenous ferrichrome. *S. pombe* Str1 is not the unique case of the MFS-type protein that mediates exogenous siderophore-iron acquisition. In other fungal species such as *S. cerevisiae*, *C. albicans*, *C. glabrata*, *U. maydis*, and *A. fumigatus*, there are MFS-type proteins that are siderophore-iron carriers (YUN *et al.* 2000; HU *et al.*

2002; KIM *et al.* 2002; PHILPOTT *et al.* 2002; HAAS 2003; NEVITT AND THIELE 2011; RAYMOND-BOUCHARD *et al.* 2012). For example, Sit1 is a plasma membrane ferrichrome importer in *C. glabrata* (NEVITT AND THIELE 2011). As observed in the case of Str1, Sit1 is predicted to contain 14 transmembrane spans that are interconnected by 13 loops. Loop 13 of Sit1 contains a conserved SITD region (NEVITT AND THIELE 2011). Primary sequence alignment of loop 13 of Str1, which corresponds to the loop present in five putative Str1 homologues (*A. fumigatus* MirB, *U. maydis* MirC, *C. albicans* Arn1, *C. glabrata* Sit1, and *S. cerevisiae* Arn1) indicated the presence of two highly conserved Tyr residues, which were found at positions 553 and 567 in Str1. In the case of Tyr^{567} in Str1, this residue corresponds to Tyr^{575} in Sit1 (*C. glabrata*) and Tyr^{577} in MirB (*A. fumigatus*) (NEVITT AND THIELE 2011; RAYMOND-BOUCHARD *et al.* 2012). Site-directed mutagenesis revealed that substitution of Tyr^{575} for Ala strongly decreased the ability of *C. glabrata* Sit1 to use exogenous ferrichrome as source of iron (NEVITT AND THIELE 2011). Similarly, substitution of Tyr^{577} for Ala in *A. fumigatus* MirB resulted in significant loss of siderophore transport activity (RAYMOND-BOUCHARD *et al.* 2012). In the case of *S. cerevisiae* Arn1, alanine substitutions of several amino acid residues found in the last extracellular loop of the protein (loop 13) led to a loss of siderophore uptake activity, to various extents (KIM *et al.* 2005). Mutation of Phe^{540} for Ala combined with Tyr^{544} substitution to Ala in Arn1 (that corresponds to Tyr^{553} in Str1) resulted in a significant loss of ferrichrome binding affinity (KIM *et al.* 2005). Given that mutations of Tyr residues in the 13^{th}-loop resulted in partial or complete loss of siderophore transport by fungal MFS-type siderophore transporters, we mutated conserved Tyr^{553} and Tyr^{567} in Str1 to assess the effect on Str1 function during spore germination. Microscopic analyses of *sib1Δ sib2Δ str1Δ* spores expressing Str1-

Y553A/Y567A showed that substitutions of Tyr^{553} and Tyr^{567} markedly decreased the spore ability to form a typical elongated germ tube when compared to *sib1Δ sib2Δ str1Δ* spores expressing a wild-type *str1*$^{+}$ allele. Consistently, the ferrichrome signal was significantly lower in extracts from *sib1Δ sib2Δ str1Δ* spores expressing Str1-Y553A/Y567A that had grown in the presence of exogenous ferrichrome compared to control spores expressing *str1*$^{+}$. Based on these observations, conserved Tyr^{553} and Tyr^{567} residues may be involved to capture ferrichrome and to move it safely in the cavity of Str1, which would be found under an outward-opening state conformation. After ferrichrome loading, Str1 would adopt an occluded conformation that triggers a shift to an inward conformation to release the ferrichrome. The resulting clamp-and-switch mechanism (YAN 2015; QUISTGAARD *et al.* 2016) would allow transport of ferrichrome across the membrane for its assimilation within the cell.

Under iron-limiting conditions, Str1-GFP was first detected after 4 h of induction of germination. Its initial detection revealed that Str1 localized at the cell contour of swollen spores. At later developmental stages, Str1 remained at the cell surface but concentrated at the periphery of the outgrowing germ tube that produced the nascent daughter cell. This cellular localization pattern was reminiscent of that observed in the case of *A. fumigatus* siderophore transporter MirB during conidial swelling (RAYMOND-BOUCHARD *et al.* 2012). In the case of MirB, the protein is enriched at the periphery of a germ tube from which the new mycelium originates and hyphal tips are produced (RAYMOND-BOUCHARD *et al.* 2012). The fact that Str1 localized to the spore contour and the periphery of nascent daughter cells in either the absence or presence of ferrichrome may reflect the critical importance

of siderophore utilization during spore outgrowth in *S. pombe*. In *C. glabrata*, the ferrichrome transporter Sit1 is primarily found at the cell surface under conditions of iron insufficiency, even in the absence of ferrichrome (NEVITT AND THIELE 2011). In contrast, ferrichrome transport through *S. cerevisiae* Arn1 is more complex and requires the presence of ferrichrome to induce the plasma membrane localization of Arn1 and its transport activity (KIM *et al.* 2002; KIM *et al.* 2005). In the absence of ferrichrome, trafficking of Arn1 to the plasma membrane is blocked and the protein is sorted directly from the secretory pathway to the vacuole for degradation (DENG *et al.* 2009). These examples illustrate the fact that there are fundamental differences with respect to the mechanism of ferrichrome acquisition in fungi. Nonetheless, our results clearly showed the ability of *S. pombe* to produce and to acquire ferrichrome as an essential step for outgrowth during spore germination under iron deficiency.

ACKNOWLEDGMENTS

We are indebted to Dr. Gilles Dupuis for critical review of the manuscript and for his valuable comments. We gratefully acknowledge Dr. Léonid Volkov for excellent assistance in flow cytometry experiments. The *S. pombe* strain FY12806 was provided by the Yeast Genetic Resource Center of Japan (YGRC/NBRP; http://yeast.lab.nig.ac.jp/nig/). S.P. is the recipient of an Alexander Graham Bell Canada Graduate Doctoral studentship from the Natural Sciences and Engineering Research Council of Canada (NSERC). This study was supported by the Natural Sciences and Engineering Research Council of Canada (NSERC, grant #RGPIN-2015/2020-04878) to S.L.

CONFLICT OF INTEREST

The authors declare that they have no conflict of interest with the content of this article.

AUTHOR CONTRIBUTIONS

S.P. performed the experiments. S.P. and S.L. designed and analyzed data. S.P. and S.L. conceptualized research and wrote the manuscript. All authors reviewed the results and approved the final version of the manuscript.

Footnotes

[1] Abbreviations used are: bp, base pair(s); BPS, bathophenanthroline disulfonate; DIC, differential interference contrast; Dip, 2, 2'-dipyridyl; FSC, forward light scatter; GFP, green fluorescent protein; MFS, Major Facilitator Superfamily; ORF, open reading frame; PCR, polymerase chain reaction; SDS, sodium dodecyl sulfate; SITD, SIderophore Transporter Domain; SSC, side-scatter; TLC, thin-layer chromatography; WT, wild-type; YES, yeast extract plus supplements.

Literature Cited

Askwith, C., and J. Kaplan, 1997 An oxidase-permease-based iron transport system in *Schizosaccharomyces pombe* and its expression in *Saccharomyces cerevisiae*. J. Biol. Chem. 272**:** 401-405.

Blyth, J., V. Makrantoni, R. E. Barton, C. Spanos, J. Rappsilber *et al.*, 2018 Genes Important for Schizosaccharomyces pombe Meiosis Identified Through a Functional Genomics Screen. Genetics 208**:** 589-603.

Bohnsack, B. L., and K. K. Hirschi, 2004 Nutrient regulation of cell cycle progression. Annu. Rev. Nutr. 24**:** 433-453.

Bonazzi, D., J. D. Julien, M. Romao, R. Seddiki, M. Piel *et al.*, 2014 Symmetry breaking in spore germination relies on an interplay between polar cap stability and spore wall mechanics. Dev. Cell 28**:** 534-546.

Brault, A., T. Mourer and S. Labbé, 2015 Molecular basis of the regulation of iron homeostasis in fission and filamentous yeasts. IUBMB Life 67**:** 801-815.

Brault, A., C. Rallis, V. Normant, J. M. Garant, J. Bahler *et al.*, 2016 Php4 is a key player for iron economy in meiotic and sporulating cells. G3 6**:** 3077-3095.

Chen, D., W. M. Toone, J. Mata, R. Lyne, G. Burns *et al.*, 2003 Global transcriptional responses of fission yeast to environmental stress. Mol. Biol. Cell 14**:** 214-229.

Coluccio, A. E., R. K. Rodriguez, M. J. Kernan and A. M. Neiman, 2008 The yeast spore wall enables spores to survive passage through the digestive tract of *Drosophila*. PLoS One 3**:** e2873.

Das, M., D. J. Wiley, X. Chen, K. Shah and F. Verde, 2009 The conserved NDR kinase Orb6 controls polarized cell growth by spatial regulation of the small GTPase Cdc42. Curr. Biol. 19**:** 1314-1319.

Deng, Y., Y. Guo, H. Watson, W. C. Au, M. Shakoury-Elizeh *et al.*, 2009 Gga2 mediates sequential ubiquitin-independent and ubiquitin-dependent steps in the trafficking of ARN1 from the trans-Golgi network to the vacuole. J. Biol. Chem. 284**:** 23830-23841.

Dworkin, J., and I. M. Shah, 2010 Exit from dormancy in microbial organisms. Nat. Rev. Microbiol. 8**:** 890-896.

Egel, R., M. Willer, S. Kjaerulff, J. Davey and O. Nielsen, 1994 Assessment of pheromone production and response in fission yeast by a halo test of induced sporulation. Yeast 10**:** 1347-1354.

Eisendle, M., H. Oberegger, I. Zadra and H. Haas, 2003 The siderophore system is essential for viability of *Aspergillus nidulans*: functional analysis of two genes encoding l-ornithine N 5-monooxygenase (sidA) and a non-ribosomal peptide synthetase (sidC). Mol. Microbiol. 49**:** 359-375.

Eisendle, M., M. Schrettl, C. Kragl, D. Muller, P. Illmer *et al.*, 2006 The intracellular siderophore ferricrocin is involved in iron storage, oxidative-stress resistance, germination, and sexual development in *Aspergillus nidulans*. Eukaryot. Cell 5**:** 1596-1603.

Fukunishi, K., K. Miyakubi, M. Hatanaka, N. Otsuru, A. Hirata *et al.*, 2014 The fission yeast spore is coated by a proteinaceous surface layer comprising mainly Isp3. Mol. Biol. Cell 25**:** 1549-1559.

Garcia, I., V. Tajadura, V. Martin, T. Toda and Y. Sanchez, 2006 Synthesis of alpha-glucans in fission yeast spores is carried out by three alpha-glucan synthase paralogues, Mok12p, Mok13p and Mok14p. Mol. Microbiol. 59**:** 836-853.

Haas, H., 2003 Molecular genetics of fungal siderophore biosynthesis and uptake: the role of siderophores in iron uptake and storage. Appl. Microbiol. Biotechnol. 62**:** 316-330.

Hatanaka, M., and C. Shimoda, 2001 The cyclic AMP/PKA signal pathway is required for initiation of spore germination in *Schizosaccharomyces pombe*. Yeast 18**:** 207-217.

Hissen, A. H., A. N. Wan, M. L. Warwas, L. J. Pinto and M. M. Moore, 2005 The *Aspergillus fumigatus* siderophore biosynthetic gene sidA, encoding L-ornithine N5-oxygenase, is required for virulence. Infect. Immun. 73**:** 5493-5503.

Hu, C. J., C. Bai, X. D. Zheng, Y. M. Wang and Y. Wang, 2002 Characterization and functional analysis of the siderophore-iron transporter CaArn1p in *Candida albicans*. J. Biol. Chem. 277**:** 30598-30605.

Jbel, M., A. Mercier, B. Pelletier, J. Beaudoin and S. Labbé, 2009 Iron activates in vivo DNA binding of *Schizosaccharomyces pombe* transcription factor Fep1 through its amino-terminal region. Eukaryot. Cell 8**:** 649-664.

Keeney, J. B., and J. D. Boeke, 1994 Efficient targeted integration at *leu1-32* and *ura4-294* in *Schizosaccharomyces pombe*. Genetics 136**:** 849-856.

Kim, Y., S. M. Lampert and C. C. Philpott, 2005 A receptor domain controls the intracellular sorting of the ferrichrome transporter, ARN1. EMBO J. 24**:** 952-962.

Kim, Y., C. W. Yun and C. C. Philpott, 2002 Ferrichrome induces endosome to plasma membrane cycling of the ferrichrome transporter, Arn1p, in *Saccharomyces cerevisiae*. EMBO J. 21**:** 3632-3642.

Kloimwieder, A., and F. Winston, 2011 A Screen for Germination Mutants in *Saccharomyces cerevisiae*. G3 1**:** 143-149.

Labbé, S., M. G. Khan and J. F. Jacques, 2013 Iron uptake and regulation in *Schizosaccharomyces pombe*. Curr. Opin. Microbiol. 16**:** 669-676.

Marston, A. L., and A. Amon, 2004 Meiosis: cell-cycle controls shuffle and deal. Nat. Rev. Mol. Cell Biol. 5**:** 983-997.

Matzanke, B. F., E. Bill, A. X. Trautwein and G. Winkelmann, 1987 Role of siderophores in iron storage in spores of *Neurospora crassa* and *Aspergillus ochraceus*. J. Bacteriol. 169**:** 5873-5876.

Mercier, A., and S. Labbé, 2010 Iron-dependent remodeling of fungal metabolic pathways associated with ferrichrome biosynthesis. Appl. Environ. Microbiol. 76**:** 3806-3817.

Mercier, A., S. Watt, J. Bahler and S. Labbé, 2008 Key function for the CCAAT-binding factor Php4 to regulate gene expression in response to iron deficiency in fission yeast. Eukaryot. Cell 7**:** 493-508.

Moore, R. E., Y. Kim and C. C. Philpott, 2003 The mechanism of ferrichrome transport through Arn1p and its metabolism in *Saccharomyces cerevisiae*. Proc. Natl. Acad. Sci. U S A 100**:** 5664-5669.

Mourer, T., J. F. Jacques, A. Brault, M. Bisaillon and S. Labbé, 2015 Shu1 is a cell-surface protein involved in iron acquisition from heme in *Schizosaccharomyces pombe*. J. Biol. Chem. 290**:** 10176-10190.

Mourer, T., V. Normant and S. Labbé, 2017 Heme assimilation in *Schizosaccharomyces pombe* requires cell-surface-anchored protein Shu1 and vacuolar transporter Abc3. J. Biol. Chem. 292**:** 4898-4912.

Nevitt, T., and D. J. Thiele, 2011 Host iron withholding demands siderophore utilization for *Candida glabrata* to survive macrophage killing. PLoS Pathog. 7**:** e1001322.

Normant, V., T. Mourer and S. Labbé, 2018 The major facilitator transporter Str3 is required for low-affinity heme acquisition in *Schizosaccharomyces pombe*. J. Biol. Chem. 293**:** 6349-6362.

Pelletier, B., J. Beaudoin, Y. Mukai and S. Labbé, 2002 Fep1, an iron sensor regulating iron transporter gene expression in *Schizosaccharomyces pombe*. J. Biol. Chem. 277**:** 22950-22958.

Pelletier, B., J. Beaudoin, C. C. Philpott and S. Labbé, 2003 Fep1 represses expression of the fission yeast *Schizosaccharomyces pombe* siderophore-iron transport system. Nucleic Acids Res. 31**:** 4332-4344.

Philpott, C. C., O. Protchenko, Y. W. Kim, Y. Boretsky and M. Shakoury-Elizeh, 2002 The response to iron deprivation in *Saccharomyces cerevisiae*: expression of siderophore-based systems of iron uptake. Biochem. Soc. Trans. 30**:** 698-702.

Philpott, C. C., J. Rashford, Y. Yamaguchi-Iwai, T. A. Rouault, A. Dancis *et al.*, 1998 Cell-cycle arrest and inhibition of G1 cyclin translation by iron in AFT1-1(up) yeast. EMBO J. 17**:** 5026-5036.

Plante, S., V. Normant, K. M. Ramos-Torres and S. Labbé, 2017 Cell-surface copper transporters and superoxide dismutase 1 are essential for outgrowth during fungal spore germination. J. Biol. Chem. 292**:** 11896-11914.

Pouliot, B., M. Jbel, A. Mercier and S. Labbé, 2010 *abc3*$^{+}$ encodes an iron-regulated vacuolar ABC-type transporter in *Schizosaccharomyces pombe*. Eukaryot. Cell 9**:** 59-73.

Quistgaard, E. M., C. Low, F. Guettou and P. Nordlund, 2016 Understanding transport by the major facilitator superfamily (MFS): structures pave the way. Nat. Rev. Mol. Cell Biol. 17**:** 123-132.

Rad, A. M., B. Janic, A. S. Iskander, H. Soltanian-Zadeh and A. S. Arbab, 2007 Measurement of quantity of iron in magnetically labeled cells: comparison among different UV/VIS spectrometric methods. Biotechniques 43**:** 627-628.

Raymond-Bouchard, I., C. S. Carroll, J. R. Nesbitt, K. A. Henry, L. J. Pinto *et al.*, 2012 Structural requirements for the activity of the MirB ferrisiderophore transporter of *Aspergillus fumigatus*. Eukaryot. Cell 11**:** 1333-1344.

Roman, D. G., A. Dancis, G. J. Anderson and R. D. Klausner, 1993 The fission yeast ferric reductase gene *frp1*$^{+}$ is required for ferric iron uptake and encodes a protein that is homologous to the gp91-phox subunit of the human NADPH phagocyte oxidoreductase. Mol. Cell. Biol. 13**:** 4342-4350.

Sabatinos, S. A., and S. L. Forsburg, 2009 Measuring DNA content by flow cytometry in fission yeast. Methods Mol. Biol. 521**:** 449-461.

Sabatinos, S. A., and S. L. Forsburg, 2010 Molecular genetics of *Schizosaccharomyces pombe*. Methods Enzymol. 470**:** 759-795.

Schrettl, M., E. Bignell, C. Kragl, Y. Sabiha, O. Loss *et al.*, 2007 Distinct roles for intra- and extracellular siderophores during *Aspergillus fumigatus* infection. PLoS Pathog. 3**:** 1195-1207.

Schrettl, M., G. Winkelmann and H. Haas, 2004 Ferrichrome in *Schizosaccharomyces pombe*-an iron transport and iron storage compound. Biometals 17**:** 647-654.

Schwecke, T., K. Gottling, P. Durek, I. Duenas, N. F. Kaufer *et al.*, 2006 Nonribosomal peptide synthesis in *Schizosaccharomyces pombe* and the architectures of ferrichrome-type siderophore synthetases in fungi. Chembiochem 7**:** 612-622.

Shah, I. M., M. H. Laaberki, D. L. Popham and J. Dworkin, 2008 A eukaryotic-like Ser/Thr kinase signals bacteria to exit dormancy in response to peptidoglycan fragments. Cell 135**:** 486-496.

Shi, L., Z. Li, H. Tachikawa, X. D. Gao and H. Nakanishi, 2014 Use of yeast spores for microencapsulation of enzymes. Appl. Environ. Microbiol. 80**:** 4502-4510.

Shigehisa, A., D. Okuzaki, T. Kasama, H. Tohda, A. Hirata *et al.*, 2010 Mug28, a meiosis-specific protein of *Schizosaccharomyces pombe*, regulates spore wall formation. Mol. Biol. Cell 21**:** 1955-1967.

Shimoda, C., 1980 Differential effect of glucose and fructose on spore germination in the fission yeast *Schizosaccharomyces pombe*. Can. J. Microbiol. 26**:** 741-745.

Tatebe, H., K. Nakano, R. Maximo and K. Shiozaki, 2008 Pom1 DYRK regulates localization of the Rga4 GAP to ensure bipolar activation of Cdc42 in fission yeast. Curr. Biol. 18**:** 322-330.

Yan, N., 2015 Structural biology of the Major Facilitator Superfamily transporters. Annu. Rev. Biophys. 44**:** 257-283.

Yuan, W. M., G. D. Gentil, A. D. Budde and S. A. Leong, 2001 Characterization of the *Ustilago maydis sid2* gene, encoding a multidomain peptide synthetase in the ferrichrome biosynthetic gene cluster. J. Bacteriol. 183**:** 4040-4051.

Yun, C. W., J. S. Tiedeman, R. E. Moore and C. C. Philpott, 2000 Siderophore-iron uptake in *Saccharomyces cerevisiae*. Identification of ferrichrome and fusarinine transporters. J. Biol. Chem. 275**:** 16354-16359.

Discussion

La majorité des résultats que j'ai obtenus ont été décrits et discutés dans les manuscrits inclus dans cette thèse. Je me concentrerai dans les prochaines sections sur les principales interrogations et pistes d'investigation qui découlent de ces résultats. Je me baserai sur des résultats non publiés que j'ai obtenus et des observations rapportées en littérature.

1. Régulation de la germination

1.1. Déterminants nutritionnels

La germination se doit d'être finement régulée. La réalisation de ce processus qui permet la transition de l'état de spore vers une forme végétative en croissance représente un risque audacieux pour les mycètes. Les spores doivent être vigilantes au moment de s'engager en germination, puisqu'il s'agit pour eux de croître dans un nouvel environnement qu'ils auront jugé adéquat pour leur prolifération. La cellule fongique adopte un état de spore pour sa survie. Une épaisse paroi autour de la spore, des molécules protectrices qui s'accumulent dans le cytoplasme et un métabolisme au ralenti limitent les interactions avec des facteurs potentiellement nocifs. Au contraire, si l'environnement extracellulaire est favorable, les spores abandonnent leurs composantes protectrices pour initier le cycle cellulaire et commencer à croître. La régulation de la germination doit assurer d'abord que les spores ne s'y engagent pas accidentellement. Les spores jaugent minutieusement le statut nutritionnel de leur environnement afin de détecter les conditions adéquates pour leur germination. Une attention particulière a été accordée à l'étude des déterminants nutritionnels nécessaires pour l'initiation de la

germination fongique. Les observations accumulées dans un grand nombre d'espèces permettent de conclure que la présence d'eau et de sucre fermentable sont des signaux généralisés, incluant chez *S. pombe*, qui enclenchent la germination. Par contre, les déterminants qui régulent les autres étapes de la germination sont peu connus.

Nos travaux ont mis en évidence qu'un apport adéquat en ions Cu et Fe est strictement nécessaire pour l'éclosion des spores et l'émergence d'une projection germinative. Ces résultats ajoutent à notre compréhension de la régulation tout au long de la germination. L'éclosion est une étape sensible de la germination puisqu'elle mène à la croissance d'une projection hors de la paroi protectrice de la spore. L'assimilation de Cu et de Fe sert donc de point de contrôle qui autorise la complétion de cette étape charnière.

Les ions Cu et Fe sont des cofacteurs essentiels pour le métabolisme des cellules végétatives. L'activation de la SOD1 et l'accumulation de FC intracellulaire semblent être des événements importants dans l'activation du métabolisme des spores en germination. Sans ces événements, les cellules suspendent leur croissance pour s'abriter au sein de la paroi protectrice de la spore.

1.2. Régulation globale transcriptionnelle

La germination comprend d'importants changements métaboliques et morphologiques qui doivent être finement coordonnés afin d'accélérer ce processus. Il est vital pour les spores se retrouvant dans une nouvelle niche de reprendre rapidement la croissance puisque, dans la nature, plusieurs microorganismes se livrent inévitablement une compétition pour les nutriments présents dans l'environnement. La rapidité de la germination est aussi un élément déterminant pour la

pathogénèse. Les spores de *A. fumigatus* ou *C. neoformans*, qui se logent dans les alvéoles pulmonaires, engagent une course au système immunitaire afin de germer rapidement dans le but de coloniser leur hôte (Nevitt and Thiele, 2011).

Des travaux chez *S. cerevisiae*, *A. fumigatus* et *A. niger* ont permis de mieux comprendre les changements transcriptionnels globaux qui entraînent la germination (Geijer et al., 2012; Joseph-Strauss et al., 2007; van Leeuwen et al., 2013; Oda et al., 2017). Ces études révèlent des changements importants dans l'abondance d'ARN au cours de la germination. Plus particulièrement, les changements les plus importants surviennent à l'activation de spores. La sortie des spores de leur état de dormance s'accompagne d'une répression de gènes associés au stress et à la sporulation. Le profil transcriptionnel des spores activés révèle aussi l'activation du métabolisme qui sollicite une consommation d'énergie importante. Les gènes associés à la transcription d'ARN, la biogénèse des ribosomes et la traduction sont rapidement induits après l'enclenchement de la germination. Le métabolisme du glucose est aussi activé. D'une part, la respiration cellulaire est positivement régulée à l'initiation de la germination; d'autre part, la néoglucogénèse semble réprimée. Par la suite, il y a une régulation positive du cycle cellulaire et de la synthèse et réplication de l'ADN à l'étape de croissance isotrope. La polarisation de la croissance lors de la germination chez *A. niger* et *A. nidulans* implique étonnamment de faibles changements transcriptionnels (van Leeuwen et al., 2013; Oda et al., 2017).

Les travaux chez *S. cerevisiae* ont permis d'identifier un réseau de facteurs de transcription orchestrant le programme d'expression génique (Geijer et al., 2012). Ce réseau inclut d'abord Hsf1. L'activité de ce facteur est présumément requise

lors de l'initiation de la germination, alors que les spores métabolisent leurs réserves de tréhalose qui serviraient de molécules protectrices. Il semble qu'il y ait ensuite un pic d'activité des facteurs Sok2, Yap6 et Phd1 qui sont impliqués dans le phénomène d'oscillation métabolique et respiratoire. Subséquemment, il y a induction des gènes impliqués dans la ribogénèse, qui impliquerait notamment les facteurs Fhl1 et Sfp1. Le programme transcriptionnel qui a été identifié chez *S. cerevisiae* révèle que lors de la germination, les gènes qui sont induits codent pour des protéines impliquées dans l'adaptation métabolique en réponse aux nouvelles conditions nutritionnelles des spores en éclosion.

Nos travaux ont permis de caractériser l'adaptation des spores en germination à la carence en ions Cu ou Fe. Nous avons pu déterminer le profil transcriptionnel de certains gènes spécifiques codant pour les composantes d'acquisition des ions Cu et Fe et nous avons identifié les facteurs de transcription impliqués dans la régulation de la transcription de ces gènes. Par contre, le profil transcriptionnel global des spores de *S. pombe* en germination n'est toujours pas connu. Plusieurs techniques, tel le séquençage à haut débit de l'ARN (RNAseq), nous permettront de caractériser les changements du transcriptome à chaque étape de la germination. Il serait certainement intéressant d'explorer plus largement les régulations transcriptionnelles qui surviennent durant la germination. Cela nous permettrait d'améliorer notre portrait de l'adaptation métabolique qui survient au cours de la germination chez *S. pombe*.

2. Espèces réactives de l'oxygène et développement

Nos résultats ont mis en évidence que la superoxyde dismutase SOD1 a un rôle crucial dans la complétion de la germination chez *S. pombe*. Plus précisément, l'activation de la SOD1 qui requiert le cofacteur Cu pour son activité catalytique est requise pour l'éclosion des spores et l'émergence d'une projection germinative. Sans son activité de disproportion des anions superoxydes, les spores restent rondes et ne présentent pas de signe de croissance polarisée. Ce résultat suggère que des anions superoxydes sont présents à ces étapes et doivent être éliminés pour la progression de la germination.

Les anions superoxydes peuvent être détectés *in vivo* grâce au nitrobleu de tétrazolium (NBT) (Bournonville and Díaz-Ricci, 2011). Les anions superoxydes oxydent ce composé, ce qui résulte en un précipité violet qui se détecte facilement en microscopie optique de type Nomarski. Des spores de type sauvage ont été induites en germination dans un milieu basal. Un échantillon de ces spores a été prélevé à différents moments après l'induction de la germination. Les spores ont été exposées à 2,5mM NBT à 30 °C dans le noir, puis ont été rapidement analysées par microscopie Nomarski (figure 10). Dès leur activation (2h), les spores ont une forte coloration au NBT, comparativement aux spores en dormance (0h) qui ne colorent pratiquement pas. Cela laisse supposer que les spores activées contiennent une grande quantité d'anions superoxydes. La marque du NBT reste aussi forte pour les spores en croissance isotrope. Après l'éclosion et l'émergence d'une projection, les spores présentent une coloration au NBT différente. La spore mère semble dépourvue d'anions superoxydes. La coloration au NBT est limitée exclusivement à l'extrémité en croissance de la projection (figure 10, 8-9-10h). La SOD1 est l'enzyme spécialisée qui métabolise les anions superoxydes. L'activité

SOD1 en germination pourrait donc être nécessaire parce que les spores en croissance isotrope ont accumulé beaucoup d'anions superoxydes et que l'éclosion subséquente demande qu'il y ait réduction des ROS.

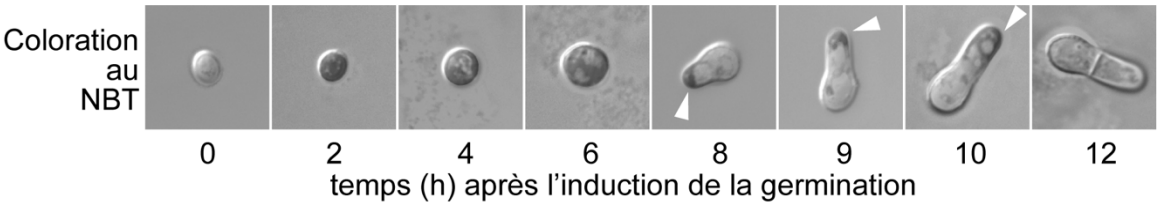

Figure 10 – Coloration au NBT au cours de la germination.
Des spores de type sauvage ont été synchronisées en germination dans un milieu YES basal. Aux temps indiqués après l'induction de la germination, 2,5mM NBT ont été ajoutés à un échantillon de la culture. Après 30 minutes de coloration, les cellules ont été observées par microscopie Nomarski. Les pointes de flèche blanches indiquent les portions marquées au NBT dans les projections en croissance.

2.1. NADPH oxydase impliquée dans la dominance apicale

Des évidences de plus en plus nombreuses accordent des rôles physiologiques aux ROS qui dépassent leur simple nature de sous-produits métaboliques avec des charges électroniques excédentaires. Notamment, la production localisée de ROS a été associée avec des processus de développement, de différenciation et de croissance polarisée chez plusieurs espèces fongiques et même lors la germination des grains de pollen (*A. thaliana*) (Aguirre et al., 2005; Scott and Eaton, 2008; Semighini and Harris, 2008; Smirnova et al., 2014). Les NADPH oxydases (NOXs) sont responsables de la production localisée d'anions superoxydes pour le contrôle de la croissance chez *A. nidulans*, *Epichloë festucae*, *N. crassa*, *Podospora anserin*a et *C. albicans* (Cano-Domínguez et al., 2008; Malagnac et al., 2004; Rossi et al., 2017; Tanaka et al., 2008). La production de ROS par les NOXs a été

visualisée par coloration au NBT. Elle se concentre à l'extrémité des hyphes ou des projections germinatives en croissance. Les anions superoxydes générés serviraient de molécules de signalisation qui favoriseraient la stabilisation de la croissance polarisée. Il s'agit d'un processus nommé "dominance apicale".

La localisation des anions superoxydes que j'ai pu observer dans les spores de *S. pombe* en germination (figure 10) est très semblable à la localisation rapportée des ROS générées par le NOXs dans différentes espèces fongiques. Cette ressemblance peut suggérer que des mécanismes similaires régulent la dominance apicale lors de l'émergence de projection germinative chez *S. pombe*. Dans cette espèce, seulement deux protéines, nommées Frp1 et Frp2, sont homologues aux nombreuses NOXs fongiques. Frp1 agit comme une réductase de Fe à la surface des cellules. Dans le cas de Frp2, bien que cette protéine ait été annotée comme une ferriréductase, sa localisation cellulaire et son rôle biologique ne sont toujours pas connus. Les ferriréductases divergent des NOX A, B et C fongiques étant donné qu'elles couplent l'oxydation du NADPH à la réduction des ions Fe (Aguirre et al., 2005).

Toutefois, il n'est pas exclu que Frp1 et/ou Frp2 puissent générer des anions superoxydes. Le pathogène opportuniste *C. albicans* peut passer d'une forme de levure à bourgeon unicellulaire à un hyphe multicellulaire. Cette transition morphologique dépend d'une accumulation de ROS qui a été attribuée à la protéine Fre8 (Rossi et al., 2017). Initialement, cette protéine été annotée comme une ferriréductase, mais il semble qu'elle catalyse la réduction de l'oxygène en anions superoxydes. Il est donc possible que les délétions *frp1*Δ, *frp2*Δ, ou encore *frp1*Δ *frp2*Δ engendrent des défauts dans l'accumulation de ROS. Si c'est le cas, ces défauts seraient visibles par une diminution de la coloration au NBT. Un manque

dans la formation de ROS à l'extrémité en croissance de la projection germinative pourrait d'ailleurs avoir une incidence sur la croissance. Les spores de mutants *frp1*Δ, *frp2*Δ, et *frp1*Δ *frp2*Δ pourraient donc avoir des projections plus courtes ou être incapables de former des projections lors du programme de germination.

3. Rôles des sidérophores en germination

La ferritine chez les animaux et des protéines homologues chez les plantes et les bactéries servent à emmagasiner le Fe (Arosio and Levi, 2002). Par contre, le génome des mycètes ne semble pas coder pour de telles protéines. L'utilisation des sidérophores est une stratégie adoptée par les mycètes pour le stockage du Fe. Toutes les levures productrices de sidérophores étudiées jusqu'à maintenant possèdent des sidérophores intracellulaires qui sont de la famille des ferrichromes (Haas et al., 2008). *S. pombe*, *U. maydis* et *U. sphaerogena* accumulent le ferrichrome, alors que les espèces *Aspergillus, N. crassa*, *F. graminaerum* et *M grisea* accumulent plutôt la ferricrocine. Le Fe lié aux sidérophores compte pour 50 % du Fe total chez *U. maydis* et jusqu'à 64% chez *A. nidulans* (Haas et al., 2008). Les sidérophores ont aussi un rôle dans le développement sexuel et asexuel de différentes espèces *Aspergillus*. Les sidérophores chélatent de 47 % à 74 % du Fe total dans les spores d'*A. fumigatus* et *A. nidulans* (Eisendle et al., 2006; Matzanke et al., 1987; Schrettl et al., 2007). D'ailleurs, les sidérophores intracellulaires servent d'importants facteurs de germination pour les spores d'*A. fumigatus*, *A. nidulans* et *N. crassa*. Plus précisément, des travaux chez *A. fumigatus* ont révélé que l'inhibition de la synthèse des sidérophores intracellulaires diminue l'activité de la catalase A dans les spores (Schrettl et al., 2007). La sporulation chez *A. fumigatus* se produit sur des hyphes aériens qui emergent du milieu

de culture. Les sidérophores intracellulaires servent de véhicules pour la distribution du Fe. Sans ces sidérophores le contenu des spores en Fe est faible, expliquant la diminution d'activité Fe-dépendantes comme la catalase. Étant donné que cet enzyme est le principal acteur dans la détoxification du peroxyde, cela provoque une diminution de la résistance au stress oxydatif chez ces conidies. De manière similaire, des travaux chez *U. maydis* suggèrent un rôle du ferrichrome intracellulaire dans la résistance au stress oxydatif (Leong and Winkelmann, 1998). Le rationnel proposé est que les ions Fe liés par les sidérophores ne seraient plus disponibles pour la réaction de Fenton.

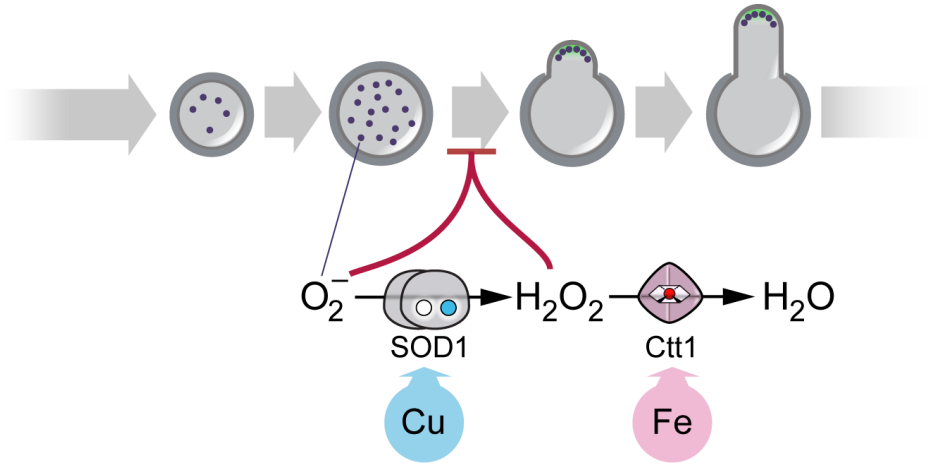

Figure 11 – Modèle de l'implication des ions Cu et Fe au cours de la germination chez *S. pombe*.
Les anions superoxydes (points violets) s'accumulant dans les spores en croissance isotrope sont disproportionnés par la SOD1 qui requiert du Cu pour son activité. Le produit de réaction de la SOD1, le peroxyde d'hydrogène, est à son tour détoxifié grâce à l'activité catalase Ctt1 qui nécessite un groupement hème, composé de Fe. Ces deux activités enzymatiques sont cruciales pour le bon déroulement de l'éclosion, puisque l'accumulation des anions superoxydes et du peroxyde d'hydrogène inhibe la croissance polarisée.

La participation des sidérophores à la résistance au stress oxydatif est une fonction qui paraît avoir du sens dans le contexte où la disproportion des anions superoxydes est une activité indispensable pour l'éclosion des spores en germination. Puisque la réaction catalysée par la SOD1 produit le peroxyde d'hydrogène, sa détoxification par la catalase pourrait être cruciale (figure 11). Les sidérophores pourraient participer à l'émergence d'une projection germinative en distribuant leur ion métallique à des sentiers Fe dépendants tel celui impliqué dans l'activation de la catalase. L'activité de la catalase Cat1 de *S. pombe* pourrait être dépendante de la présence du FC intracellulaire comme il a été observé chez *A. fumigatus*. La déficience en activité de la catalase CatA dans les spores de cette espèce contribuerait en partie à un délai dans leur germination. De manière cohérente, la surexpression de la catalase Cat1 chez *Metarhizium anisopliae* raccourcit le temps de germination des spores (Morales Hernandez et al., 2010). Il serait intéressant de tester si les spores de *S. pombe* dépourvues de catalase (*cat1*Δ) peuvent compléter le programme de germination de manière similaire à des spores de type sauvage.

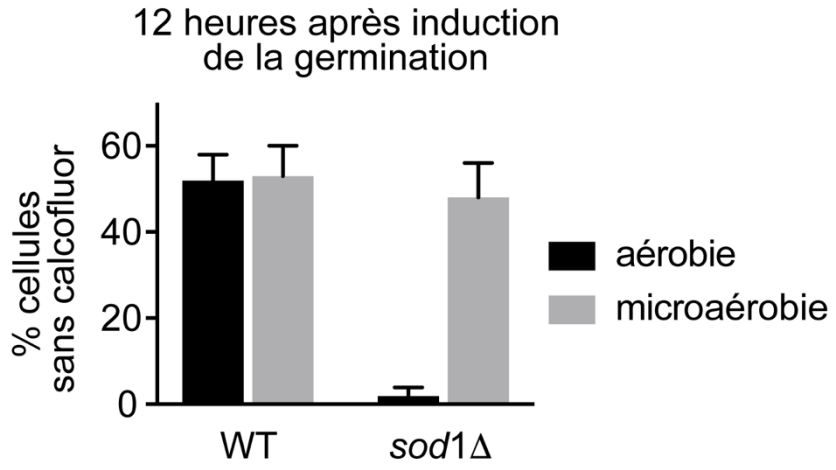

Figure 12 – Germination des spores *sod1*Δ en microaérobie
Des spores de type sauvage ou *sod1*Δ ont été synchronisées en germination dans un milieu YES basal en condition aérobie ou microaérobie (jarre BD GasPak system). 12 heures après l'induction de la germination, la proportion de cellules dépourvue de calcofluor a été comptée. Les résultats sont la moyenne ± déviation standard de trois réplicas.

De plus, l'arrêt des spores *sod1*Δ en germination peut être renversé en induisant la germination dans une jarre microaérobique (Figure 12). Le rationnel pour expliquer ce résultat est que le stress oxydatif induit par la déficience en SOD1 qui cause l'arrêt de germination peut être amenuiser en diminuant la concentration d'oxygène dans l'environnement de spores. Notre hypothèse est que l'arrêt de germination associé à une déficience en FC peut être expliqué par leur implication dans la résistance au stress oxydatif. Si c'est le cas, la germination de spores *sib1*Δ *sib2*Δ devrait être rétablie dans un environnement microaérophilique.

4. Rôles de la vacuole dans la régulation du ferrichrome

Les protéines Str1, Str2 et Str3 chez *S. pombe* ont une homologie de séquence avec les transporteurs de sidérophores Arn1 à 4 de *S. cerevisiae*. Les résultats que j'ai obtenus révèlent que Str1 est le transporteur de FC à la membrane plasmique. Str3 a plutôt un rôle dans le transport de l'hème (Normant et al., 2018). Quant à Str2, son rôle physiologique reste à être déterminé. Des expériences d'expression hétérologue dans une souche de *S. cerevisiae* mutante pour l'acquisition du Fe suggèrent que Str2 peut transporter du ferrichrome et de la ferrioxamine B (Pelletier et al., 2003). La délétion du gène *str2*$^{+}$ (*str2*Δ) cause une forte inhibition de la croissance cellulaire sur un milieu carencé en Fe avec 100 μM Dip (figure 13A). Ce phénotype est carence-dépendant puisque la souche mutante

croît aussi bien que la souche de type sauvage sur un milieu YES contrôle contenant suffisamment de fer. Le défaut de croissance causé par la délétion *str2*Δ est associé au FC puisque la croissance de la souche mutante en présence du chélateur Dip est rétablie par l'ajout de 10 μM FC exogène (figure 13a, Dip+FC). Cependant, les résultats que j'ai obtenus suggèrent que Str2 n'agit pas dans l'assimilation de FC exogène. L'expression dans les cellules *str2*Δ de la protéine Str2 étiquetée avec GFP rétablit une croissance semblable à une souche de type sauvage en présence du chélateur Dip (figure 13a). Ce résultat suggère que la protéine Str2-GFP est fonctionnelle. Des cellules *str2*Δ exprimant Str2-GFP en croissance exponentielle ont été traitées avec 250μM Dip ou 100μM $FeCl_3$ durant 5 heures. La protéine Str2-GFP est localisée à la membrane des vacuoles en carence de Fe (figure 13b). La membrane des vacuoles a été marquée à l'aide du fluorophore FM4-64 afin de confirmer la localisation de Str2-GFP. Il s'agit, à ma connaissance, du premier exemple d'un transporteur fongique de sidérophore localisé à la membrane vacuolaire.

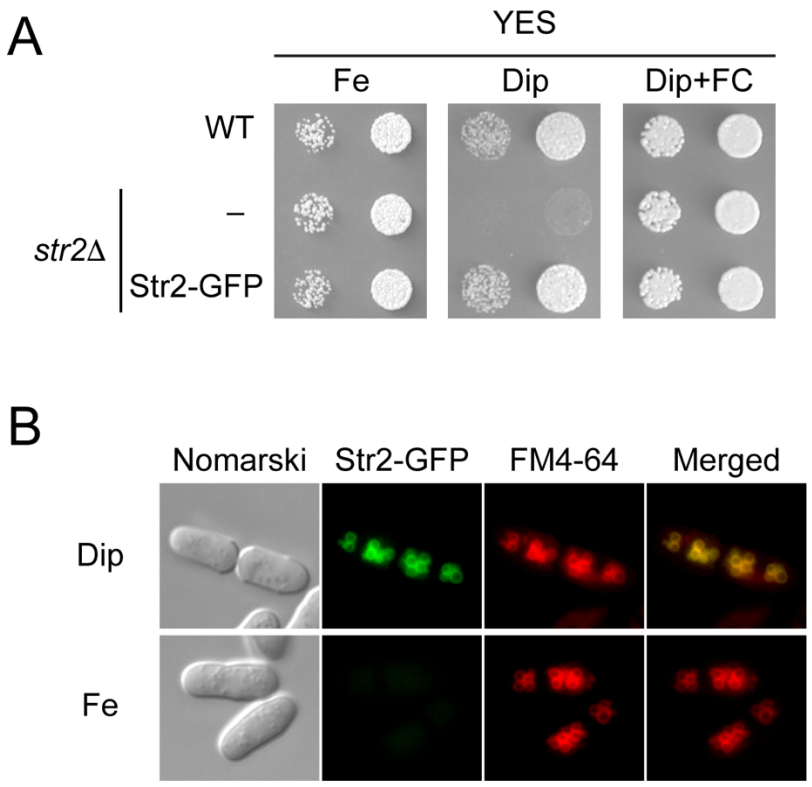

Figure 13 – Croissance inhibée du mutant *str2*Δ en carence de Fe.
A) les souches isogéniques de *S. pombe* de type sauvage, *str2*Δ, ou str2Δ exprimant un allèle codant pour Str2-GFP, ont été déposées sur un milieu YES supplémenté de 50µM $FeCl_3$, un milieu YES additionné de 100 µM Dip, ou un milieu contenant du Dip (100 µM) supplémenté de 10 µM FC (Dip + FC). Les plaques ont ensuite été incubées à 30°C durant 4 jours avant d'être photographiées. B) la souche *str2*Δ exprimant Str2-GFP en croissance exponentielle dans un milieu YES basal a été traitée soit avec 250 µM Dip ou 100 µM $FeCl_3$ durant 5 heures à 30°C. Juste avant l'analyse au microscope, les membranes vacuolaires ont été colorées au FM4-64 (REF). Depuis la gauche; image Nomarski, la fluorescence GFP (vert), la fluorescence du FM4-64 (rouge), et la superposition des images en fluorescence (Merged).

L'utilisation d'un analogue fluorescent du FC a permis de suivre l'assimilation du complexe FC-Fe chez la levure *U. maydis* (Ardon et al., 1998). À la suite de l'exposition des levures à l'analogue de ferrichrome, les auteurs rapportent avoir détecté sa fluorescence concentrée dans des vésicules intracellulaires. La nature de ces vésicules n'a pas été spécifiée, mais leur forme sphérique régulière pourrait

suggérer qu'il s'agisse de vacuoles. Un fait intéressant est qu'il semble qu'une portion des analogues de ferrichrome accumulés dans ces vésicules soit sous forme desferri *i.e.* sans ligand Fe (Ardon et al., 1997). L'accumulation de desferrichrome est cohérente avec un mécanisme de navette des sidérophores. Le ligand des sidérophores est extrait et les sidérophores apo peuvent ensuite être recyclés pour l'assimilation d'autres ions Fe. Un tel mécanisme a été suggéré chez le producteur de ferrichrome *Ustilago sphaerogena* et serait commun pour les mycètes utilisateurs du sidérophore coprogène (Emery, 1971). De manière similaire, le FC et la ferricrocine s'accumulent chez *S. pombe* et les espèces *Aspergillus*, respectivement, sous forme apo (Eisendle et al., 2006; Schrettl et al., 2004). Le sort des sidérophores varie entre les familles et entre les espèces. Le ferrichrome s'accumule chez *S. cerevisiae* dans le cytoplasme sous forme de complexe intacte avec le Fe, alors que la triacétylfusarinine C est hydrolysée après son internalisation chez *A. fumigatus* et *A. nidulans* (Kragl et al., 2007; Moore et al., 2003).

Les données préliminaires que j'ai obtenues suggèrent que la protéine Str2 chez *S. pombe* serait impliquée dans l'accumulation du desferrichrome. Une souche de type sauvage en croissance logarithmique a été incubée durant cinq heures en présence de 250 μM Dip. Puis, les sidérophores ont été extraits, soit de manière native (sans ajout de $FeCl_3$ au tampon d'extraction) ou en saturant les sidérophores de Fe en ajoutant du $FeCl_3$ au tampon d'extraction (figure 14a). La visualisation des sidérophores de la souche de type sauvage par CCM montre que seulement une petite portion des sidérophores intracellulaires totaux sont liés au Fe. Au contraire, les sidérophores de la souche mutante *str2*Δ soumise aux mêmes conditions semblent être en très grande majorité liés au Fe. L'expression de la protéine Str2 étiquetée avec GFP dans la souche *str2*Δ rétablit la présence

de desferrichrome (figure 14b). L'analyse par CCM ne révèle pas une différence marquée pour la quantité totale de ferrichrome intracellulaire, seulement quant à la nature du statut du ferrichrome. Cependant, une analyse plus fine du contenu en sidérophores par chromatographie liquide se révèlerait plus adéquate pour quantifier les sidérophores. Les sidérophores chez *S. pombe* ont déjà été séparés d'un extrait cellulaire par chromatographie en phase inverse (Schrettl et al., 2004). Les sidérophores liés au Fe sont ensuite détectés spectrophotométriquement. Cette procédure pourrait être appliquée pour la quantification des niveaux de ferrichrome lié ou non au Fe.

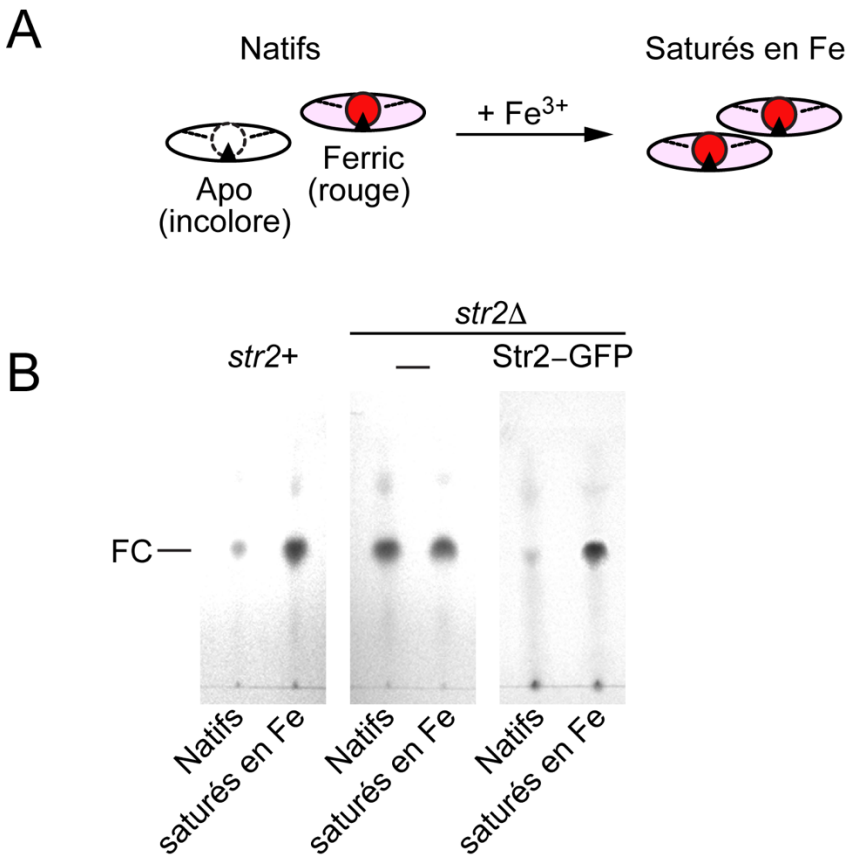

Figure 14 – Effets de la délétion de *str2* sur le métabolisme du FC.
A) l'extraction native des sidérophores permet de récupérer le FC apo et lié au Fe (ferric). Seul le FC lié au Fe contribue au spot visible sur CCM, puisque le FC apo

est incolore. L'ajout de Fe durant l'extraction des sidérophores force la métallation du FC apo (Fe saturation). B) Les souches isogéniques de *S. pombe* de type sauvage, *str2*Δ, et *str2*Δ exprimant un allèle codant pour Str2-GFP, en croissance exponentielle dans un milieu YES ont été exposées à 250 µM Dip durant cinq heures. Une moitié des sidérophores extraits a été conservée sous forme native et l'autre moitié a été saturée en Fe. Les sidérophores ont ensuite été visualisés par CCM.

L'accumulation de desferrichrome modulée par Str2 semble donc essentielle pour la croissance en carence de Fe. Les données obtenues chez le producteur de sidérophores *U. maydis* concernant l'accumulation d'un analogue de FC sous forme *apo* dans des vésicules permettent de supposer que Str2 transporte le FC vers la lumière vacuolaire (figure 15). L'utilisation d'un tel analogue fluorescent de FC chez *S. pombe* permettrait d'explorer cette hypothèse. Ces molécules ne sont cependant pas disponibles commercialement, mais leur schéma de synthèse a été publié (Besserglick et al., 2017). De manière alternative, la fonction de Str2 à la vacuole pourrait être examinée par l'analyse du contenu en FC des vacuoles. Les vacuoles peuvent être purifiées à partir de cellules végétatives de *S. pombe* par centrifugation différentielle (Mourer et al., 2017; Sooksa-nguan et al., 2009). Si Str2 transporte effectivement du FC vers l'intérieur des vacuoles, alors le contenu en FC des vacuoles purifiées d'une souche *str2*Δ devrait être diminué par rapport aux vacuoles purifiées d'une souche de type sauvage.

La lumière acide des vacuoles serait un environnement favorable à la séparation du complexe Fe et FC. La protonation des groupements hydroxamate du FC dans un environnement à bas pH diminue effectivement l'affinité du FC pour le ligand Fe(III) (Ahmed and Holmström, 2014). Une activité enzymatique intracellulaire pourrait être impliquée dans la réduction du Fe(III) lié en Fe(II), contribuant ainsi

au bris du complexe avec le sidérophore (figure 15). Cependant, la protéine impliquée dans une telle activité n'a toujours pas été identifiée.

Le mécanisme de navette du ferrichrome proposé chez *U. Sphaerogena* implique l'accumulation d'un intermédiaire desferrichrome qui serait ensuite sécrété dans l'environnement pour compléter une nouvelle ronde d'assimilation de Fe. Or, très peu de détails sont connus concernant les mécanismes d'excrétion des sidérophores chez les organismes fongiques. De futurs travaux sur la protéine Str2 de *S. pombe* permettraient d'explorer cet aspect du métabolisme des sidérophores fongiques. Dans la mesure où il semble que Str2 soit impliquée dans l'accumulation des desferrichromes intracellulaires, ce transporteur pourrait donc avoir une incidence sur l'excrétion du ferrichrome.

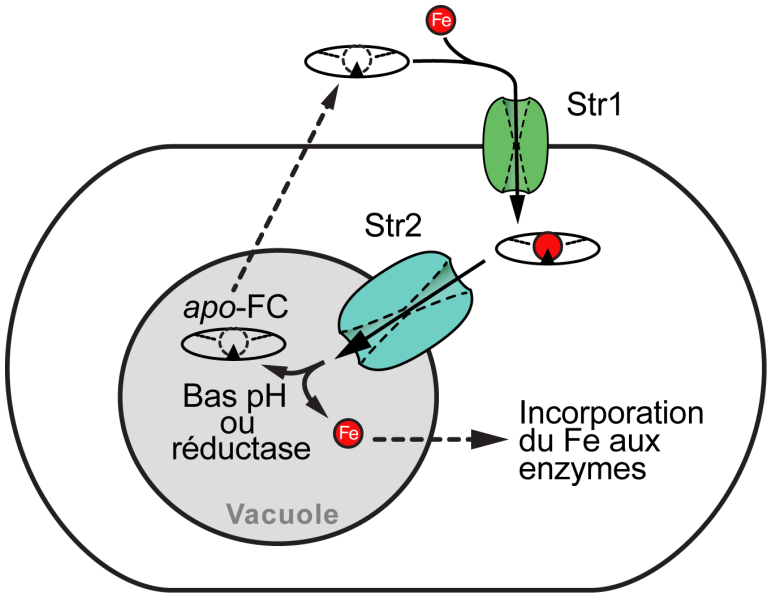

Figure 15 – Modèle de la fonction de Str2 dans le métabolisme du FC chez *S. pombe*.
Le FC intracellulaire est pris en charge par Str2 qui le transporte à l'intérieure des vacuoles. Dans celles-ci, le Fe est libéré du FC par une réductase inconnue ou le bas pH vacuolaire. Le Fe peut alors être incorporé au enzymes Fe-dépendantes, alors que le FC apo peut être excrété dans l'environnement pour l'acquisition de Fe.

5. Les sidérophores fongiques comme cibles thérapeutiques

Il est clair que la synthèse et le transport des sidérophores est un élément central dans l'homéostasie des ions Fe chez la plupart des organismes fongiques. Les sidérophores fonctionnent comme chélateurs extracellulaires de Fe qui sont utilisés par les microorganismes pour l'acquisition de l'ion métallique. Les sidérophores intracellulaires sont aussi impliqués dans la résistance au stress oxydatif, la croissance des cellules et le programme de reproduction sexuelle et asexuelle des levures.

De plus, les sidérophores ont un rôle crucial dans le maintien de l'interaction des organismes fongiques avec leur environnement. L'association symbiotique entre *E. fustucae* et l'herbe est dépendante de la production de sidérophores extracellulaires (Johnson, 2008). La virulence des levures pathogènes de plantes (comme *F. graminearum* et *M. grisea*) ou chez les animaux (comme *A. fumigatus*) est dépendante de la production de sidérophores extracellulaires et intracellulaires (Haas et al., 2008; Schrettl et al., 2007). Ce rôle crucial des sidérophores se reflète par la présence d'au moins deux protéines chez les mammifères, les lipocalines Lcn1 et Lcn2, qui sont capables de séquestrer les sidérophores. Lcn2, aussi connue sous le nom de sidérocaline, a un rôle protecteur contre l'infection par *Escherichia coli* rendu possible grâce à la séquestration de l'entérobactine bactérienne afin d'éviter que cette dernière soit réutilisée comme source de nutriment par les bactéries (Flo et al., 2004; Fluckinger et al., 2004).

Les enzymes impliquées dans la synthèse des sidérophores ou les transporteurs de sidérophores sont effectivement des cibles thérapeutiques très prometteuses puisqu'il s'agit de protéines qui n'ont pas d'homologues chez les mammifères ou

les plantes. Déjà, des composés antibactériens qui ciblent précisément la synthèse des sidérophores ont été développés (Quadri, 2007). Notamment, ces composés ne présentent pas de toxicité contre des cellules mammifères *in vitro*.

Une autre stratégie exploitant la nature unique du système d'acquisition des sidérophores est la conjugaison d'un composé antifongique avec un sidérophore. La caractérisation du potentiel d'action d'un antibiotique couplé à des sidérophores contre différentes espèces *Candida* (Bernier et al., 2005) a montré que son efficacité dépend de l'affinité de l'espèce pour le sidérophore utilisé. Les produits conjugués contenant l'antibiotique desketoneoenactin avec des groupements hydroxamate sont assimilés par des mécanismes communs aux sidérophores naturels (Bernier et al., 2005). Une meilleure compréhension des mécanismes moléculaires de l'acquisition des sidérophores permettra certainement de concevoir de meilleurs conjugués avec une activité antifongique améliorée. Il sera, de plus, possible d'envisager la conjugaison de composés à des sidérophores pour augmenter leur assimilation par les levures ou augmenter leur spécificité à cibler des composantes vitales pour la croissance des cellules fongiques.

Conclusions générales

La germination est un aspect relativement peu exploré du cycle de vie des mycètes. Alors que l'activation de la germination a reçu une attention particulière, l'étude plus large de la germination permettrait de mieux comprendre les changements métaboliques qui surviennent au cours des différentes étapes de ce processus essentiel. Le métabolisme des sidérophores est une composante importante dans la régulation de la germination. Or, plusieurs aspects restent encore

à explorer, *e.g.* les détails du transport des sidérophores, les mécanismes de leur excrétion ou encore les mécanismes qui permettent l'extraction du Fe.

Remerciements

Je tiens d'abord à remercier le Pr Simon Labbé. Alors que je finissais ma maîtrise dans son labo, il m'a donné la chance de poursuivre des études au doctorat. Je suis reconnaissant pour le dévouement et la confiance qu'il porte à tous ses étudiants. L'intérêt et la passion qui l'animent dans ses recherches ont été des plus inspirants.

Je remercie tous les membres du laboratoire Labbé que j'ai eu la chance de côtoyer au cours de mes études. Raphaël Ioannoni, Thierry Mourer, Philippe Vachon, Ariane Brault, Jude Beaudoin, Jean-François Jacques, ainsi que plusieurs stagiaires, en particulier Isabelle Hébert-Milette, Ariane Millette St-Hilaire et Émilie Jolibois, par leur aide, leurs conseils, ou seulement leur bonne humeur, ont contribué au succès de mes études.

Merci particulièrement à Jude. Il a consacré beaucoup de son temps à mon encadrement et à me transmettre ses connaissances et son savoir-faire. Je suis très reconnaissant pour la patience dont il a fait preuve à mon égard durant mes stages au laboratoire.

Ariane mérite aussi un remerciement spécial. Son support a été très apprécié et a certainement contribué à la réussite de mes travaux. Elle et plusieurs autres membres du département ont su égailler mes longues journées au laboratoire, mais surtout ils ont été présents quand j'avais besoin de me changer les idées.

Finalement, un grand merci à ma famille et amis qui ont un été d'un grand support pour moi durant mes études.

Liste des références

Adams, T.H., Wieser, J.K., and Yu, J.H. (1998). Asexual sporulation in Aspergillus nidulans. Microbiol. Mol. Biol. Rev. *62*, 35–54.

Aguirre, J., Ríos-Momberg, M., Hewitt, D., and Hansberg, W. (2005). Reactive oxygen species and development in microbial eukaryotes. Trends Microbiol. *13*, 111–118.

Ahmed, E., and Holmström, S.J.M. (2014). Siderophores in environmental research: roles and applications. Microbial Biotechnology *7*, 196–208.

Allen, P.J. (1965). Metabolic Aspects of Spore Germination in Fungi. Annual Review of Phytopathology *3*, 313–342.

Ardon, O., Weizman, H., Libman, J., Shanzer, A., Chen, Y., and Hadar, Y. (1997). Iron uptake in Ustilago maydis: studies with fluorescent ferrichrome analogues. Microbiology *143*, 3625–3631.

Ardon, O., Nudelman, R., Caris, C., Libman, J., Shanzer, A., Chen, Y., and Hadar, Y. (1998). Iron Uptake in Ustilago maydis: Tracking the Iron Path. Journal of Bacteriology *180*, 2021–2026.

Arosio, P., and Levi, S. (2002). Ferritin, iron homeostasis, and oxidative damage. Free Radic. Biol. Med. *33*, 457–463.

Banci, L., Bertini, I., Cantini, F., Felli, I.C., Gonnelli, L., Hadjiliadis, N., Pierattelli, R., Rosato, A., and Voulgaris, P. (2006). The Atx1-Ccc2 complex is a metal-mediated protein-protein interaction. Nat. Chem. Biol. *2*, 367–368.

Barhoom, S., and Sharon, A. (2004). cAMP regulation of "pathogenic" and "saprophytic" fungal spore germination. Fungal Genet. Biol. *41*, 317–326.

Beaudoin, J., and Labbé, S. (2006). Copper induces cytoplasmic retention of fission yeast transcription factor cuf1. Eukaryotic Cell *5*, 277–292.

Beaudoin, J., and Labbé, S. (2007). Crm1-mediated nuclear export of the Schizosaccharomyces pombe transcription factor Cuf1 during a shift from low to high copper concentrations. Eukaryotic Cell *6*, 764–775.

Beaudoin, J., Mercier, A., Langlois, R., and Labbé, S. (2003). The Schizosaccharomyces pombe Cuf1 is composed of functional modules from two distinct classes of copper metalloregulatory transcription factors. J. Biol. Chem. *278*, 14565–14577.

Beaudoin, J., Thiele, D.J., Labbé, S., and Puig, S. (2011a). Dissection of the relative contribution of the Schizosaccharomyces pombe Ctr4 and Ctr5 proteins to the copper transport and cell surface delivery functions. Microbiology (Reading, Engl.) *157*, 1021–1031.

Beaudoin, J., Ioannoni, R., López-Maury, L., Bähler, J., Ait-Mohand, S., Guérin, B., Dodani, S.C., Chang, C.J., and Labbé, S. (2011b). Mfc1 is a novel forespore membrane copper transporter in meiotic and sporulating cells. J. Biol. Chem. *286*, 34356–34372.

Becher, P.G., Flick, G., Rozpędowska, E., Schmidt, A., Hagman, A., Lebreton, S., Larsson, M.C., Hansson, B.S., Piškur, J., Witzgall, P., et al. (2012). Yeast, not fruit volatiles mediate Drosophila melanogaster attraction, oviposition and development. Functional Ecology *26*, 822–828.

Bellemare, D.R., Shaner, L., Morano, K.A., Beaudoin, J., Langlois, R., and Labbe, S. (2002). Ctr6, a vacuolar membrane copper transporter in Schizosaccharomyces pombe. J. Biol. Chem. *277*, 46676–46686.

Beltran, F.F., Castillo, R., Vicente-Soler, J., Cansado, J., and Gacto, M. (2000). Role for trehalase during germination of spores in the fission yeast Schizosaccharomyces pombe. FEMS Microbiol Lett *193*, 117–121.

Bernier, G., Girijavallabhan, V., Murray, A., Niyaz, N., Ding, P., Miller, M.J., and Malouin, F. (2005). Desketoneoenactin-siderophore conjugates for Candida: evidence of iron transport-dependent species selectivity. Antimicrob. Agents Chemother. *49*, 241–248.

Besserglick, J., Olshvang, E., Szebesczyk, A., Englander, J., Levinson, D., Hadar, Y., Gumienna-Kontecka, E., and Shanzer, A. (2017). Ferrichrome Has Found Its Match: Biomimetic Analogues with Diversified Activity Map Discrete Microbial Targets. Chemistry *23*, 13181–13191.

Blaby-Haas, C.E., and Merchant, S.S. (2014). Lysosome-related Organelles as Mediators of Metal Homeostasis. J Biol Chem *289*, 28129–28136.

Boer, W. de, Folman, L.B., Summerbell, R.C., and Boddy, L. (2005). Living in a fungal world: impact of fungi on soil bacterial niche development. FEMS Microbiol. Rev. *29*, 795–811.

Bonazzi, D., Julien, J.-D., Romao, M., Seddiki, R., Piel, M., Boudaoud, A., and Minc, N. (2014). Symmetry Breaking in Spore Germination Relies on an Interplay between Polar Cap Stability and Spore Wall Mechanics. Developmental Cell *28*, 534–546.

Bonfante, P. (2018). The future has roots in the past: the ideas and scientists that shaped mycorrhizal research. New Phytol. *220*, 982–995.

Botha, A. (2011). The importance and ecology of yeasts in soil. Soil Biology and Biochemistry *43*, 1–8.

Botstein, D., Chervitz, S.A., and Cherry, J.M. (1997). Yeast as a Model Organism. Science *277*, 1259–1260.

Bournonville, C.F.G., and Díaz-Ricci, J.C. (2011). Quantitative determination of superoxide in plant leaves using a modified NBT staining method. Phytochem Anal *22*, 268–271.

Boyd, S.D., Calvo, J.S., Liu, L., Ullrich, M.S., Skopp, A., Meloni, G., and Winkler, D.D. (2019). The yeast copper chaperone for copper-zinc superoxide dismutase (CCS1) is a multifunctional chaperone promoting all levels of SOD1 maturation. J. Biol. Chem. *294*, 1956–1966.

Brault, A., Mourer, T., and Labbé, S. (2015). Molecular basis of the regulation of iron homeostasis in fission and filamentous yeasts. IUBMB Life *67*, 801–815.

Brault, A., Rallis, C., Normant, V., Garant, J.-M., Bähler, J., and Labbé, S. (2016). Php4 Is a Key Player for Iron Economy in Meiotic and Sporulating Cells. G3 (Bethesda) *6*, 3077–3095.

Bruns, T.D., Peay, K.G., Boynton, P.J., Grubisha, L.C., Hynson, N.A., Nguyen, N.H., and Rosenstock, N.P. (2009). Inoculum potential of Rhizopogon spores increases with time over the first 4 yr of a 99-yr spore burial experiment. New Phytol. *181*, 463–470.

Bunyard, B.A. (2007). Legerdemain in the Fungal Domain: The Use and Abuse of Insects by Fungi. American Entomologist *53*, 236–239.

Bushley, K.E., Ripoll, D.R., and Turgeon, B.G. (2008). Module evolution and substrate specificity of fungal nonribosomal peptide synthetases involved in siderophore biosynthesis. BMC Evol Biol *8*, 328.

Calhim, S., Halme, P., Petersen, J.H., Læssøe, T., Bässler, C., and Heilmann-Clausen, J. (2018). Fungal spore diversity reflects substrate-specific deposition challenges. Scientific Reports *8*, 5356.

Callan, B.E., and Carris, L.M. (2004). 7 - FUNGI ON LIVING PLANT SUBSTRATA, INCLUDING FRUITS. In Biodiversity of Fungi, G.M. Mueller, G.F. Bills, and M.S. Foster, eds. (Burlington: Academic Press), pp. 105–126.

Cano-Domínguez, N., Alvarez-Delfín, K., Hansberg, W., and Aguirre, J. (2008). NADPH oxidases NOX-1 and NOX-2 require the regulatory subunit NOR-1 to control cell differentiation and growth in Neurospora crassa. Eukaryotic Cell *7*, 1352–1361.

Chitarra, G.S., Abee, T., Rombouts, F.M., Posthumus, M.A., and Dijksterhuis, J. (2004). Germination of Penicillium paneum Conidia Is Regulated by 1-Octen-3-ol, a Volatile Self-Inhibitor. Appl. Environ. Microbiol. *70*, 2823–2829.

Cobine, P.A., Ojeda, L.D., Rigby, K.M., and Winge, D.R. (2004). Yeast contain a non-proteinaceous pool of copper in the mitochondrial matrix. J. Biol. Chem. *279*, 14447–14455.

Cobine, P.A., Pierrel, F., and Winge, D.R. (2006). Copper trafficking to the mitochondrion and assembly of copper metalloenzymes. Biochim. Biophys. Acta *1763*, 759–772.

Coluccio, A.E., Rodriguez, R.K., Kernan, M.J., and Neiman, A.M. (2008). The Yeast Spore Wall Enables Spores to Survive Passage through the Digestive Tract of Drosophila. PLOS ONE *3*, e2873.

Culotta, V.C., Klomp, L.W.J., Strain, J., Casareno, R.L.B., Krems, B., and Gitlin, J.D. (1997). The Copper Chaperone for Superoxide Dismutase. J. Biol. Chem. *272*, 23469–23472.

Dainty, S.J., Kennedy, C.A., Watt, S., Bähler, J., and Whitehall, S.K. (2008). Response of Schizosaccharomyces pombe to zinc deficiency. Eukaryotic Cell *7*, 454–464.

Dancis, A., Yuan, D.S., Haile, D., Askwith, C., Eide, D., Moehle, C., Kaplan, J., and Klausner, R.D. (1994). Molecular characterization of a copper transport protein in S. cerevisiae: an unexpected role for copper in iron transport. Cell *76*, 393–402.

Das, M., Drake, T., Wiley, D., Buchwald, P., Vavylonis, D., and Verde, F. (2012). Oscillatory dynamics of Cdc42 GTPase in the control of polarized growth. Science *337*, 239–243.

Davis, L., and Smith, G.R. (2001). Meiotic recombination and chromosome segregation in Schizosaccharomyces pombe. PNAS *98*, 8395–8402.

Doxastakis, M., Sum, A.K., and de Pablo, J.J. (2005). Modulating Membrane Properties: The Effect of Trehalose and Cholesterol on a Phospholipid Bilayer. J. Phys. Chem. B *109*, 24173–24181.

Drinnenberg, I.A., Weinberg, D.E., Xie, K.T., Mower, J.P., Wolfe, K.H., Fink, G.R., and Bartel, D.P. (2009). RNAi in budding yeast. Science *326*, 544–550.

Eisendle, M., Schrettl, M., Kragl, C., Müller, D., Illmer, P., and Haas, H. (2006). The Intracellular Siderophore Ferricrocin Is Involved in Iron Storage, Oxidative-Stress Resistance, Germination, and Sexual Development in Aspergillus nidulans. Eukaryot Cell *5*, 1596–1603.

Emery, T. (1971). Role of ferrichrome as a ferric ionophore in Ustilago sphaerogena. Biochemistry *10*, 1483–1488.

d'Enfert, C. (1997). Fungal Spore Germination: Insights from the Molecular Genetics ofAspergillus nidulansandNeurospora crassa. Fungal Genetics and Biology *21*, 163–172.

Feo, C.J.D., Aller, S.G., Siluvai, G.S., Blackburn, N.J., and Unger, V.M. (2009). Three-dimensional structure of the human copper transporter hCTR1. PNAS *106*, 4237–4242.

Field, L.S., Luk, E., and Culotta, V.C. (2002). Copper chaperones: personal escorts for metal ions. J. Bioenerg. Biomembr. *34*, 373–379.

Flo, T.H., Smith, K.D., Sato, S., Rodriguez, D.J., Holmes, M.A., Strong, R.K., Akira, S., and Aderem, A. (2004). Lipocalin 2 mediates an innate immune response to bacterial infection by sequestrating iron. Nature *432*, 917–921.

Florenzano, G., Balloni, W., and Materassi, R. (1977). Contributo alla ecologia dei lieviti Schizosaccharomyces sulle uve. Vitis.

Fluckinger, M., Haas, H., Merschak, P., Glasgow, B.J., and Redl, B. (2004). Human tear lipocalin exhibits antimicrobial activity by scavenging microbial siderophores. Antimicrob. Agents Chemother. *48*, 3367–3372.

Forsburg, S.L. (2001). The art and design of genetic screens: yeast. Nat. Rev. Genet. *2*, 659–668.

Fukunishi, K., Miyakubi, K., Hatanaka, M., Otsuru, N., Hirata, A., Shimoda, C., and Nakamura, T. (2014). The fission yeast spore is coated by a proteinaceous surface

layer comprising mainly Isp3. Mol. Biol. Cell *25*, 1549–1559.

Geijer, C., Pirkov, I., Vongsangnak, W., Ericsson, A., Nielsen, J., Krantz, M., and Hohmann, S. (2012). Time course gene expression profiling of yeast spore germination reveals a network of transcription factors orchestrating the global response. BMC Genomics *13*, 554.

Gerwien, F., Skrahina, V., Kasper, L., Hube, B., and Brunke, S. (2018). Metals in fungal virulence. FEMS Microbiol. Rev. *42*.

Glerum, D.M., Shtanko, A., and Tzagoloff, A. (1996). Characterization of COX17, a yeast gene involved in copper metabolism and assembly of cytochrome oxidase. J. Biol. Chem. *271*, 14504–14509.

Goffeau, A., Barrell, B.G., Bussey, H., Davis, R.W., Dujon, B., Feldmann, H., Galibert, F., Hoheisel, J.D., Jacq, C., Johnston, M., et al. (1996). Life with 6000 genes. Science *274*, 546, 563–567.

Gomes, F.C.O., Pataro, C., Guerra, J.B., Neves, M.J., Corrêa, S.R., Moreira, E.S.A., and Rosa, C.A. (2002). Physiological diversity and trehalose accumulation in Schizosaccharomyces pombe strains isolated from spontaneous fermentations during the production of the artisanal Brazilian cachaça. Can. J. Microbiol. *48*, 399–406.

Haas, H. (2014). Fungal siderophore metabolism with a focus on Aspergillus fumigatus. Nat Prod Rep *31*, 1266–1276.

Haas, H., Eisendle, M., and Turgeon, B.G. (2008). Siderophores in fungal physiology and virulence. Annu Rev Phytopathol *46*, 149–187.

Halliwell, B., and Gutteridge, J.M. (1992). Biologically relevant metal ion-dependent hydroxyl radical generation. An update. FEBS Lett. *307*, 108–112.

Harigaya, Y., and Yamamoto, M. (2007). Molecular mechanisms underlying the mitosis-meiosis decision. Chromosome Res. *15*, 523–537.

Hassett, R., and Kosman, D.J. (1995). Evidence for Cu(II) reduction as a component of copper uptake by Saccharomyces cerevisiae. J. Biol. Chem. *270*, 128–134.

Hatanaka, M., and Shimoda, C. (2001). The cyclic AMP/PKA signal pathway is required for initiation of spore germination in Schizosaccharomyces pombe. Yeast *18*, 207–217.

Hedges, S.B. (2002). The origin and evolution of model organisms. Nat. Rev. Genet. *3*, 838–849.

Heinemann, I.U., Jahn, M., and Jahn, D. (2008). The biochemistry of heme biosynthesis. Archives of Biochemistry and Biophysics *474*, 238–251.

Heymann, P., Gerads, M., Schaller, M., Dromer, F., Winkelmann, G., and Ernst, J.F. (2002). The Siderophore Iron Transporter of Candida albicans (Sit1p/Arn1p) Mediates Uptake of Ferrichrome-Type Siderophores and Is Required for Epithelial Invasion. Infection and Immunity *70*, 5246–5255.

Hoffman, C.S., Wood, V., and Fantes, P.A. (2015). An Ancient Yeast for Young Geneticists: A Primer on the Schizosaccharomyces pombe Model System. Genetics *201*, 403–423.

Horng, Y.-C., Cobine, P.A., Maxfield, A.B., Carr, H.S., and Winge, D.R. (2004). Specific copper transfer from the Cox17 metallochaperone to both Sco1 and Cox11 in the assembly of yeast cytochrome C oxidase. J. Biol. Chem. *279*, 35334–35340.

Howard, D.H. (1999). Acquisition, Transport, and Storage of Iron by Pathogenic Fungi. Clin Microbiol Rev *12*, 394–404.

Inoue, H., and Shimoda, C. (1981). Changes in trehalose content and trehalase activity during spore germination in fission yeast, Schizosaccharomyces pombe. Arch. Microbiol. *129*, 19–22.

Ioannoni, R., Beaudoin, J., Mercier, A., and Labbé, S. (2010). Copper-dependent trafficking of the Ctr4-Ctr5 copper transporting complex. PLoS ONE *5*, e11964.

Janes, S.M., Palcic, M.M., Scaman, C.H., Smith, A.J., Brown, D.E., Dooley, D.M., Mure, M., and Klinman, J.P. (1992). Identification of topaquinone and its consensus sequence in copper amine oxidases. Biochemistry *31*, 12147–12154.

Jbel, M., Mercier, A., Pelletier, B., Beaudoin, J., and Labbé, S. (2009). Iron activates in vivo DNA binding of Schizosaccharomyces pombe transcription factor Fep1 through its amino-terminal region. Eukaryotic Cell *8*, 649–664.

Jbel, M., Mercier, A., and Labbé, S. (2011). Grx4 monothiol glutaredoxin is required for iron limitation-dependent inhibition of Fep1. Eukaryotic Cell *10*, 629–645.

Jeffares, D.C. (2018). The natural diversity and ecology of fission yeast. Yeast *35*, 253–260.

Jeffares, D.C., Rallis, C., Rieux, A., Speed, D., Převorovský, M., Mourier, T., Marsellach, F.X., Iqbal, Z., Lau, W., Cheng, T.M.K., et al. (2015). The genomic and phenotypic diversity of Schizosaccharomyces pombe. Nature Genetics *47*, 235–241.

Johnson, L. (2008). Iron and siderophores in fungal-host interactions. Mycol. Res. *112*, 170–183.

Joseph-Strauss, D., Zenvirth, D., Simchen, G., and Barkai, N. (2007). Spore germination in Saccharomyces cerevisiae: global gene expression patterns and cell cycle landmarks. Genome Biol. *8*, R241.

Kampfenkel, K., Kushnir, S., Babiychuk, E., Inzé, D., and Montagu, M.V. (1995). Molecular Characterization of a Putative Arabidopsis thaliana Copper Transporter and Its Yeast Homologue. J. Biol. Chem. *270*, 28479–28486.

Kang, S.H., Khang, C.H., and Lee, Y.-H. (1999). Regulation of cAMP-dependent protein kinase during appressorium formation in Magnaporthe grisea. FEMS Microbiol Lett *170*, 419–423.

Kaplan, J., and Ward, D.M. (2013). The essential nature of iron usage and regulation. Current Biology *23*, R642–R646.

Kendrick, B. (2011). Fungi: Ecological Importance and Impact on Humans. In ELS, (American Cancer Society), p.

Kim, B.-E., Nevitt, T., and Thiele, D.J. (2008). Mechanisms for copper acquisition, distribution and regulation. Nat. Chem. Biol. *4*, 176–185.

Kim, Y., Yun, C.-W., and Philpott, C.C. (2002). Ferrichrome induces endosome to plasma membrane cycling of the ferrichrome transporter, Arn1p, in Saccharomyces cerevisiae. EMBO J *21*, 3632–3642.

Kodama, H., Fujisawa, C., and Bhadhprasit, W. (2012). Inherited Copper Transport Disorders: Biochemical Mechanisms, Diagnosis, and Treatment. Curr Drug Metab *13*, 237–250.

Komori, H., and Higuchi, Y. (2015). Structural insights into the O2 reduction mechanism of multicopper oxidase. J. Biochem. *158*, 293–298.

Kragl, C., Schrettl, M., Abt, B., Sarg, B., Lindner, H.H., and Haas, H. (2007). EstB-Mediated Hydrolysis of the Siderophore Triacetylfusarinine C Optimizes Iron Uptake of Aspergillus fumigatus. Eukaryotic Cell *6*, 1278–1285.

Kulkarni, R.D., Kelkar, H.S., and Dean, R.A. (2003). An eight-cysteine-containing CFEM domain unique to a group of fungal membrane proteins. Trends in Biochemical Sciences *28*, 118–121.

Kuramae, E.E., Robert, V.J.M., Snel, B., and Boekhout, T. (2006). Conflicting phylogenetic position of Schizosaccharomyces pombe. Genomics *88*, 387–393.

Kuznets, G., Vigonsky, E., Weissman, Z., Lalli, D., Gildor, T., Kauffman, S.J., Turano, P., Becker, J., Lewinson, O., and Kornitzer, D. (2014). A relay network of extracellular heme-binding proteins drives C. albicans iron acquisition from hemoglobin. PLoS Pathog. *10*, e1004407.

Laliberté, J., Whitson, L.J., Beaudoin, J., Holloway, S.P., Hart, P.J., and Labbé, S. (2004). The Schizosaccharomyces pombe Pccs protein functions in both copper trafficking and metal detoxification pathways. J. Biol. Chem. *279*, 28744–28755.

Lamb, A.L., Wernimont, A.K., Pufahl, R.A., Culotta, V.C., O'Halloran, T.V., and Rosenzweig, A.C. (1999). Crystal structure of the copper chaperone for superoxide dismutase. Nat. Struct. Biol. *6*, 724–729.

Lamb, A.L., Torres, A.S., O'Halloran, T.V., and Rosenzweig, A.C. (2001). Heterodimeric structure of superoxide dismutase in complex with its metallochaperone. Nat. Struct. Biol. *8*, 751–755.

Lee, J., Prohaska, J.R., Dagenais, S.L., Glover, T.W., and Thiele, D.J. (2000). Isolation of a murine copper transporter gene, tissue specific expression and functional complementation of a yeast copper transport mutant. Gene *254*, 87–96.

Lee, S.C., Ni, M., Li, W., Shertz, C., and Heitman, J. (2010). The Evolution of Sex: a Perspective from the Fungal Kingdom. Microbiol. Mol. Biol. Rev. *74*, 298–340.

van Leeuwen, M.R., Krijgsheld, P., Bleichrodt, R., Menke, H., Stam, H., Stark, J.,

Wösten, H. a. B., and Dijksterhuis, J. (2013). Germination of conidia of Aspergillus niger is accompanied by major changes in RNA profiles. Stud. Mycol. *74*, 59–70.

Leong, S.A., and Winkelmann, G. (1998). Molecular biology of iron transport in fungi. Met Ions Biol Syst *35*, 147–186.

Lin, S.J., Pufahl, R.A., Dancis, A., O'Halloran, T.V., and Culotta, V.C. (1997). A role for the Saccharomyces cerevisiae ATX1 gene in copper trafficking and iron transport. J. Biol. Chem. *272*, 9215–9220.

Lindegren, C.C. (1932). The Genetics of Neurospora. I. The Inheritance of Response to Heat- Treatment. Bulletin of the Torrey Botanical Club *59*, 85–102.

Liti, G. (2015). The fascinating and secret wild life of the budding yeast S. cerevisiae. ELife *4*, e05835.

Magazù, S., Maisano, G., Migliardo, P., and Villari, V. (1999). Experimental simulation of macromolecules in trehalose aqueous solutions: A photon correlation spectroscopy study. J. Chem. Phys. *111*, 9086–9092.

Malagnac, F., Lalucque, H., Lepère, G., and Silar, P. (2004). Two NADPH oxidase isoforms are required for sexual reproduction and ascospore germination in the filamentous fungus Podospora anserina. Fungal Genet. Biol. *41*, 982–997.

Marcus, S., Polverino, A., Chang, E., Robbins, D., Cobb, M.H., and Wigler, M.H. (1995). Shk1, a homolog of the Saccharomyces cerevisiae Ste20 and mammalian p65PAK protein kinases, is a component of a Ras/Cdc42 signaling module in the fission yeast Schizosaccharomyces pombe. Proc. Natl. Acad. Sci. U.S.A. *92*, 6180–6184.

Mata, J., Wilbrey, A., and Bähler, J. (2007). Transcriptional regulatory network for sexual differentiation in fission yeast. Genome Biol. *8*, R217.

Matzanke, B.F., Bill, E., Trautwein, A.X., and Winkelmann, G. (1987). Role of siderophores in iron storage in spores of Neurospora crassa and Aspergillus ochraceus. J. Bacteriol. *169*, 5873–5876.

McCord, J.M., and Fridovich, I. (1969). Superoxide dismutase. An enzymic function for erythrocuprein (hemocuprein). J. Biol. Chem. *244*, 6049–6055.

Mehra, A., Shi, M., Baker, C.L., Colot, H.V., Loros, J.J., and Dunlap, J.C. (2009). A role for Casein Kinase 2 in the mechanism underlying circadian temperature compensation. Cell *137*, 749–760.

Mercier, A., and Labbé, S. (2009). Both Php4 function and subcellular localization are regulated by iron via a multistep mechanism involving the glutaredoxin Grx4 and the exportin Crm1. J. Biol. Chem. *284*, 20249–20262.

Mercier, A., and Labbé, S. (2010). Iron-dependent remodeling of fungal metabolic pathways associated with ferrichrome biosynthesis. Appl. Environ. Microbiol. *76*, 3806–3817.

Mercier, A., Pelletier, B., and Labbé, S. (2006). A transcription factor cascade involving Fep1 and the CCAAT-binding factor Php4 regulates gene expression in response to

iron deficiency in the fission yeast Schizosaccharomyces pombe. Eukaryotic Cell *5*, 1866–1881.

Mercier, A., Watt, S., Bähler, J., and Labbé, S. (2008). Key function for the CCAAT-binding factor Php4 to regulate gene expression in response to iron deficiency in fission yeast. Eukaryotic Cell *7*, 493–508.

Merlini, L., Dudin, O., and Martin, S.G. (2013). Mate and fuse: how yeast cells do it. Open Biol *3*, 130008.

Moore, R.E., Kim, Y., and Philpott, C.C. (2003). The mechanism of ferrichrome transport through Arn1p and its metabolism in Saccharomyces cerevisiae. PNAS *100*, 5664–5669.

Morales Hernandez, C.E., Padilla Guerrero, I.E., Gonzalez Hernandez, G.A., Salazar Solis, E., and Torres Guzman, J.C. (2010). Catalase overexpression reduces the germination time and increases the pathogenicity of the fungus Metarhizium anisopliae. Appl. Microbiol. Biotechnol. *87*, 1033–1044.

Mourer, T., Jacques, J.-F., Brault, A., Bisaillon, M., and Labbé, S. (2015). Shu1 is a cell-surface protein involved in iron acquisition from heme in Schizosaccharomyces pombe. J. Biol. Chem. *290*, 10176–10190.

Mourer, T., Normant, V., and Labbé, S. (2017). Heme Assimilation in Schizosaccharomyces pombe Requires Cell-surface-anchored Protein Shu1 and Vacuolar Transporter Abc3. J. Biol. Chem. *292*, 4898–4912.

Nevitt, T., and Thiele, D.J. (2011). Host Iron Withholding Demands Siderophore Utilization for Candida glabrata to Survive Macrophage Killing. PLOS Pathogens *7*, e1001322.

Nevitt, T., Ohrvik, H., and Thiele, D.J. (2012). Charting the travels of copper in eukaryotes from yeast to mammals. Biochim. Biophys. Acta *1823*, 1580–1593.

Nielsen, O., and Davey, J. (1995). Pheromone communication in the fission yeast Schizosaccharomyces pombe. Seminars in Cell Biology *6*, 95–104.

Normant, V., Mourer, T., and Labbé, S. (2018). The major facilitator transporter Str3 is required for low-affinity heme acquisition in Schizosaccharomyces pombe. J. Biol. Chem. *293*, 6349–6362.

Nosanchuk, J.D. (2015). Review of Human Pathogenic Fungi: Molecular Biology and Pathogenic Mechanisms. Front Microbiol *6*.

Oda, K., Bignell, E., Kang, S.E., and Momany, M. (2017). Transcript levels of the Aspergillus fumigatus Cdc42 module, polarisome, and septin genes show little change from dormancy to polarity establishment. Med. Mycol. *55*, 445–452.

Okada, M., and Miura, T. (2016). Copper(I) stabilization by cysteine/tryptophan motif in the extracellular domain of Ctr4. J. Inorg. Biochem. *159*, 45–49.

Okada, M., Miura, T., and Nakabayashi, T. (2017). Comparison of extracellular Cys/Trp motif between Schizosaccharomyces pombe Ctr4 and Ctr5. J. Inorg. Biochem. *169*,

97–105.

Otsubo, Y., and Yamamoto, M. (2012). Signaling pathways for fission yeast sexual differentiation at a glance. J Cell Sci *125*, 2789–2793.

Ottilie, S., Miller, P.J., Johnson, D.I., Creasy, C.L., Sells, M.A., Bagrodia, S., Forsburg, S.L., and Chernoff, J. (1995). Fission yeast pak1+ encodes a protein kinase that interacts with Cdc42p and is involved in the control of cell polarity and mating. EMBO J. *14*, 5908–5919.

Park, H.-S., and Yu, J.-H. (2012). Genetic control of asexual sporulation in filamentous fungi. Current Opinion in Microbiology *15*, 669–677.

Park, Y.-S., Kim, T.-H., Chang, H.-I., Sung, H.-C., and Yun, C.-W. (2006). Cellular iron utilization is regulated by putative siderophore transporter FgSit1 not by free iron transporter in Fusarium graminearum. Biochem. Biophys. Res. Commun. *345*, 1634–1642.

Park, Y.-S., Kim, J.-Y., and Yun, C.-W. (2016). Identification of ferrichrome- and ferrioxamine B-mediated iron uptake by Aspergillus fumigatus. Biochem. J. *473*, 1203–1213.

Pelletier, B., Beaudoin, J., Mukai, Y., and Labbé, S. (2002). Fep1, an iron sensor regulating iron transporter gene expression in Schizosaccharomyces pombe. J. Biol. Chem. *277*, 22950–22958.

Pelletier, B., Beaudoin, J., Philpott, C.C., and Labbé, S. (2003). Fep1 represses expression of the fission yeast Schizosaccharomyces pombe siderophore-iron transport system. Nucleic Acids Res. *31*, 4332–4344.

Pelletier, B., Trott, A., Morano, K.A., and Labbé, S. (2005). Functional characterization of the iron-regulatory transcription factor Fep1 from Schizosaccharomyces pombe. J. Biol. Chem. *280*, 25146–25161.

Peña, M.M.O., Puig, S., and Thiele, D.J. (2000). Characterization of the Saccharomyces cerevisiae High Affinity Copper Transporter Ctr3. J. Biol. Chem. *275*, 33244–33251.

Perez-Nadales, E., Almeida Nogueira, M.F., Baldin, C., Castanheira, S., El Ghalid, M., Grund, E., Lengeler, K., Marchegiani, E., Mehrotra, P.V., Moretti, M., et al. (2014). Fungal model systems and the elucidation of pathogenicity determinants. Fungal Genetics and Biology *70*, 42–67.

Peter, C., Laliberté, J., Beaudoin, J., and Labbé, S. (2008). Copper distributed by Atx1 is available to copper amine oxidase 1 in Schizosaccharomyces pombe. Eukaryotic Cell *7*, 1781–1794.

Plante, S., Ioannoni, R., Beaudoin, J., and Labbé, S. (2014). Characterization of Schizosaccharomyces pombe copper transporter proteins in meiotic and sporulating cells. J. Biol. Chem. *289*, 10168–10181.

Pope, C.R., Flores, A.G., Kaplan, J.H., and Unger, V.M. (2012). Structure and function of copper uptake transporters. Curr Top Membr *69*, 97–112.

Pufahl, R.A., Singer, C.P., Peariso, K.L., Lin, S.J., Schmidt, P.J., Fahrni, C.J., Culotta, V.C., Penner-Hahn, J.E., and O'Halloran, T.V. (1997). Metal ion chaperone function of the soluble Cu(I) receptor Atx1. Science *278*, 853–856.

Puig, S., Lee, J., Lau, M., and Thiele, D.J. (2002). Biochemical and genetic analyses of yeast and human high affinity copper transporters suggest a conserved mechanism for copper uptake. J. Biol. Chem. *277*, 26021–26030.

Quadri, L.E.N. (2007). Strategic paradigm shifts in the antimicrobial drug discovery process of the 21st century. Infect Disord Drug Targets *7*, 230–237.

Quistgaard, E.M., Löw, C., Guettou, F., and Nordlund, P. (2016). Understanding transport by the major facilitator superfamily (MFS): structures pave the way. Nature Reviews Molecular Cell Biology *17*, 123–132.

Reddi, A.R., and Culotta, V.C. (2013). SOD1 Integrates Signals from Oxygen and Glucose to Repress Respiration. Cell *152*, 224–235.

Renshaw, J.C., Robson, G.D., Trinci, A.P.J., Wiebe, M.G., Livens, F.R., Collison, D., and Taylor, R.J. (2002). Fungal siderophores: structures, functions and applications. Mycological Research *106*, 1123–1142.

Rinaldi, A.C., Porcu, C.M., Oliva, S., Curreli, N., Rescigno, A., Sollai, F., Rinaldi, A., Finazzi-Agró, A., and Sanjust, E. (1998). Biosynthesis of the topaquinone cofactor in copper amine oxidases--evidence from model studies. Eur. J. Biochem. *251*, 91–97.

Riquelme, M., Yarden, O., Bartnicki-Garcia, S., Bowman, B., Castro-Longoria, E., Free, S.J., Fleissner, A., Freitag, M., Lew, R.R., Mouriño-Pérez, R., et al. (2011). Architecture and development of the Neurospora crassa hypha -- a model cell for polarized growth. Fungal Biol *115*, 446–474.

Roman, D., Dancis, A., Anderson, G.J., and Klausner, R.D. (1993). The fission yeast ferric reductase gene frp1+ is required for ferric iron uptake and encodes a protein that is homologous to the gp91-phox subunit of the human NADPH phagocyte oxidoreductase. Molecular and Cellular Biology *13*, 4342–4350.

Rossi, D.C.P., Gleason, J.E., Sanchez, H., Schatzman, S.S., Culbertson, E.M., Johnson, C.J., McNees, C.A., Coelho, C., Nett, J.E., Andes, D.R., et al. (2017). Candida albicans FRE8 encodes a member of the NADPH oxidase family that produces a burst of ROS during fungal morphogenesis. PLoS Pathog. *13*, e1006763.

Rutherford, J.C., and Bird, A.J. (2004). Metal-Responsive Transcription Factors That Regulate Iron, Zinc, and Copper Homeostasis in Eukaryotic Cells. Eukaryot Cell *3*, 1–13.

Schmidt, P.J., Rae, T.D., Pufahl, R.A., Hamma, T., Strain, J., O'Halloran, T.V., and Culotta, V.C. (1999). Multiple Protein Domains Contribute to the Action of the Copper Chaperone for Superoxide Dismutase. J. Biol. Chem. *274*, 23719–23725.

Schmidt, P.J., Kunst, C., and Culotta, V.C. (2000). Copper activation of superoxide dismutase 1 (SOD1) in vivo. Role for protein-protein interactions with the copper

chaperone for SOD1. J. Biol. Chem. *275*, 33771–33776.

Schrettl, M., Winkelmann, G., and Haas, H. (2004). Ferrichrome in Schizosaccharomyces pombe--an iron transport and iron storage compound. Biometals *17*, 647–654.

Schrettl, M., Bignell, E., Kragl, C., Sabiha, Y., Loss, O., Eisendle, M., Wallner, A., Jr, H.N.A., Haynes, K., and Haas, H. (2007). Distinct Roles for Intra- and Extracellular Siderophores during Aspergillus fumigatus Infection. PLOS Pathogens *3*, e128.

Schwecke, T., Göttling, K., Durek, P., Dueñas, I., Käufer, N.F., Zock-Emmenthal, S., Staub, E., Neuhof, T., Dieckmann, R., and von Döhren, H. (2006). Nonribosomal peptide synthesis in Schizosaccharomyces pombe and the architectures of ferri-chrome-type siderophore synthetases in fungi. Chembiochem *7*, 612–622.

Scott, B., and Eaton, C.J. (2008). Role of reactive oxygen species in fungal cellular differentiations. Curr. Opin. Microbiol. *11*, 488–493.

Semighini, C.P., and Harris, S.D. (2008). Regulation of apical dominance in Aspergillus nidulans hyphae by reactive oxygen species. Genetics *179*, 1919–1932.

Severance, S., Chakraborty, S., and Kosman, D.J. (2004). The Ftr1p iron permease in the yeast plasma membrane: orientation, topology and structure-function relationships. Biochem J *380*, 487–496.

Shatwell, K.P., Dancis, A., Cross, A.R., Klausner, R.D., and Segal, A.W. (1996). The FRE1 ferric reductase of Saccharomyces cerevisiae is a cytochrome b similar to that of NADPH oxidase. J. Biol. Chem. *271*, 14240–14244.

Shimoda, C. (1980). Differential effect of glucose and fructose on spore germination in the fission yeast, Schizosaccharomyces pombe. Can. J. Microbiol. *26*, 741–745.

Silar, P. (2014). Simple Genetic Tools to Study Fruiting Body Development in Fungi. The Open Mycology Journal *8*.

Silva, B., and Faustino, P. (2015). An overview of molecular basis of iron metabolism regulation and the associated pathologies. Biochimica et Biophysica Acta (BBA) - Molecular Basis of Disease *1852*, 1347–1359.

Smirnova, A.V., Matveyeva, N.P., and Yermakov, I.P. (2014). Reactive oxygen species are involved in regulation of pollen wall cytomechanics. Plant Biol (Stuttg) *16*, 252–257.

Sooksa-nguan, T., Yakubov, B., Kozlovskyy, V.I., Barkume, C.M., Howe, K.J., Thannhauser, T.W., Rutzke, M.A., Hart, J.J., Kochian, L.V., Rea, P.A., et al. (2009). Drosophila ABC Transporter, DmHMT-1, Confers Tolerance to Cadmium DmHMT-1 AND ITS YEAST HOMOLOG, SpHMT-1, ARE NOT ESSENTIAL FOR VACUOLAR PHYTOCHELATIN SEQUESTRATION. J. Biol. Chem. *284*, 354–362.

Spiro, T.G., Allerton, S.E., Renner, J., Terzis, A., Bils, R., and Saltman, P. (1966). The Hydrolytic Polymerization of Iron(III). J. Am. Chem. Soc. *88*, 2721–2726.

Tanaka, K., and Hirata, A. (1982). Ascospore development in the fission yeasts Schizosaccharomyces pombe and S. japonicus. J. Cell. Sci. *56*, 263–279.

Tanaka, A., Takemoto, D., Hyon, G.-S., Park, P., and Scott, B. (2008). NoxA activation by the small GTPase RacA is required to maintain a mutualistic symbiotic association between Epichloë festucae and perennial ryegrass. Molecular Microbiology *68*, 1165–1178.

Thevelein, J.M. (1984). Regulation of Trehalose Mobilization in Fungi. MICROBIOL. REV. *48*, 18.

Valko, M., Morris, H., and Cronin, M.T.D. (2005). Metals, toxicity and oxidative stress. Curr. Med. Chem. *12*, 1161–1208.

Wallace, M.A., Liou, L.-L., Martins, J., Clement, M.H.S., Bailey, S., Longo, V.D., Valentine, J.S., and Gralla, E.B. (2004). Superoxide inhibits 4Fe-4S cluster enzymes involved in amino acid biosynthesis. Cross-compartment protection by CuZn-superoxide dismutase. J. Biol. Chem. *279*, 32055–32062.

Welton, R.M., and Hoffman, C.S. (2000). Glucose monitoring in fission yeast via the Gpa2 galpha, the git5 Gbeta and the git3 putative glucose receptor. Genetics *156*, 513–521.

Winkelmann, G. (2007). Ecology of siderophores with special reference to the fungi. Biometals *20*, 379–392.

Winkelmann, G., and Huschka, H. (1984). A study on the mechanism of siderophore transport - a proton symport. Journal of Plant Nutrition *7*, 479–487.

Wood, V., Gwilliam, R., Rajandream, M.-A., Lyne, M., Lyne, R., Stewart, A., Sgouros, J., Peat, N., Hayles, J., Baker, S., et al. (2002). The genome sequence of Schizosaccharomyces pombe. Nature *415*, 871–880.

Yamamoto, M. (1996). Regulation of meiosis in fission yeast. Cell Struct. Funct. *21*, 431–436.

Yan, N. (2015). Structural Biology of the Major Facilitator Superfamily Transporters. Annual Review of Biophysics *44*, 257–283.

Yanagida, M. (2002). The model unicellular eukaryote, Schizosaccharomyces pombe. Genome Biol *3*, comment2003.1-comment2003.4.

Yuan, D.S., Stearman, R., Dancis, A., Dunn, T., Beeler, T., and Klausner, R.D. (1995). The Menkes/Wilson disease gene homologue in yeast provides copper to a ceruloplasmin-like oxidase required for iron uptake. Proc. Natl. Acad. Sci. U.S.A. *92*, 2632–2636.

Yuan, S., Sharma, A.K., Richart, A., Lee, J., and Kim, B.-E. (2018). CHCA-1 is a copper-regulated CTR1 homolog required for normal development, copper accumulation, and copper-sensing behavior in Caenorhabditis elegans. J. Biol. Chem. *293*, 10911–10925.

Yun, C.W., Tiedeman, J.S., Moore, R.E., and Philpott, C.C. (2000). Siderophore-iron uptake in saccharomyces cerevisiae. Identification of ferrichrome and fusarinine transporters. J. Biol. Chem. *275*, 16354–16359.

Zhou, B., and Gitschier, J. (1997). hCTR1: A human gene for copper uptake identified by complementation in yeast. Proc Natl Acad Sci U S A *94*, 7481–7486.

Zhou, H., and Thiele, D.J. (2001). Identification of a novel high affinity copper transport complex in the fission yeast Schizosaccharomyces pombe. J. Biol. Chem. *276*, 20529–20535.

Zhou, H., Cadigan, K.M., and Thiele, D.J. (2003). A Copper-regulated Transporter Required for Copper Acquisition, Pigmentation, and Specific Stages of Development in Drosophila melanogaster. J. Biol. Chem. *278*, 48210–48218.

Znaidi, S., Pelletier, B., Mukai, Y., and Labbé, S. (2004). The Schizosaccharomyces pombe corepressor Tup11 interacts with the iron-responsive transcription factor Fep1. J. Biol. Chem. *279*, 9462–9474.

ANNEXES

Dans le but de faciliter le travail des évaluateurs, je joins ici les articles inclues dans cette thèse dans leur format publié.

Plante S., Normant V., Ramos-Torres KM, and Labbé S (2017), Cell-surface copper transporters and superoxide dismutase 1 are essential for outgrowth during fungal spore germination, *J Biol Chem*, 292, 11896-11914

Plante S, and Labbé S (2019), Spore Germination Requires Ferrichrome Biosynthesis and the Siderophore Transporter Str1 in Schizosaccharomyces pombe, *Genetics*, 211, 893-911